UNIVERSITÀ DEGLI STUDI DI MILANO

PhD Course in Environmental Sciences

XXIX Cycle

Homogenized sunshine duration (1936-2013) and global radiation (1959-2013) instrumental time series over Italy: variability and trends

PhD Thesis

Veronica MANARA

R10545-R24

Scientific tutor: Prof. Maurizio MAUGERI

Scientific co-tutor: Dr. Michele BRUNETTI PhD

Academic year: 2015-2016

SSD: FIS/06; FIS/07; GEO/12
Thesis performed at the Department of Physics, Università degli Studi di Milano (Milan, Italy) in collaboration with ISAC-CNR (Institute of Atmospheric Sciences and Climate - National Research Council, Bologna, Italy).

Contents

Abstract

Daily sunshine duration (SD) and global radiation ($E_{g\downarrow}$) series were recovered for the whole Italian territory for the periods 1936-2013 and 1959-2013, respectively. To obtain reliable series, useful to study the variability and trends, it has been necessary to solve a number of problems concerning the quality of the data, their completeness and their spatial distribution. Specifically, all the corresponding monthly records were subjected to a detailed quality control and homogenization procedure in order to eliminate non climatic signals and then the missing values were estimated. Moreover, all the series were converted into seasonal and annual anomaly series and a 1°x1° gridded version of the dataset has been generated. Finally, two regional records (northern and southern Italy) were obtained by averaging the corresponding grid-point series. Besides to all-sky records, clear-sky anomaly records were also obtained selecting only the clear days in the original series by comparison with corresponding total cloud cover (TCC) series.

The all-sky SD and $E_{g\downarrow}$ anomaly regional records show a decreasing tendency ("Global dimming") between the 1950s and 1980s while in the subsequent period they show an increasing tendency ("Brightening period"). The SD series, covering a longer period, show also an increasing tendency between the mid-1930s and the mid-1950s ("Early brightening"). The intensity and the length of the signals depend on the considered variable, region and season. The comparison between SD records with corresponding TCC records shows that the expected negative correlation between these variables is often not evident, especially between the 1960s and 1980s. This suggests that during the dimming period there is an important fraction of SD evolution that cannot be explained by TCC. It must therefore depend on other factors, as for example, changes in aerosol optical thickness.

The clear-sky SD and $E_{g\downarrow}$ series show longer and more significant trends than the all-sky series for almost all the seasons. The most relevant changes are observed in winter and autumn for both variables, highlighting the important role of clouds under all-sky conditions.

The resulting trends under clear-sky conditions are in agreement with changes in anthropogenic aerosols suggesting that they have a relevant role on $E_{g\downarrow}$ variability. Nevertheless, an high correlation coefficient between $E_{g\downarrow}$ series and the Sahel Precipitation index, especially in the southern region, suggests also a significant contribution of natural aerosols. This can justify the stronger dimming during spring, summer and autumn in the south than in the north. Moreover, the fact that the intensity of the dimming/brightening trends

change in all seasons removing the cloud contribution supports the hypothesis that clouds contribute in a significant way to the $E_{g\downarrow}$ variability under all-sky conditions.
The results highlight that the agreement between SD and $E_{g\downarrow}$ decadal variability and long-term trends, over the common period (1959-2013), depends on the considered region, season and period. Specifically, $E_{g\downarrow}$ clear-sky series show stronger tendencies than SD, both during the dimming and brightening periods. In order to investigate whether the differences in the clear-sky trends are due to a different sensitivity to atmospheric turbidity changes, a model has been applied with the aim of estimating how large are SD and $E_{g\downarrow}$ relative variations when atmospheric turbidity (expressed by means of the Turbidity Linke Factor - T_L) changes. For low T_L, $E_{g\downarrow}$ is expected to be much more sensitive than SD while for high T_L, SD is expected to be slightly more sensitive than $E_{g\downarrow}$. These results give evidence that the use of SD as a proxy variable for clear-sky $E_{g\downarrow}$ may be problematic, especially if T_L is low or if it shows significant changes in time. The comparison between the modelled and the observed relative trends highlights a very good agreement with the only exception of the dimming period in winter and autumn in northern region. These disagreement could be both connected to instrumental problems or to the influence of other meteorological variables.
Finally, a methodology to estimate $E_{g\downarrow}$ normal values for any interval of a period in which a SD anomaly series is available has been set up (it is very useful for example to evaluate the ability of a RCM-GCM (Regional Climate Model - Global Climate Model) in capturing the spatial distribution of $E_{g\downarrow}$), and then, for each period during which the $E_{g\downarrow}$ normal values are available, to estimate the corresponding climatologies.

Riassunto

Le serie giornaliere di eliofania (SD) e radiazione globale ($E_{g\downarrow}$) disponibili per il territorio italiano, sono state raccolte rispettivamente per i periodi 1936-2013 e 1959-2013. Al fine di ottenere serie di dati realistiche, utilizzabili per studiare la variabilità e i trend, è stato necessario risolvere una serie di problemi riguardanti la qualità dei dati, la completezza delle serie e la loro distribuzione spaziale. In particolare, tutte le corrispondenti serie mensili sono state sottoposte a un minuzioso controllo di qualità ed omogeneizzazione con il fine di eliminare eventuali segnali di tipo non climatico, e poi per ognuna di queste serie, sono stati stimati i valori mancanti. Tutte le serie sono state poi convertite in serie di anomalie stagionali e annuali ed è stata calcolata la versione su griglia del dataset con una risoluzione di 1°x1°. Infine, sono state ottenute due serie regionali (nord e sud Italia) mediando le corrispondenti serie ottenute per ciascun punto di griglia. Parallelamente alle serie in condizioni di "all-sky", sono state ottenute le serie in condizioni di cielo sereno ("clear-sky"), selezionando solo i giorni sereni mediante confronto con le corrispondenti serie di copertura nuvolosa (TCC).

Le serie regionali di anomalia ottenute per SD e $E_{g\downarrow}$ in condizioni di "all-sky", mostrano un trend negativo ("Global dimming") tra gli anni '50 e gli anni '80 mentre nel periodo successivo, mostrano un trend positivo ("Brightening period"). Le serie di SD, coprendo un periodo più lungo, mostrano un trend positivo anche tra la metà degli anni '30 e la metà degli anni '50 ("Early brightening"). L'intensità dei trend dipende dalla variabile, dalla regione e dalla stagione che viene considerata. Il confronto tra le serie di SD e le corrispondenti serie di TCC mostra che l'attesa anti-correlazione tra queste due variabili non è sempre presente, specialmente tra gli anni '60 e gli anni '80. Questo suggerisce che durante il periodo di "dimming" c'è un'importante frazione della variabilità dell'SD che non può essere spiegata con una variazione della copertura nuvolosa. Essa deve quindi dipendere da altri fattori, come per esempio, la variazione dello spessore ottico degli aerosol.

Le serie di SD e $E_{g\downarrow}$ in condizioni di "clear-sky" mostrano in quasi tutte le stagioni dei trend con un'intensità maggiore e una maggiore significatività rispetto ai corrispondenti ottenuti in condizioni di "all-sky". Le maggiori differenze si osservano in inverno e autunno per entrambe le variabili, evidenziando l'importante ruolo delle nubi in condizioni di "all-sky".

I trend ottenuti in condizioni di "clear-sky" sono in accordo con le variazioni osservate per gli aerosol di origine antropogenica, suggerendo in questo modo, un loro importante ruolo

nella variabilità di $E_{g\downarrow}$. Tuttavia, l'elevata correlazione tra le serie di $E_{g\downarrow}$ e le serie di "Sahel Precipitation Index", specialmente in sud Italia, suggerisce anche un significativo contributo degli aerosol di origine naturale. Questo potrebbe giustificare nel periodo di "dimming", la più intensa diminuzione di $E_{g\downarrow}$ osservata in primavera, estate e autunno al sud rispetto a quella osservata al nord. Inoltre, il fatto che rimuovendo il contributo delle nubi, l'intensità dei trend durante il periodo di "dimming/brightening" cambi in tutte le stagioni, supporta l'ipotesi che le nubi contribuiscono in maniera significativa in condizioni di "all-sky" alla variazione di $E_{g\downarrow}$.

I risultati mostrano che l'accordo tra la variabilità a scala decennale tra SD e $E_{g\downarrow}$, nel periodo comune alle due variabili (1959-2013), dipende dalla regione, dalla stagione e dal periodo che si considera. In modo particolare, le serie di $E_{g\downarrow}$ in condizioni di "clear-sky" mostrano variazioni più intense rispetto a quelle osservate per SD sia durante il periodo di "dimming" che durante il periodo di "brightening". Al fine di comprendere meglio se le differenze osservate nei trend in condizioni di "clear-sky" siano dovute a una diversa sensitività alle variazioni della torbidità atmosferica, è stato applicato un modello con lo scopo di stimare quanto variano SD e $E_{g\downarrow}$ al variare della torbidità (espressa tramite il "Turbidity Linke Factor" - T_L). Per bassi valori di T_L, $E_{g\downarrow}$ è attesa essere molto più sensitiva di SD, mentre per alti valori di T_L, SD è attesa essere leggermente meno sensitiva di $E_{g\downarrow}$. Questi risultati mostrano che l'uso di SD come variabile proxy per $E_{g\downarrow}$ in condizioni di "clear-sky" può essere problematico, specialmente se T_L è basso e se mostra significative variazioni nell'arco del tempo. Il confronto tra i trend osservati e stimati mostra un ottimo accordo con la sola eccezione del periodo di "dimming" in inverno e autunno al nord. Queste discrepanze potrebbero essere legate a problemi di tipo strumentale e all'influenza di altre variabili meteorologiche.

In fine, è stata sviluppata una metodologia per stimare i valori normali di $E_{g\downarrow}$ per ogni intervallo di tempo nel quale una serie di anomalia di SD è disponibile (è molto utile per esempio per valutare l'abilità di un RCM-GCM (Regional Climate Model - Global Climate Model, Modello a scala regionale - Modelo a scala globale) nel prevedere la distribuzione spaziale di $E_{g\downarrow}$), e quindi, per ognuno dei periodi per i quali i valori normali di $E_{g\downarrow}$ sono disponibili, stimare le corrispondenti climatologie.

Chapter 1

Introduction

1.1 Climate change: a general overview

As described in the Contribution of the Working Group I to the latest IPCC (Intergovernmental Panel on Climate Change) report ([16]) and in the contributions to the previous reports, *weather* describes the conditions of the atmosphere at a certain place and time with reference to temperature, pressure, humidity, wind, and other key parameters, while *climate* is defined as the average weather, or more rigorously, as the statistical description in terms of mean and variability of relevant quantities over a period of time, ranging from months to thousands or million of years. Classically, the period for averaging these variables is 30 years. *Climate change* referes to a change in the state of the climate that can be identified by changes in the mean and/or the variability of its properties, and that persists for an extended period, typically decades or longer.

The *climate system*, which is a complex, interactive system consisting of the atmosphere, land surface, snow and ice, oceans and other bodies of water, and living things ([60]), evolves in time under the influence of its own internal dynamics and due to changes in external factors that affect climate. External forcing includes natural phenomena such as volcanic eruptions and solar variations, as well as human-induced changes in atmospheric composition.

The Earth's climate system is powered by solar radiation (Figure 1.1). About half of the incoming solar radiation (shortwave radiation - SWR), is absorbed by the Earth's surface. The fraction of SWR reflected back to space by gases, aerosols, clouds and by the Earth's surface (albedo) is approximately 30%, and about 20% is absorbed in the atmosphere ([16]).

The radiation emitted from the Earth (longwave radiation - LWR), also referred to infrared radiation, is largely absorbed by some atmospheric constituents (greenhouse gases - GHG_s) like water vapour, carbon dioxide (CO_2), methane (CH_4), nitrous oxide (N_2O) and clouds, which themselves emit LWR into all directions. The downward directed component of LWR adds heat to the lower layers of the atmosphere and to the Earth's surface (greenhouse effect) ([16]).

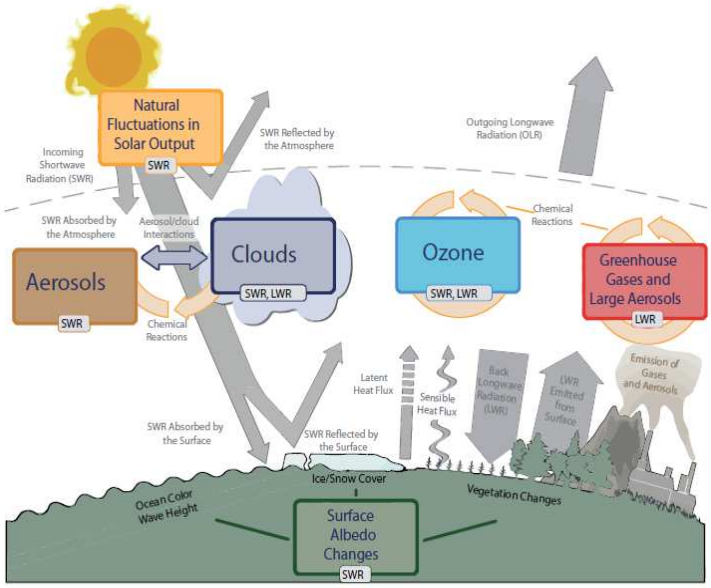

Figure 1.1: Main drivers of climate change ([16]).

The Sun provides its energy to the Earth primarily in the tropics and the subtropics; this energy is then partially redistributed to middle and high latitudes by atmospheric and oceanic transport processes.

Changes in the global energy budget can derive from either changes in the net SWR or changes in the LWR. The former can be due to changes in the Sun's output of energy, changes in the orbital parameters of the Earth or changes in the Earth's albedo. Changes in the outgoing LWR can result from changes in the temperature of the Earth's surface or atmosphere or changes in the emissivity of LWR from either the atmosphere or the Earth's surface. For the atmosphere, these changes in emissivity are due predominantly to changes in cloud cover and cloud properties, in GHG_s and in aerosol concentrations.
Human activities contribute to climate change by causing variations in the amount of GHG_s and aerosols altering incoming and outgoing SWR and LWR. Changing the atmospheric abundance or properties of these gases and particles can lead to a warming or cooling of the climate system.
Since the start of the industrial era (about 1750), the overall effect of human activities on climate has been a warming influence (the change in global surface temperature relative to 1951-1980 average temperature is -0.19°C for 1880 and 0.87°C for 2015 (Figure 1.2) ([39])). There is evidence of that from multiple independent climate indicators, from high up in the atmosphere to the depths of the oceans. They include changes in surface, atmospheric and oceanic temperatures, glaciers, snow cover, sea ice, sea level and atmospheric water vapour. The human impact on climate during this era greatly exceeds that due to known changes in natural processes, such as changes in solar irradiance and vulcanic eruptions ([21]). This is confirmed by simulations which fail to reproduce late 20^{th} century global warming if driven only by natural forcings. However, simulations including both

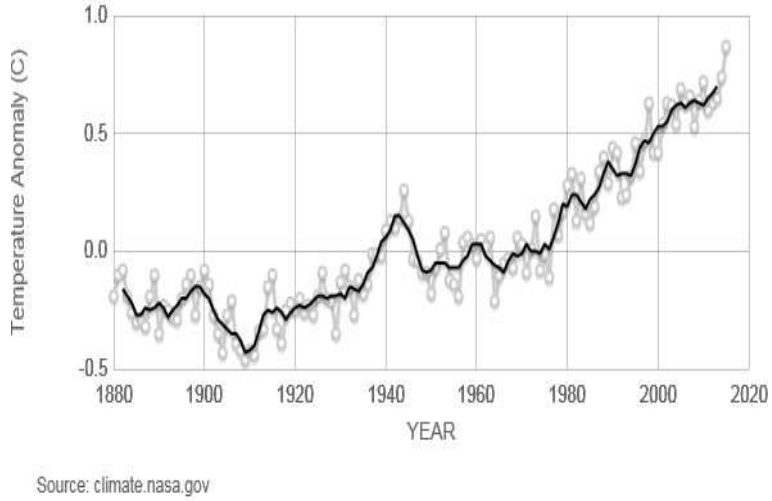

Figure 1.2: Change in global surface temperature relative to 1951-1980 average temperatures. The gray line represents the annual mean while the black line represents the 5 year mean ([39]).

natural and human-caused forcings provide a much better representation of the time rate of change and spatial pattern of observed surface temperature change ([6]).
The principal GHG_s are:

- Water vapour: human activities have only a small direct influence on the amount of atmospheric water vapour (e.g., anthropogenic emissions through irrigation or power plant cooling). Indirectly, human have the potential to affect it by changing climate because the amount of water vapour in the atmosphere is controlled mostly by air temperature, rather than by emissions;

- Carbon dioxide (CO_2): it is emitted by fossil fuel combustion, building heating and cooling, deforestation and so on. The main features in the contemporary CO_2 records are the long-term increase and the seasonal cycle resulting from photosynthesis and respiration by the terrestrial biosphere, mostly in the northern hemisphere ([24]). The global mean concentrations varied from 278±2ppm in 1750 (based on measurements of air extracted from ice cores and from firn [19]) to about 400ppm nowadays ([40]). The longest record of direct measurements of CO_2 in the atmosphere is that of Mauna Loa (Figure 1.3). They were started by C. David Keeling of the Scripps Institution of Oceanography in March of 1958 at a facility of the National Oceanic and Atmospheric Administration ([26]);

- Methane (CH_4): it results from human activities related to agriculture and natural gas distribution ([24]). Direct atmospheric measurements of CH_4 of sufficient spatial coverage to calculate global annual means began at the beginning of the 1980s (Figure 1.4). During this period, methane shows a decreasing growth rate from the early 1980s until 1998, a period of stabilization from 1999 to 2006, and then an increasing atmospheric burden from 2007 to 2011 ([18]; [47]). The global mean concentrations

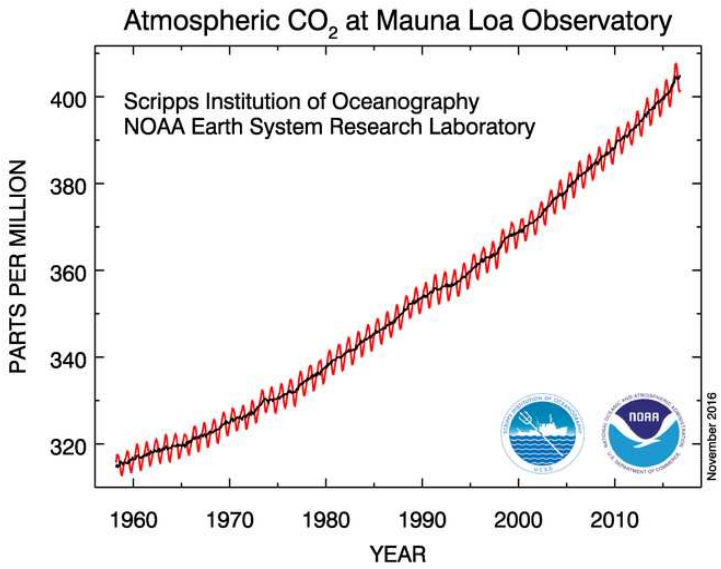

Figure 1.3: The red curve represents CO_2 data measured at Mauna Loa (dry mole fraction defined as the number of molecules of carbon dioxide divided by the number of molecules of dry air multiplied by one million - ppm) and the black curve represents the seasonally corrected data ([40]).

varied from 722±25ppb in 1750 (after correction to the NOAA-2004 CH_4 standard scale) ([17], [20]) to about 1830ppb nowadays ([41]);

- Nitrous oxide (N_2O): it is emitted by human activities such as fertilizer and fossil fuel burning ([24]). The concentrations varied from 270±7ppb in 1750 to about 330ppb nowadays ([42]) (Figure 1.5). The annually concentrations of N_2O show a persistent latitudinal gradient (maximum in the northern subtropic) that contain information about anthropogenic emissions from fertilizer use at the northern tropical to mid-latitudes and natural emissions from soil and ocean upwelling in regions of the tropics;

- Holocarbon gas concentrations (chlorofluorocarbons - CFC): they were used extensively as refrigeration agents and in other industrial processes before their presence in the atmosphere was found to cause stratospheric ozone depletion. The abundance of chlorofluorocarbon gases is now decreasing as a result of international regulations designed to protect the ozone layer (Montreal Protocol) ([24]);

- Ozone: it is a GHG that is continuously produced and destroyed in the atmosphere by photo-chemical reactions. In the troposphere, human activities have increased ozone concentrations through the realase of gases (carbon monoxide, hydrocarbons...) which chemically react to produce ozone. The tropospheric ozone with a radiative forcing of $0.40\pm0.20 Wm^{-2}$ also impacts human health and vegetation. Its average atmospheric lifetime of a few weeks produces a global distribution highly variable by season, altitude and location. These characteristics and the paucity

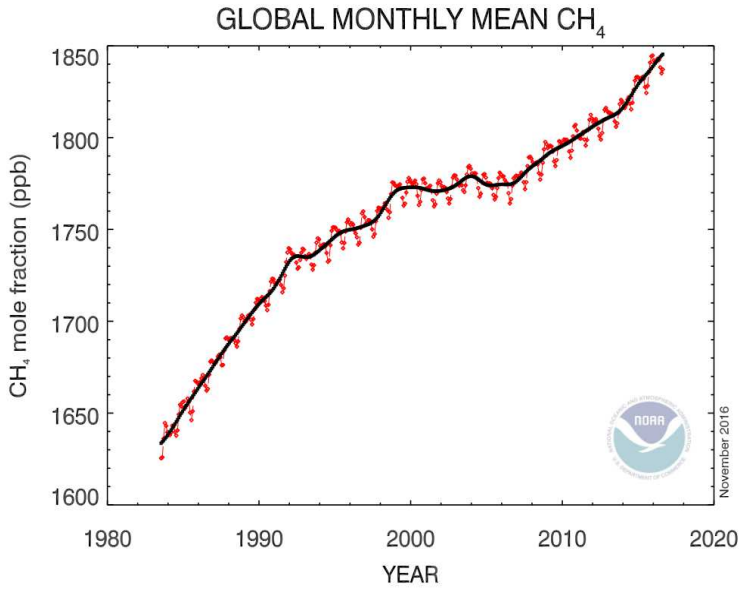

Figure 1.4: Globally-averaged, monthly mean atmospheric CH_4 abundance centered on the middle of each month (red line) and the long-term trend where the average seasonal cycle has been removed (black line) ([41]).

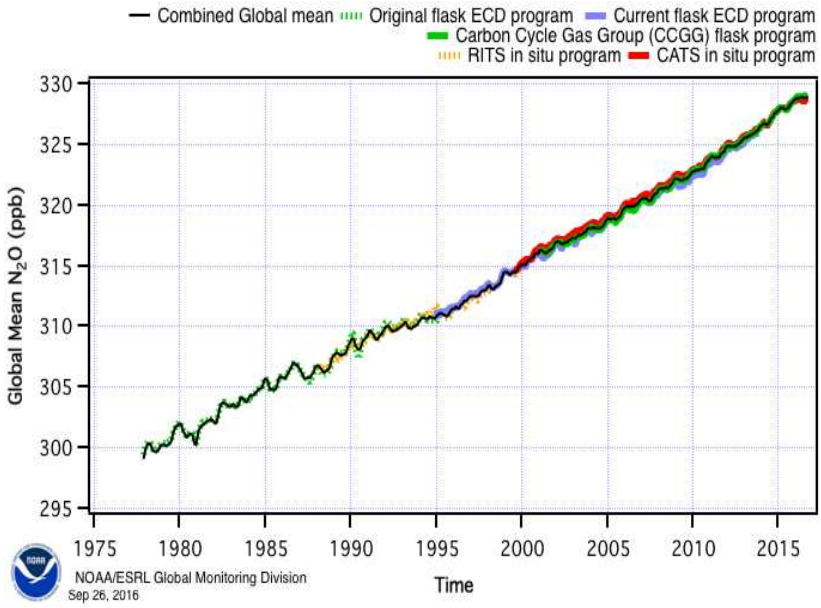

Figure 1.5: Different measurement programs' calculated global means. Measured monthly means from the different programs are statistically combined to create a long-term NOAA/ESRL GMD dataset (black line) ([42]).

of long-term measurements make the assessment of long-term global ozone trends challenging. Owing to methodological changes, free tropospheric ozone observations are most reliable since the mid-1990s. Ozone has decreased above Europe since 1998 ([29]) and is largely unchanged above Japan ([43]). The remaining regions with measurements (North America, North Pacific ocean, South hemisphere) show a range of positive trends.

The forcings for all GHG_s are positive and since the preindustrial era, CO_2 increases have caused the largest forcing (Figure 1.6).
Besides GHG_s, aerosols have a relevant effect in the global energy budget. Aerosols are particles present in the atmosphere with widely varying size, concentration and chemical composition and because of the short lifetime of tropospheric aerosols (the typical lifetime is between one day and two weeks in the troposphere while it reaches one year in the stratosphere), trends have a strong regional signature. They influence radiative forcing directly through reflection and absorption of solar and infrared radiation in the atmosphere. Aerosol scattering generally makes the planet more reflective, and tends to cool the climate, while aerosol absorption has the opposite effect, and tends to warm the climate system. Specifically, when aerosols scatter solar radiation, less solar radiation reaches the surface which leads to a localised cooling. Then, the atmospheric circulation and mixing processes spread the cooling regionally and in vertical. Differently, when aerosols absorb solar radiation the aerosol layer is warmed while the surface is cooled locally because it receives less solar radiation. Then, the atmospheric circulation and mixing processes redistribute the thermal energy and so at large scale there is a net warming of the surface and atmosphere. The balance between cooling and warming depends on aerosol properties and environmental conditions (Figure 1.6). One of the remaining uncertainties comes from black carbon because it is difficult to measure and also induces a complicated cloud response ([7]).
However, the direct radiative forcing summed over all aerosols is negative which has masked some of the global warming from greenhouse gases that would have occurred in their absence. The projected decrease in emissions of anthropogenic aerosols in the future, in response to air quality policies, would eventually unmask this warming.
Some of the aerosols are emitted directly into the atmosphere while others are formed from compounds emitted as gases. Aerosols contain both naturally occurring compounds and those emitted as a result of human activities. Natural aerosols include mineral dust released from the surface, sea salt, biogenic emissions from land and oceans and sulphate and dust produced by vulcanic eruptions. Owing to interannual variability, long-term trends in aerosols from natural sources are more difficult to identify. Fossil fuel and biomass burning have increased aerosols containing sulphur, organic compounds and black carbon. However, anthropogenic aerosols emissions have decreased in some developed countries during about the last three decades while they are increased in many developing countries.
Aerosols also serve as condensation and ice nucleation sites, on which cloud droplets and ice

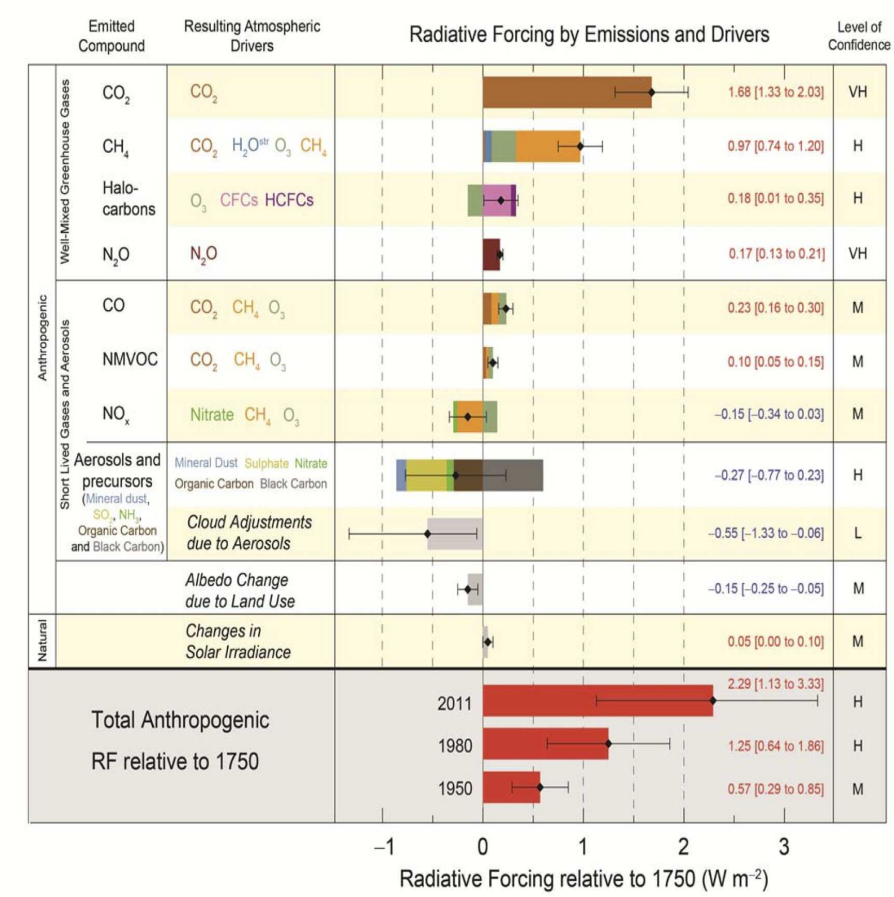

Figure 1.6: Radiative forcing estimates in 2011 relative to 1750 and aggregated uncertainties for the main drivers of climate change ([25]).

particles can form. However, quantifying the overall impact of aerosols on cloud amounts and properties is understandably difficult.

Another key element in the energy balance is the cloud cover. Clouds affect the climate system in a variety of ways. They produce precipitation (rain and snow) that is necessary for most life on land. Clouds strongly affect the flows in both sunlight (cooling the planet as it is radiated to space) and infrared light (warming the planet) through the atmosphere. Because clouds interact so strongly with both sunlight and infrared light, small changes in cloudiness can have a powerful effect on the climate system.

Many possible types of cloud-climate feedbacks have been suggested, involving changes in cloud amount, cloud top height and/or cloud reflectivity. The literature shows that high clouds amplify global warming as they interact with infrared light emitted by the atmosphere and surface. Low clouds reflect a lot of sunlight back to space but, for a given state of the atmosphere and surface, they have only a weak effect on the infrared light that is emitted to space by the Earth. As a result, they have a net cooling effect on the present climate; to a lesser extent, the same holds for mid-level clouds ([7]).

Figure 1.7: Pyranometer (http://www.kippzonen.com/).

1.2 Global radiation

The Earth's climate system is powered by solar radiation ([23]), governing a large number of processes like for example: evaporation, snow and glacier melting, plant photosynthesis and the diurnal and seasonal course of surface temperature ([64], [66]). Knowing the temporal behavior and spatial distribution of global radiation (also known as surface solar radiation $E_{g\downarrow}$), is useful not only for scientific interest but it has also profound environmental, societal and economic implications influencing, for example, the agricultural production and the solar power generation ([56]; [59]; [69]). During the last years, it has also become of interest in the tourism and health care field (e.g. due to its links with ultraviolet radiation and the associated risk of skin cancer).
Specifically, $E_{g\downarrow}$ is the solar radiation received from a solid angle of $2\pi sr$ on a horizontal surface. It includes the radiation received directly from the solid angle of the sun's disc (direct radiation - E), as well as the diffuse sky radiation that has been scattered in traversing the atmosphere (diffuse radiation - $E_{d\downarrow}$) and it is measured with a pyranometer ([71]) (Figure 1.7).

Continuous observations by thermoelectric pyranometers at the Earth's surface date back to 1920s, as for example the Stockholm record that is available since 1923 ([64]) (Figure 1.8). However, $E_{g\downarrow}$ measurements started to become available on a widespread basis only in the late 1950s, with the establishment of numerous radiation sites during the International Geophysical Year (IGY) 1957-1958 ([56]), in order to provide accurate and comparable measurements of the Earth's radiation balance ([58]).
For this reason, it is very useful to estimate $E_{g\downarrow}$ temporal variability from other climatic variables (proxy variables) such as total cloud cover (TCC), visibility, or daily temperature range but probably the most appropriate is sunshine duration (SD).
The advantage of this variable is that it is available since the late nineteenth century ([52]) covering a much longer period than $E_{g\downarrow}$ series ([64]). Moreover, it is less subjective than TCC and visibility observations and it is directly correlated to $E_{g\downarrow}$ through Ångström-Prescott formula ([4]; [44]). According to the World Meteorological Organization (WMO), SD for a given day is defined as the length of time during which E is above $120 W m^{-2}$ ([72]). Most of SD data have been recorded with the Campbell-Stokes sunshine recorder

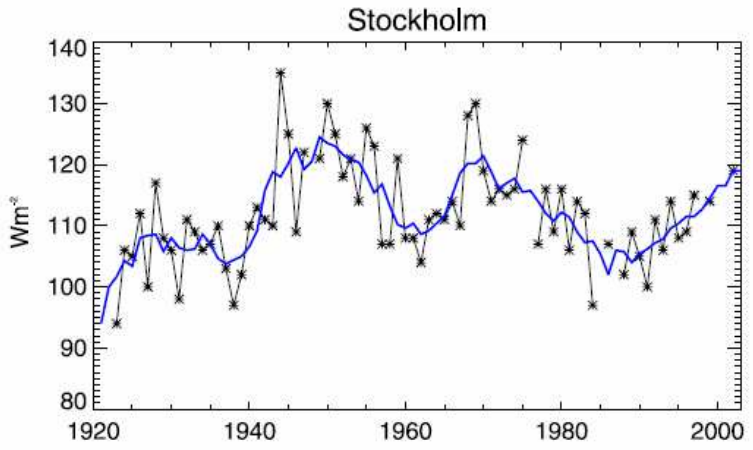

Figure 1.8: Annual mean surface solar radiation as observed at Stockholm, the longest observational record available from GEBA (since 1923). Five year moving average shown in blue. Units are Wm^{-2}([64])

Figure 1.9: Campbell-Stokes sunshine recorder [photo by M^a Victoria Fernández Arboleya].

(Figure 1.9). It consists of a spherical lens that focuses E onto a paper strip, burning a trace if the irradiance exceeds the instrumental threshold ([54]; [57]). The definition of a correct value for this threshold is not an easy issue: $120Wm^{-2}$ was proposed by WMO as resulting mean after some investigations performed at different stations. However, it can vary between 70 and about $280Wm^{-2}$ depending on a number of factors including the atmospheric turbidity and the moisture content of the paper strip ([70]).

In the last decades, the scientific community has become aware of the fact that $E_{g\downarrow}$ is not constant on decadal time scales ([68]). It shows decadal fluctuations which exceed the accuracy limit of observational irradiance measurements (2% on an annual basis and 5% on a daily basis as established by the WMO) ([22]). Specifically, the literature reports a decrease called "Global dimming" from the 1950s to the 1980s of about 3-9Wm^{-2} ([58]; [59]) and a subsequent increase called "Brightening period" since the beginning of 1980s

of about 1-4Wm^{-2} ([65]; [67]). Some studies, that cover a longer period, report also an increase during the 1930s and 1940s, known as "Early brightening" (see Wild ([66]) for a recent review). These variations are highlighted not only by studies focusing on specific regions (e.g., [11]; [28]; [31]; [49]; [50]; [51]; [53]; [62]) but also by studies focusing on worldwide datasets (e.g., [3]; [22]; [59]; [63]; [64]; [66]).
The causes of these decadal variations are not completely clear: it has been suggested that changes in aerosols concentrations and cloud cover can be major causes (e.g., [59]; [64]; [66]), while changes in radiatively active gas concentrations have, at least, globally a minor effect ([27]; [48]). Aerosols and clouds can interact in various ways and are therefore not completely independent ([46]). Aerosols act as a modulator of $E_{g\downarrow}$ by absorption or scattering of solar radiation (direct effect) ([45]; [61]) and by changing the number of cloud condensation nuclei particles (indirect aerosol effect) that also change albedo and cloud lifetime ([2]; [30]). The increase in anthropogenic aerosol emissions in the 20^{th} century is thought to have been the major cause of the observed decadal $E_{g\downarrow}$ reduction until the 1980s, while measures to reduce air pollution in the late 20^{th} century are possibly responsible for the renewed increase in $E_{g\downarrow}$. Nevertheless, the relative contribution of clouds and aerosols is not yet clear, especially when comparing studies regarding different areas.

1.3 A dataset for climate change studies

In order to study climate variability and changes, datasets that contain high-quality climatic instrumental time series covering a long period are essential.
The main steps to set up a dataset that contains reliable series are:

1. Data and metadata rescue;

2. Data quality: homogeneity issue;

3. Gap filling and spatial interpolation;

1.3.1 Data and metadata rescue

One of the main points to set up a dataset useful for climate change studies is to recover as much as possible and as long as possible high quality instrumental time series together with the corresponding metadata.
Metadata are *data about the data* and they should reflect *how*, *where*, *when* and by *whom* information was collected. They have a key role to interpret measurements and observations because a detailed knowledge of the station history helps to anticipate and preview which problems we may find in the data and when they should appear ([1]).

1.3.2 Data quality: homogeneity issue

A homogeneous climate time series is defined as one where variations are caused only by variations in climate. In the last decades, the scientific community has become aware of the fact that, most long-term climatological time series are affected by a number of non-climatic factors that make these data unrepresentative of the actual climate variation. These factors are due to changes in: instruments, observing practices, station locations, station environment and so on. Some of these changes cause sharp discontinuities while other changes, particularly changes in the environment around the station, can cause gradual biases in the data.
So, at present, the statement that time series of meteorological data cannot be used for climate research without a clear knowledge about the state of the data in terms of homogeneity has very large consent ([9]). It is important, therefore to remove the inhomogeneities or at least determine the possible errors they may cause ([1]).
Meteorological series can be tested for homogeneity and homogenized both by direct and indirect methodologies. The first approach is based on objective information that can be extracted from the station history (metadata) or from some other sources, the latter uses statistical methods, generally based on comparison with other series. Direct methods have the advantage of providing detailed information about the time location of the inhomogeneities and the sources that caused them. Unfortunately, metadata are not always available and complete. Moreover, it is generally difficult to convert them into quantitative values useful to correct the discontinuities (breaks). On the other hand, indirect methods are more suitable to calculate correcting factors to eliminate breaks, but the identification of inhomogeneities is not always easy and unambiguous, as (1) inhomogeneities and errors are present in all meteorological series, making it difficult to objectively assign the breaks to one or another of them and (2) correlation among data series depends on various factors (regional patterns, climate elements under analysis, time resolution of data and so on) and when the common variance between the test series and the reference series is too low, the potential discontinuity signal in an homogeneity test disappears into statistical noise.
The choice of the most suitable method depends on the characteristics of the dataset (metadata availability, station density and so on) and on the examined region but probably the best solution is to use an indirect method supported by metadata.

1.3.3 Gap filling and spatial interpolation

Together with the data, metadata rescue and the homogeneity issue, the main problem that is necessary to solve is that most of the series are not complete in the period covered by the corresponding dataset. The gaps in the series make a direct estimation of an average series impossible. Such series would in fact be highly vulnerable to fluctuations in spatial coverage. For this reason, it is necessary to transform the records into anomaly records before averaging them.
The basis assumption is that the spatio-temporal behavior of a variable over a given area

can be described by the superimposition of two fields: the climate normals over a given reference period (i.e. the climatologies) and the departures (difference or ratio) from them (i.e. anomalies). The advantage of the anomaly series is that their variations take place on a much larger spatial scale. Such a greater spatial coherence causes the anomalies to be much less vulnerable to missing data and much more suitable for the calculation of regional average or gridded series. The shortcoming of the anomaly series is that they contain less information than the corresponding absolute value series. The climatologies are instead linked to geographical features of the territory and they can manifest remarkable spatial gradients ([12]).
In order to transform the absolute value records into anomaly ones, it is necessary filling the gaps in the monthly series, at least in the period used as reference to convert the data into anomalies.
The last step before averaging the series in order to obtain a regional series is to generate a gridded version of the anomaly series with the aim to balance the contribution of areas with a higher number of stations with those that have a lower station coverage.

1.4 State of art and Thesis organization

An Italian research group based on a cooperation between the Department of Physics of the University of Milan and ISAC-CNR (Institute of Atmospheric Sciences and Climate - National Research Council) has been set up in the mid-1990s. In order to focus on the study of climate variability and change, it concentrated the scientific efforts on recovering and studying the secular records of precipitation and temperature, which were available for Italy and for the surrounding areas ([8]; [9]; [10]; [12]; [13]; [14]). The activities focused also on sea level pressure and on TCC ([38]), whereas solar radiation has not yet been studied in depth. Indeed, scientific literature contains only very limited information on the spatial distribution of this variable in Italy while no information are available about the temporal behavior ([11]; [55]).
In this context, my PhD project aimed to improve the knowledge of solar radiation in Italy setting up a database of instrumental time series for SD and $E_{g\downarrow}$ and studying their variability and trends in relation to changes in other variables like cloudiness and aerosols. The largest part of the series, used to set up the two datasets, come from the Council for Agricultural Research and Agricultural Economy Analysis (CREA - Consiglio per la ricerca in agricoltura e l'analisi dell'economia agraria) and the Italian Air Force (AM - Aeronautica Militare Italiana). It is interesting to underline that a part of the SD records that come from the CREA archive were digitalized within this project (Figure 1.10) and that nowaday only less than 30% of the available data in this archive have been transferred to computer readable form ([5]). The series were then subjected to a quality check and homogenization procedure to ensure the reliability of the resulting trends and after the gap-filling procedure they were transformed into anomaly series and interpolated onto a regular grid. Finally, they were averaged in order to get regional records useful to study

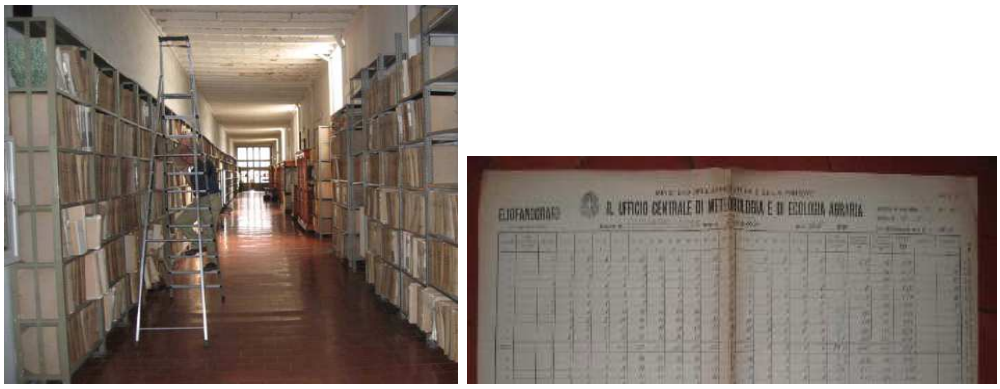

Figure 1.10: (left side) The seat of the Meteorological Archive at CREA; (right side) Sample of data in manuscript version ([5]).

the variability and trends.
The obtained records (both the station and the gridded records) are also useful to validate output from models, satellite data and as input data to study the spatial distribution of solar radiation. Specifically, the thesis is organized as follow:

- Chapter 2: Presentation of the main steps to set up a SD dataset for the period 1936-2013 over the Italian territory. Moreover, the SD temporal evolution is presented and discussed in the light of a comparison with trends found in observations of TCC and with results from two neighboring regions (the Alps and Spain). The study presented in this chapter has been published on *Journal Geophysical Research: Atmospheres* ([33]);

- Chapter 3: Presentation of the main steps to set up a $E_{g\downarrow}$ dataset for the period 1959-2013 over the Italian territory. Moreover, the series under clear-sky conditions were obtained by comparison with corresponding TCC series. The temporal evolution of the regional series both under all-sky and clear-sky conditions is presented and discussed in order to determine to what extent $E_{g\downarrow}$ variability depends on aerosols or clouds variations. The study presented in this chapter has been published on *Atmospheric Chemistry and Physics* ([35]);

- Chapter 4: Presentation of additional details concerning the data availability, the homogenization and gap-filling procedures developed to set up the SD and $E_{g\downarrow}$ dataset. This work underlines how the real climate signal in the original series of meteorological data is generally hidden behind non-climatic noise and how time series of meteorological data should not be used for climate research without facing this issue. Moreover, the need to fill the gaps in the series before using them is shown together with the main steps of the adopted methodology. The study presented in this chapter has been published as Conference proceeding during the 14^{th} *IMEKO TC10 Workshop Technical Diagnostics New Perspectives in Measurements, Tools and Techniques for system's reliability, maintainability and safety* ([34]);

- Chapter 5: Presentation of additional details and examples about the homogenization procedure (Craddock homogeneity test) applied to check the reliability of the SD and $E_{g\downarrow}$ series. The study presented in this chapter has been published as Conference proceeding during the *International Radiation Symposium* ([36]);

- Chapter 6: Presentation of the comparison between the SD and $E_{g\downarrow}$ series for the northern and southern Italy under all-sky and clear-sky conditions over the common period (1959-2013). The agreement/disagreement in the obtained SD and $E_{g\downarrow}$ clear-sky records is discussed in relation to the variations estimated by means of a model based on Lambert-Beer's law and on a simple estimation of diffuse radiation. The study presented in this chapter has been submitted to *Journal of Geophysical Research: Atmospheres* ([37]).

- Chapter 7: Presentation of a methodology to estimate Sicily $E_{g\downarrow}$ 1961-2000 monthly climatologies from already available climatologies (2002-2011) and from a regional SD anomaly series. Moreover, the comparison with corresponding climatologies from 4 RCM-GCMs (Regional Climate Model - Global Climate Models) combinations is presented together with the climatologies for the period 2001-2050 and 2051-2100. This study ([15]) was developed in the framework of an European project (ECLISE - http://www.eclise-project.eu/) that aimed to take the first step towards the realisation of an European Climate Service. In particular, the work was developed on the basis of SIAS (Agrometeorological Service of Sicily Regional Administration) needing that needed this kind of information to develop the 2014-2020 PSR (Rural Development Plan). Moreover, it has been published as Conference proceeding during the *Second annual conference of the Italian Society of Climate Sciences* ([32]);

Bibliography

[1] Aguilar E., Auer I., Brunet M., Peterson T.C., Wieringa J. (2003): *Guidelines on Climate Metadata and Homogenization*, WMO-TD No. 1186, pp. 52, World Meteorological Organization, Geneva, Switzerland;

[2] Albrecht B.A. (1989): *Aerosols, cloud microphysics, and fractional cloudiness*, Science, Vol. 245(4923), pp. 1227-1230, doi:10.1126/science.245.4923.1227;

[3] Alpert P., Kishcha P., Kaufman Y.J., Schwarzbard R. (2005): *Global dimming or local dimming?: Effect of urbanization on sunlight availability*, Geophys. Res. Lett., Vol. 32(17), L17802, doi:10.1029/2005GL023320;

[4] Ångström A. (1924): *Solar and terrestrial radiation*, Q. J. Royal. Meteor. Soc., Vol. 50(210), pp. 121-126;

[5] Beltrano M.C., Esposito S., Iafrate L. (2012): *The archive and library of the former Italian Central Office for Meteorology and Climatology*, Adv. Sci. Res., Vol. 8, pp. 58-65, doi:10.5194/asr-8-59-2012;

[6] Bindoff N.L., Stott P.A., AchutaRao K.M., Allen M.R., Gillett N., Gutzler D., Hansingo K., Hegerl G., Hu Y., Jain S., Mokhov I.I., Overland J., Perlwitz J., Sebbari R., Zhang X. (2013): *Detection and Attribution of Climate Change: from Global to Regional*. In: Climate Change 2013: The Physical Science Basis. Contribution of Working Group I to the Fifth Assessment Report of the Intergovernmental Panel on Climate Change [Stocker, T.F., D. Qin, G.-K. Plattner, M. Tignor, S.K. Allen, J. Boschung, A. Nauels, Y. Xia, V. Bex and P.M. Midgley (eds.)]. Cambridge University Press, Cambridge, United Kingdom and New York, NY, USA;

[7] Boucher O., Randall D., Artaxo P., Bretherton C., Feingold G., Forster P., Kerminen V.M., Kondo Y., H. Liao, Lohmann U., Rasch P., Satheesh S.K., Sherwood S., Stevens B., Zhang X.Y. (2013): *Clouds and Aerosols*. In: Climate Change 2013: The Physical Science Basis. Contribution of Working Group I to the Fifth Assessment Report of the Intergovernmental Panel on Climate Change [Stocker, T.F., D. Qin, G.-K. Plattner, M. Tignor, S.K. Allen, J. Boschung, A. Nauels, Y. Xia, V. Bex and P.M. Midgley (eds.)]. Cambridge University Press, Cambridge, United Kingdom and New York, NY, USA;

[8] Brunetti M., Buffoni L., Mangianti F., Maugeri M., Nanni T. (2004): *Temperature, precipitation and extreme events during the last century in Italy*, Glob. Planet. Change, Vol. 40, pp. 141-149;

[9] Brunetti M., Maugeri M., Monti F., Nanni T. (2006): *Temperature and precipitation variability in Italy in the last two centuries from homogenized instrumental time series*, Int. J. Climatol., Vol. 26(3), pp. 345-381, doi:10.1002/joc.1251;

[10] Brunetti M., Maugeri M., Nanni T., Auer I., Böhm R., Schöner W. (2006): *Precipitation variability and changes in the greater Alpine region over the 1800-2003 period*, J. Geophys. Res., Vol. 111, D11107, doi:10.1029/2005JD006674;

[11] Brunetti M., Lentini G., Maugeri M., Nanni T., Auer I., Böhm R., Schöner W. (2009): *Climate variability and change in the Greater Alpine Region over the last two centuries based on multi-variable analysis*, Int. J. Climatol., Vol. 29(15), pp. 2197-2225, doi:10.1002/joc.1857;

[12] Brunetti M., Lentini G., Maugeri M., Nanni T., Simolo C., Spinoni J. (2009): *Estimating local records for Northern and Central Italy from a sparse secular temperature network and from 1961-1990 climatologies*, Adv. Sci. Res., Vol. 3, pp. 63-71;

[13] Brunetti M., Lentini G., Maugeri M., Nanni T., Simolo C., Spinoni J. (2012): *Projecting North Eastern Italy temperature and precipitation secular records onto*

a high-resolution grid, Physics and Chemistry of the Earth, Vol. 40-41, pp. 9-22, doi:10.1016/j.pce.2009.12.005;

[14] Brunetti M., Maurizio M., Nanni T., Simolo C., Spinoni J. (2013): *High-resolution temperature climatology for Italy: interpolation methods intercomparison*, Int. J. Climatol, doi:10.1002/joc.3764;

[15] Brunetti M., Simolo C., Maugeri M., Manara V., Pasotti L. (2014): *Report on future evolution of sunshine duration and solar radiation over Sicily*, WP6-Energy, Task 6.6 - Past and future solar radiation estimation for Sicily, Deliverable 6.13, ECLISE, *http : //www.eclise − project.eu/content/mm_files/do_*868/*D*6.13 *_ECLISE_WP*6*_Task_*6*_*6*_Deliv_*6*_*13*_ISAC_CNR.pdf*;

[16] Cubasch U., Wuebbles D., Chen D., Facchini M.C., Frame D., Mahowald N., Winther J.G. (2013): *Introduction*. In: Climate Change 2013: The Physical Science Basis. Contribution of Working Group I to the Fifth Assessment Report of the Intergovernmental Panel on Climate Change [Stocker T.F., Qin D., Plattner G.K., Tignor M., Allen S.K., Boschung J., Nauels A., Xia Y., Bex V., Midgley P.M. (eds.)]. Cambridge University Press, Cambridge, United Kingdom and New York, NY, USA;

[17] Dlugokencky E.J., Myers R.C., Lang P.M., Masarie K.A., Crotwell A.M., Thoning K.W., Hall B.D., Elkins J.W., Steele L.P. (2005): *Conversion of NOAA atmospheric dry air CH_4 mole fractions to a gravimetrically prepared standard scale*, J. Gephys. Res, Vol. 110, D18306, doi:10.1029/2005JD006035;

[18] Dlugokencky E.J., Bruhwiler L., White J.W.C., Emmons L.K., Novelli P.C., Montzka S.A., Masarie K.A., Lang P.M., Crotwell A.M., Miller,J.B., Gatti L.V. (2009): *Observational constraints on recent increases in the atmospheric CH_4 burden*, Geophys. Res. Lett., Vol. 36(18), L18803, pp. 1944-8007, doi:10.1029/2009GL039780;

[19] Etheridge D.M., Steele L.P., Langenfelds R.L., Francey R.J., Barnola J.M., Morgan V.I. (1996): *Natural and anthropogenic changes in atmospheric CO_2 over the last 1000 years from air in Antarctic ice and firn*, J. Geophys. Res. Atm., Vol. 101, No. D2, pp. 4115-4128;

[20] Etheridge D.M., Steele L.P., Francey R.J., Langenfelds R.L. (1998): *Atmospheric methane between 1000 A.D. and present: evidence of anthropogenic emissions and climatic variability*, J. Geophys. Res., Vol. 103, No. D13, pp. 15979-15993;

[21] Forster P., Ramaswamy V., Artaxo P., Berntsen T., Betts R., Fahey D.W., Haywood J., Lean J., Lowe D.C., Myhre G., Nganga J., Prinn R., Raga G., Schulz M., Van Dorland R. (2007): *Changes in Atmospheric Constituents and in Radiative Forcing*. In: Climate Change 2007: The Physical Science Basis. Contribution of Working Group I to the Fourth Assessment Report of the Intergovernmental Panel on Climate Change [Solomon, S., D. Qin, M. Manning, Z. Chen, M. Marquis, K.B. Averyt,

M.Tignor and H.L. Miller (eds.)]. Cambridge University Press, Cambridge, United Kingdom and New York, NY, USA;

[22] Gilgen H., Wild M., Ohmura A. (1998): *Means and trends of shortwave irradiance at the surface estimated from global energy balance archive data*, J. Clim., Vol. 11, pp. 2042-2061, doi:10.1175/1520-0442-11.8.2042;

[23] Hartmann D.L., Ramanathan V., Berroir A., Hunt G.E. (1986): *Earth radiation budget data and climate research*, Rev. Geophys., Vol. 24(2), pp. 439-468, doi:10.1029/RG024i002p00439;

[24] Hartmann D.L., Klein Tank A.M.G., Rusticucci M., Alexander L.V., Brnnimann S., Charabi Y., Dentener F.J., Dlugokencky E.J, Easterling D.R., Kaplan A., Soden B.J., Thorne P.W., Wild M., Zhai P.M. (2013): *Observations: Atmosphere and Surface.* In: Climate Change 2013: The Physical Science Basis. Contribution of Working Group I to the Fifth Assessment Report of the Intergovernmental Panel on Climate Change [Stocker, T.F., D. Qin, G.-K. Plattner, M. Tignor, S.K. Allen, J. Boschung, A. Nauels, Y. Xia, V. Bex and P.M. Midgley (eds.)]. Cambridge University Press, Cambridge, United Kingdom and New York, NY, USA;

[25] IPCC (2013): *Summary for Policymakers.* In: Climate Change 2013: The Physical Science Basis. Contribution of Working Group I to the Fifth Assessment Report of the Intergovernmental Panel on Climate Change [Stocker, T.F., D. Qin, G.-K. Plattner, M. Tignor, S.K. Allen, J. Boschung, A. Nauels, Y. Xia, V. Bex and P.M. Midgley (eds.)]. Cambridge University Press, Cambridge, United Kingdom and New York, NY, USA;

[26] Keeling C.D., Bacastow R.B., Bainbridge A.E., Ekdahl C.A., Guenther P.R., Waterman L.S. (1976): *Atmospheric carbon dioxide variations at Mauna Loa Observatory*, Hawaii, Tellus, Vol. 28, pp. 538-551;

[27] Kvalevåg M.M. and Myhre G. (2007): *Human impact on direct and diffuse solar radiation during the industrial era*, J. Clim., Vol. 20, pp. 4874-4883, doi:10.1175/JCLI4277.1;

[28] Liang F. and Xia X.A. (2005): *Long-term trends in solar radiation and the associated climatic factors over China for 1961-2000*, Ann. Geophys., Vol. 23(7), pp. 2425-2432, doi:10.5194/angeo-23-2425-2005;

[29] Logan J.A., Staehelin J., Megretskaia I.A., Cammas J.P., Thouret V., Claude H., De Backer H., Steinbacher M., Scheel H.E., Stübi R., Fröhlich M., Derwent R. (2012): *Changes in ozone over Europe: analysis of ozone measurements from sondes, regular aircraft (MOZAIC) and alpine surface sites*, J. Geophys. Res., Vol. 117, D09301, doi:10.1029/2011JD016852;

[30] Lohmann U. and Feichter J. (2005): *Global indirect aerosol effects: a review*, Atmos. Chem. Phys., Vol. 5, pp. 715-737, doi:1680-7324/acp/2005-5-715;

[31] Long C.N., Dutton E.G., Augustine J.A., Wiscombe W., Wild M., McFarlane S.A., Flynn C.J. (2009): *Significant decadal brightening of downwelling shortwave in the continental United States*, J. Geophys. Res., Vol. 114, D00D06, doi:10.1029/2008JD011263;

[32] Manara V., Brunetti M., Maugeri M., Pasotti L., Simolo C. (2014): *Past and future solar radiation variability and change over Sicily*, Conference proceeding: Climate change: scenarios, impacts and policy SISC Second Annual Conference, Venice, Italy, September 2014, ISBN: 978-88-97666-04-2, pp. 397-415, *http* : $//www.sisclima.it/wp - content/uploads/2014/10/SISC\_Conference\_Proceedings - 2014.pdf$;

[33] Manara V., Beltrano M.C., Brunetti M., Maugeri M., Sanchez-Lorenzo A., Simolo C., Sorrenti S. (2015): *Sunshine duration variability and trends in Italy from homogenized instrumental time series (1936-2013)*, J. Geophys. Res. Atmos., Vol. 1, No. 120, pp. 3622-3641, doi:10.1002/2014JD022560;

[34] Manara V., Brunetti M., Maugeri M.(2016): *Reconstructing sunshine duration and solar radiation long-term evolution for Italy: a challenge for quality control and homogenization procedures*, Conference proceeding of the 14^{th} IMEKO T10 Workshop Technical Diagnostics - New Perspectives in Measurements, Tools and Techniques for system's reliability, maintainability and safety, 27-28 June 2016, Milan, Italy, pp: 13-18, ISBN: 978-92-990073-9-6, *http* : $//www.imeko.org/publications/tc10 - 2016/IMEKO - TC10 - 2016 - 002.pdf$;

[35] Manara V., Brunetti M., Celozzi A., Maugeri M., Sanchez-Lorenzo A., Wild M. (2016): *Detection of dimming/brightening in Italy from homogenized all-sky and clear-sky surface solar radiation records and underlying causes (1959-2013)*, Atmos. Chem. Phys., Vol. 16, pp. 11145-11161, doi:10.5194/acp-16-11145-2016;

[36] Manara V., Brunetti M., Maugeri M., Sanchez-Lorenzo A., Wild M. (2017): *Homogenization of a surface solar radiation dataset over Italy*, Radiation Processes in the Atmosphere and Ocean (IRS2016), AIP Conference Proceedings, Vol. 1810, 090004-1-090004-4, doi: 10.1063/1.4975544, Published by AIP Publishing, ISBN: 978-0-7354-1478-5;

[37] Manara V., Brunetti M., Maugeri M., Sanchez-Lorenzo A., Wild M.: *Sunshine duration and global radiation trends in Italy (1959-2013): to what extent do they agree?*, submitted to J. Geophys. Res. Atmos.;

[38] Maugeri M., Bagnati Z., Brunetti M., Nanni T. (2001): *Trends in italian total cloud amount, 1951-1996*, Geophys. Res. Lett., Vol. 28(24), pp. 4551-4554, doi: 10.1029/2001GL013754;

[39] $http://climate.nasa.gov/vital-signs/global-temperature/$

[40] Ed Dlugokencky and Pieter Tans, NOAA/ESRL ($www.esrl.noaa.gov/gmd/ccgg/trends/$);

[41] Ed Dlugokencky, NOAA/ESRL ($www.esrl.noaa.gov/gmd/ccgg/trends\_ch4/$);

[42] $http://www.esrl.noaa.gov/gmd/hats/combined/N2O.html$;

[43] Oltmans S.J, Lefohn A.S., Shadwick D., Harris J.M., Scheel H.E., Galbally I., Tarasick D.W., Johnson B.J., Brunke E.G., Claude H., Zeng G., Nichol S., Schmidlin F., Davies J., Cuevas E., Redondas A., Naoe H., Nakano T., Kawasato T (2013): *Recent tropospheric ozone changes - A pattern dominated by slow or no growth*, Atm. Env., Vol. 67, pp. 331-351;

[44] Prescott J.A. (1940): *Evaporation from a water surface in relation to solar radiation*, Trans. R. Soc. S. Austr., Vol. 64, pp. 114-118;

[45] Radke L.F., Coakley J.A., King M.D. (1989): *Direct and remote sensing observations of the effects of ships on clouds*, Science, Vol. 246(4934), pp. 1146-1149, doi:10.1126/science.246.4934.1146;

[46] Ramanathan V., Crutzen P.J., Kiehl J.T., Rosenfeld D. (2001): *Aerosol, climate, and the hydrological cycle*, Science, Vol. 294(5549), pp. 2119-2124, doi:10.1126/science.1064034;

[47] Rigby M., Prinn R.G., Fraser P.J., Simmonds P.G., Langenfelds R.L., Huang J., Cunnold D.M., Steele L.P., Krummel P.B., Weiss R.F., O'Doherty S., Salameh P.K., Wang H.J., Harth C.M., Mühle J., Porter L.W. (2008): *Renewed growth of atmospheric methane*, Geophys. Res. Lett, Vol. 35(22), L22805, pp. 1944-8007, doi:10.1029/2008GL036037;

[48] Romanou A., Liepert B., Schmidt G.A., Rossow W.B., Ruedy R.A., Zhang Y. (2007): *20th Century Changes in Surface Solar Irradiance in Simulations and Observations*, Geophys. Res. Lett., Vol. 34(5), doi:10.1029/2006GL028356;

[49] Sanchez-Lorenzo A. and Wild M. (2012): *Decadal variations in estimated surface solar radiation over Switzerland since the late 19th century*, Atmos. Chem. Phys., Vol. 12(18), pp. 8635-8644, doi:10.5194/acp-12-8635-2012;

[50] Sanchez-Lorenzo A., Brunetti M., Calbo J., Martin-Vide J. (2007): *Recent spatial and temporal variability and trends of sunshine duration over the Iberian Peninsula from a homogenized data set*, J. Geophys. Res., Vol. 112, D20115, doi:10.1029/2007JD008677;

[51] Sanchez-Lorenzo A., Calbó J., Wild M. (2013): *Global and diffuse solar radiation in Spain: Building a homogeneous dataset and assessing their trends*, Glob. Planet. Change, Vol. 100, pp. 343-352, doi:10.1016/j.gloplacha.2012.11.010;

[52] Sanchez-Lorenzo A., Calbó J., Wild M., Azorin-Molina C., Sanchez-Romero A. (2013): *New insights into the history of the Campbell-Stokes sunshine recorder*, Weather, Vol. 68(12), pp. 327-331, doi:10.1002/wea.2130;

[53] Sanchez-Lorenzo A., Wild M., Brunetti M., Guijarro J.A., Hakuba M.Z., Calbó J., Mystakidis S., Bartok B. (2015): *Reassessment and update of long-term trends in downward surface shortwave radiation over Europe (1939-2012)*, J. Geophys. Res. Atm., Vol. 120(18), pp. 9555-9569, doi:10.1002/2015JD023321;

[54] Sanchez-Romero A., Gonzalez J.A., Calbó J., Sanchez-Lorenzo A. (2015): *Using digital image processing to characterize the Campbell-Stokes sunshine recorder and to derive high-temporal resolution direct solar irradiance*, Atm. Meas. Tech., Vol. 8, pp. 183-194, doi:10.5194/amt-8-183-2015;

[55] Spinoni J., Brunetti M., Maugeri M., Simolo C. (2012): *1961-1990 monthly high-resolution solar radiation climatologies for Italy*, Adv. Sci. Res., Vol. 8, pp. 19-25, doi:10.5194/asr-8-19-2012;

[56] Stanhill G. (1983): *The distribution of global solar radiation over the land surfaces of the Earth*, Solar Energy, Vol. 31(1), pp. 95-104;

[57] Stanhill G. (2003): *Through a glass brightly: Some new light on the Campbell-Stokes sunshine recorder*, Weather, Vol. 58(1), pp. 3-11;

[58] Stanhill G. (2005): *Global dimming: A new aspect of climate change*, Weather, Vol. 60(1), pp. 11-14, doi:10.1256/wea.210.03;

[59] Stanhill G. and Cohen S.: Global dimming (2001): *A review of the evidence for a widespread and significant reduction in global radiation with discussion of its probable causes and possible agricultural consequences*, Agr. Forest. Meteorol., Vol. 107(4), pp. 255-278, doi:10.1016/S0168-1923(00)00241-0;

[60] Le Treut H., Somerville R., Cubasch U., Ding Y., Mauritzen C., Mokssit A., Peterson T., Prather M. (2007): *Historical Overview of Climate Change*. In: Climate Change 2007: The Physical Science Basis. Contribution of Working Group I to the Fourth Assessment Report of the Intergovernmental Panel on Climate Change [Solomon, S., D. Qin, M. Manning, Z. Chen, M. Marquis, K.B. Averyt, M. Tignor and H.L. Miller (eds.)]. Cambridge University Press, Cambridge, United Kingdom and New York, NY, USA.

[61] Twomey S.A., Piepgrass M., Wolfe T.L. (1984): *An assessment of the impact of pollution on global cloud albedo*, Tellus Ser. B, Vol. 36, pp. 356-366, doi:10.1111/j.1600-0889.1984.tb00254.x;

[62] Wang Y.W. and Yang Y.H. (2014): *China's dimming and brightening: evidence, causes and hydrological implications*, Ann. Geophys., Vol. 32, pp. 41-55, doi:10.5194/angeo-32-41-2014;

[63] Wang K.C., Dickinson R.E., Wild M., Liang S. (2012): *Atmospheric impacts on climatic variability of surface incident solar radiation*, Atmos. Chem. Phys., Vol. 12(20), pp. 9581-9592, doi:10.5194/acp-12-9581-2012;

[64] Wild M. (2009): *Global dimming and brightening: A review*, J. Geophys. Res., Vol. 114, D00D16, doi:10.1029/2008JD011470;

[65] Wild M. (2012): *Enlightening Global Dimming and Brightening*, Bull. Am. Meteorol. Soc., Vol. 93, pp. 27-37, doi:10.1175/BAMS-D-11-00074.1;

[66] Wild M. (2016): *Decadal changes in radiative fluxes at land and ocean surfaces and their relevance for global warming*, Wiley Interdisciplinary Reviews: Climate Change, Vol. 7(1), pp. 91-107, doi:10.1002/wcc.372;

[67] Wild M., Gilgen H., Roesch A., Ohmura A., Long C.N., Dutton E.G., Forgan B., Kallis A., Russak V., Tsvetkov A. (2005): *From Dimming to Brightening: Decadal Changes in Solar Radiation at Earth's Surface*, Science, Vol. 308(5723), pp. 847-850, doi:10.1126/science.1103215;

[68] Wild M., Trssel B., Ohmura A., Long C.N., Knig-Langlo G., Dutton E.G., Tsvetkov A. (2009): *Global dimming and brightening: An update beyond 2000*, J. Geophys. Res. Atm., Vol. 114, D00D13, doi:10.1029/2008JD011382;

[69] Wild M., Folini D., Henschel F., Fischer N., Möller B. (2015): *Projections of long-term changes in solar radiation based on CMIP5 climate models and their influence on energy yields of photovoltaic systems*, Solar Energy, Vol. 116, pp. 12-24, doi:10.1016/j.solener.2015.03.039;

[70] WMO-No.8 (1969): *Chapter 9, Solar radiation and Sunshine duration*, World Meteorological Organization, Guide to meteorological instruments and observing practices, Third edition;

[71] WMO-No.8 (2008): *Chapter 7, Measurement of Solar Radiation*, World Meteorological Organization, Guide to Meteorological Instruments and Methods of Observation, Geneva, Switzerland, ISBN:978-92-63-10008-5;

[72] WMO-No.8 (2008): *Chapter 8, Measurement of Sunshine Duration*, World Meteorological Organization, Guide to Meteorological Instruments and Methods of Observation, Geneva, Switzerland, ISBN:978-92-63-10008-5;

Chapter 2

Sunshine duration variability and trends in Italy from homogenized instrumental time series (1936-2013)

Abstract

A dataset of quality checked daily sunshine duration measurements was collected from 104 Italian sites over the 1936-2013 period. Monthly mean values were homogenized, projected onto a grid and subjected to a Principle Component Analysis, which identified two significantly different regions: North and South. Sunshine duration temporal evolution is presented and possible reasons for differences between the two regions are discussed in the light of a comparison with the trends found in observations of total cloud cover and with results from two neighboring regions: the Alps and Spain. In addition, trends for irradiance records, estimated from sunshine duration records using the Ångström-Prescott formula, are presented too. The major feature of the trends, an increase in sunshine duration from the mid of the 1980s, was common to both northern and southern Italy; the decrease in the preceding 30 year period was not, as northern Italy had a lower rate of decrease than southern Italy. The few records available during the earliest period of the dataset indicate that sunshine duration in Italy increased from the mid-1930s to the mid-1950s. The further steps needed to identify and quantify the mechanisms giving rise to the observed trends and to the reported regional differences in dimming and brightening are outlined.

2.1 Introduction

Downward solar irradiance at the Earth's surface (global radiation) is the primary energy source for the Earth's climate system. It has a central role in the surface energy balance (e.g., [17]; [35]; [86]), driving a large number of processes like diurnal surface and atmospheric boundary layer heating, water evaporation, snow and glacier melting, plant photosynthesis and related terrestrial carbon uptake (e.g., [80]; [83]). Along with the scientific interest, there is also a strong socio-economic benefit in the knowledge of the spatial distribution of global radiation and its temporal trends: it is useful in a wide spectrum of fields such as solar energy production, agriculture, health care and tourism.

Temporal variations in global radiation depend on many factors, which can be external and internal to the climate system: the most important are cloud cover and atmospheric aerosols ([43]; [65]). Variations in aerosol concentration can depend on natural causes (e.g., volcanic eruptions), but in many areas there is also a significant contribution related to human activities. Changes in aerosol concentration can also cause variations in cloud cover as the condensation of atmospheric water vapor is influenced by aerosol particles ([24]; [45]).

Temporal variability of global radiation in the last decades is discussed in a large number of papers (see Wild ([80]) for a review), with Goldberg and Klein ([16]) and Suraqui et al. ([72]) as two of the pioneering studies. The results suggest a widespread reduction between the 1960s and the beginning of the 1980s (e.g. [36]; [48]; [69]) and a tendency toward an opposite trend after the 1980s (e.g., [84]). The first phenomenon is known as "Global dimming" ([66]), the second as "Brightening period" ([79]). The causes of this temporal variability are very complex and they are not completely understood yet. The most relevant drivers of these decadal changes seem to be anthropogenic pollutant emissions ([81]). Thus, the recent brightening is associated to air pollution regulatory actions in developed countries and to declining industrialization in some European countries in the late 1980s ([59]; [64]; [71]).

One of the main problems in studying global radiation temporal variability is the small number of sites with reliable long-term records. Extensive networks of pyranometers cover in fact a rather short period ([53]; [80]). It is therefore very useful to estimate global radiation temporal variability from other climatic variables (proxy measures) such as total cloud cover (TCC), or daily temperature range (DTR), but probably the most appropriate is sunshine duration (SD) ([64]; [76]).

According to the World Meteorological Organization (WMO), the SD for a given period is defined as the length of time during which direct solar radiation is above $120 Wm^{-2}$ ([89]). It has been generally measured with the Campbell-Stokes SD recorder composed of a spherical lens that focuses direct solar radiation onto a paper strip, burning a trace if the irradiance exceeds the instrumental threshold ([55]). This threshold ranges from 70 to $280 Wm^{-2}$, depending on a number of factors, the most relevant being the moisture content of the paper strip ([56]; [88]), although in 1981 the WMO recommended a threshold

mean value of $120 W m^{-2}$ ([89]).
A very important advantage of SD records is that they are available since the late of the 19^{th} century ([55]), covering a much longer period than global radiation records ([80]). Moreover, they are less subjective than TCC observations. Equally, SD is directly correlated to global radiation through Ångström-Prescott formula ([3]; [40]; for a review see Martinez-Lozano et al. [27]).
Many studies have investigated the temporal behavior of SD for many areas ([76]) including, e.g. the Alpine region ([5]; [12]), Western Europe ([51]), Eastern Europe ([8]), Switzerland ([36]; [49]), Poland ([29]), Greece ([21]), China ([20]; [22]; [74];[78]; [90]), USA ([2]; [26]; [67]), South America ([42]), Iran ([41]), India ([62]), Australia ([19]) and Japan ([68]).
As far as Italy is concerned, papers on the temporal evolution of global radiation or SD in the last decades are not available. The best available information concerns TCC and DTR. Maugeri et al. ([30]) studied the temporal evolution of TCC over Italy for the 1951-1996 period by means of 35 synoptic stations. They found a highly significant annual and seasonal negative trend, mainly due to a strong decrease after the 1970s. The stations of the northern part of Italy were then extended and updated to 2005 within the EU FP5 ALP-IMP Project (Multi-centennial climate variability in the Alps based on Instrumental data, Model simulations and Proxy data) and were included in the HISTALP database (Historical Instrumental climatological Surface Time series of the greater Alpine regions)([5]): they confirmed the strong decrease since the 1970s ([12]).
Brunetti et al. ([10]) studied the temporal evolution of DTR for the 1865-2003 period by means of 48 Italian secular stations with daily minimum and maximum temperatures. Their results are in good agreement with the global dimming and brightening signals in all seasons with the only exception of autumn, during which DTR does not increase in the brightening period. It is also worth noting that the Italian DTR records show an increasing trend in the first decades of the 20^{th} century, which is known as "Early brightening period" (e.g., [34]; [80]).
In this context, we recently set up a research program aiming at collecting, checking for quality, homogenizing and analyzing Italian SD records as much as possible. The main steps of this research program and the results of the analyses we performed are presented in this paper. After the introduction, Section 2.2 describes the data sources and Section 2.3 discusses quality control, homogenization, gap filling, gridding and clustering into homogenous regions. In Section 2.4 the average regional records are subjected to trend analysis and compared with records of other areas and with Italian TCC records. Finally, in Section 2.5 some conclusive remarks are outlined.

2.2 Data

The SD records used in this paper were obtained from three main data sources: (a) the paper archive of the former Italian Central Office for Meteorology (24 records), which is managed by CRA-CMA, a research unit of the National Agricultural Research Council (Consiglio per la Ricerca e la Sperimentazione in Agricoltura), (b) the database of Italian Air Force synoptic stations (AM - Aeronautica Militare) (47 records), and (c) the National Agrometeorological database (BDAN - Banca Dati Agrometeorologica Nazionale) (59 records), which is also managed by CRA-CMA. In addition, we considered four records (Pontremoli, Varese, Modena and Trieste) from universities and local observatories.
Specifically, CRA-CMA hosts the archive of the former Italian Central Office for Meteorology. The digitalization of this archive is in progress even though up to now less than 30% of the available data have been transferred to computer readable form ([6]; [7]) and included in the BDAN. We digitalized daily SD data from 24 observatories.
The Italian Air Force records were already available in digital form. A brief summary on the history of these observations is recorded in a report of the Italian Air Force ([18]), which shows also some statistics on data availability, highlighting a much better situation for SD with respect to solar radiation.
BDAN includes records from automatic stations and from the CRA-CMA traditional network (only 25 stations of this network are still in operation). The automatic stations are from AM network, from Italian agency for civil aviation (ENAV - Ente Nazionale Assistenza al Volo) network, and from the National Agrometeorological network (RAN - Rete Agrometeorologica Nazionale).
Pontremoli and Varese records were collected, respectively, at "Osservatorio Meteorologico Marsili" and at "Centro Geofisico Prealpino". The former observatory is managed by the Italian Society for Meteorology ([44]), the latter is managed by a local meteorological association. Modena and Trieste records were collected, respectively, since 1893 at "Osservatorio Geofisico" of Modena University ([25]) and since 1886 at different sites all located within 1.6km in the city of Trieste ([70]). We consider here only the data since 1936 as the focus of this paper is on the entire Italian territory and before 1936 there are only these two series.
For some sites we set up composite records, merging data of the same station from different sources. Moreover, for some records we merged data from different sites. They concern stations at short distances and belonging to areas with homogeneous geographical features. Additional information on the SD records is shown in Table 2.1, 2.2 that lists the records by data sources, providing station names, coordinates and elevations. The table also provides information on the SD recorders, on the years supplying data and on composite and merged records.
The final dataset encompasses 104 SD daily records covering the entire Italian territory for the 1936-2013 period. The spatial distribution of the stations (Figure 2.1) is uniform, with the only exception of the Alps and Apennines. So, most of the stations are located in

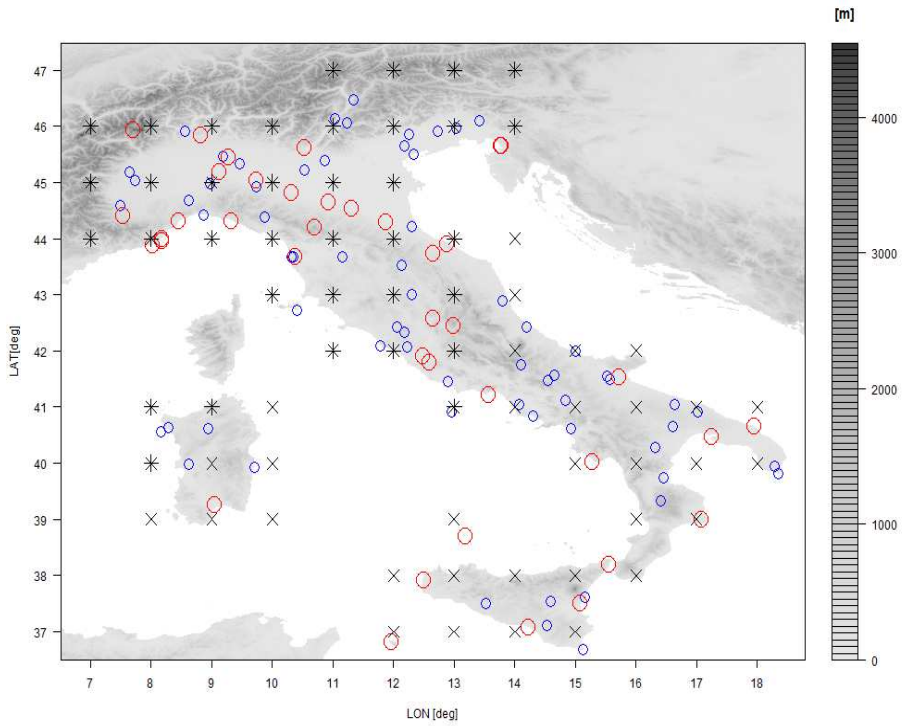

Figure 2.1: Spatial distribution of the stations and points of the grid-mode version of the dataset (see Section 2.3.5): stars and crosses represent, respectively, northern and southern Italy grid-points. The figure also shows the orography of the region and gives evidence of the length of the station records, with big red circles indicating stations with more than 30 years of data.

the Italian plains or coastal areas. Data availability versus time is rather inhomogeneous (Figure 2.2). The best data coverage concerns 1958-1964, 1971-1977 and 1982-2013, while the period with the most critical situation corresponds to the first 22 years (1936-1957).

2.3 Data pre-processing

2.3.1 Quality check and calculation of monthly values

All daily records were checked in order to find out and correct gross errors ([1]). Moreover, station coordinates were checked matching the consistency of the coordinates with the information from station metadata and controlling elevation in relation to position. All records were expressed in hours and tenths of hour. Monthly records were calculated when the fraction of missing data did not exceed 10%. They were then converted into relative SD records that express the ratio between measured and maximum possible SD.

2.3.2 Data homogenization

Climatic records are often affected by non-climatic signals which have to be identified and eliminated ([1]). They can be caused by changes in the condition or in the management of the corresponding meteorological station and by changes in the area surrounding

Network/Data Source	Region	Station number	Station	Latitude (°)	Longitude (°)	Elevation (m)	Period	Composite record	Instrument
AM	N	1	Alghero	40.633	8.283	23	1958-1989	No	Campbell-Stokes sunshine duration recorder
		2	Bologna Borgo Panigale	44.530	11.300	36	1958-1991	No	
		3	Bolzano	46.467	11.333	241	1958-1990	No	
		4	Capo Caccia	40.560	8.164	202	1990-2004	No	
		5	Cervia	44.217	12.300	10	1989-2013	Yes	
		6	Elba	42.733	10.400	397	1984-2004	No	
		7	Genova Sestri	44.413	8.868	2	1962-1989	No	
		8	Milano Linate	45.450	9.270	107	1958-2000	No	
		9	Monte Cimone	44.194	10.700	2165	1958-2004	No	
		10	Monte Terminillo	42.451	12.983	1874	1958-2004	No	
		11	Paganella	46.143	11.037	2125	1990-2004	No	
		12	Pisa San Giusto	43.680	10.380	7	1958-2004	Yes	
		13	Plateau Rosa	45.933	7.700	3488	1958-1999	No	
		14	Ponza	40.917	12.950	185	1991-2004	No	
		15	Torino Bric della Croce	45.030	7.730	710	1982-2004	No	
		16	Torino Caselle	45.187	7.646	301	1958-1993	No	
		17	Udine Rivolto	45.967	13.033	53	1982-2004	No	
		18	Venezia Tessera	45.500	12.330	2	1961-1989	No	
		19	Vigna di Valle	42.080	12.220	262	1982-2013	Yes	
		20	Viterbo	42.433	12.050	308	1992-2004	No	
		21	Campobasso	41.570	14.650	793	1973-2004	No	
	S	22	Crotone	38.996	17.080	155	1958-1997	No	
		23	Monte Scuro	39.333	16.400	1710	1993-2004	No	
		24	Napoli Capodichino	40.850	14.300	88	1958-1997	No	
		25	Pantelleria	36.817	11.967	191	1958-2004	No	
		26	Pescara	42.430	14.200	10	1958-1990	No	
		27	Ustica	38.700	13.183	250	1958-2004	No	
AM - updated by BDAN (ENAV and AM networks)	N	28	Capo Mele	43.954	8.169	220	1963-2013	No	Campbell-Stokes sunshine duration recorder - SIAP-Micros transducer
		29	Piacenza	44.917	9.733	138	1991-2008	No	
		30	Roma Ciampino	41.800	12.583	129	1958-2009	No	
		31	Treviso Sant'Angelo	45.650	12.183	18	1988-2008	No	
		32	Trieste	45.650	13.783	8	1958-2013	No	
		33	Verona Villafranca	45.383	10.867	68	1991-2009	No	
	S	34	Brindisi	40.650	17.950	15	1958-2013	No	
		35	Capo Bellavista	39.934	9.710	138	1992-2013	No	
		36	Capo Palinuro	40.024	15.275	184	1958-2013	No	
		37	Cozzo Spadaro	36.686	15.132	46	1992-2013	No	
		38	Foggia Amendola	41.533	15.717	60	1959-2009	No	
		39	Gela	37.076	14.225	11	1971-2013	No	
		40	Grazzanise	41.050	14.067	9	1992-2013	Yes	
		41	Messina	38.201	15.553	59	1960-2013	No	
		42	Santa Maria di Leuca	39.817	18.350	104	1993-2013	No	
		43	Termoli	42.004	14.996	44	1991-2013	No	
		44	Trapani Birgi	37.917	12.500	7	1961-2009	No	
		45	Cagliari Elmas	39.250	9.050	4	1958-2006	No	

Table 2.1: Details on the records 1-45 in the SD dataset

Table 2.2: Details on the records 46-104 in the SD dataset

Network/Data Source	Region	Station number	Station	Latitude (°)	Longitude (°)	Elevation (m)	Period	Composite record	Instrument
RAN/BDAN	N	46	Borgo San Michele	41.450	12.900	12	1995-2013	No	SIAP-Micros transducer, threshold: $120 Wm^{-2}$, range: $0 \div 1500 Wm^{-2}$, spectrum: $0.2 \div 1.1 \mu$m, accuracy: $2.4 Wm^{-2}$, 300° continuous scan
		47	Caprarola	42.327	12.177	650	1994-2013	No	
		48	Carpeneto	44.683	8.624	230	1994-2013	No	
		49	Cividale	46.091	13.419	130	1997-2013	No	
		50	Chilivani	40.617	8.936	216	1994-2013	No	
		51	Fiume Veneto	45.921	12.724	19	1996-2013	No	
		52	Marsciano	43.005	12.303	229	1991-2013	Yes	
		53	Montanaso Lombardo	45.332	9.457	83	1994-2013	No	
		54	Piubega	45.226	10.533	40	1994-2013	Yes	
		55	San Casciano	43.671	11.152	230	1994-2013	No	
		56	San Piero a Grado	43.669	10.348	3	1994-2013	No	
		57	Santa Fista	43.523	12.129	311	1994-2013	No	
		58	Susegana	45.852	12.259	67	1994-2013	No	
		59	Verzuolo	44.598	7.484	420	1995-2013	No	
		60	Vigalzano	46.068	11.234	539	1999-2013	No	
	S	61	Aliano	40.283	16.315	250	1998-2013	No	
		62	Campochiaro	41.475	14.538	502	1994-2013	No	
		63	Castel di Sangro	41.750	14.098	810	1998-2013	No	
		64	Libertinia	37.543	14.583	183	1994-2013	No	
		65	Matera	40.654	16.613	370	1999-2013	Yes	
		66	Monsampolo	42.888	13.797	43	1994-2013	No	
		67	Palo del Colle	41.054	16.633	191	1994-2013	No	
		68	Piano Cappelle	41.114	14.828	152	1994-2013	Yes	
		69	Pietranera	37.506	13.517	158	1994-2013	No	
		70	Pontecagnano	40.620	14.921	29	1997-2013	No	
		71	Santa Lucia	39.978	8.619	14	1994-2013	No	
		72	Santo Pietro	37.119	14.525	313	1994-2013	No	
		73	Sibari	39.739	16.450	10	1994-2013	No	
		74	Turi	40.921	17.011	230	1994-2013	No	
CRA-CMA	N	75	Alassio	44.000	8.170	32	1937-2013	Yes	Campbell-Stokes SD recorder
		76	Chiavari	44.315	9.323	25	1937-2001	No	
		77	Civitavecchia	42.083	11.783	23	1969-1992	No	
		78	Cuneo	44.400	7.533	536	1961-1993	No	
		79	Faenza	44.287	11.879	55	1949-1992	No	
		80	Imperia	43.877	8.016	54	1952-2011	No	
		81	Milano Brera	45.472	9.188	147	1948-1971	No	
		82	Parma	44.804	10.315	53	1936-2008	No	
		83	Pavia	45.183	9.129	82	1936-1974	No	
		84	Pesaro	43.902	12.883	14	1937-2007	No	
		85	Piacenza Collegio Alberoni	45.035	9.726	72	1941-1998	No	
		86	Pisa	43.679	10.320	2	1957-1989	Yes	
		87	Roma Collegio Romano	41.898	12.481	57	1942-2013	No	
		88	Salo	45.608	10.522	110	1946-2013	No	
		89	Savona	44.307	8.457	24	1946-2011	No	
		90	Urbino	43.725	12.653	476	1943-1999	No	
		91	Verbania Pallanza	45.917	8.550	241	1975-1991	No	
		92	Voghera	44.983	8.967	108	1974-1984	No	
		93	Terni	42.567	12.650	170	1961-2000	No	
	S	94	Acireale Agrumicultura	37.620	15.152	208	1971-1984	Yes	
		95	Catania	37.504	15.079	65	1940-1977	No	
		96	Foggia Podere	41.500	15.563	90	1950-1962	No	
		97	Foggia Quindicinella	41.550	15.519	50	1951-1962	No	
		98	Gaeta	41.220	13.567	50	1939-1998	No	
		99	Lucugnano	39.948	18.292	130	1938-1969	No	
		100	Taranto	40.467	17.254	22	1937-2013	No	
University and local observatory	N	101	Modena	44.648	10.930	76	1936-1984	No	
		102	Pontremoli	44.377	9.877	257	1994-2013	No	
		103	Trieste Hortis	45.648	13.766	35	1936-2010	No	
		104	Varese	45.834	8.820	427	1983-2013	No	Campbell-Stokes SD recorder and LSI-Lastem SD recorder, threshold: $120 Wm^{-2}$, range: $0 \div 1500 Wm^{-2}$, spectrum: 300÷110nm, accuracy: $5 Wm^{-2}$

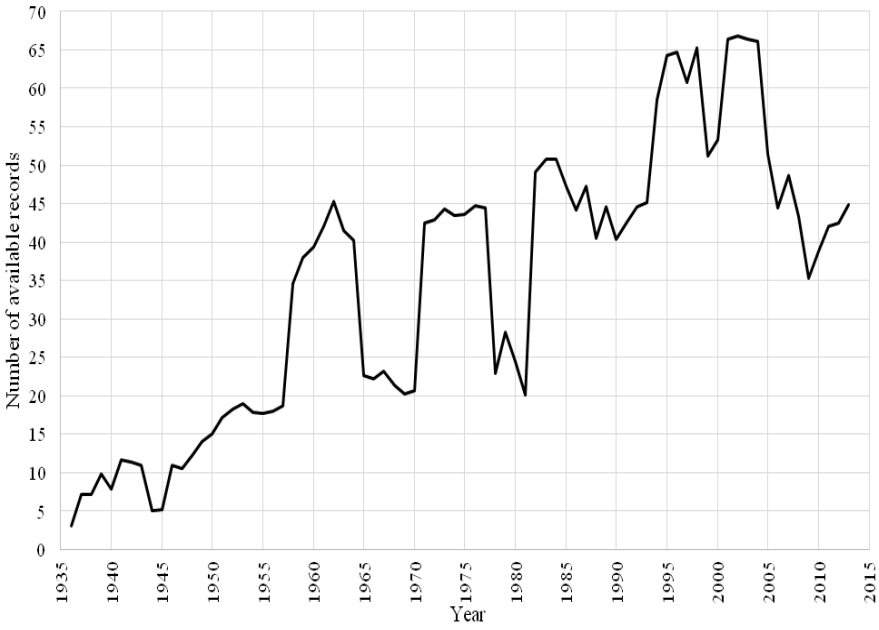

Figure 2.2: Temporal evolution of the number of available records.

the station ([10]). As far as Italian sunshine duration data are concerned, a major issue is linked to the different instrumentation used to measure sunshine duration in the different networks (see Table 2.1; 2.2).

We subjected therefore all our monthly records to a homogenization procedure based on a relative homogeneity test as described by Brunetti et al. ([10]). In this procedure, each series is tested against 10 other series by means of the Craddock test ([15]). When a break is identified in the test series, some reference series are chosen among those that prove to be homogeneous in a sufficiently large period centered on the break and that correlate well with the test series. Several series are used in order to better identify the break and to get adjustments that are more reliable. When a break is identified, the preceding portion of the series is corrected, leaving the most recent portion unchanged. This allows updating the records without considering adjustment factors.

The ability of the procedure to detect breaks depends on the spatial coherence of the data and on the density of the record network. Some information on such issues is given in Figure 2.3. It shows that the common variance between two stations falls to about 50% at a distance of 150km and that it is extremely difficult to apply the homogenization procedure before 1946. In this period, in fact, there is a very low number of records within a radius of 150km from each station with available data.

After homogenization, only 34 out of 104 records resulted homogeneous, whereas the remaining 70 were homogenized. A total number of 116 breaks were found. By plotting

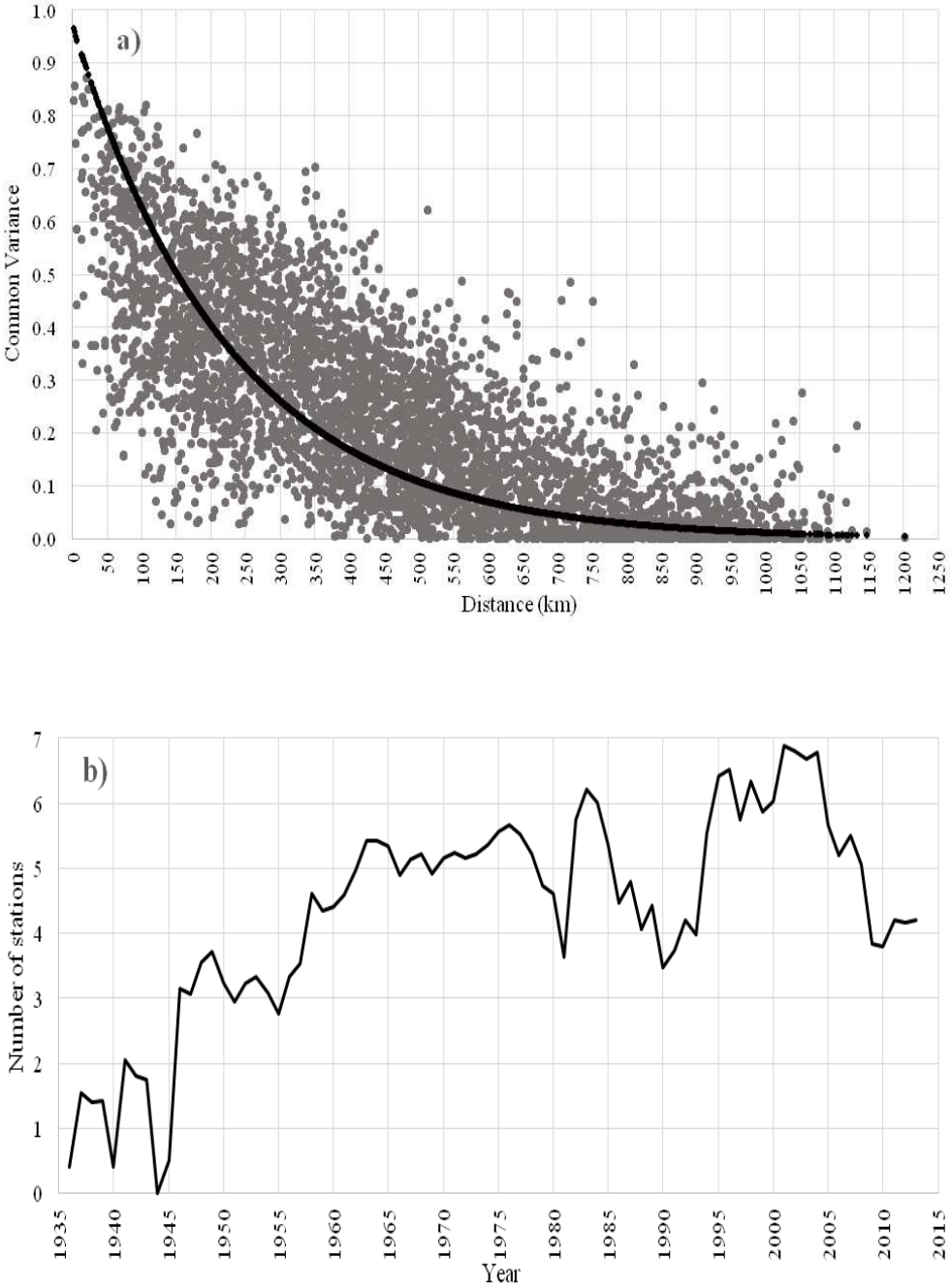

Figure 2.3: (a) Common variance versus distance of monthly sunshine duration records. In order to remove the effect of the annual cycle, common variance has been calculated after deseasonalization of the records; (b) temporal evolution of the average number of available stations within a radius of 150km from each station with available data.

the number of detected breaks versus time, we found a significant increase (Figure 2.4); this is an expected result as the probability of breaks is indeed linked to data availability (Figure 2.2). However, there is an increase in the number of detected breaks even when we normalize them with respect to the number of available series per year (Figure 2.4), due to the very low number of breaks before 1950. This is related to the higher performances of all relative homogeneity tests with the increase of station density. In order to better understand the effect of the homogenization procedure, we analyzed the adjustment series obtained performing the ratio between the homogenized and the original series. Figure 2.5 shows the curve obtained by averaging the mean annual adjustments over all single records, together with their absolute range. The large absolute range underlines how homogenization is important to get reasonable single station series. This is particularly evident for some records of the archive of the former Italian Central Office for Meteorology (i.e. Cagliari, Cuneo and Taranto), with adjustments up to 1.5. Even though the adjustments cover a wide range of values, their average is rather close to one, especially since 1980. In the 1961-1979 period, the average adjustments (from 1.02 to 1.06) are higher than 1.0, this means that the original data were systematically increased to get homogenous data; however it is due only to a few records with rather large adjustments. In the years before the 1960s (adjustments from 0.96 to 1) there is a tendency to have smaller values in the homogenized records with respect to the original ones. The necessity of reducing SD before 1960 to get homogeneous series may be due to the strong urbanization which occurred in Italy in the following decades, causing a reduction in the sky view factor for some urban observatories of the CRA-CMA network and producing relatively lower SD in the following years.

2.3.3 Gap filling and calculation of monthly anomaly records

After homogenisation, we filled the gaps in each monthly record. The record to be used as reference for the estimation of a missing datum was selected among those fulfilling two conditions: distance within 500km from the record under analysis and availability of at least 10 monthly values in common with it in the month of the gap. If no records fulfilled these conditions, the missing datum was not estimated. The records fulfilling these conditions were ranked considering the product of a distance and an elevation factor. These factors were defined as in Brunetti et al. ([13]), using Gaussian weights. For distance, the weight decreases to 0.5 at 300km. For elevation difference, if station elevation is under 500m, it decrease to 0.5 at 250, whereas for higher stations it decreases to 0.5 at half of station elevation. The record with the highest rank was then selected as reference record and the gap was filled under the assumption of the constancy of the ratio between incomplete and reference series. The procedure has been checked with a leave-one-out approach, considering each available value of each record as missing and estimating it: about 50% of the ratios between the original values and the estimated ones resulted between 0.95 and 1.05; about 90% of them resulted between 0.85 and 1.15.

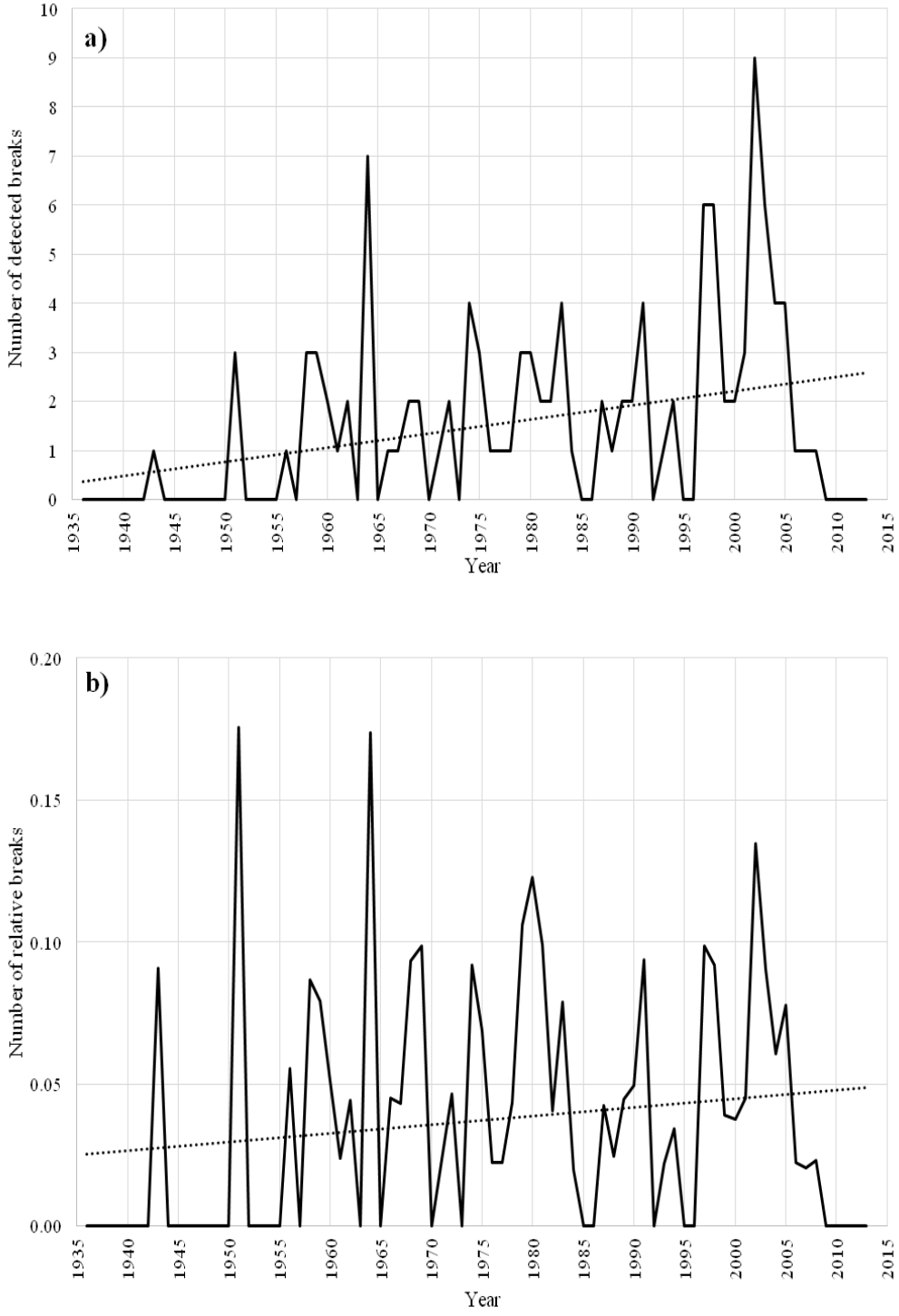

Figure 2.4: (a) Number of detected breaks per year in the SD dataset and (b) number of detected breaks normalized by the number of available series. The linear regression lines are shown (dotted lines) too.

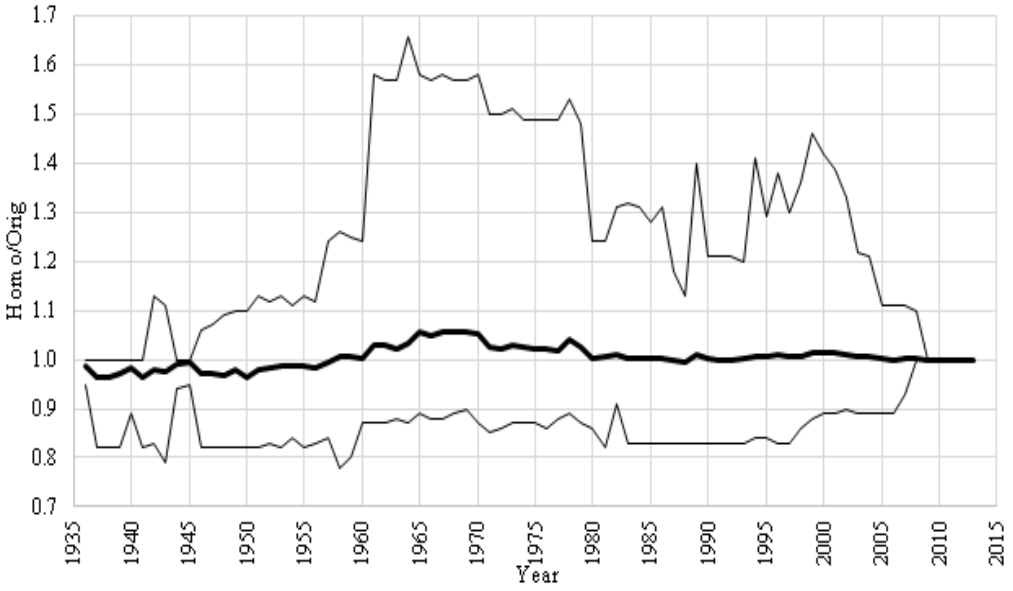

Figure 2.5: Mean annual adjustment series obtained by calculating the annual average adjustment overall series (bold line). The figure shows the maximum range in the adjustments too.

After gap filling, we considered only the 95 records for which at least 90% of the data were available in the 1984-2013 period and transformed them into anomaly records, with respect to the monthly 1984-2013 normals. Besides monthly anomaly records, also seasonal and annual anomaly records were produced. Seasons are defined according to the scheme DJF, MAM, JJA and SON and winter is dated according to the year in which January and February fall. Years are defined by the December-November period. For the first year the winter season is calculated only with January and February while the year is calculated only with the January-November period.

2.3.4 Gridding

Starting from the 95 gap-filled anomaly series, we generated a gridded version of the monthly, seasonal and annual SD anomalies. The aim was to balance the contribution of areas with a higher number of stations with those that have a lower station coverage. We used a grid of $1^\circ \times 1^\circ$ following the technique described by Brunetti et al. ([10]) and Sanchez-Lorenzo et al. ([50]), which is based on an Inverse Distance Weighting approach with the addition of an angular term to take into account the anisotropy in spatial distribution of stations.
Distance weights (w_i^d) were calculated as for the gap-filling procedure, with a decrease to 0.5 for distance equal to $\frac{\bar{d}}{2}$ from the grid point under analysis. Here $\bar{d}$ is defined as the

	Non-rotated			Varimax Rotated		
EOF	**Eigenvalues**	**Variance (%)**	**Total variance (%)**	**Eigenvalues**	**Variance (%)**	**Total variance (%)**
1	40.3	59.3	59.3	29.1	42.3	42.3
2	11.9	17.6	76.9	23.2	34.1	76.9
3	3.0	4.5	81.4			
4	2.7	3.9	85.3			
5	1.6	2.3	87.6			
6	1.1	1.6	89.2			

[a]Eigenvalues, explained variances, and cumulative explained variances of nonrotated and rotated EOFs obtained from the PCA applied to the gridded dataset.

Table 2.3: PCA of the Gridded Dataset[a]

mean distance from one grid point to the next one calculated over all adjacent points of the grid: it turns out to be about 130km. The angular term (α_i) is that used by New et al. ([32]). The station weights were then obtained as in New et al. ([32]) by means of $w_i = w_i^d(1 + \alpha_i)$. Gridded values were calculated only when either a minimum of two stations at a distance smaller than $\bar{d}$ were available or a minimum of one station at a distance smaller than $\frac{\bar{d}}{2}$. Grid values were calculated by considering all stations within a distance of $\bar{d}$.
The grid spans from 7° to 19° E and from 37° to 47° N, with 68 points over the Italian territory (Figure: 2.1).

2.3.5 PCA and regional average records for Italian main climatic regions

Monthly anomaly records were subjected to Principal Component Analysis (PCA) in order to identify areas with similar SD temporal variability. This technique allows the identification of a small number of variables, known as Principal Components (PCs), which are linear functions of the original data, and which maximize their explained variance ([39]; [87]). The analysis focused on the 1958-2013 period because here we had more available data.
We applied PCA both to station and grid-point records. As the results are very similar, we discuss only the grid-point results. Table 2.3 shows the eigenvalues, the explained variances, and the cumulative explained variances of the first 6 eigenvectors, which are those with eigenvalues greater than 1. They explain more than 89% of the total variance of the dataset.

To obtain more physically meaningful patterns ([73]), we selected to rotate, by means of a VARIMAX rotation, the first two Empirical Orthogonal Functions (EOFs), which are those that account for more than 5% of the original variance of the dataset. The loading patterns (figure not shown) allowed to identify two regions: northern Italy (36 grid-points) and southern Italy (32 grid-points) (Figure 2.1). Finally, we calculated the regional monthly, seasonal and annual mean series from the gridded dataset simply by averaging all corresponding grid-point anomaly records.

2.4 Results and Discussion

2.4.1 Trend analysis of the seasonal and annual regional records

The average northern and southern Italy seasonal and annual SD records are shown in Figure 2.6, together with a low-pass filter working on 11-year windows that considers Gaussian weights decreasing to e^{-1} at 3 years from the center of the window.

These curves indicate an increase starting from the 1980s. This signal concerns both northern and southern Italy and all seasons, with the only exception of autumn, that shows an increasing tendency only in northern Italy starting from about 1995. Before this brightening signal, there is a decreasing tendency: it is however less evident than the more recent increase. In northern Italy, it concerns spring and summer and the period from about mid of the 1960s to the beginning of the 1980s; in southern Italy, it concerns also winter and seems to start from about the end of the 1950s. In the early period, from the 1930s to the 1950s there is some evidence of an increasing tendency. This early brightening signal concerns however a period in which data availability is low, causing a greater uncertainty in the regional records. Moreover, it is rather weak and different for northern and southern Italy, both in terms of seasons and corresponding periods taken into account.

In order to better investigate the increasing and decreasing tendencies highlighted by Figure 2.6, we subjected the records to running trend analysis ([11]). Specifically, we estimated slopes by applying linear least square regression to all sub-intervals of at least 20 years of the 1936-2013 period. The results are shown in Figure 2.7, where window widths and the starting years of the windows that the trends refer to are represented on y and x axes, respectively. Slopes are represented by the colors of the corresponding pixels. Pixels are plotted only for trends with a significance level of 0.1. Significances are evaluated by the Mann-Kendall non-parametric test ([61]). This type of running trend analysis is an instrument to investigate trends in depth and to produce plots that show trends on a wide range of timescales.

First, in Figure 2.7 it underlines the evident brightening of the last decades of the study period: it is significant in all cases, with increases up to near 10%/decade, with the only exception of autumn in southern Italy. The highest increase concerns the decades starting at the beginning of the 1980s. Secondly, it shows that also the dimming signals highlighted by Figure 2.6 are significant. In northern Italy, they concern only spring and summer for the sub-periods ending in the 1980s, whereas in southern Italy there is a dimming period also in winter and at annual scale. Thus, in this region the dimming period is more evident and slightly anticipated with respect to northern Italy. Thirdly, it shows that the early brightening signal is significant only in autumn in northern Italy. This latter signal, even though not significant at a seasonal level, is significant in some cases for the annual record both for northern and southern Italy.

Figure 2.7 (left column) highlights that in northern Italy the brightening of the last decades is both stronger and longer than the previous dimming. In fact, also in the seasons that

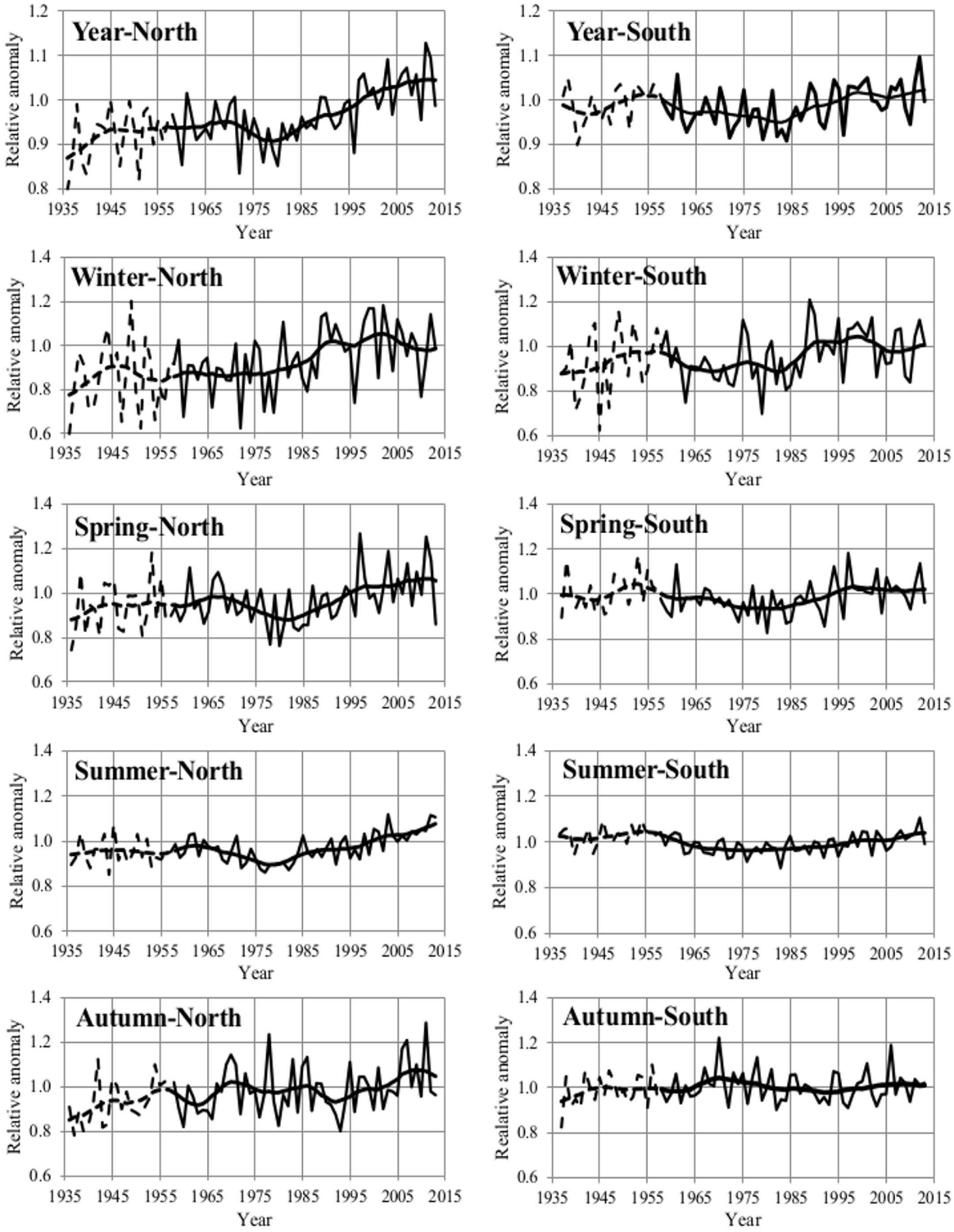

Figure 2.6: Average annual and seasonal northern (left column) and southern (right column) Italy sunshine duration series (thin lines), plotted together with an 11-y window - 3-y standard deviation Gaussian low-pass filter (thick lines). The series are expressed as relative deviations from the 1984-2013 means. Dashed lines are used prior to 1958 owing to the lower number of records for the initial period. Annual graphs are expressed with an expanded scale with respect to seasonal ones.

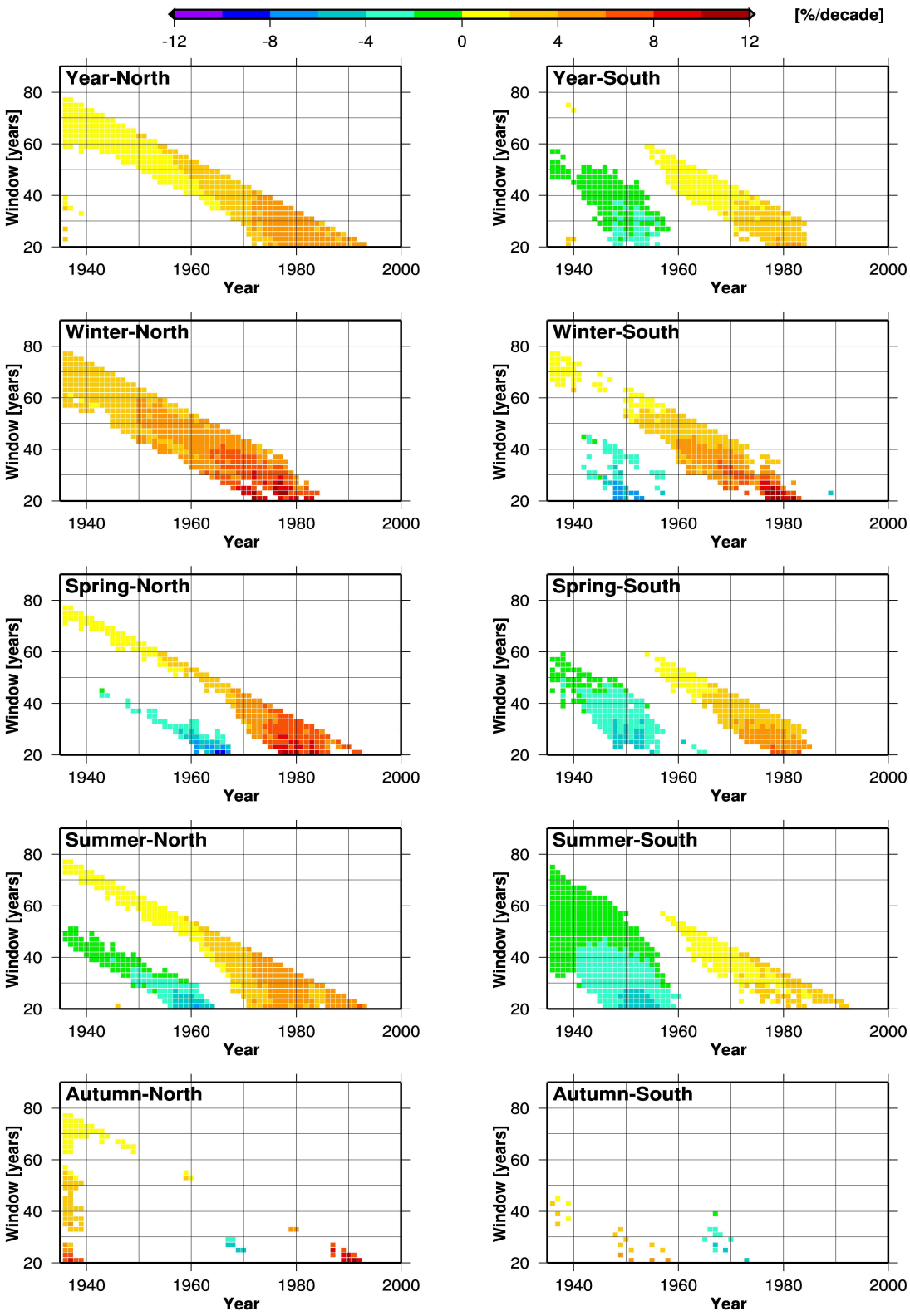

Figure 2.7: Running trend analysis for the northern Italy (left column) and southern Italy (right column) annual and seasonal records. The y axis represents window width, and the x axis represents starting year of the window over which the trend is calculated. Only trends with significance level of at least 0.1 are plotted.

show a significant dimming in the 1960s and 1970s, the trend over the widest windows is significantly positive: for the 1936-2013 period it ranges from $1.1 \pm 0.3\% decade^{-1}$ in summer to $2.8 \pm 0.7\% decade^{-1}$ in autumn. On the contrary, Figure 2.7 (right column) gives evidence that in southern Italy the dimming and the following brightening are comparable in slope and length, with the only exception of autumn where these signals are not present. Therefore, the trend of the widest windows is generally not significant. In this region, there is a significant positive long-term trend only for the winter record ($1.5 \pm 0.6\% decade^{-1}$ over the 1936-2013 period) and for a few windows for the annual record, whereas in summer there are some rather wide windows with negative trends.
In order to get a first estimation of global radiation trends, we estimated global irradiance data from the corresponding SD records by means of Ångström-Prescott formula ([3]; [40]). Specifically, we used the coefficients reported by Spinoni et al. ([63]), which give a preliminary estimation of this formula for Italy. The resulting records were then transformed into anomalies with respect to the monthly averages of the 1984-2013 period and were used to get northern and southern Italy global radiation (expressed as mean irradiance, in Wm^{-2}) anomaly records. The trends of these records are presented in Table 2.4 for five periods, i.e. the entire period covered by the data, the period with best data availability and three intervals (1951-1980, 1981-2000 and 1981-2013), which can be useful for comparison with other studies. The results for the annual records give evidence of a decrease in the global dimming period (1951-1980), which is not significant in northern Italy and is slightly above $3Wm^{-2}$ per decade in southern Italy. Southern Italy trend is in line with trends reported in other worldwide areas ([23]; [66]; [80]; [81]) and Europe ([14]; [33]; [54]). The increase in the following period is significantly stronger in northern Italy (over $5Wm^{-2}$ per decade), whereas it is comparable to the previous decrease in southern Italy. Also in this period, at an annual scale, southern Italy results are in good agreement with reported trends in Europe ([53]; [55]; [80]; [81]). Nevertheless, northern Italy trends exhibit a tendency towards higher increase as compared to most of the sites in Europe, even in Central Europe ([38]; [47]; [49]), although a trend of around $5Wm^{-2}$ is also reported in Germany during the period 1985-2005 ([85]) and the region of the Po Valley and Central Europe over the period 1980-2012 ([31]).

2.4.2 Comparison with sunshine duration records of other areas

SD is one of the variables considered by the HISTALP Project that aimed at setting up a wide dataset of instrumental time series for the Greater Alpine Region (GAR, $4 - 19°$ E, $43 - 49°$ N) ([5]). This dataset has been analyzed by Brunetti et al. ([12]) in a paper discussing and comparing long-term changes and high-frequency variability of these variables: they studied four regions representing different GAR low-level areas (northwest, northeast, southwest, southeast) and an additional mean series for high-level locations. The southwest and southeast records concern a wide area covering also the northern part of Italy. When the HISTALP dataset had been set up, no long-term SD records were available

		Annual	**Winter**	**Spring**	**Summer**	**Autumn**
North	1936-2013	**1.5±0.3**	**1.3±0.3**	**1.8±0.6**	**1.7±0.5**	**1.1±0.3**
	1958-2013	**2.1±0.4**	**1.8±0.5**	**2.5±1.0**	**3.3±0.8**	1.0±0.6
	1951-1980	-	+	-	**-3.4±1.6**	+
	1981-2000	**5.7±1.3**	**5.3±2.2**	**10.6±4.1**	**7.4±3.1**	-
	1981-2013	**5.1±0.8**	+	**7.7±2.2**	**8.9±1.4**	2.4±1.3
South	1936-2013	+	0.8±0.4	+	-	+
	1958-2013	**1.2±0.4**	**1.4±0.5**	**1.8±0.8**	**1.6±0.7**	-
	1951-1980	**-3.1±0.9**	-2.0±1.3	**-6.2±1.9**	**-7.0±1.6**	+
	1981-2000	**5.1±1.7**	**7.0±2.5**	+	5.7±2.9	-
	1981-2013	**3.0±0.8**	+	**3.9±1.8**	**5.1±1.4**	+

[a] Values are expressed in Wm^{-2} per decade. Values are shown only for significance greater than 90%, whereas bold characters indicate significance greater than 95%. For not significant trends, only the sign of the slope is given.

Table 2.4: Global radiation Trends [a]

for Italy. Therefore, the HISTALP southwest and southeast SD records were constructed without considering Italian series. Thus, it is very interesting to compare northern Italy SD records with the corresponding HISTALP southwest and southeast records, which are here combined in an average record representative of the southern part of the GAR.
This comparison is shown in Figure 2.8 (left column) for the annual and seasonal low-pass filter records for the period of best common data availability (1958-2007). Figure 2.8 shows good agreement between HISTALP records and those considered in this paper, as for both datasets the recent brightening signal is clearer than the previous dimming signal. It is worth noting that the Italian and the HISTALP SD records have been set up using completely independent data and homogenization procedures. Therefore, the good agreement between these records is not only interesting, as it shows that long-term SD exhibits a rather coherent signal over a large region such as the southern part of the GAR, but it is also useful to increase our confidence in the quality of the regional SD records both for HISTALP and Italian datasets. This point is very important also to shed light on some apparent inconsistencies between the HISTALP SD and TCC records detected by Brunetti et al. ([12]): the authors highlighted a disagreement between the long-term tendencies of the two variables, suggesting that some biases could affect one of these variables or both of them. The agreement between HISTAL SD records and our new SD dataset suggests that the inconsistencies between the HISTALP SD and TCC records are possibly due to problems in the HISTALP TCC records.
The behavior of northern Italy and GAR southern regions is indeed rather peculiar, as most publications do not report a significant increase either for SD or for global radiation in the 1958-2007 period. Thus, the SD records of this area could support the hypothesis of Wang et al. ([77]) that suggests that the dimming period in global radiation records could have been overestimated, due to some instrumental problems. More specifically, Wang et al. ([77]) compared global radiation records measured by single pyranometers with those obtained by summing diffuse and direct components, which are measured by shaded

pyranometers and pyrheliometers, respectively. They conclude that there are statistically significant differences between both methods to estimate global radiation, and state that the trend rates during the dimming period, when only single pyranometers were available, would have been lower if measured using global radiation from shaded pyranometer and pyrheliometer data. Further research is needed on this issue; in this paper, based on comparison with TCC records (see Section 2.4.3), we suggest however that the behavior of northern Italy SD is linked to a peculiar evolution of TCC.
As far as southern Italy is concerned, we perform the comparison with a more Mediterranean-like area, such as Spain. We show therefore in Figure 2.8 (right column) southern Italy annual and seasonal low-pass filter records together with corresponding records from Sanchez-Lorenzo et al. ([50]) for the period 1961-2004. Specifically, we consider the eastern Spain records shown in the first column of Figure 2.7 of that paper. The results indicate that in southern Italy the dimming in the 1960s and 1970s is indeed weaker than in Spain. The agreement seems to be better for the subsequent brightening that seems to start both in southern Italy and in Spain at the beginning of the 1980s. Overall, there are no significant long-term trends since the 1960s in both southern Italy and eastern Spain series, unlike the clear tendency observed in northern Italy.

2.4.3 Comparison of sunshine duration records with total cloud cover records

The comparison between TCC and SD records over Italy has been performed over the 1958-1995 period, using the dataset of Maugeri et al. ([30]), with data available until 1995. This dataset contains only TCC data, whereas no information is available for cloud amount by low and middle clouds, which would be a better variable for investigating the cloudiness-SD relationship (e.g. [28]; [90]).
The TCC-SD comparison is shown in Figure 2.9 separately for northern and southern Italy, with all records expressed in terms of relative anomalies from the averages over the 1958-1995 period. Here, as well as in Figure 2.8, we show only the low-pass filter records.
The figure highlights that the negative correlation expected between SD and TCC is often not evident in the low-pass filter records. A clear example concerns the annual series in the period from about the beginning of 1960s to the beginning of the 1980s: here both SD and TCC have a decreasing tendency. This low negative correlation, beside the annual records, is particularly evident in summer which shows very weak correlation also for the unfiltered records; the correlation coefficients for annual and summer records are, respectively, -0.53 and -0.55 for northern Italy and -0.39 and -0.54 for southern Italy. These results are in agreement with previous findings for Spain ([52]), which also highlight a disagreement between both variables from the 1960s to the mid-1980s, especially in summer months. On the contrary, if the residuals (relative deviations) from low-pass filter are considered, the negative correlation is much higher, with correlation coefficients ranging from -0.90 (spring) to -0.96 (autumn) for northern Italy and from -0.85 (summer) to -0.91 (spring)

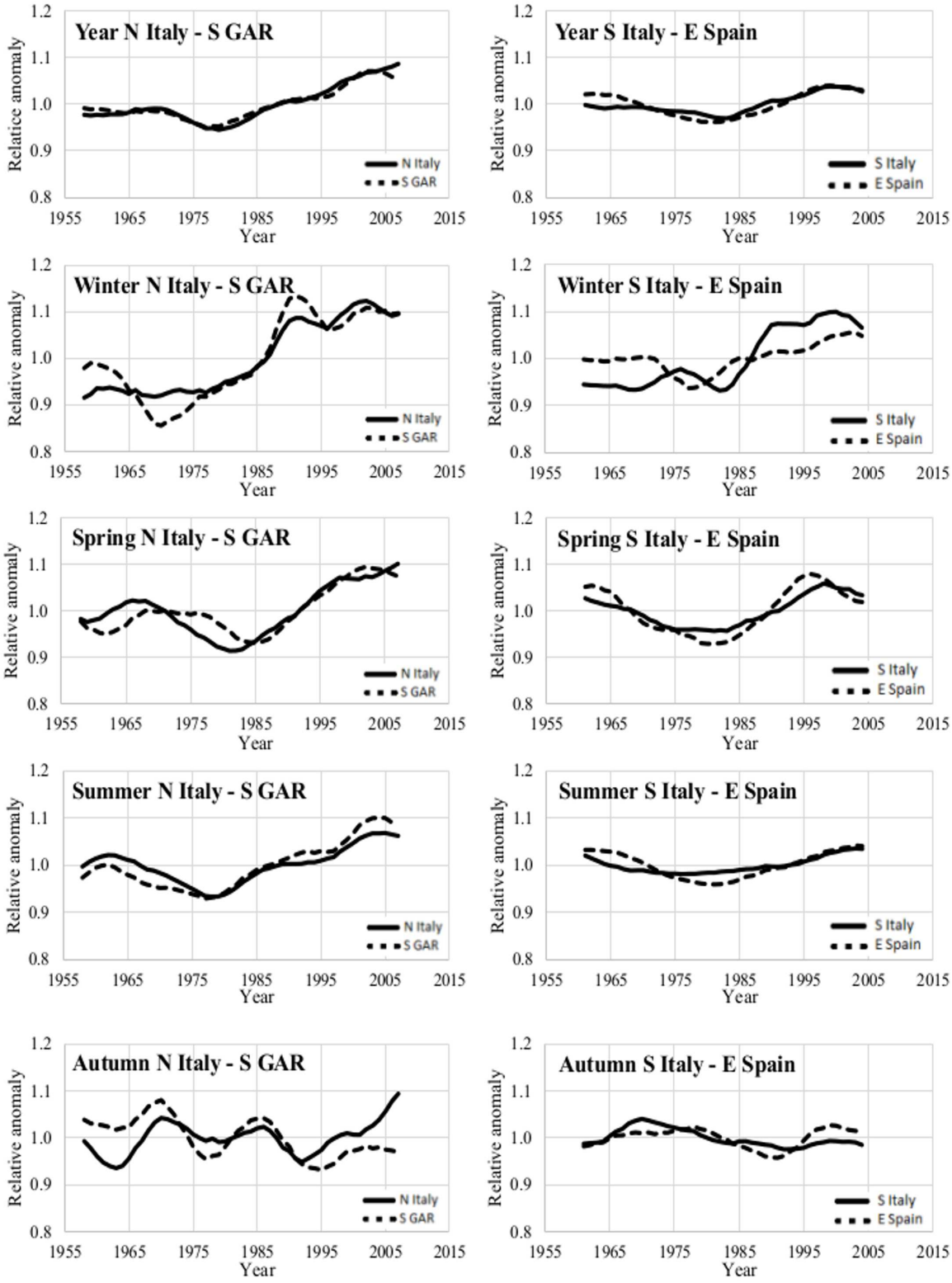

Figure 2.8: Sunshine duration low-pass-filter annual and seasonal records for northern Italy and the southern part of the Greater Alpine Region (left column, 1958-2007 period) and for southern Italy and eastern Spain (right column, 1961-2004 period). The filter is the same as in Figure 2.6. All records are expressed in terms of relative anomalies from the 1958-2007/1961-2004 averages.

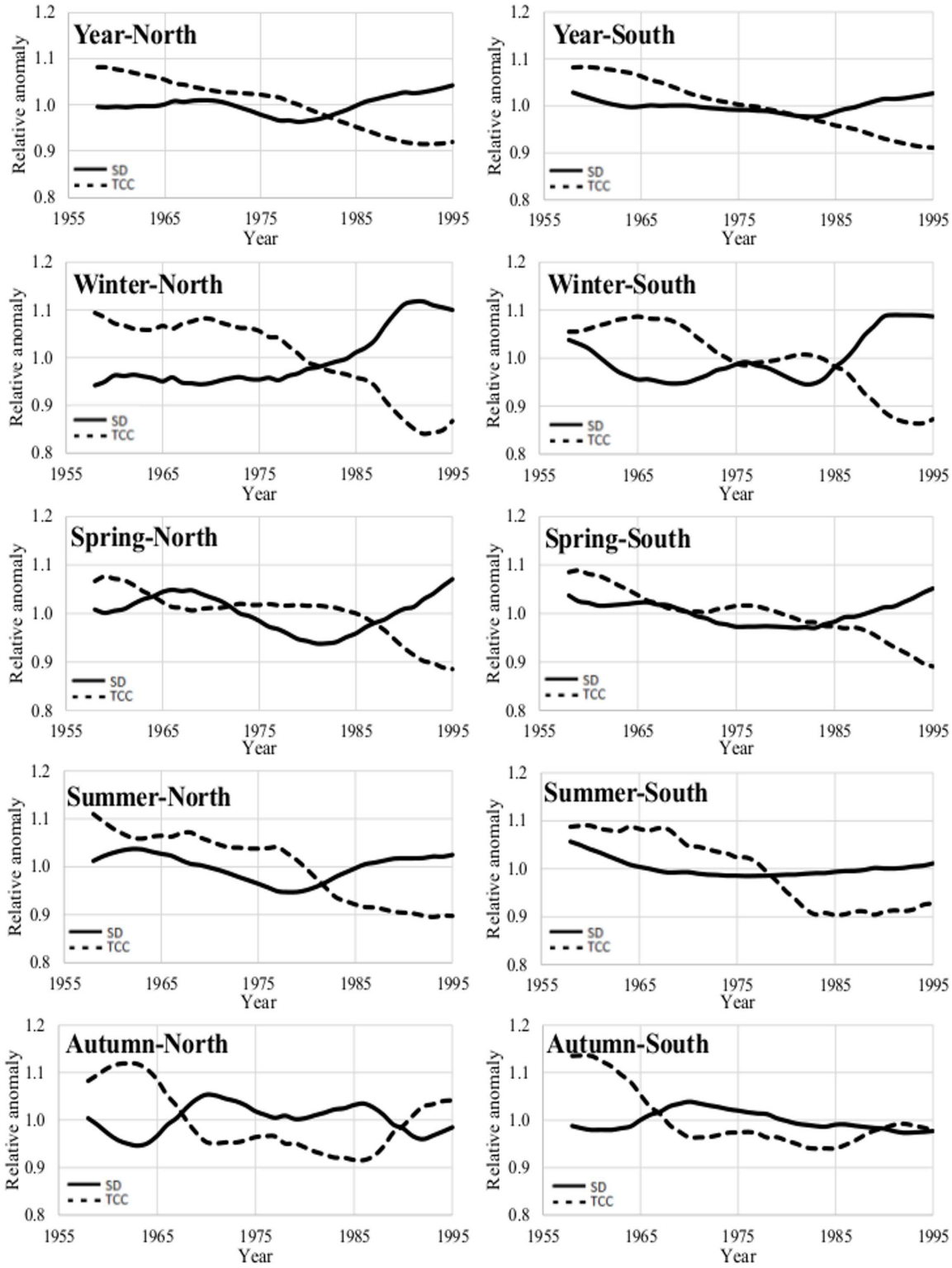

Figure 2.9: Sunshine duration (SD) and total cloud cover (TCC) low-pass filter annual and seasonal records (1958-1995) for northern (left column) and southern Italy (right column). The filter is the same as in Figure 2.6. All records are expressed in terms of relative anomalies from the 1958-1995 averages.

for southern Italy. This suggests the existence of different factors affecting the long-term tendencies in the two variables, as reported by Wang et al. ([76]).
To highlight the role of TCC in driving SD, we created virtual SD annual and seasonal records using TCC as predictor, by exploiting the relationship between SD and TCC residuals: in particular, we evaluated the linear relationship between SD and TCC residuals and extended it to the real records. This linear relationship shows highest regression coefficients in winter (-0.92±0.06 for northern Italy; -0.96±0.09 for southern Italy) and spring (-0.90±0.07 for northern Italy; -0.77±0.06 for southern Italy), whereas in summer the regression coefficients are much lower (-0.45±0.03 for northern Italy; -0.21±0.02 for southern Italy).
Once we got these virtual SD records, we followed a technique suggested by other authors (e.g., [33]; [52]) to remove the cloud effect from the real SD records and to detect whether there are signals linked to other factors than TCC. It consists in obtaining residual series by simply dividing the real SD records by the corresponding virtual SD records. These residual series should represent the SD tendency without the contribution due to TCC (i.e. keeping TCC constant). Results are shown in Figure 2.10. In order to give better evidence of the influence of TCC on SD, we also report in this figure the real SD low-pass filter curves (see Figure 2.6) that are here expressed in terms of anomalies with respect to the 1958-1995 means.

This figure shows a clear decrease from the end of the 1950s to the beginning of the 1980s (of about 15% at an annual scale) both in northern and southern Italy. This signal indicates that during this period there is an important fraction of SD long-term evolution that cannot be explained by TCC: it must therefore depend on other factors such as changes in aerosol optical thickness, cloud properties, and/or water vapor content. The clear dimming caused by these factors has been partially masked, especially in northern Italy, by a strong TCC reduction. Therefore, the regional peculiarity of northern Italy very low SD reduction in the dimming period could simply be a consequence of a stronger decrease in TCC experienced by this region ([30]). After the beginning of the 1980s, the curves in Figure 2.10 do not show strong variations. Therefore, we can conclude that the effect of the other factors on SD becomes less relevant. The Italian brightening, at least up to 1995, seems therefore to be dominated by a TCC decrease.
It is also worth noting that the curves in Figure 2.10 have in most cases relevant minima in the periods 1982-1983 and 1992-1993. These pronounced minima, which have also been observed by other authors ([52]), might be a consequence of El Chichón (April 1982) and Pinatubo (June 1991) volcanic eruptions, which injected high amounts of sulfur dioxide (SO_2) into the stratosphere causing a worldwide reduction in direct solar radiation.
The results of Figure 2.10 are in reasonable agreement with anthropogenic emissions of pollutants and associated aerosol loads in the atmosphere over Europe (e.g., [46]; [59]; [60]; [71]). The agreement is good especially for the decrease between the beginning of the 1960s and the early 1980s, which corresponds to a strong increase in aerosol loads, whereas after 1980 the agreement is less evident as emissions and aerosol loads show a

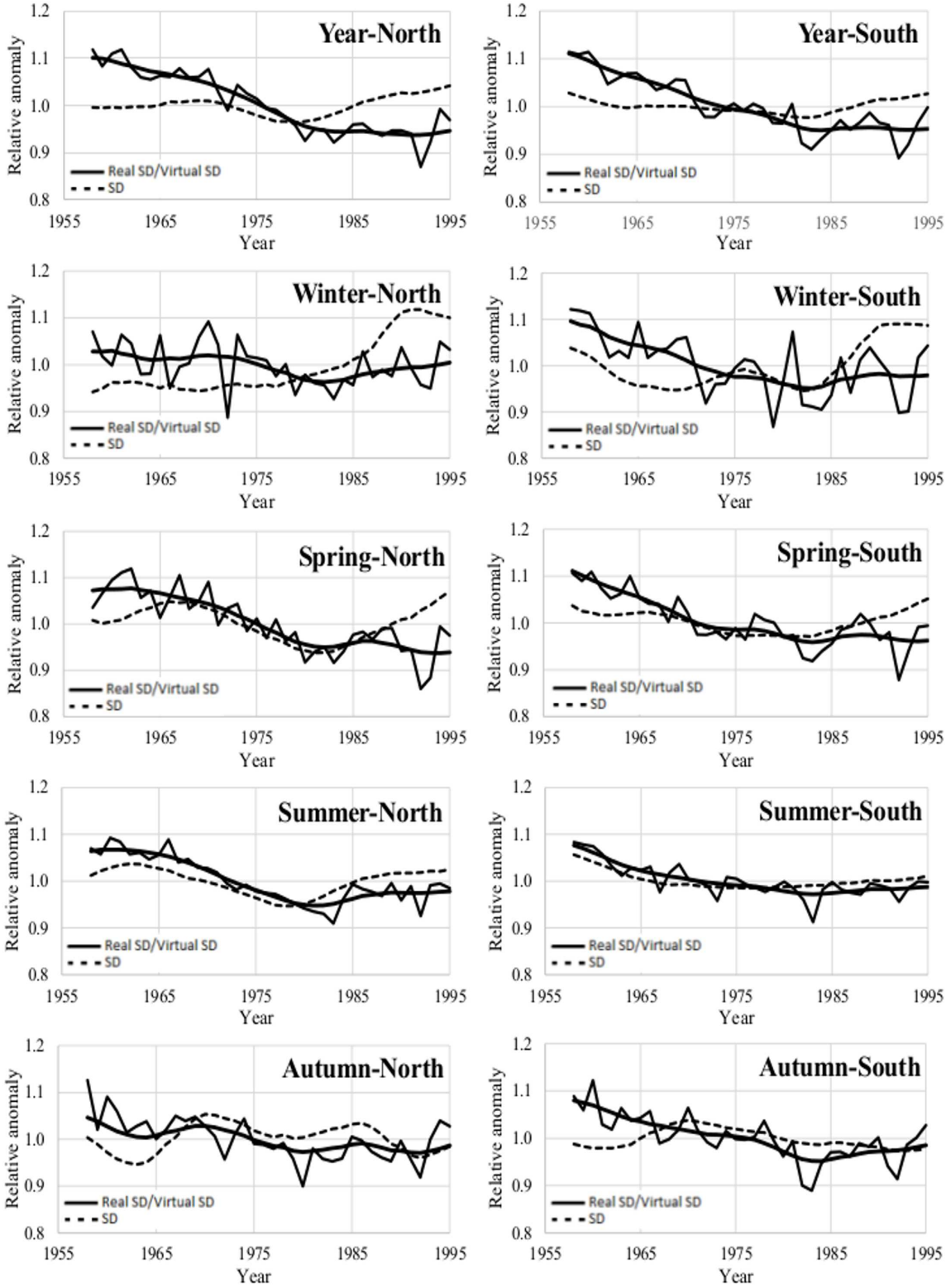

Figure 2.10: Continuous lines: ratios between the real sunshine duration (SD) anomalies and the virtual SD anomalies as predicted by total cloud cover anomalies for northern Italy (left column) and southern Italy (right column). Heavy lines represent Gaussian low-pass filter (3-year standard deviation 11-year window) records. Dashed lines: real SD low-pass filter curves expressed as anomalies from the 1958-1995 means.

strong decrease that does not correspond to a clear increase of the curves in Figure 2.10. Anyway, the short period of Italy TCC records after the 1980s does not allow us better investigating this issue.

2.4.4 Sunshine duration and air temperature

Global radiation can have a significant influence on temperature evolution at the Earth's surface (e.g., [37]; [38]; [75]; [82]). It is therefore interesting to investigate whether the differences in the evolution of SD in northern and southern Italy correspond to differences in the evolution of air temperature.
Air temperature variability in Italy is discussed by Brunetti et al. ([10]) who analysed a network of 67 secular records. Their results do not show relevant differences between northern and southern Italy. The same result is reported by Simolo et al. ([58]) who analysed 67 stations to study northern and southern Italy temperature trends (daily minimum and maximum temperatures - Tn and Tx -) for the 1951-2008 period, showing rather low differences between northern and southern Italy seasonal and annual trends.
As a conclusion, the overall picture of air temperature in Italy does not give evidence of a strong link with the temporal evolution of SD: strong temperature trends are present also where SD trends are not present and important regional differences in SD trends do not correspond to significant differences in temperature trends. The lack of a strong SD effect on temperature long-term variability is probably caused by the fact that an increase in SD, besides producing an increase in daily maximum temperatures, produces a decrease in daily minimum values, linked to a reduction in cloudiness. This effect is also clear in very low correlation between Italian regional temperature and DTR records ([9]).

2.5 Conclusions

A new dataset of Italian quality checked sunshine duration records has been set up collecting data from different sources. The records have then been homogenized, completed and projected onto a regular grid ($1^\circ \times 1^\circ$ resolution) covering the entire Italian territory and clustered into two main regions by means of a Principal Component Analysis: northern Italy and southern Italy. The records of these areas were averaged in order to get the corresponding regional records for the 1936-2013 period.
The clearest feature of Italy sunshine duration records is an increasing tendency starting in the 1980s. Before this brightening signal, there is a decreasing tendency, which is, however, less evident than the more recent increasing trend, especially in northern Italy. In the early period, from mid of the 1930s to the 1950s there is some evidence of an increasing tendency although this early brightening signal concerns a period in which data availability is very low, causing a greater uncertainty in regional records ([4]). The overall picture of Italian sunshine duration trends is therefore in reasonable agreement with the early brightening - dimming - brightening phases observed in many areas of the world

([80]), even though some relevant regional peculiarities are evident especially in northern Italy.

Italian sunshine duration records turn out to be in good agreement with corresponding records from neighboring areas, specifically from the southern part of the Greater Alpine Region and from eastern Spain. This good agreement is both interesting as it shows that sunshine duration exhibits a rather coherent signal over large regions, and useful, because it increases our confidence in the quality of records for Italy and neighboring regions.

The comparison of sunshine duration records with corresponding total cloud cover records shows that the expected negative correlation of these variables is often not evident as far as long term tendencies are concerned ([76]). On the contrary, the residuals from the low-pass filter records show a very high negative correlation. This robust relationship was used here to separate the effect of cloud cover on sunshine duration from other factors. This separation suggests that during the global dimming period there is an important fraction of sunshine duration evolution that cannot be explained by total cloud cover. It must therefore depend on other factors as, for example, changes in aerosol optical thickness. Nevertheless, in Italy, especially in the northern region, the clear dimming caused by these other factors (e.g. aerosol optical thickness) has been partially masked by a strong reduction in total cloud cover. Therefore, the regional peculiarity of northern Italy - very low sunshine duration reduction in the dimming period - could simply be a consequence of a strong decrease in total cloud cover. Also the strong brightening observed in Italy after the beginning of the 1980s is probably, at least up to 1995, dominated by a decrease in total cloud cover.

A more detailed understanding of the mechanism in Italy driving sunshine duration variability and trends calls for further research that should start with setting up a new cloudiness dataset, which would extend the time period covered by the records considered in this paper, and, include the cloud amount by low and middle clouds. We plan to set up this dataset in the near future. This new dataset, together with a corresponding dataset of daily temperature range records, will provide us with data to investigate a wider time interval and to study the relationship between SD, cloud cover, DTR (see e.g. [57]; [91]) and aerosol load.

Bibliography

[1] Aguilar E., Auer I., Brunet M., Peterson T.C., Wieringa J. (2003): *Guidelines on Climate Metadata and Homogenization*, WMO-TD No. 1186, pp. 52, World Meteorological Organization, Geneva, Switzerland;

[2] Angell J.K. (1990): *Variation in United States cloudiness and sunshine duration between 1950 and the drought year of 1988*, J. Clim., Vol. 3, pp. 296308, doi:10.1175/1520-0442(1990)003<0296:VIUSCA>2.0.CO;2;

[3] Ångström A. (1924): *Solar and terrestrial radiation*, Q. J. Royal. Meteor. Soc., Vol. 50(210), pp. 121-126;

[4] Antón M., Vaquero J.M., Aparicio A.J.P. (2014): *The controversial early brightening in the first half of 20th century: a contribution from pyrheliometer measurements in Madrid (Spain)*, Glob. Planet. Change, Vol. 115, pp. 71-75, doi:10.1016/j.gloplacha.2014.01.013;

[5] Auer I., Böhm R., Jurkovic A., Lipa W., Orlik A., Potzmann R., Schöner W., Ungersböck M., Matulla C., Briffa K., Jones P., Efthymiadis D., Brunetti M., Nanni T., Maugeri M., Mercalli L., Mestre O., Moisselin J.M., Begert M., Müller-Westermeier G., Kveton V., Bochnicek O., Stastny P., Lapin M., Szalai S., Szentimrey T., Cegnar T., Dolinar M., Gajic-Capka M., Zaninovic K., Majstorovic Z., Nieplova E. (2007): *HISTALP-Historical instrumental climatological surface time series of the Greater Alpine Region*, Int J. Climatol., Vol. 27(1), pp. 17-46, doi:10.1002/joc.1377;

[6] Beltrano M.C., Dal Monte G., Esposito S., Iafrate L. (2012): *The CRA-CMA archive and library for agricultural meteorology and phenology: A heritage to know, preserve and share*, Ital. J. Agrometeorol., Vol. 17(3), pp. 15-24;

[7] Beltrano M.C., Esposito S., Iafrate L. (2012): *The archive and library of the former Italian Central Office for Meteorology and Climatology*, Adv. Sci. Res., Vol. 8, pp. 58-65, doi:10.5194/asr-8-59-2012;

[8] Brazdil R., Flocas A.A., Sahsamanoglou H.S. (1994): *Fluctuation of sunshine duration in central and south-eastern Europe*, Int. J. Climatol., Vol. 14, pp. 1017-1034;

[9] Brunetti M., Buffoni L., Maugeri M., Nanni T. (2000): *Trends of Minimum and Maximum Daily Temperatures in Italy from 1865 to 1996*, Theor. Appl. Climatol., Vol. 66, pp. 49-60;

[10] Brunetti M., Maugeri M., Monti F., Nanni T. (2006): *Temperature and precipitation variability in Italy in the last two centuries from homogenized instrumental time series*, Int. J. Climatol., Vol. 26(3), pp. 345-381, doi:10.1002/joc.1251;

[11] Brunetti M., Maugeri M., Nanni T., Auer I., Böh R., Schöner W. (2006): *Precipitation variability and changes in the greater Alpine region over the 1800-2003 period*, J. Geophys. Res., Vol. 111, D11107, doi:10.1029/2005JD006674;

[12] Brunetti M., Lentini G., Maugeri M., Nanni T., Auer I., Böhm R., Schöner W. (2009): *Climate variability and change in the Greater Alpine Region over the last two centuries based on multi-variable analysis*, Int. J. Climatol., Vol. 29(15), pp. 2197-2225, doi:10.1002/joc.1857;

[13] Brunetti M., Maugeri M., Nanni T., Simolo C., Spinoni J. (2013): *High-resolution temperature climatology for Italy: Interpolation method intercomparison*, Int. J. Climatol., Vol. 34(4), pp. 1278-1296, doi:10.1002/joc.3764;

[14] Chiacchio M. and Wild M. (2010): *Influence of NAO and clouds on long-term seasonal variations of surface solar radiation in Europe*, J. Geophys. Res., Vol. 115, D00D22, doi:10.1029/2009JD012182;

[15] Craddock J.M. (1979): *Methods of comparing annual rainfall records for climatic purposes*, Weather, Vol. 34(9), pp. 332-346, doi:10.1002/j.1477-8696.1979.tb03465.x;

[16] Golderg B. and Klein W.H. (1971): *Comparison of normal incident solar energy measurements at Washington*, D.C. Solar Energy, Vol. 13, pp. 311-321;

[17] Hartmann D.L., Ramanathan V., Berroir A., Hunt G.E. (1986): *Earth radiation budget data and climate research*, Rev. Geophys., Vol. 24(2), pp. 439-468, doi:10.1029/RG024i002p00439;

[18] Italian Air Force (Vergari S.) (2012): *La radiazione solare globale e la durata del soleggia mento in Italia dal 1991 al 2010*, Aeronautica Militare, Reparto di Sperimentazioni di Meteorologia Aeronautica;

[19] Jones P.A. and Henderson-Sellers A. (1992): *Historical records of cloudiness and sunshine in Australia*, J. Clim., Vol. 5, pp. 260-267, doi:10.1175/1520-0442(1992)005<0260:HROCAS>2.0.CO;2;

[20] Kaiser D.P. and Qian Y. (2002): *Decreasing trends in sunshine duration over China for 19541998: Indication of increased haze pollution?*, Geophys. Res. Lett., Vol. 29(21), pp. 2042, doi:10.1029/2002GL016057;

[21] Kitsara G., Papaioannou G., Papathanasiou A., Retalis A. (2013): *Dimming/brightening in Athens: trends in sunshine duration, cloud cover and reference evapotranspiration*, Water Resour. Manage., Vol. 27, pp. 1623-1633, doi: 10.1007/s11269-012-0229-4;

[22] Liang F. and Xia X.A. (2005): *Long-term trends in solar radiation and the associated climatic factors over China for 1961-2000*, Ann. Geophys., Vol. 23(7), pp. 2425-2432, doi:10.5194/angeo-23-2425-2005;

[23] Liepert B.G. (2002): *Observed reductions of surface solar radiation at sites in the United States and worldwide from 1961 to 1990*, Geophys. Res. Lett., Vol. 29(10), 1421, doi:10.1029/2002GL014910;

[24] Lohmann U. and Feichter J. (2005): *Global indirect aerosol effects: a review*, Atmos. Chem. Phys., Vol. 5, pp. 715-737, doi:10.5194/acp-5-715-2005;

[25] Lombroso L. and Quattrocchi S. (2008): *L'Osservatorio di Modena: 180 anni di misure meteorologiche*, Società Meteorologica Subalpina Edition (Castello Borello, Bussoleto (TO), Italy, ISBN 978-88-903023-2-9;

[26] Magee B.N., Melaas E., Finocchio P.M., Jardel M., Noonan A., Iacono M.J. (2014): *Blue hill observatory sunshine: Assessment of climate signals in the longest continuous meteorological record in North America*, Bull. Am. Meteorol. Soc., doi:10.1175/BAMS-D-12-00206.1;

[27] Martinez-Lozano J. A., Tena F., Onrubia J. E., De La Rubia J. (1984): *The historical evolution of the ngström formula and its modifications: Review and bibliography*, Agr. Forest Meteorol., Vol.33(23), pp. 109-128;

[28] Matuszko D. (2012): *Influence of cloudiness on sunshine duration*, Int. J. Climatol, Vol. 32, pp. 1527-2536, doi:10.1002/joc.2370;

[29] Matuszko D. (2014): *Long-term variability in solar radiation in Krakow based on measurements of sunshine duration*, Int. J. Climatol., Vol. 34, pp. 228-234, doi:10.1002/joc.3681;

[30] Maugeri M., Bagnati Z., Brunetti M., Nanni T. (2001): *Trends in italian total cloud amount, 1951-1996*, Geophys. Res. Lett., Vol. 28(24), pp. 4551-4554, doi:10.1029/2001GL013754;

[31] Nabat P., Somot S., Mallet M., Sanchez-Lorenzo A., Wild M. (2014): *Contribution of anthropogenic sulfate aerosols to the changing Euro-Mediterranean climate since 1980*, Geophys. Res. Lett., Vol. 41, pp. 5605-5611, doi:10.1002/2014GL060798;

[32] New M., Hulme M., Jones P.D. (2000): *Representing twentieth-century space-time climate variability. Part II: Development of 1901-96 monthly grids of terrestrial surface climate*, J. Clim., Vol. 13, pp. 2217-2238;

[33] Norris J.R. and Wild M. (2007): *Trends in aerosol radiative effects over Europe inferred from observed cloud cover, solar "dimming", and solar "brightening"*, J. Geophys. Res., Vol. 112, D08214, doi:10.1029/2006JD007794;

[34] Ohmura A. (2009): *Observed decadal variations in surface solar radiation and their causes*, J. Geophys. Res., Vol. 114, D00D05, doi:10.1029/2008JD011290;

[35] Ohmura A. and Gilgen H. (1993): *Re-evaluation of the global energy*, in Interactions Between Global Climate Subsystems the Legacy of Hann, American Geophysical Union, edited by G.A. McBean and M. Hantel, Washington, D. C.., doi:10.1029/GM075p0093;

[36] Ohmura A. and Lang H. (1989), *Secular variation of global radiation in Europe*, in IRS88: Current Problems in Atmospheric Radiation, edited by J. Lenoble and J.-F. Geleyn, pp. 298-301, A. Deepak, Hampton, Va;

[37] Oldenborg G.J., Drijfhout S., van Ulden A., Haarsma R., Sterl A., Severijns C., Hazeleger W., Dijkstra H. (2009): *Western Europe is warming much faster than expected*, Clim. Past, Vol. 5, pp. 1-12;

[38] Philipona R., Behrens K., Ruckstuhl C. (2009): *How declining aerosols and rising greenhouse gases forced rapid warming in Europe since the 1980s*, Geophys. Res. Lett., Vol. 36, L02806, doi:10.1029/2008GL036350;

[39] Preisendorfer R.W. (1988): *Principal Component Analysis in Meteorology and Oceanography*, 425 pp., Elsevier, New York;

[40] Prescott J.A. (1940): *Evaporation from a water surface in relation to solar radiation*, Trans. R. Soc. S. Austr., Vol. 64, pp. 114-118;

[41] Rahimzadeh F., Sanchez-Lorenzo A., Hamedi M., Kruk M., Wild M. (2014): *New evidence on the dimming/brightening phenomenon and decreasing diurnal temperature range in Iran (19612009)*, Int. J. Climatol., Vol. 35(8), pp. 2065-2079, doi:10.1002/joc.4107;

[42] Raichijk C. (2012): *Observed trends in sunshine duration over South America*, Int. J. Climatol., Vol. 32, pp. 669-680, doi:10.1002/joc.2296;

[43] Ramanathan V., Crutzen P.J., Kiehl J.T., Rosenfeld D. (2001): *Aerosol, climate, and the hydrological cycle*, Science, Vol. 294(5549), pp. 2119-2124, doi:10.1126/science.1064034;

[44] Ratti M. (2010): *Il clima del 2010 a Pontremoli: Temperature quasi normali e piovositá straordinaria, Società meteorologica italiana*, Nimbus, http://www.nimbus.it/clima/2010/110204PontremoliClima2010.htm;

[45] Rosenfeld D., Andreae M.O., Asmi A., Chin M., de Leeuw G., Donovan D. P., Kahn R., Kinne S., Kiveks N., Kulmala M., Lau W., Schmidt K.S., Suni T., Wagner T., Wild M., Quaas J. (2014): *Global observations of aerosol-cloud-precipitation-climate interactions*, Rev. Geophys., Vol. 52, doi:10.1002/2013RG000441;

[46] Ruckstuhl C. and Norris J.R. (2009): *How do aerosol histories affect solar "dimming" and "brightening" over Europe?: IPCC-AR4 models versus observations*, J. Geophys. Res, Vol. 114, D00D04, doi:10.1029/2008JD011066;

[47] Ruckstuhl C., Philipona R., Behrens K., Coen M.C., Dürr B., Heimo A., Mätzler C., Nyeki S., Ohmura A., Vuilleumier L., Weller M., Wehrli C., Zelenka A. (2008), *Aerosol and cloud effects on solar brightening and the recent rapid warming*, Geophys. Res. Lett., Vol. 35, L12708, doi:10.1029/2008GL034228;

[48] Russak V. (1990): *Trends of solar radiation, cloudiness and atmospheric transparency during recent decades in Estonia*, Tellus Ser. B, Vol. 42, pp. 206-210;

[49] Sanchez-Lorenzo A. and Wild M. (2012): *Decadal variations in estimated surface solar radiation over Switzerland since the late 19th century*, Atmos. Chem. Phys., Vol. 12, pp. 8635-8644, doi:10.5194/acp-12-8635-2012;

[50] Sanchez-Lorenzo A., Brunetti M., Calbo J., Martin-Vide J. (2007): *Recent spatial and temporal variability and trends of sunshine duration over the Iberian Peninsula from a homogenized data set*, J. Geophys. Res., Vol. 112, D20115, doi:10.1029/2007JD008677;

[51] Sanchez-Lorenzo A., Calbo J., Martine-Vide J. (2008): *Spatial and temporal trends in sunshine duration over Western Europe (1938-2004)*, J. Climate, Vol. 21, pp. 6089-6098, doi:10.1175/2008JCLI2442.1;

[52] Sanchez-Lorenzo A., Calbó J., Brunetti M., Deser C. (2009): *Dimming/brightening over the Iberian Peninsula: trends in sunshine duration and cloud cover and their relations with atmospheric circulation*, J. Geophys. Res., Vol. 114, D00D09, doi:10.1029/2008JD0111394;

[53] Sanchez-Lorenzo A., Calbo J., Wild M. (2013): *Global and diffuse solar radiation in Spain: building a homogeneous dataset and assessing their trends*, Glob. Planet. Change, Vol. 100, pp. 343-352, doi:10.1016/j.gloplacha.2012.11.010;

[54] Sanchez-Lorenzo A., Wild M., Trentmann J. (2013): *Validation and stability assessment of the monthly mean CM SAF surface solar radiation dataset over Europe against a homogenized surface dataset (1983-2005)*, Remote Sens. Environ., Vol. 134, pp. 355-366, doi:10.1016/j.rse.2013.03.012;

[55] Sanchez-Lorenzo A., Calbó J., Wild M., Azorin-Molina C., Sanchez-Romero A. (2013): *New insights into the history of the Campbell-Stokes sunshine recorder*, Weather, Vol. 68(12), pp. 327-331, doi:10.1002/wea.2130;

[56] Sanchez-Romero A., Sanchez-Lorenzo A., Calbo J., Gonzalez J. A., Azorin-Molina C. (2014): *The signal of aerosol induced changes in sunshine duration records: A review of the evidence*, J. Geophys. Res. Atmos., Vol. 119, pp. 4657-4673, doi:10.1002/2013JD021393;

[57] Shen X., Liu B., Li G., Wu Z., Jin Y., Yu P., Zhou D. (2015): *Spatio-temporal change of diurnal temperature range and its relationship with sunshine duration and precipitation in China*, J. Geophys. Res. Atmos., doi:10.1002/2014JD022326;

[58] Simolo C., Brunetti M., Maugeri M., Nanni T., Speranza A. (2010): *Understanding climate change-induced variations in daily temperature distributions over Italy*, J. Geophys. Res., Vol. 115, D22110, doi:10.1029/2010JD014088;

[59] Smith S.J. and Bond T.C. (2014): *Two hundred fifty years of aerosols and climate: the end of the age of aerosols*, Atmos. Chem. Phys, Vol. 14, pp. 537-549, doi:10.5194/acp-14-537-2014;

[60] Smith S.J., van Aardenne J., Klimont Z., Andres R.J., Volke A., Delgado Arias S. (2011): *Anthropogenic sulfur dioxide emission: 1850-2005*, Atmos. Chem. Phys., Vol. 11, pp. 1101-1116, doi:5194/acp-11-1101-2011;

[61] Sneyers R. (1992): *On the use of statistical analysis for the objective determination of climatic change*, Meteorol. Z., Vol. 1(5), pp. 247-256;

[62] Soni V.K., Pandithurai G., Pai D.S. (2012): *Evaluation of long-term changes of solar radiation in India*, Int. J. Climatol., Vol. 32, pp. 540-551, doi:10.1002/joc.2294;

[63] Spinoni J., Brunetti M., Maugeri M., Simolo C. (2012): *1961-1990 monthly high-resolution solar radiation climatologies for Italy*, Adv. Sci. Res., Vol. 8, pp. 19-25, doi:10.5194/asr-8-19-2012;

[64] Stanhill G. (2005): *Global dimming: a new aspect of climate change*, Weather, Vol. 60(1), pp. 11-14, doi:10.1256/wea.210.03;

[65] Stanhill G. (2007): *A perspective on global warming, dimming, and brightening*, Eos. Trans. Amer. Geophys. Union, Vol. 88(5), pp. 58-59, doi:10.1029/2007EO050007;

[66] Stanhill G. and Cohen S. (2001): *Global dimming: A review of the evidence for a widespread and significant reduction in global radiation with discussion of its probable causes and possible agricultural consequences*, Agric. For. Meteorol., Vol. 107, pp. 255-278, doi:10.1016/S0168-1923(00)00241-0;

[67] Stanhill G. and Cohen S. (2005): *Solar radiation changes in United States during the twentieth century: Evidence from sunshine duration measurements*, J. Clim., Vol. 18, pp. 1503-1512, doi:10.1175/JCLI3354.1;

[68] Stanhill G. and Cohen S. (2008): *Solar radiation changes in Japan during the 20th century: Evidence from sunshine duration measurements*, J. Meteorol. Soc. Jpn., Vol. 86(1), pp. 57-67, doi:10.2151/jmsj.86.57;

[69] Stanhill G. and Moreshet S. (1992): *Global radiation climate changes: The world network*, Clim. Change, Vol. 21, pp. 57-75, doi:10.1007/BF00143253;

[70] Stravisi F. (2004): *Dati orari di eliofania: Trieste 1886-2003*, Universitá degli Studi di Trieste-Dipartimento di Scienze della Terra, Rap n104, OM 04/6;

[71] Streets D.G., Wu Y., Chin M.(2006): *Two-decadal aerosol trends as a likely explanation of the global dimming/brightening transition*, Geophys. Res. Lett., Vol. 33, L15806, doi:10.1029/2006GL026471;

[72] Suraqui S., Tabor H., Klein W.H., Goldberg B. (1974): *Solar radiation changes at Mt. St. Katherine after forty years*, Solar Energy, Vol. 16, pp. 155-158;

[73] Von Storch H. (1995): *Spatial patterns: EOFs and CCA*, in Analysis of Climate Variability: Applications of Statistical Techniques, edited by H. von Storch and A. Navarra, pp. 227-258, Springer, New York;

[74] Wang K.C. (2014): *Meausement biases explain discrepancies between the observed and simulated decadal variability of surface incident solar radiation*, Sci. Rep., Vol. 4(6144), doi:10.1038/srep06144;

[75] Wang K.C. and Dickinson R. (2013): *Contribution of solar radiation to decadal temperature variability over land*, Proc. Natl. Acad. Sci. U.S.A., Vol. 110(37), pp. 14877-14882, doi:10.1073/pnas.1311433110;

[76] Wang K.C., Dickinson R.E., Wild M., Liang S. (2012): *Atmospheric impacts on climatic variability of surface incident solar radiation*, Atmos. Chem. Phys., Vol. 12, pp. 9581-9592, doi:105194/acp-12-9581-2012;

[77] Wang K.C, Dickinson R.E., Ma Q., Augustine J.A., Wild M. (2013): *Measurement methods affect the observed global dimming and brightening*, J. Clim., Vol. 26, pp. 4112-4120, doi:10.1175/JCLI-D-12-00482.1;

[78] Wang Y.W. and Yang Y.H. (2014): *Chinas dimming and brightening: evidence, causes and hydrological implications*, Ann. Geophys., Vol. 32, pp. 4155, doi:10.5194/angeo-32-41-2014;

[79] Wild M. (2005): *From dimming to brightening: decadal changes in solar radiation at Earths surface*, Science, Vol. 308(5723), pp. 847-850, doi:101126/science-1103215;

[80] Wild M. (2009): *Global dimming and brightening: A review*, J. Geophys. Res., Vol. 114, D00D16, doi:10.1029/2008JD011470;

[81] Wild M. (2012): *Enlightening global dimming and brightening*, Bull. Amer. Meteor. Soc., Vol. 93, pp. 27-37, doi:10.1175/BAMS-D-11-00074.1;

[82] Wild M., Ohmura A., Makowski K. (2007): *Impact of global dimming and brightening on global warming*, Geophys. Res. Lett., Vol. 34, L04702, doi:10.1029/2006GL028031;

[83] Wild M., Ohmura A., Gilgen H., Rosenfeld D. (2004): *On the consistence of trends in radiation and temperature records and implications for the global hydro-logical cycle*, Geophys. Res. Lett., Vol. 31, L11201, doi:10.1029/2003GL019188;

[84] Wild M., Gilgen H., Roesch A., Ohmura A., Long C.N., Dutton E.G., Forgan B., Kallis A., Russak V., Tsvetkov A. (2005): *From dimming to brightening: Decadal changes in surface solar radiation at Earths surface*, Science, Vol. 308(5723), pp. 847-850, doi:10.1126/science.1103215;

[85] Wild M., Trüssel B., Ohmura A., Long C.N., König-Langlo G., Dutton E.G., Tsvetkov A. (2009): *Global dimming and brightening: An update beyond 2000*, J. Geophy. Res. Atm., Vol. 114, D00D13, doi:10.1029/2008JD011382;

[86] Wild M., Folini D., Schaer C., Loeb N., Dutton E. G., Koning-Langlo G. (2013): *The global energy balance from a surface perspective*, Clim. Dynamics, Vol. 40, pp. 3107-3134, doi:10.1007/s00382-012-1569-8;

[87] Wilks D.S. (1995): *Statistical methods in the atmospheric sciences*, Int. Geophys. Ser., Vol. 59, 2nd ed., 464 pp, Academic Press, New York;

[88] WMO-No.8 (1969): *Chapter 9, Solar radiation and Sunshine duration*, World Meteorological Organization, Guide to meteorological instruments and observing practices, Third edition;

[89] WMO-No.8 (2008): *Chapter 8, Measurement of Sunshine Duration*, World Meteorological Organization, Guide to Meteorological Instruments and Methods of Observation, Geneva, Switzerland, ISBN:978-92-63-10008-5;

[90] Xia X. (2010): *Spatiotemporal changes in sunshine duration and cloud amount as well as their relationship in China during 1954-2005*, J. Geophys. Res., Vol. 115, D00K06, doi:10.1029/2009JD012879;

[91] Xia X. (2013): *Variability and trend of diurnal temperature range in China and their relationship to total cloud cover and sunshine duration*, Ann. Geophys., Vol. 31, pp. 795-804, doi: 10.5194/angeo-31-795-2013.

Chapter 3

Detection of dimming/brightening in Italy from homogenized all-sky and clear-sky surface solar radiation records and underlying causes (1959-2013)

Abstract

A dataset of 54 daily Italian downward surface solar radiation (SSR) records has been set up collecting data for the 1959-2013 period. Special emphasis is given to the quality control and the homogenization of the records in order to ensure the reliability of the resulting trends. This step has been shown as necessary due to the large differences obtained between the raw and homogenized dataset, especially during the first decades of the study period. In addition, SSR series under clear-sky conditions were obtained considering only the cloudless days from corresponding ground-based cloudiness observations. Subsequently, records were interpolated onto a regular grid and clustered into two regions, northern and southern Italy, which were averaged in order to get all-sky and clear-sky regional SSR records. Their temporal evolution is presented, and possible reasons for differences between all-sky and clear-sky conditions and between the two regions are discussed in order to determine to what extent SSR variability depends on aerosols or clouds. Specifically, the all-sky SSR records show a decrease until the mid-1980s (dimming period), and a following increase until the end of the series (brightening period) even though strength and persistence of tendencies are not the same in all seasons. Clear-sky records present stronger tendencies than all-sky records during the dimming period in all seasons and during the brightening period in winter and autumn. This suggests that, under all-sky conditions, the variations caused by the increase/decrease in the aerosol content have

been partially masked by cloud cover variations, especially during the dimming period. Under clear sky the observed dimming is stronger in the south than in the north. This peculiarity could be a consequence of a significant contribution of mineral dust variations to the SSR variability.

3.1 Introduction

The fraction of solar radiation that reaches the Earth's surface is the source of energy which drives the majority of the processes in the atmosphere and in the oceans and plays a crucial role in a large number of sectors (e.g., agriculture, tourism, solar energy production) ([21]; [79]; [80]). For these reasons, it is very important to study the spatial distribution and the temporal behavior of surface solar radiation (SSR). Continuous observations by thermoelectric pyranometers at the Earth's surface date back to the 1920s, for example at the Stockholm site since 1923 ([63]; [83]). Surface radiation measurements started to become available on a widespread basis only in the late 1950s, with the establishment of numerous radiation sites during the International Geophysical Year (IGY) 1957-1958.
Studies of the last decades have demonstrated that SSR has not been constant over time ([14]; [27]; [42]; [52]; [66]), as shown by decadal fluctuations which exceed the accuracy limit of observational irradiance measurements (2% on an annual basis) ([18]). They report a decrease in SSR, "global dimming", of about 3-9Wm^{-2} from the 1950s to the 1980s and a subsequent increase, "brightening", of about 1-4Wm^{-2} from the beginning of the 1980s ([80]). These two periods are highlighted not only by studies focusing on specific regions ([24]; [31]; [55]; [57]; [58]; [78]) but also by studies focusing on worldwide datasets ([4]; [18]; [25]; [64]; [77]; [82], [83]).
The causes of these decadal variations are not completely clear: it has been suggested that changes in the anthropogenic aerosols and cloud cover can be major causes (e.g., [27]; [64]; [79]; [81]), while changes in radiatively active gas concentrations have, at least, globally a minor effect ([23]; [51]). Aerosols and clouds can interact in various ways and are therefore not completely independent ([49]). Aerosols act as a modulator of SSR by absorption or scattering of solar radiation (direct effect) ([48]; [72]) and by changing the number of cloud condensation nuclei particles (indirect aerosol effect) that also change albedo and cloud lifetime ([2]; [29]). The increase in anthropogenic aerosol emissions in the 20^{th} century is thought to have been the major cause of the observed decadal SSR reduction until the 1980s (e.g., [26]; [39]; [64]), while measures to reduce air pollution in the late 20^{th} century are possibly responsible for the renewed increase in SSR ([10]; [15]; [16]; [20]; [37]). Nevertheless, the relative contribution of clouds and aerosols is not yet clear, especially after comparing studies regarding different areas.
For these reasons, it is interesting to understand to what extent the SSR variability depends on aerosol variations or on changes in cloud characteristics. Different studies tried to estimate this distinction by using global climate models, satellite-derived products and ground-based observations, finding a good agreement between clear-sky SSR variations and

changes in aerosol emissions and concentrations, indicating aerosols as a major contributor to SSR variability at decadal scale ([81]). In addition, some studies analyzing all-sky SSR have highlighted the important contribution of clouds especially at an interannual scale ([17]; [34]; [39]; [43]; [85]; [86]). Other studies confirmed that changes in aerosols play a major role in the decadal variations in SSR ([28]; [88]), although there is a tendency to underestimate the dimming and brightening obtained with models with respect to trends obtained with ground-based observations. This has been attributed to possible deficiencies in aerosol emission inventories or an underestimation of aerosol direct radiative forcing ([3]; [9]; [17]; [53]). As concerns the aerosol radiative forcing, some studies tried to analyze the problem combining SSR series with optical depth and aerosol concentration observations finding a comparable or higher contribution of the direct aerosol effect with respect to the indirect aerosol effect ([37]; [38]; [41]; [54]; [71]). However, few studies have used only ground-based observations to obtain clear-sky and all-sky SSR series in order to investigate the aerosol-cloud effect ([24]; [25]; [31]; [54]; [82]); this is due to the difficulty in recovering high-temporal-resolution SSR series together with additional information on cloudiness or direct/diffuse radiation to discriminate clear-sky conditions ([30]; [79]).

In Italy, there have been no studies on the temporal evolution of SSR and its relation to aerosol concentrations and cloud cover variability. The best available information concerns sunshine duration (SD) for the 1936-2013 period ([33] - Chapter 2). It shows an increasing tendency starting in the 1980s preceded by a less evident decreasing tendency. Comparing these trends with corresponding cloud amount series, Manara et al. ([33] - Chapter 2) found that the expected negative correlation of these two variables is often not evident. This suggested that during the global dimming/brightening periods there is an important fraction of SD evolution that cannot be explained by cloud cover changes which must therefore depend on other factors such as changes in aerosol optical thickness. The temporal variations in aerosol optical thickness of the last decades seem to be mainly driven by anthropogenic emissions ([69]; [70]), even though, especially for southern Italy, mineral particles originating from Sahara and Sahel areas may also have a significant role, as recently suggested for Spain by Sanchez-Romero et al. ([60]). This natural atmospheric aerosol, with emissions that are highly variable from year to year, is a significant component of the Mediterranean area ([44]; [74]) causing reflection and absorption of the incoming solar radiation and therefore affecting the energy balance together with anthropogenic aerosols ([89]).

In this context, this work aims at collecting, quality checking, homogenizing (Section 3.2) and analyzing an extensive database of Italian SSR records in order to obtain average regional series under both all-sky (Section 3.3.1) and clear-sky conditions (Section 3.3.2). By doing this, we want to describe how SSR has changed in Italy during about the last 60 years and to explain how these variations depend on aerosols or cloud variability (Section 3.3.3, Section 3.4).

3.2 Data and data preprocessing

3.2.1 Data

The Italian SSR series used in this work were obtained at daily scale from the Italian Air Force stations (AM, Aeronautica Militare, 29 series - 1959-2013 period) and from the National Agro-meteorological Database (BDAN, Banca Dati Agrometeorologica Nazionale, 19 series - 1994-2013 period). Some information about the history of the AM observations are available in a report of the Italian Air Force ([22]) and the data for the 1964-2013 period are also available in the World Radiation Data Centre (WRDC) of the Main Geophysical Observatory in St. Petersburg. In order to increase data availability, especially for the Alpine region, we considered also the series from the meteorological observatory of Trieste (1971-2013 period) ([68]) and five series from Switzerland, close to the Italian border, from the Swiss Federal Office of Meteorology and Climatology (MeteoSwiss - 1981-2013 period).
The data that come from the AM stations and from the meteorological observatory of Trieste were recorded with the Robitzsch bimetallic actinograph until the 1980s. This instrument was then replaced with the Kipp & Zonen CM11 pyranometer in the first case and with different types of Kipp & Zonen CM pyranometers in the second one (for more details about AM instruments and instrument changes, see http://wrdc.mgo.rssi.ru/; for more details about Trieste instruments, see Stravisi [67]). The CM11 pyranometer was also used in the stations included in the BDAN database, with the only exception of two stations that used a Middleton EP07 pyranometer. Finally, the data that come from MeteoSwiss were measured with a Kipp & Zonen CM21 pyranometer.
The main difference between the Robitzsch bimetallic actinograph and the Keep & Zonen pyranometer is that the measure is mechanical in the first case and thermoelectrical in the second. Specifically, the Robitzsch pyranometer consists of a black metallic strip located between two white metallic strips. Due to differential absorption, a temperature difference is created between the strips which serves as a measure of radiation intensity. This temperature difference drives the position of a pen which allows recording of radiation intensity on a paper strip chart. The sensitivity range covers the entire spectrum of solar radiation; only radiation above 2μm in not included this, however, contributes only very little to the solar irradiance.
The Kipp & Zonen and Middleton pyranometers are based on a black-coated surface which is warmed up by solar radiation. The thermal energy is converted into measurable voltage, which is used to measure the solar irradiance. These pyranometers are provided with an automatic acquisition system which allows for recording of solar irradiance on a digital support. The spectral range covers the interval of 0.3-2.8μm.
The final dataset is composed of 54 daily series with data for the 1959-2013 period. All series have at least 15 years of data (Figure 3.1 and Table 3.1). The spatial distribution of the stations and the length of the series in relation to their location is uniform, the only exception are the series in the Alps and Apennines. All series are located in the plains

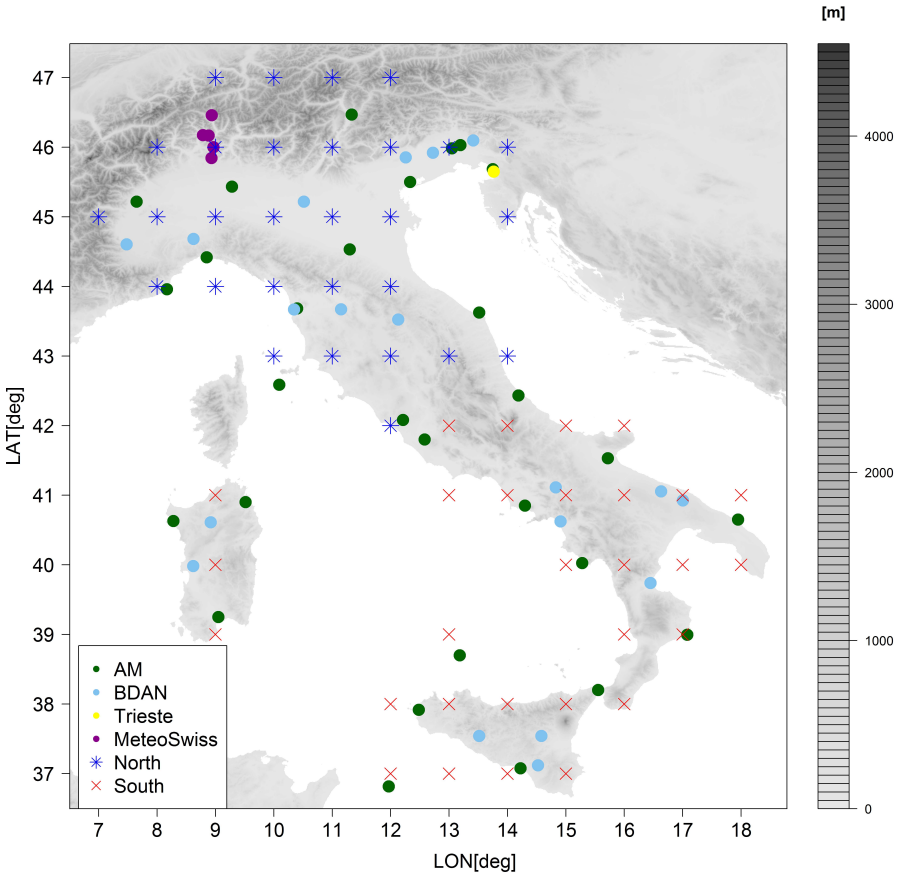

Figure 3.1: Spatial distribution of the stations and of the grid-mode version of the dataset (see Section 3.2.3): stars and crosses represent, respectively, northern (29 points) and southern (29 points) Italian grid points as clustered by a principal component analysis. The figure also shows the orography of the region and gives evidence of the sources of the station records, with green circles for AM series (29 series), blue circles for BDAN series (19 series), a yellow circle for the Trieste observatory and violet circles for MeteoSwiss series (5 series).

and coastal areas with elevation lower than 600m. Data availability versus time is rather inhomogeneous with a minimum before the beginning of the period covered by the BDAN series (Figure 3.2).

3.2.2 Data homogenization, gap filling and anomaly records

Before analyzing the time evolution of SSR, we subjected the records to a quality check and to a homogenization procedure. A quality check was performed at a daily timescale in order to find out and correct gross errors ([1]). Specifically, we searched for negative values and values exceeding the radiation at the top of the atmosphere. In addition, the reliability of station coordinates was checked by means of the comparison with station metadata and checking the elevation in relation to position. After the quality check, monthly series were calculated when the proportion of missing data did not exceed 20%.
All monthly records were subjected to homogenization in order to identify and eliminate non-climatic signals ([1]; [7]). Our aim was to identify time-dependent adjusting factors in

Network / Data Source	Station name	Country	Region	Latitude (deg)	Longitude (deg)	Elevation (m)	Period	Instrument (pyranograph, pyranometer)	Selected clear-sky 0 okta
METEO SWISS	ACQUAROSSA COMPROVASCO	CH	N	46.459	8.936	575	1988-2013	Kipp & Zonen CM21	N
AM	ALGHERO	I	S	40.630	8.280	23	1959-1989	Robitzsch	N
AM	AMENDOLA	I	S	41.530	15.720	57	1959-2010	Robitzsch and Kipp & Zonen CM11	Y
AM	ANCONA CAPPUCCINI	I	N	43.623	13.516	104	1959-1978	Robitzsch	Y
AM	BOLOGNA	I	N	44.530	11.300	36	1959-1989	Robitzsch	Y
AM	BOLZANO	I	N	46.467	11.333	241	1959-1988	Robitzsch	Y
AM	BRINDISI	I	S	40.650	17.950	15	1959-2013	Robitzsch and Kipp & Zonen CM11	Y
AM	CAGLIARI ELMAS	I	S	39.250	9.050	4	1959-2013	Robitzsch and Kipp & Zonen CM11	N
AM	CAPO MELE	I	N	43.958	8.170	220	1964-2003	Robitzsch and Kipp & Zonen CM11	Y
AM	CAPO PALINURO	I	S	40.025	15.280	184	1959-2013	Robitzsch and Kipp & Zonen CM11	Y
UCEA-BDAN	CARPENETO	I	N	44.681	8.624	230	1994-2013	Kipp & Zonen CM11	Y
UCEA-BDAN	CHILIVANI	I	S	40.610	8.919	216	1994-2013	Kipp & Zonen CM11	N
UCEA-BDAN	CIVIDALE	I	N	46.096	13.414	130	1997-2013	Kipp & Zonen CM11	Y
AM	CROTONE	I	S	38.996	17.080	155	1959-1989	Robitzsch	Y
UCEA-BDAN	FIUME VENETO	I	N	45.920	12.724	19	1996-2013	Kipp & Zonen CM11	Y
AM	GELA	I	S	37.076	14.225	33	1965-1997	Robitzsch and Kipp & Zonen CM11	Y
AM	GENOVA SESTRI	I	N	44.417	8.850	2	1959-1989	Robitzsch	Y
UCEA-BDAN	LIBERTINIA	I	S	37.541	14.581	188	1994-2013	Kipp & Zonen CM11	N
METEO SWISS	LOCARNO MONTI	CH	N	46.172	8.787	383	1981-2013	Kipp & Zonen CM21	N
METEO SWISS	LUGANO	CH	N	46.000	8.967	273	1981-2013	Kipp & Zonen CM21	Y
METEO SWISS	MAGADINO CADENAZZO	CH	N	46.167	8.883	197	1981-2013	Kipp & Zonen CM21	Y
AM	MESSINA	I	S	38.201	15.553	59	1959-2006	Robitzsch and Kipp & Zonen CM11	Y
AM	MILANO LINATE	I	N	45.433	9.283	107	1959-2010	Robitzsch and Kipp & Zonen CM11	Y
AM	NAPOLI	I	S	40.850	14.300	88	1959-1989	Robitzsch	Y
AM	OLBIA	I	S	40.900	9.517	13	1959-1988	Robitzsch	Y
UCEA-BDAN	PALO DEL COLLE	I	S	41.055	16.632	191	1994-2013	Middleton EP07	Y
AM	PANTELLERIA ISOLA	I	S	36.817	11.967	191	1959-2009	Robitzsch and Kipp & Zonen CM11	N
AM	PESCARA	I	S	42.433	14.189	10	1959-1987	Robitzsch	Y
UCEA-BDAN	PIANO CAPPELLE	I	S	41.113	14.827	152	1994-2013	Kipp & Zonen CM11	Y
AM	PIANOSA ISOLA	I	N	42.586	10.094	27	1959-1979	Robitzsch	Y
UCEA-BDAN	PIETRANERA	I	S	37.541	13.517	158	1994-2013	Kipp & Zonen CM11	Y
AM	PISA SAN GIUSTO	I	N	43.683	10.400	2	1959-2013	Robitzsch and Kipp & Zonen CM11	Y
UCEA-BDAN	PIUBEGA	I	N	45.217	10.514	38	1997-2013	Kipp & Zonen CM11	Y
UCEA-BDAN	PONTECAGNANO	I	S	40.623	14.911	38	1997-2013	Kipp & Zonen CM11	Y
AM	ROMA CIAMPINO	I	S	41.800	12.583	129	1959-2009	Robitzsch and Kipp & Zonen CM11	Y
UCEA-BDAN	SAN CASCIANO	I	N	43.670	11.151	230	1994-2013	Kipp & Zonen CM11	Y
UCEA-BDAN	SAN PIERO A GRADO	I	N	43.668	10.346	3	1994-2013	Kipp & Zonen CM11	Y
UCEA-BDAN	SANTA FISTA	I	N	43.523	12.130	311	1994-2013	Kipp & Zonen CM11	Y
UCEA-BDAN	SANTA LUCIA	I	S	39.982	8.620	14	1994-2013	Kipp & Zonen CM11	N
UCEA-BDAN	SANTO PIETRO	I	S	37.120	14.525	313	1994-2013	Kipp & Zonen CM11	Y
UCEA-BDAN	SIBARI	I	S	39.738	16.449	10	1994-2013	Kipp & Zonen CM11	Y
METEO SWISS	STABIO	CH	N	45.843	8.932	353	1981-2013	Kipp & Zonen CM21	Y
UCEA-BDAN	SUSEGANA	I	N	45.853	12.258	67	1994-2013	Middleton EP07	Y
AM	TORINO CASELLE	I	N	45.217	7.650	301	1959-1985	Robitzsch	Y
AM	TRAPANI BIRGI	I	S	37.917	12.483	7	1959-1996	Robitzsch and Kipp & Zonen CM11	N
AM	TRIESTE	I	N	45.683	13.750	4	1959-2001	Robitzsch and Kipp & Zonen CM11	Y
Observatory of Trieste	TRIESTE HORTIS	I	N	45.648	13.766	35	1971-2013	Robitzsch and Kipp & Zonen CM	Y
UCEA-BDAN	TURI	I	S	40.924	17.005	230	1994-2013	Middleton EP07	N
AM	UDINE CAMPOFORMIDO	I	N	46.029	13.196	94	1959-1978	Robitzsch	Y
AM	UDINE RIVOLTO	I	N	45.983	13.050	51	1964-2010	Robitzsch and Kipp & Zonen CM11	Y
AM	USTICA ISOLA	I	S	38.700	13.183	250	1959-1997	Robitzsch and Kipp & Zonen CM11	Y
AM	VENEZIA TESSERA	I	N	45.500	12.333	2	1959-1989	Robitzsch	Y
UCEA-BDAN	VERZUOLO	I	N	44.603	7.480	420	1995-2013	Kipp & Zonen CM11	Y
AM	VIGNA DI VALLE	I	N	42.081	12.211	275	1959-2013	Robitzsch and Kipp & Zonen CM11	Y

Table 3.1: Details on the network, station location, instruments and length of the records in the SSR dataset. The last column shows which records have been considered to calculate the regional mean under clear-sky conditions (see Section 3.2.4).

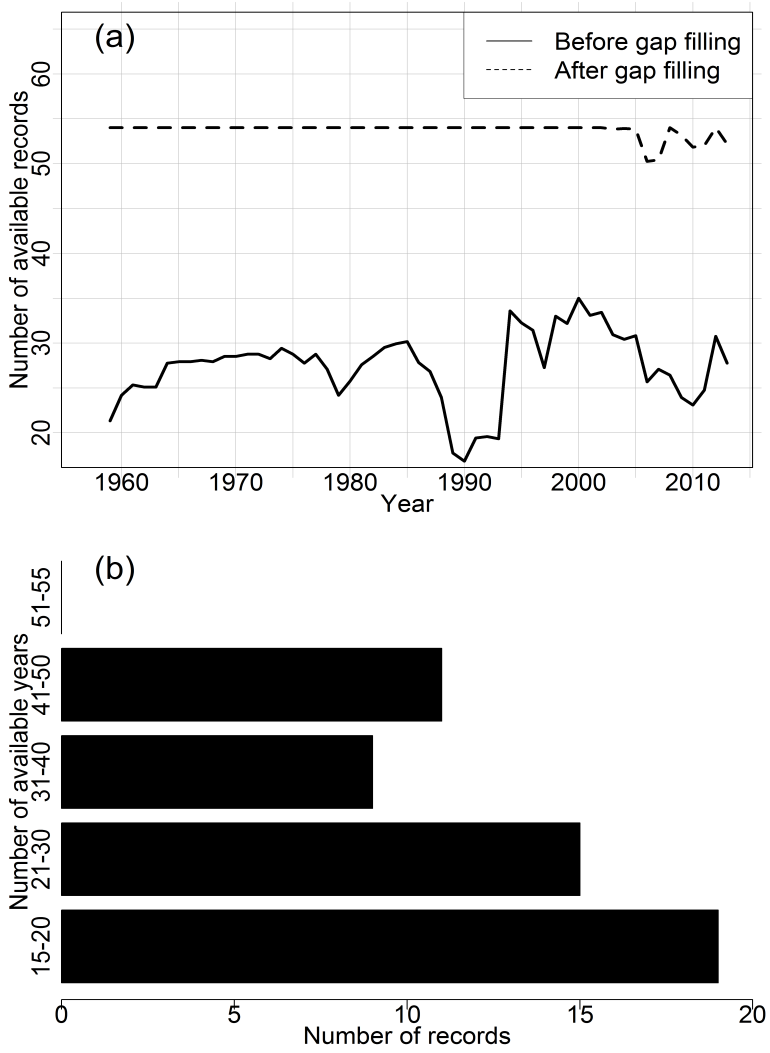

Figure 3.2: (a) Temporal evolution of the number of available records per year before (bold line) and after the gap-filling procedure (dashed line) (see Section 3.2.2); (b) The histogram shows the number of records as a function of the number of available years before the gap-filling procedure.

order to transform the original records into homogeneous ones. The homogenization of the series was performed using a procedure based on a relative homogeneity test ([7]) based on statistical methods supported by metadata information. Specifically, each test series is compared against 10 other reference series that correlate well with the test series by means of the Craddock test ([11]). This methodology is suitable to calculate correcting factors, but the identification of an inhomogeneity is not always easy and unambiguous ([7]). For this reason, we homogenize a period only when more reference series give coherent adjustment estimates. In this way, we can be more confident that the inhomogeneity is "real" and ascribable to the test series and not to the reference series. The reference series that result homogeneous in a sufficiently long sub-period centered on the break year are then selected to estimate the adjustments. We use several series to estimate the adjustments to increase their stability and to avoid unidentified outliers in the reference series from producing wrong corrections. By comparing the obtained breaks of each series with the corresponding metadata, we found in most of the cases a reasonable agreement between the breaks identified by the statistical method with information reported by metadata.
The common variance between two stations depends on their distance, and for the Italian territory, as previously found for SD ([33] - Chapter 2), it falls to 50% at a distance of about 150km. Homogenization was performed at a monthly timescale. However, a daily version of the adjustments was also generated in order to homogenize the daily series.
All analyzed series showed at least one inhomogeneous period highlighting the importance of homogenization, especially before 1980. The most relevant inhomogeneities fall in the first 20 years of the investigated period, where many instrument changes and recalibrations occurred, whereas the inhomogeneities are less relevant from the 1980s when the Robitzsch pyranograph was replaced in all AM stations by the CM11 pyranometer (Table 3.1), an instrument with higher quality, as recommended by the WMO ([22]).

Figure 3.3(a) shows the Italian average annual SSR anomaly series (relative anomalies with respect to the period 1976-2005) before and after homogenization with corresponding Gaussian low-pass filters (11-year window; 3-year standard deviation) that allow a better visualization of the decadal variability and long-term trend, while Figure 3.3(b) shows the curve obtained by averaging the mean annual adjustments over all single records, together with their absolute range. The details on how we obtained regional SSR anomaly series will be explained in the following sections.
The average annual records before and after the homogenization show a different decadal variability during the 1959-1970 and 1971-1980 periods, where increasing (average adjustment: 1.098) and decreasing (average adjustment: 0.964) correcting factors, respectively, have been applied to the original series. However, during the 1981-2013 period the two series show a similar behavior, where in fact only small correcting factors have been applied to the original series (average adjustment: 1.008). Overall, the use of the raw series hides the trends obtained during the study period, especially before the 1980s when the dimming period observed in the homogenized series is not evident during the 1960s and early 1970s.

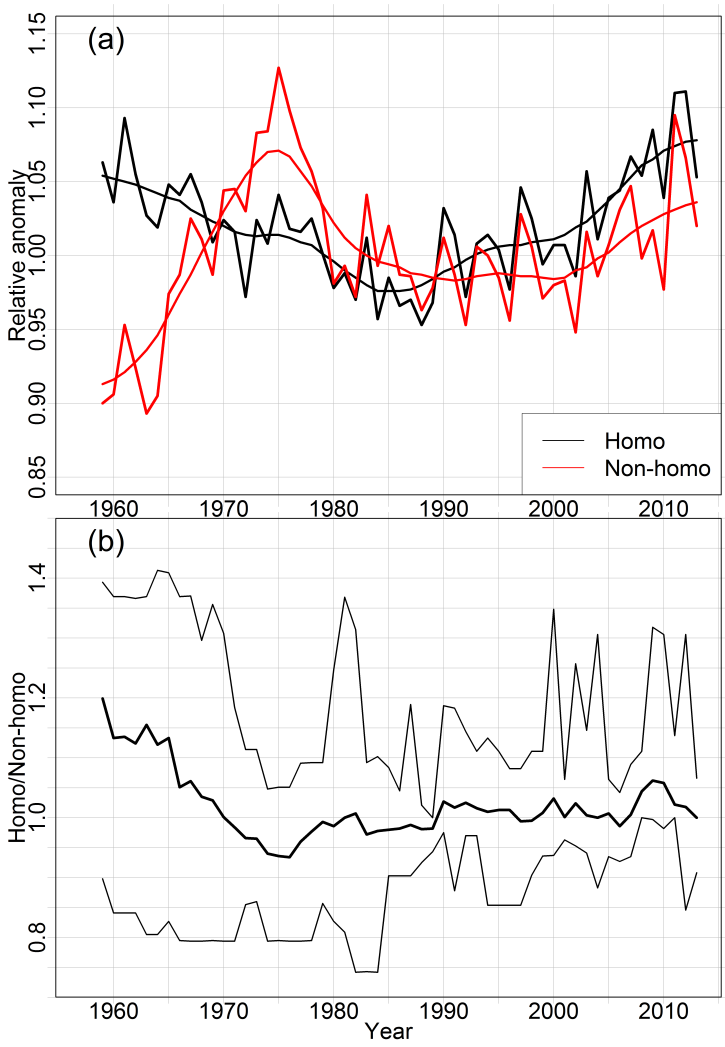

Figure 3.3: (a) Average annual Italian SSR series plotted together with an 11-year window, 3-year standard deviation Gaussian low-pass filter before (red line) and after (black line) the homogenization procedure; (b) Mean annual adjustment series is obtained by calculating the annual average adjustment over all series (bold line). The figure also shows the maximum range in the adjustments.

We filled the gaps in each monthly record using a procedure similar to that described in Manara et al. ([33] - Chapter 2). In particular, the median of a set of five estimated values, corresponding to the five highest correlated reference records, was selected in order to avoid outliers resulting from peculiar climatic conditions of the reference station. When fewer than five reference records fulfilling the requested conditions (distance within 500km from the record under analysis and at least six monthly values in common with it in the month of the gap) were available, the median was calculated with the available reference series. After the gap-filling procedure, all series had at least 90% of available data during the 1959-2013 period and 99% during the 1976-2005 period (Figure 3.2), used as the reference period to calculate the anomaly series. Therefore, all the series were transformed into monthly/seasonal/annual relative anomaly series with respect to the monthly/seasonal/annual 1976-2005 normals. Seasons are calculated according to the following scheme - December-January-February (winter), March-April-May (spring), June-July-August (summer) and September-October-November (autumn) - and the year is calculated for the December-November period. The winter season is dated to the year in which January and February fall, and, for the first year, the winter and the annual means are calculated using also the monthly mean of December 1958.

3.2.3 Gridding and regional average record

Starting from the monthly/seasonal/annual anomaly series, we generated a gridded version of the anomaly series with a resolution of 1° x 1° in order to balance the contribution of areas with a higher number of stations with the contribution of areas with a lower number of stations. This technique, explained in more detail by Brunetti et al. ([7]) and Manara et al. ([33] - Chapter 2), is based on an inverse distance weighting approach with the addition of an angular term to take into account the anisotropy in the spatial distribution of stations. The resulted grid spans from 7° to 18° E and from 37° to 47° N, with 58 grid points over the Italian territory (Figure 3.1).
Then, the monthly gridded anomaly records were subjected to a principal component analysis (PCA) in order to identify areas with similar SSR temporal variability. With this technique, it is possible to identify a small number of variables, which are linear functions of the original data and which maximize their explained variance ([46]; [84]). The analysis focused on the 1976-2005 period, the same reference period used to calculate the anomaly series. The analysis shows that the first five eigenvectors have an eigenvalue greater than 1 and they explain more than 91% of the total variance of the dataset. Then, we selected to rotate the first two empirical orthogonal functions (EOFs), which are those that account for 59% and 23%, respectively, of the original variance of the dataset, in order to obtain a more physically meaningful pattern ([76]). We decided to select these two EOFs because they account for 82% of the original variance while the other three only account for 9%. This procedure allowed to divide the Italian territory into two regions: northern Italy (29 grid points) and southern Italy (29 grid points) (Figure 3.1). Finally, we calculated the

monthly, seasonal and annual mean anomaly series for the two regions by averaging all corresponding grid point anomaly records. From here on, we refer to these series as the SSR anomaly series obtained under all-sky conditions to distinguish them from the series presented in the next section (Section 3.2.4) obtained selecting only the clear-sky days.

3.2.4 Clear sky series

Starting from the 54 homogenized daily SSR series presented in Section 3.2.1 and in Section 3.2.2, we aimed at determining clear SSR days for the 1959-2013 period. For this purpose, we used an updated version (both for number of series and for series length) of the total cloud cover (TCC) database presented by Maugeri et al. ([35]) as a reference to extract the clear-sky days. In particular, we considered only the days with a daily TCC mean of 0 okta. For the SSR series without a corresponding TCC series, we considered the data from nearby stations. The main limitation of the previous procedure is that the condition adopted to select clear-sky days (0 okta of TCC) often allow for a very low number of days to be selected. We therefore tried to apply a less restrictive condition and we also extracted the clear-sky days using 1 okta as the threshold. The average of clear-sky days per station and month is 9% for the 0 okta threshold and 18% for the 1 okta threshold. These fractions are however higher in summer when SSR is more important, reaching the maximum value in July with 17% of 0 okta days and 34% of days with less than 1 okta of TCC.
Then, the monthly mean was calculated when at least two clear-sky daily values were available in the considered month. After gap filling, the monthly/seasonal/annual relative anomaly series were obtained with respect to the 1976-2005 period using the same technique explained in Section 3.2.2. To calculate the anomaly series we considered only the series with at least 50% (for 0 okta) and 80% (for 1 okta) of available data in the 1976-2005 period after the gap filling. This reduced the series to 44 in the first case (Table 3.1). In the final step, we interpolated the anomaly series as described in Section 3.2.3 and obtained the regional anomaly series, for the two regions and the two thresholds, by averaging all corresponding grid point anomaly series.

3.3 Results

3.3.1 Trend analysis of the all-sky SSR records

The average northern and southern Italy annual and seasonal SSR records obtained under all-sky conditions are shown in Figure 3.4, together with the same low-pass filter used in Figure 3.3. In order to better understand the depth and the length of the tendencies showed in Figure 3.4, we subjected the records to a running trend analysis ([6]) estimating the trend slope of each sub-interval of at least 21 years by applying a linear regression. The results are shown in Figure 3.5. Specifically, we represent the length of the period considered for the analysis (y axes) in relation to the starting year of the

window that the trend refers to (x axes). Slopes are shown by means of the colors of the corresponding pixels, with large squares for trends with a significance level of $p \leq 0.1$ and small squares for trends with a significance level of $p > 0.1$ (considered here statistically non-significant), with significance levels estimated by means of the Mann-Kendall non parametric test ([61]).

At annual scale both regions show a decreasing tendency until the mid-1980s and a following increase until the end of the series, with a period of stabilization in the late 1990s. The trends of the two periods are comparable, especially in the southern region. In fact, the trend for the whole period under analysis (e.g., 1959-2013 period) is not statistically significant, as highlighted by the running trend analysis (Figure 3.5). However, the intensity of the dimming is slightly higher for the south than the north, especially for some windows starting in the mid-1960s (e.g., about -3% per decade for the north and about -4% per decade for the south for the 1965-1985 period), while the brightening is more intense in the north especially for the windows starting in the mid-1980s (e.g., about +4% per decade for the north and about +2% per decade for the south for the 1980-2010 period).

For the winter season, the records show a well-defined behavior with a dimming and a following brightening only in the northern region where the record shows statistically significant negative and positive tendencies for some periods starting in the 1960s and 1980s, respectively. However, the behavior is not well defined in the southern region, with a minimum in the mid-1980s and two secondary maxima during the 1970s and 1990s (Figure 3.4). As a consequence, the series shows only some sub-periods with a statistically significant trend. These sub-periods are less than 35 years long, and they start in the 1960s with a negative sign and in late 1970s/early 1980s with a positive sign. There is also a window extending 21 years, starting in 1990, with a significant decreasing tendency (-4% per decade) (Figure 3.5).

The spring season has a similar pattern to the annual one with a clear negative-positive sequence and a period of stabilization during the second half of the 1990s for both northern and southern Italy. The records show a comparable dimming for the two regions for periods longer than 30 years with variations of about -3% per decade (e.g., 1962-1992 period), while it is slightly stronger in the north if sub-periods starting in the mid-1960s with fewer than 30 years are considered in which variations range between -7% and -5% per decade. As concerns the brightening, it is stronger in the northern region, for both for long and short sub-periods, with values of about +6% per decade for some windows starting in the 1980s.

For the summer season the sequence of the dimming and brightening is evident and very similar to the annual and spring behavior only in the south. In the north, during the dimming period, there are only very few sub-periods with a significant decreasing trend, while in the south the most part of the windows starting in the 1960s have significant trends with variations of about -3% per decade (e.g., 1960-1990 period) indicating a reduction of SSR. However, the brightening period is quite comparable for the two regions

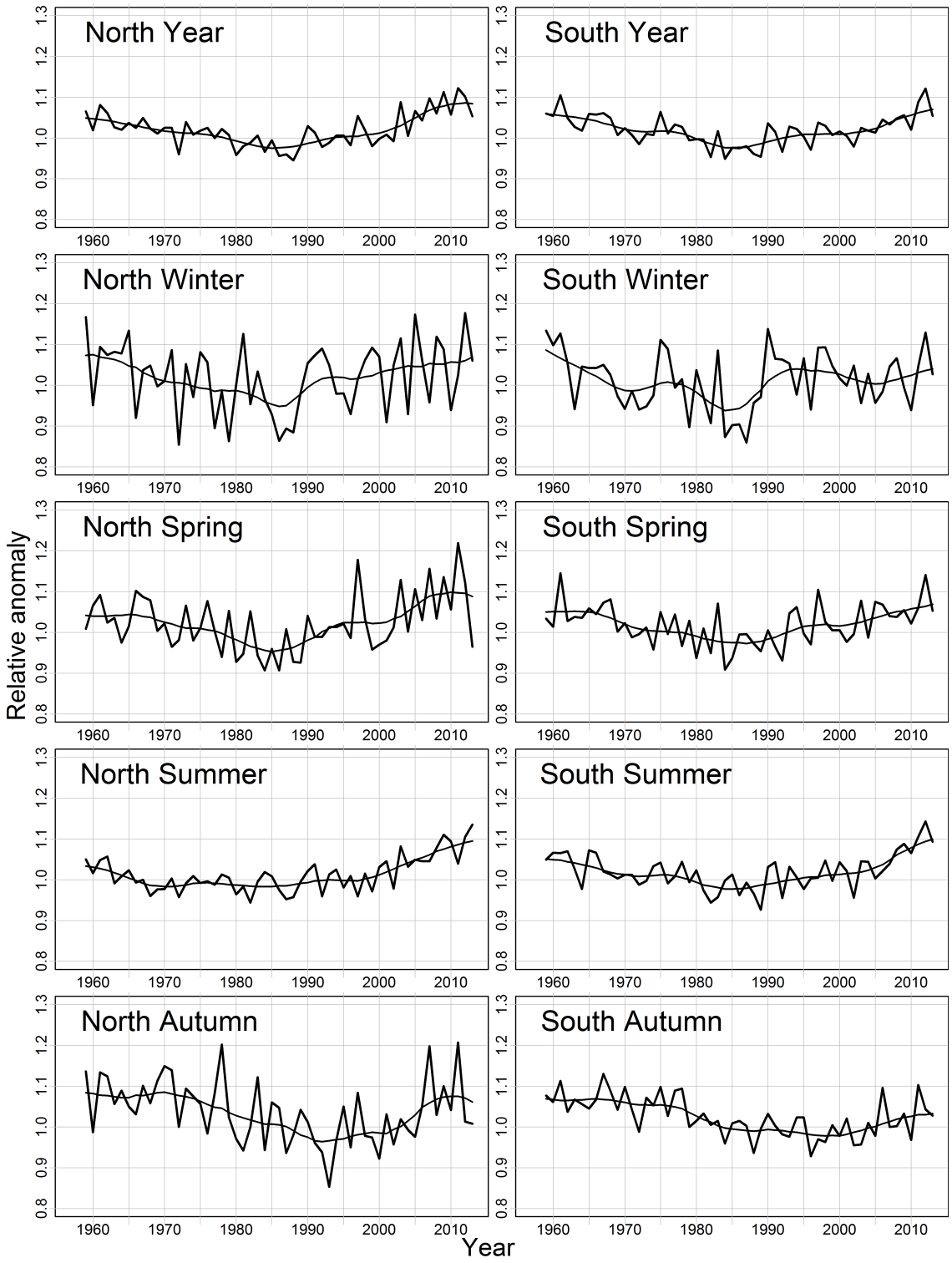

Figure 3.4: Average annual and seasonal northern (left column) and southern (right column) Italian SSR records obtained under all-sky conditions (bold lines), plotted together with an 11-year window, 3-year standard deviation Gaussian low-pass filter (thin lines). The series are expressed as relative deviations from the 1976-2005 means.

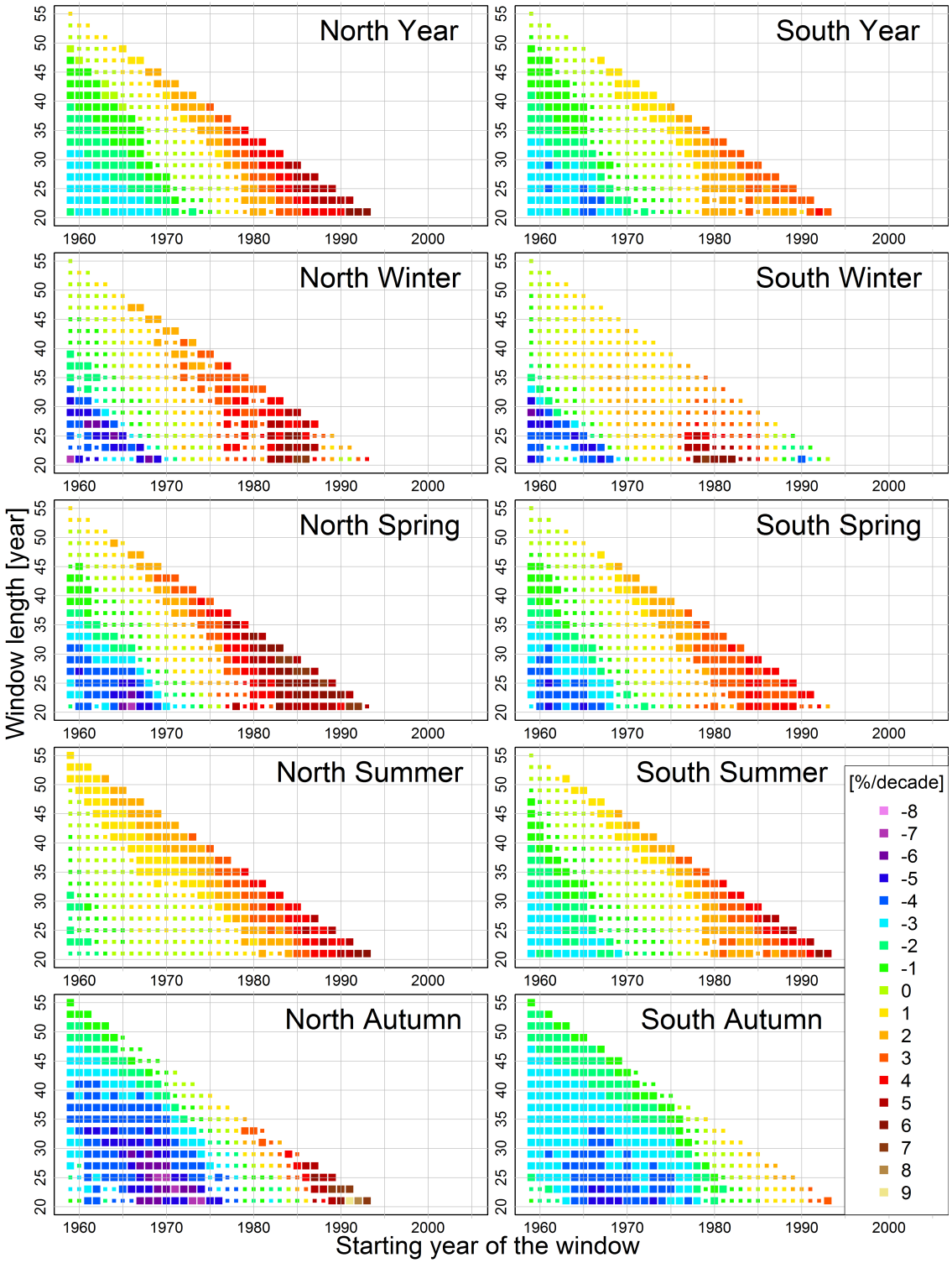

Figure 3.5: Running trend analysis for annual and seasonal northern (left column) and southern (right column) Italian SSR records obtained under all-sky conditions. The y and x axis represent the length and the first year of the period under analysis, respectively, while the colored pixels show the trend expressed in $\%decade^{-1}$ with a significance level of p≤0.1 (large squares) and p>0.1 (small squares).

		Year	Winter	Spring	Summer	Autumn
North all sky	1959-2013	+	+	+	**3.1±0.8**	**-1.5±0.7**
	1959-1985	***-4.4±0.8***	***-3.0±1.3***	***-7.2±2.2***	*-3.9±1.6*	*-3.5±1.9*
	1986-2013	***7.7±1.1***	***3.2±1.3***	***10.4±2.9***	***12.3±1.9***	***4.8±1.9***
	1970-2013	**2.9±0.7**	**1.4±0.7**	**4.8±1.5**	**6.1±1.0**	-
	1970-1985	**-4.0±1.9**	-	-	+	-7.8±4.6
	1981-2000	+	+	+	+	-
	1981-2013	**6.1±0.9**	**2.2±1.0**	**9.4±2.2**	**9.8±1.5**	+
South all sky	1959-2013	-	-	+	+	**-2.2±0.5**
	1959-1985	***-6.4±1.1***	***-4.6±1.4***	***-8.5±2.3***	***-8.1±2.0***	***-4.2±1.3***
	1986-2013	***6.0±1.2***	*+*	***7.6±2.0***	***13.5±2.3***	*+*
	1970-2013	**2.1±0.7**	+	**3.7±1.2**	**5.2±1.3**	**-1.5±0.8**
	1970-1985	-5.9±2.6	-	-	-	**-7.4±3.0**
	1981-2000	**5.0±1.9**	**6.5±2.6**	+	**9.3±3.5**	-2.4±1.7
	1981-2013	**5.4±0.9**	+	**6.9±1.7**	**11.6±1.8**	+
North clear sky estimated	1959-2013	+	-	+	+	-
	1959-1985	***-6.3±0.8***	***-3.2±0.8***	***-5.8±2.7***	***-8.2±1.6***	***-6.0±1.3***
	1986-2013	***7.6±0.9***	***3.6±0.7***	***9.7±1.6***	***10.0±1.5***	***6.5±1.3***
	1970-2013	**2.7±0.7**	0.9±0.4	**2.8±1.2**	**5.1±0.9**	**1.8±0.8**
	1970-1985	**-5.7±1.5**	-	-	**-6.9±2.4**	**-7.5±2.7**
	1981-2000	**5.3±1.6**	**3.2±1.4**	+	**7.1±2.1**	5.3±2.3
	1981-2013	**6.4±0.7**	**2.7±0.6**	**8.0±1.2**	**9.3±1.1**	**5.5±1.0**
South clear sky estimated	1959-2013	-	-	+	+	**-1.9±0.6**
	1959-1985	***-8.4±1.0***	***-4.4±1.2***	***-10.3±2.5***	***-10.7±1.8***	***-9.1±1.1***
	1986-2013	***7.9±1.0***	***3.9±1.3***	***10.2±1.6***	***11.4±1.9***	***5.4±1.1***
	1970-2013	**2.8±0.7**	**1.5±0.7**	**4.2±1.2**	**4.3±1.2**	+
	1970-1985	**-8.1±1.8**	-	**-11.3±5.2**	**-11.8±3.3**	**-10.2±2.1**
	1981-2000	**6.4±1.5**	**7.2±2.3**	**7.7±2.4**	**10.7±2.5**	+
	1981-2013	**7.1±0.8**	**3.7±1.0**	**9.2±1.2**	**10.7±1.5**	**4.5±0.8**

[a]Values are expressed in Wm^{-2} per decade. Values are shown in roman for significance level $0.05< p\leq 0.1$ and in bold for significance $p\leq 0.05$.
For not significant trends, only the sign of the slope is given.

Table 3.2: Absolute SSR trends in northern and southern Italy under all-sky conditions and estimated trends assuming no changes in cloudiness (see Section 3.3.3). The results concerning the dimming and brightening periods according to the northern and southern Italy annual records are highlighted in italic[a]

and reaches values of about +4% per decade (e.g., 1983-2013 period). The trends of the longest periods are significant and positive with values of about +1% per decade (e.g. 1959-2013 period) only in the north as a consequence of its weaker dimming in the early period.

The autumn records (Figure 3.4) start with a period without any trend for both regions and then show a decrease between the beginning of the 1970s and the beginning of the 1990s and a following increase, which is stronger in the northern than in the southern region. This picture is evident also in the running trends (Figure 3.5), especially for the brightening period, where some sub-periods have a positive trend after the beginning of the 1980s in the north and none has a positive trend in the south, with the only exception of one 21-year sub-period starting in the 1990s. However, most of the sub-periods starting in the 1960s and 1970s have significant and negative trends with values of about -3% per decade. The trend over the whole period under analysis (1959-2013 period) is significant and negative for both regions with values of about -2% per decade.

In order to give a more accurate information on the variations highlighted by Figure 3.4 and Figure 3.5, we estimated the trends in Wm^{-2} per decade for some key periods

(Table 3.2), including 1959-2013 (the entire period covered by the records), 1959-1985 and 1986-2013 (the dimming and brightening periods according to the northern and southern Italy annual records), and other periods to allow a direct comparison with some relevant dimming/brightening papers ([58]; [80]). Specifically, we calculated the absolute series for each grid point by multiplying each seasonal/annual anomaly series obtained under all-sky conditions by the corresponding seasonal/annual normals and then we calculated the seasonal and annual regional records, by averaging all corresponding grid point absolute series. The seasonal/annual normals were calculated by averaging the corresponding monthly normals obtained using the same data and the procedure explained by Spinoni et al. ([62]). In particular, the monthly normals were obtained starting from a database of SD normals for the Italian territory referring to flat and non-shaded sites. These normals were first transformed into SSR normals by means of the Ångström law and then interpolated onto the USGS GTOPO 30 digital elevation model grid ([73]) by means of an inverse distance gaussian weighting spatialization model.
As previously shown, the trend over the whole period under analysis (1959-2013) is only significant in summer in the north (+3.1Wm^{-2} per decade) and in autumn for both regions (-1.5Wm^{-2} and -2.2Wm^{-2} for the north and the south respectively). In the first case, considering the weak (and not-significant) dimming, the trend over the whole period is mostly driven by the increasing tendency of the second period while in the second case, considering the weak brightening, the trend over the whole period is mostly driven by the decreasing tendency of the first period. Considering the 1959-1985 period, as the reference for the dimming period, the trend is significant in all the seasons for both the north and the south with values ranging between -7.2Wm^{-2} per decade in spring and -3Wm^{-2} per decade in winter for the north and between -8.5Wm^{-2} per decade in spring and -4.2Wm^{-2} per decade in autumn for the south. As concerns the brightening period, considering the 1986-2013 period, the trend is significant in all the seasons in the northern region with values ranging between +3.2Wm^{-2} per decade in winter and +12.3Wm^{-2} per decade in summer, while in the southern region it is only significant at annual scale and during spring (+7.6Wm^{-2} per decade) and summer (+13.5Wm^{-2} per decade).

3.3.2 Trend analysis of the clear-ky SSR records

The average northern and southern Italy seasonal and annual SSR records obtained under clear-sky conditions using 0 okta and 1 okta as thresholds to select the clear days are shown in Figure 3.6. The correlations between the records obtained with the two thresholds are between 0.86 for the spring season and 0.97 for the winter season in the north and between 0.87 for the winter and autumn season and 0.95 for the summer season in the south. The agreement increases if the correlation between the filters is considered (it is always higher than 0.96). The decadal variability shown by the trends using the two thresholds is very similar, with the exception of a few periods where one of the two records shows a higher interannual variability causing slight differences in the resulting

trends. This is evident, for example, before the 1980s during the spring season in the north and during the winter season in the south; in both cases the 0 okta series shows higher variability than the 1 okta series. The difference in the resulting variability over the whole period under analysis (1959-2013) is particularly evident in the north where it is always higher in the 0 okta than in the 1 okta series (the standard deviation of the residuals from the low-pass filter is between 0.02 and 0.04 for the 0 okta series and between 0.01 and 0.03 for the 1 okta series), while it is less evident in the south where the two series show the same variability (the standard deviation of the residuals from the low-pass filter is between 0.02 and 0.05 for both the thresholds). The advantage of 0 okta as the threshold is that it allows for only the real clear-sky conditions to be selected, but the limitation of this choice is that it only allows for a low number of days to be selected (in the north it is particularly due to the higher frequency of cloudy days), thereby increasing the variability in the obtained series. However, using 1 okta as the threshold allows for a more stable series to be obtained because selects a higher number of days, which are, however, not completely clear.

In order to better understand the magnitude and the length of the tendencies shown in Figure 3.6, we subjected the clear-sky records to a running trend analysis ([6]), as previously illustrated for the all-sky series. The running trend obtained for the two different thresholds is very similar, so we show and discuss only the one obtained with 0 okta as threshold (Figure 3.7).

At annual scale the clear-sky records show a comparable decreasing and following increasing tendency for both the north and the south as highlighted by the lack of a significant trend for the whole period under analysis (e.g., 1959-2013 period). However, the dimming period is slightly stronger in the southern region, especially if the sub-periods with fewer than 30 years and starting before the 1970s are considered (e.g., about -4% per decade for the south and about -3% per decade for the north for the 1961-1991 period), while the brightening period is slightly more intense in the northern region (e.g., about +4% per decade for the north and about +3% per decade for the south for the 1981-2011 period). During the winter season, trends show a dimming and a subsequent brightening for both regions. The dimming is slightly stronger than the brightening and, as a consequence, the trend over almost the whole period under analysis is negative (e.g., -2% per decade during the 1959-2009 for both regions). Records show a period of stabilization during the mid-1970s and during the 2000s (Figure 3.6), and so some sub-periods, especially in the south do not show a significant trend after the beginning of the 1980s.

The spring season has a similar pattern to the annual one with a clear negative-positive sequence after a starting period without any significant trend and a period of stabilization in the 1990s, for both northern and southern Italy. The dimming period is stronger in the south than in the north where all the sub-periods with fewer than 30 years and starting before 1970 show a significant trend with values comprised between -8% per decade and -3% per decade. However, the brightening period is slightly stronger in the north especially after the mid-1980s, with values reaching +6% per decade.

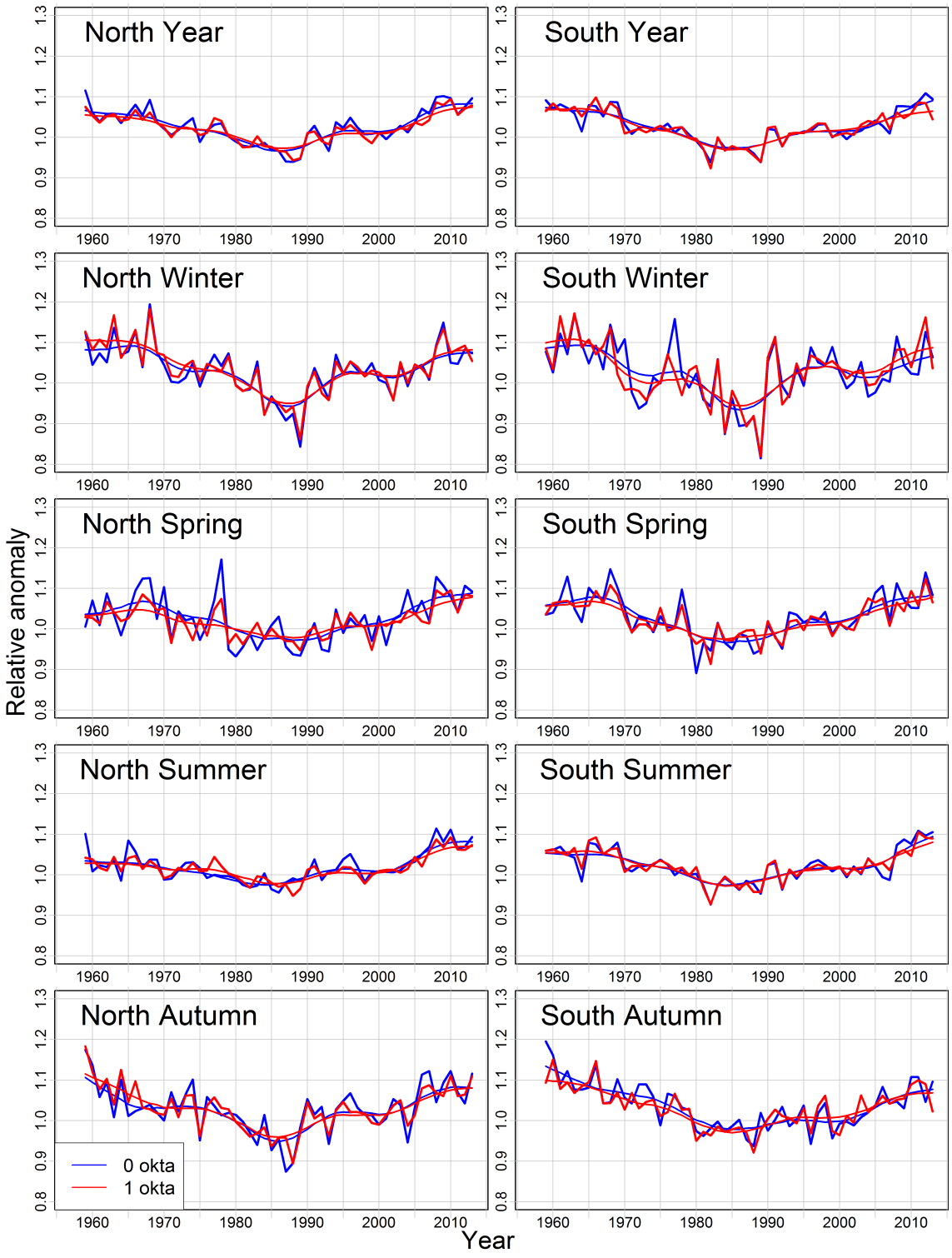

Figure 3.6: Average annual and seasonal northern (left column) and southern (right column) Italian SSR records obtained under clear-sky conditions (bold lines), plotted together with an 11-year window, 3-year standard deviation Gaussian low-pass filter (thin lines). The series are expressed as relative deviations from the 1976-2005 means. The blue lines represent the records obtained using 0 okta of TCC as the threshold to select clear days and the red lines the ones using 1 okta.

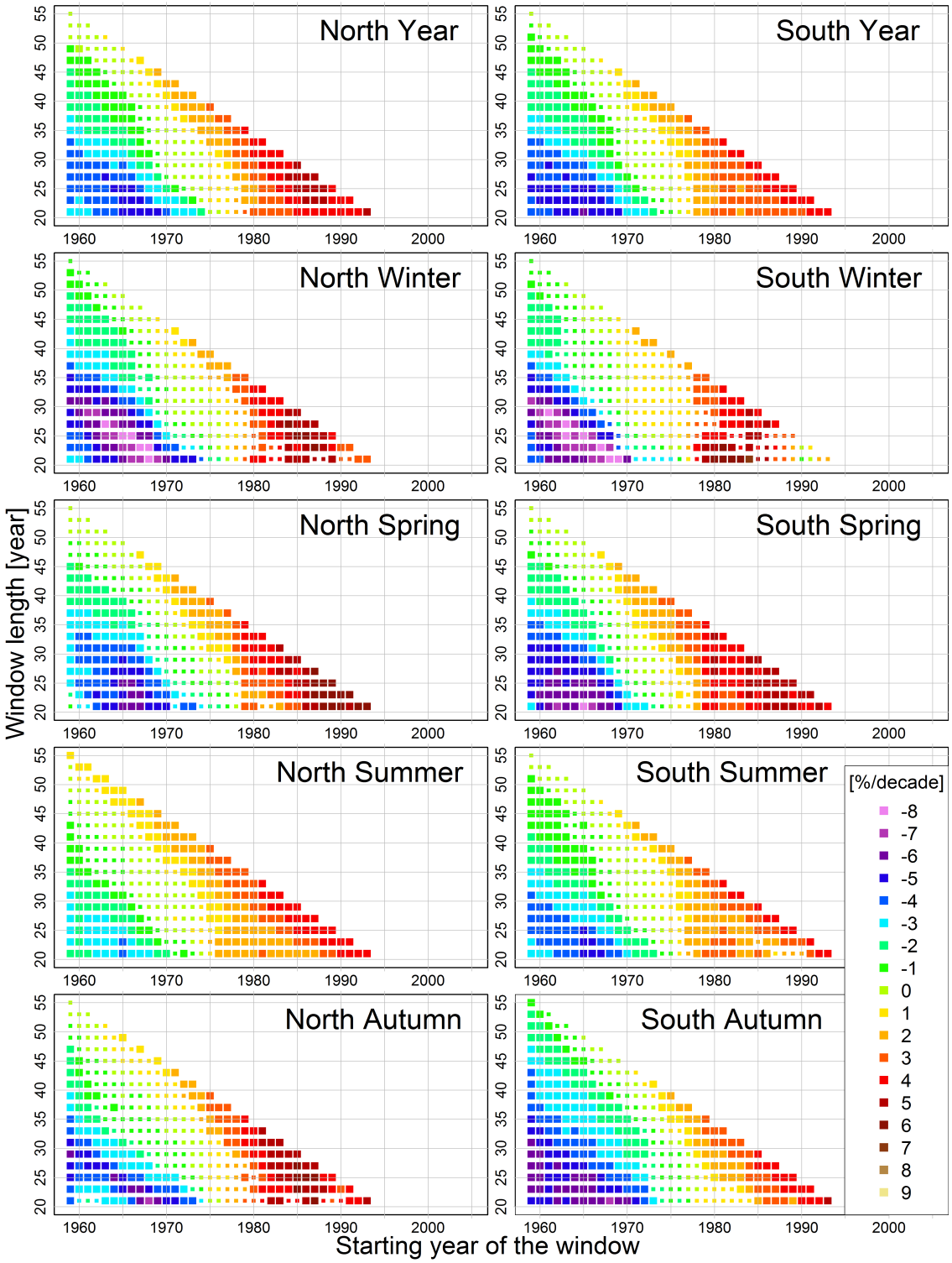

Figure 3.7: Running trend analysis for annual and seasonal northern (left column) and southern (right column) Italian SSR records obtained under clear-sky conditions (0 okta of TCC as threshold). The y and x axes represent the length and the first year of the period under analysis, respectively, while the colored pixels show the trend expressed in $\%decade^{-1}$ with a significance level of p≤0.1 (large squares) and p>0.1 (small squares).

During the summer season the two regions show a different trend with a stronger dimming period in the south than in the north (e.g., about -3% per decade for the south and about -2% per decade for the north for the 1961-1991 period) and a stronger brightening period in the north, with all the sub-periods with less than 30 years showing a significant trend. Summer in the north is the only season that shows a significant positive trend for the longest window (e.g., +1% per decade for the 1959-2013 period) while the summer season in the south, which shows a very similar behavior to the annual series, shows a negative trend for the windows that cover almost the whole period under analysis (e.g., -2% per decade for the 1959-2009 period).
For the autumn season, trends show a decrease until the mid-1980s followed by an increase until the end of the series in both regions, even if in the north a period of stabilization is observed during 1970s as already highlighted by the winter trend. The dimming period is stronger in the south than in the north (e.g., about -5% per decade for the south and about -4% per decade for the north for the 1961-1991 period), while the brightening is stronger in the north even if a period of stabilization is observed during 1990s, as already highlighted by the winter trend (e.g., about +4% per decade for the north and about +3% per decade for the south for the 1981-2011 period). Overall, in the northern region the trends of the two periods are comparable, while in the south the trend is stronger in the dimming period than in the brightening period, resulting in a significant negative trend over the whole period under analysis (e.g., about -2% per decade for the 1959-2013 period).

3.3.3 Comparison between all-sky and clear-sky SSR records

In order to better investigate the differences between the trends illustrated in Section 3.3.1 and in Section 3.3.2 and thus determine to what extent SSR variability depends on either cloud or aerosol variability, we compared the annual and seasonal low-pass filter series for all-sky and clear-sky conditions (considering 0 okta as the threshold) as shown in Figure 3.8. For clarity, only filters of the time series are indicated.

The comparison between the trends obtained under the two different conditions shows that, without the contribution of clouds, dimming and brightening become more intense and significant in all seasons for both north and south. The differences are particularly evident during winter and autumn seasons. Specifically, considering the winter season for both regions, the dimming period is more intense under clear-sky conditions than under all-sky conditions, with a significant trend for almost all sub-periods starting before the mid-1970s (see Figure 3.5 and Figure 3.7). As concern the brightening period, in the northern region it is comparable under clear and all-sky conditions if the trend intensity is considered, while it presents some differences if curve shapes are taken into account. However, in the southern region the brightening becomes stronger and significant under clear-sky conditions even if a period of stabilization is evident in the mid-1990s. After removing cloud contribution, during the autumn season the length and intensity of dim-

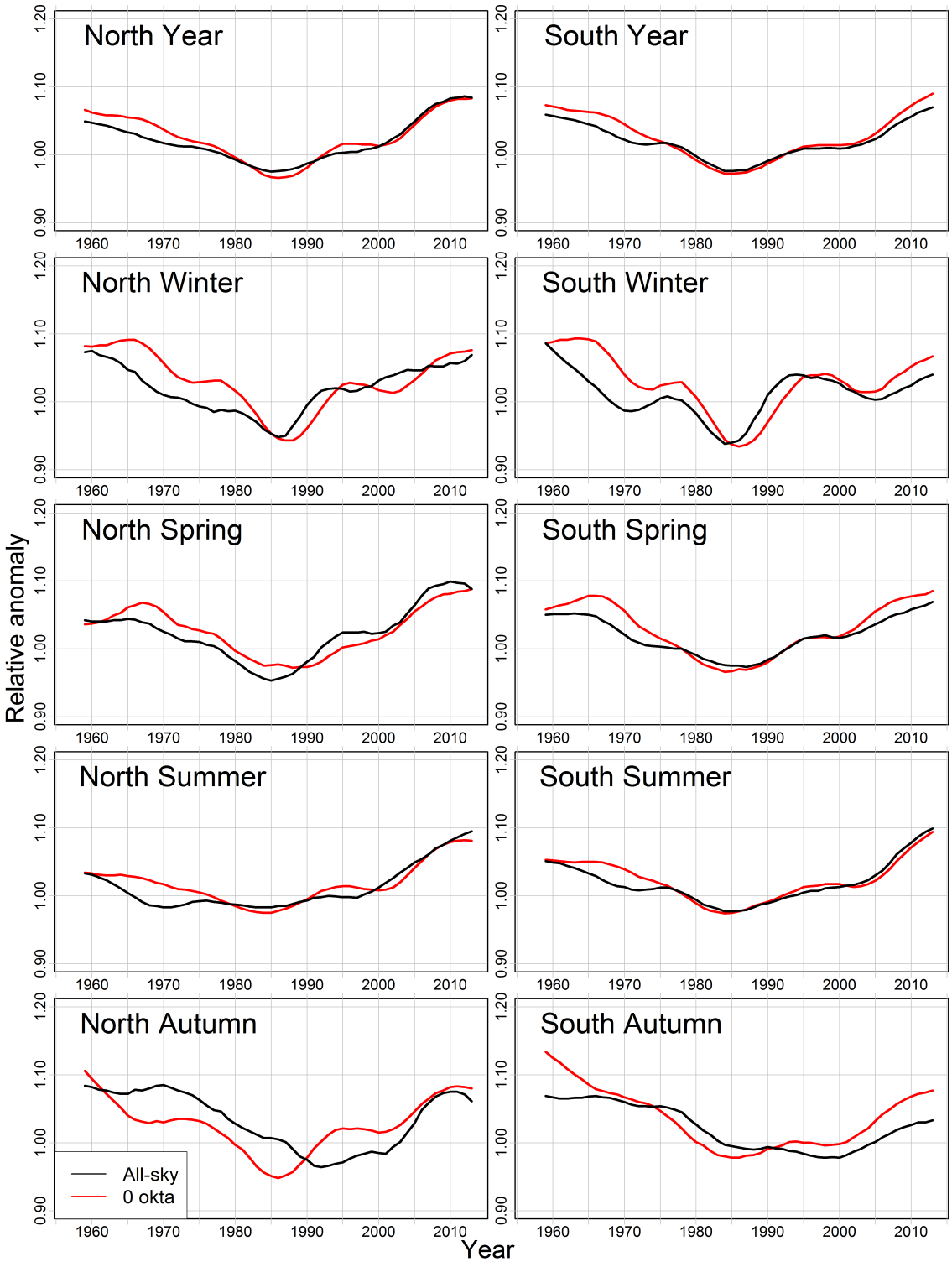

Figure 3.8: All-sky (black lines) and clear-sky 0 okta (red lines) SSR annual and seasonal low-pass filter for northern (left column) and southern (right column) Italy. The filters are the same as in Figure 3.4 and Figure 3.6.

ming and brightening periods change for both regions. This is due to a shift in the trend inversion from the beginning of the 1990s in the north and the end of the 1990s in the south to the mid-1980s as already observed for the other seasons for both all-sky and clear-sky conditions. This shift causes a shorter dimming period and a longer and more significant brightening period.

Differences between all-sky and clear-sky trends are less evident in spring and summer. Nevertheless, some differences are relevant in both seasons, especially during summer, in the north, where under all-sky conditions there is only a weak decrease, while it becomes more intense and significant under clear-sky conditions.

The differences between the all-sky and clear-sky anomaly records are also highlighted considering the ratios between the latter and the former records. Before 1980, low-pass filters applied to these ratios (figures not shown) show values higher than 1 in all seasons, with the only exception of autumn. Also, at annual scale, ratios are higher than 1 before about 1980, with maxima of 1.025 in the north (1967) and 1.024 in the south (1968) and a clear decrease in the 1970s. These results seem to suggest that, in Italy, global dimming has been partially hidden by a decreasing tendency of cloudiness and that without these changes in cloudiness the decrease in SSR in the dimming period would have been greater.

The comparison between clear-sky and all-sky anomaly records also allows for quantification of the effect of cloudiness on the observed SSR trends and thus the effect due to other factors. In this case, we have assumed that if cloudiness did not change, clear-sky and all-sky anomaly records would have had the same behavior. With this hypothesis, virtual constant-cloudiness SSR trends were estimated by transforming, by means of the all-sky normals already presented in Section 3.3.1, the trends of the clear-sky anomaly records (obtained with 0 okta as the threshold) into constant-cloudiness all-sky absolute trends. Trends expressed in Wm^{-2} per decade for the same periods considered in Table 3.2 for the all-sky series were calculated and the results are reported in the same table.

These values confirm what has already been highlighted by Figure 3.8. Assuming no changes in cloudiness, at the annual scale the trend during the dimming period (1959-1985) decreases to -6.3Wm^{-2} per decade in the north and -8.4Wm^{-2} per decade in the south (the corresponding all-sky trends are -4.4 and -6.4Wm^{-2} per decade, respectively), confirming that the variations in cloudiness partially masked the all-sky decreasing trends. However, the influence of the cloudiness variability is not evident during the brightening period (1986-2013) in the north where the all-sky and estimated constant-cloudiness records have almost the same trend, while it is more important in the south, where the trend increases from +6.0Wm^{-2} per decade (all sky) to +7.9Wm^{-2} per decade (estimated constant cloudiness). This behavior reflects the variations observed during winter, spring and summer. During autumn the cloudiness variability significantly influenced both periods and regions. In particular, during the brightening period the trend changes in the north from +4.8Wm^{-2} per decade (all sky) to +6.5Wm^{-2} per decade (estimated constant cloudiness) and in the south from a non-significant value (all sky) to +5.4Wm^{-2} per decade (estimated constant cloudiness).

Without cloud contribution, the correlation between north and south becomes higher: the correlation coefficients range from 0.53 (winter) to 0.78 (year) under all-sky conditions and from 0.67 (autumn) to 0.86 (year) under clear-sky conditions. The largest variation is observed in winter, the season more affected by clouds, where the correlation coefficient increases from 0.53 (all sky) to 0.84 (clear sky) while the smallest variation is observed in summer where the correlation coefficient changes from 0.74 (all sky) to 0.76 (clear sky). Under all-sky conditions the correlation between the two regions is higher in spring (0.64 for anomalies and 0.94 for filters) and summer (0.74 for anomalies and 0.89 for filters), while under clear-sky conditions the correlation is higher in winter (0.84 for anomalies and 0.96 for filters).

3.4 Discussion and conclusions

A new dataset of long-term Italian SSR records has been set up for collecting data from different sources. Particular emphasis is placed upon the quality control and the homogenization of the records in order to ensure the reliability of the resulting trends, which can be affected by non-climatic signals. The majority of the inhomogeneities detected in the series happen before 1980, when many recalibrations, changes in instruments and station relocations occurred, while they become less relevant in the subsequent period. This is also highlighted by the Italian annual mean series, where the dimming observed in the homogenized series is not evident in the raw series during the 1960s and early 1970s, showing how, at regional level, systematic biases in the original records can hide a significant part of the long-term trend.

Starting from the homogenized daily records, besides SSR series under all-sky conditions, SSR series under clear-sky conditions were also obtained by selecting clear days from corresponding ground-based TCC observations. Then, these series were projected onto a regular grid (1° x 1°) covering the entire Italian territory and clustered in two regions (northern and southern Italy) by means of a principal component analysis. The records of these areas were averaged in order to get the corresponding regional all-sky and clear-sky SSR records for the 1959-2013 period.

The clearest feature of the Italian all-sky SSR is a significant dimming from the beginning of the series to the mid-1980s and a subsequent brightening until the end of the series for the annual mean, as well as during winter and spring in the northern region and spring and summer in the southern region. The trend over the whole period (1959-2013) is only significant during summer (positive) in the north and during autumn (negative) for both regions, as a consequence of a very weak dimming in the first case and a very weak brightening in the second case.

In the clear-sky SSR records, dimming and brightening trends become stronger, and they are significant for all seasons and for both regions. The strength of the clear-sky trends is higher than that observed for the all-sky records, especially during winter in the south and during summer in the north. The most evident differences between all-sky and clear-sky

series are observed in autumn for both regions where not only the variations become more intense and significant but also the change point from dimming to brightening moves from the mid-1990s to the mid-1980s. Thus, the fact that the change point under all-sky and clear-sky conditions differs by several years in autumn and the intensity of the two periods changes in all seasons supports the hypothesis that clouds contribute in a significant way to the SSR variability under all-sky conditions and confirms the hypothesis formulated by Manara et al. ([33] - Chapter 2) for SD, suggesting that cloud cover variations have partially masked the dimming caused by the increasing aerosol concentration, especially in the northern region. This is also confirmed by Maugeri et al. ([35]) who found a highly significant negative trend in TCC all over Italy during the period 1951-1996.

The resulting trends without the contribution of the clouds show a more coherent pattern over the Italian territory. The peculiarities of a very weak dimming in summer for the north and a very weak brightening in winter for the south, as well as a strong and long dimming in autumn for both regions and the subsequent absence of brightening, are in fact attenuated under clear-sky conditions. The resulting trends under clear-sky conditions for both regions are in agreement with the changes in aerosol and aerosol precursor emissions that occurred during the period under analysis. More specifically, in Italy sulphur dioxide emissions, which can be converted to sulfate aerosols, show an increasing tendency until the 1980s due to the combustion of solid and liquid fuels ([36]) and a decreasing tendency in the following years ([32]; [75]). In parallel, the trends of black carbon and particulate organic matter show a change in tendency starting in the mid-1970s, which is earlier with respect to the sulfate aerosols due to the reduction in coal use in residential and commercial sectors as well as improved diesel engines ([40]). Therefore, the combination of these trends could to some degree explain the SSR variability under clear-sky conditions, suggesting anthropogenic aerosols to be a relevant contributor of SSR variations in Italy under clear-sky conditions.

The dimming in the south in spring, summer and autumn is stronger than in the north under clear-sky, and this fact may challenge the above hypothesis as the north is more affected by air pollution due to higher emissions. Nevertheless, southern Italy is more affected by coarse aerosols ([5]), causing a significant contribution of natural aerosols to SSR variability such as mineral dust intrusions from the Sahara and Sahel ([47]). In particular, we highlight that a comparison between the northern and southern Italian clear-sky SSR variations and the Sahel precipitation index shows a good agreement, especially in southern Italy and during the Sahel rainy season (summer and autumn). The correlation coefficients between these two variables over the period 1959-2013 are 0.85 and 0.79 for the south and 0.74 and 0.79 for the north, respectively, for the summer and autumn seasons, suggesting a possible connection between SSR and Sahel precipitation index variability. Equally, they show a similar behavior with a decreasing tendency from the beginning of the series until the mid-1980s and an increasing tendency in the following period. The results are also coherent with the fact that mineral dust transportation from northern Africa into Europe shows a pronounced seasonal cycle with a maximum in summer and

a minimum in winter ([44]; [74]) and a distinct gradient with the highest values near the northern coast of Africa ([19]; [47]).
Long-term variations in dust transport into Europe are confirmed by measurements of dust accumulation in Alpine snow, which show a clear increase in mineral dust since the early 1970s with quite high values after the 1980s. This suggests an increase in dust mobilization and transport from northern Africa to the north across the Mediterranean and into Europe ([13]; [32]) during the first part of the period covered by the SSR series. All this information supports the hypothesis that mineral dust contributes in a significant way to the SSR variability, with a higher contribution in the southern part of Italy than in the northern part especially during summer and autumn. This could also explain why the summer correlation between the north and the south remains low even under clear-sky conditions, suggesting that cloud cover is not the cause of this low correlation, thus pointing to a different source, such as dust transport, that affects the two regions in a different way. However, the stronger dimming observed in the north during winter could be a consequence of higher concentrations of anthropogenic aerosols in that region with respect to the south. However, in order to confirm all these hypotheses on the role of natural and anthropogenic aerosols, there is a need for a better understanding of the factors influencing dust generation and transport, as well as a better understanding of the spatial distribution and temporal evolution of the different types of aerosols that characterize the atmosphere in northern and southern Italy.
It is also worth noticing that the time series, both for all-sky conditions and for clear-sky conditions, show relevant minima in some seasons in the periods 1982-1983 and 1992-1993, possibly as a consequence of the El Chichón (April 1982) and Pinatubo (June 1991) volcanic eruptions, which injected high amounts of sulfur dioxide into the stratosphere, causing a worldwide reduction in direct solar radiation (e.g., [50]; [56]).
The observed trends under all-sky conditions are in good agreement with those observed in other worldwide areas and Europe. In particular, we compared the Italian trends with those obtained by Sanchez-Lorenzo et al. ([58]), using a new version of the GEBA (Global Energy Balance Archive) dataset updated to 2012, for southern Europe. This comparison shows similar trends in the dimming period, while in the brightening period the trends are significantly stronger for Italy than for southern Europe. This is in agreement with the SD trends reported by Manara et al. ([33] - Chapter 2) for Italy, where the brightening especially in the northern region appeared to be stronger compared to Europe.
The all-sky SSR trends presented for the Italian territory show some discrepancies with respect to the trends of SD obtained for the same areas reported by Manara et al. ([33] - Chapter 2), despite the fact that the correlations between the two variables over the period 1959-2013 are between 0.71 in autumn and 0.88 in spring in the north and between 0.58 in autumn and 0.75 in spring in the south. The deviation of the SSR series with respect to the SD series is a trend reversal shifted from the mid-1980s to the beginning of the 1980s and a dimming period that is more intense and significant. The agreement between the two variables increases if the correlations between the residuals (ratio between the

anomaly series and the filter) are considered; they are between 0.72 in summer and 0.91 in winter in the north and 0.62 at annual scale and 0.84 in spring for the south highlighting a good year-to-year correlation between the two variables.
The fact that the dimming in SD is weaker than in SSR could indicate that the long-term increase in aerosols affects the two variables in a different way inducing a more significant reduction in the intensity of SSR than in SD. The discrepancies between SSR and SD trends could also be a consequence of a different sensitivity to changes in the diurnal cycle and decadal variability of cloud cover, temperature and humidity that could modify the measurements of SD differently than SSR, but the reasons for these differences need further research. However, in a review, Sanchez-Romero et al. ([59]) reported some studies that found similar discrepancies between SD and SSR trends in different areas of the world such as Germany ([45]), China ([8]; [87]), the United States ([65]) and the Canadian Prairies ([12]).
A more detailed understanding of the mechanisms driving the SSR variability in Italy under both all-sky and clear-sky conditions calls for further research including also the study of other variables such as temperature, visibility, aerosols and cloudiness.

Bibliography

[1] Aguilar E., Auer I., Brunet M., Peterson T.C., Wieringa J. (2003): *Guidelines on Climate Metadata and Homogenization*, WMO-TD No. 1186, pp. 52, World Meteorological Organization, Geneva, Switzerland;

[2] Albrecht B.A. (1989): *Aerosols, cloud microphysics, and fractional cloudiness*, Science, Vol. 245(4923), pp. 1227-1230, doi:10.1126/science.245.4923.1227;

[3] Allen R.J., Norris J.R., Wild M. (2013): *Evaluation of multidecadal variability in CMIP5 surface solar radiation and inferred underestimation of aerosol direct effects over Europe, China, Japan, and India*, J. Geophys. Res. Atmos., Vol. 118(12), pp. 6311-6336, doi:10.1002/jgrd.50426;

[4] Alpert P., Kishcha P., Kaufman Y.J., Schwarzbard R. (2005): *Global dimming or local dimming?: Effect of urbanization on sunlight availability*, Geophys. Res. Lett., Vol. 32(17), L17802, doi:10.1029/2005GL023320;

[5] Bonasoni P., Cristofanelli P., Calzolari F., Bonafé U., Evangelisti F., Stohl A., Sajani Zauli S., van Dingenen R., Colombo T., Balkanski Y. (2004): *Aerosol-ozone correlations during dust transport episodes*, Atmos. Chem. Phys., Vol. 4, pp. 1201-1215, doi:1680-7324/acp/2004-4-1201;

[6] Brunetti M., Maugeri M., Nanni T., Auer I., Bhm R. and Schner W. (2006): *Precipitation variability and changes in the greater Alpine region over the 1800-2003 period*, J. Geophys. Res. Atmos., Vol. 111(11), pp. 129, doi:10.1029/2005JD006674;

[7] Brunetti M., Maugeri M., Monti F., Nanni T. (2006): *Temperature and precipitation variability in Italy in the last two centuries from homogenised instrumental time series*, Int. J. Climatol., Vol. 26(3), pp. 345-381, doi:10.1002/joc.1251;

[8] Che H.Z., Shi G.Y., Zhang X.Y., Arimoto R., Zhao J.Q., Xu L., Wang B., Chen Z.H. (2005): *Analysis of 40 years of solar radiation data from China, 1961-2000*, Geophys. Res. Lett., Vol. 32, L06803, doi:10.1029/2004GL022322;

[9] Cherian R., Quaas J., Salzmann M., Wild M. (2014): *Pollution trends over Europe constrain global aerosol forcing as simulated by climate models*, Geophys. Res. Lett., Vol. 41, pp. 2176-2181, doi:10.1002/2013GL0587151;

[10] Chiacchio M. and Wild M. (2010): *Influence of NAO and clouds on long-term seasonal variations of surface solar radiation in Europe*, J. Geophys. Res., Vol. 115, D00D22, doi:10.1029/2009JD012182;

[11] Craddock J.M. (1979): *Methods of comparing annual rainfall records for climatic purposes*, Weather, Vol. 34(9), pp. 332-346;

[12] Cutforth H.W. and Judiesch D. (2007): *Long-term changes to incoming solar energy on the Canadian Prairie*, Agr. Forest Meteorol., Vol. 145, pp. 167-175, doi:10.1016/j.agrformet.2007.04.011;

[13] De Angelis M. and Gaudichet A. (1991): *Saharan dust deposition over Mont Blanc (French Alps) during the last 30 years*, Tellus Ser. B, Vol. 43, pp. 61-75;

[14] Dutton E.G., Stone R.S., Nelson D.W., Mendonca B.G. (1991): *Recent interannual variations in solar radiation, cloudiness, and surface temperature at the South Pole*, J. Clim., Vol. 4(8), pp. 848-858;

[15] Dutton E.G., Farhadi A., Stone R.S., Long C.N., Nelson D.W. (2004): *Long-term variations in the occurrence and effective solar transmission of clouds as determined from surface-based total irradiance observations*, J. Geophys. Res. Atmos., Vol. 109(D3), doi:10.1029/2003JD003568;

[16] Dutton E.G., Nelson D.W., Stone R.S., Longenecker D., Carbaugh G., Harris J.M., Wendell J. (2006): *Decadal variations in surface solar irradiance as observed in a globally remote network*, J. Geophys. Res. Atmos., Vol. 111(D19), pp. 1-10, doi:10.1029/2005JD006901;

[17] Folini D. and Wild M. (2011): *Aerosol emissions and dimming/brightening in Europe: Sensitivity studies with ECHAM5-HAM*, J. Geophys. Res. Atmos., Vol. 116(D21), pp. 1-15, doi:10.1029/2011JD016227;

[18] Gilgen H., Wild M., Ohmura A. (1998): *Means and trends of shortwave irradiance at the surface estimated from global energy balance archive data*, J. Clim., Vol. 11, pp. 2042-2061, doi:10.1175/1520-0442-11.8.2042;

[19] Gkikas A., Hatzianastassiou N., Mihalopoulos N., Katsoulis V., Kazadzis S., Pey J., Querol X., Torres O. (2013): *The regime of intense desert dust episodes in the Mediterranean based on contemporary satellite observations and ground measurements*, Atmos. Chem. Phys., Vol. 13(23), pp. 12135-12154, doi:10.5194/acp-13-12135-2013;

[20] Hansen J., Sato M., Ruedy R. (1997): *Radiative forcing and climate response*, J. Geophys. Res.: Atm., Vol. 102(D6), pp. 6831-6864, doi:10.1029/96JD03436;

[21] Hartmann D.L., Ramanathan V., Berroir A., Hunt G.E. (1986): *Earth radiation budget data and climate research*, Rev. Geophys., Vol. 24(2), pp. 439-468, doi:10.1029/RG024i002p00439;

[22] Italian Air Force (2012): *La radiazione solare globale e la durata del soleggiamento in Italia dal 1991 al 2010*, Areonautica Militare, Reparto di Sperimentazione di Meteorologica Areonautica, pp. 1-53;

[23] Kvalevåg M.M. and Myhre G. (2007): *Human impact on direct and diffuse solar radiation during the industrial era*, J. Clim., Vol. 20, pp. 4874-4883, doi:10.1175/JCLI4277.1;

[24] Liang F. and Xia X.A. (2005): *Long-term trends in solar radiation and the associated climatic factors over China for 1961-2000*, Ann. Geophys., Vol. 23(7), pp. 2425-2432, doi:10.5194/angeo-23-2425-2005;

[25] Liepert B.G. (2002): *Observed reductions of surface solar radiation at sites in the United States and worldwide from 1961 to 1990*, Geophys. Res. Lett., Vol. 29(10), pp. 1421, doi:10.1029/2002GL014910;

[26] Liepert B. and Tegen I. (2002): *Multidecadal solar radiation trends in the United States and Germany and direct tropospheric aerosol forcing*, J. Geophys. Res. Atmos., Vol. 107(D12), AAC 7-1 - AAC 7-15, doi:10.1029/2001jD000760;

[27] Liepert B., Fabian P., Grassl H. (1994): *Solar radiation in Germany - observed trends and an assessment of their causes. Part I: regional approach, Contributions to Atmospheric Physics*, Vol. 67(1), pp. 15-29;

[28] Li Z., Xia X., Cribb M., Mi W., Holben B., Wang P., Chen H., Tsay S.C., Eck T.F., Zhao F., Dutton E.G., Dickerson R.E. (2007): *Aerosol optical properties and their radiative effects in northern China*, J. Geophys. Res. Atmos., Vol. 112(22), pp. 1-11, doi:10.1029/2006JD007382;

[29] Lohmann U. and Feichter J. (2005): *Global indirect aerosol effects: a review*, Atmos. Chem. Phys., Vol. 5, pp. 715-737, doi:1680-7324/acp/2005-5-715;

[30] Long C.N. and Ackerman T.P. (2000): *Identification of clear skies from broadband pyranometer measurements and calculation of downwelling shortwave cloud effects*, J. Geophys. Res., Vol. 105(D12), pp. 15609-15626, doi:10.1029/2000JD900077;

[31] Long C.N., Dutton E.G., Augustine J.A., Wiscombe W., Wild M., McFarlane S.A., Flynn C.J. (2009): *Significant decadal brightening of downwelling shortwave in the continental United States*, J. Geophys. Res., Vol. 114, D00D06, doi:10.1029/2008JD011263;

[32] Maggi V., Villa S., Finizio A., Delmonte B., Casati P., Marino F. (2006): *Variability of anthropogenic and natural compounds in high altitude-high accumulation alpine glaciers*, Hydrobiologia, Vol. 562, pp. 4356, doi:10.1007/s10750-005-1804-y;

[33] Manara V., Beltrano M.C., Brunetti M., Maugeri M., Sanchez-Lorenzo A., Simolo C., Sorrenti S. (2015): *Sunshine duration variability and trends in Italy from homogenized instrumental time series (1936-2013)*, J. Geophys. Res. Atmos., Vol. 120(9), pp. 3622-3641, doi:10.1002/2014JD022560;

[34] Mateos D., Sanchez-Lorenzo A., Antón M., Cachorro V.E., Calbó J., Costa M.J., Torres B., Wild M. (2014): *Quantifying the respective roles of aerosols and clouds in the strong brightening since the early 2000s over the Iberian Peninsula*, J. Geophys. Res. Atmos., Vol. 119(17), pp. 10382-10393, doi:10.1002/2014JD022076;

[35] Maugeri M., Bagnati Z., Brunetti M., Nanni T. (2001): *Trends in italian total cloud amount, 1951-1996*, Geophys. Res. Lett., Vol. 28(24), pp. 4551-4554, doi: 10.1029/2001GL013754;

[36] Mylona S. (1996): *Sulphur dioxide emissions in Europe 1880-1991 and their effect on sulphur concentrations and depositions*, Tellus Ser. B, Vol. 48, pp. 662-689;

[37] Nabat P., Somot S., Mallet M., Sanchez-Lorenzo A., Wild M. (2014): *Contribution of anthropogenic sulfate aerosols to the changing Euro-Mediterranean climate since 1980*, Geophys. Res. Lett., Vol. 41(15), pp. 5605-5611, doi:10.1002/2014GL060798;

[38] Nabat P., Somot S., Mallet M., Sevault F., Chiacchio M., Wild M. (2015): *Direct and semi-direct aerosol radiative effect on the Mediterranean climate variability using a coupled regional climate system model*, Clim. Dynamics, Vol. 44(3), pp. 1127-1155, doi:10.1007/s00382-014-2205-6;

[39] Norris J.R. and Wild M. (2007): *Trends in aerosol radiative effects over Europe inferred from observed cloud cover, solar "dimming", and solar "brightening"*, J. Geophys. Res., Vol. 112, D08214, doi:10.1029/2006JD007794;

[40] Novakov T., Ramanathan V., Hansen J.E., Kirchstetter T.W., Sato M., Sinton J.E., Sathaye J.A. (2003): *Large historical changes of fossil-fuel black carbon aerosols*, Geophys. Res. Lett., Vol. 30(6), pp. 1324, doi:10.1029/2002GL016345;

[41] Ohmura A. (2009): *Observed decadal variations in surface solar radiation and their causes*, J. Geophys. Res., Vol. 114, D00D05, doi:10.1029/2008JD011290;

[42] Ohmura A. and Lang H. (1989), *Secular variation of global radiation in Europe*, in IRS88: Current Problems in Atmospheric Radiation, edited by J. Lenoble and J.-F. Geleyn, pp. 298-301, A. Deepak, Hampton, Va;

[43] Parding K., Olseth J.A., Dagestad K.F., Liepert B.G. (2014): *Decadal variability of clouds, solar radiation and temperature at a high-latitude coastal site in Norway*, Tellus Ser. B, Vol. 66, doi:10.3402/tellusb.v66.25897;

[44] Pey J., Querol X., Alastuey A., Forastiere F., Stafoggia M. (2013): *African dust outbreaks over the Mediterranean Basin during 2001-2011: PM10 concentrations, phenomenology and trends, and its relation with synoptic and mesoscale meteorology*, Atmos. Chem. Phys., Vol. 13(3), pp. 1395-1410, doi:10.5194/acp-13-1395-2013;

[45] Power H.C. (2003): *Trends in solar radiation over Germany and an assessment of the role of aerosols and sunshine duration*, Theor. Appl. Climatol., Vol. 76, pp. 4763, doi:10.1007/s00704-003-0005-8;

[46] Preisendorfer R.W. (1988): *Principal component analysis in meteorology and oceanography*, edited by Elsevier, New York.;

[47] Prospero J.M. (1996): *Saharan dust transport over the North Atlantic Ocean and Mediterranean: An overview, The Impact of Desert Dust across the Mediterranean*, Vol. 11, pp. 133-151, doi:10.1007/978-94-017-3354-0;

[48] Radke L.F., Coakley J.A., King M.D. (1989): *Direct and remote sensing observations of the effects of ships on clouds*, Science, Vol. 246(4934), pp. 1146-1149, doi:10.1126/science.246.4934.1146;

[49] Ramanathan V., Crutzen P.J., Kiehl J.T., Rosenfeld D. (2001): *Aerosol, climate, and the hydrological cycle*, Science, Vol. 294(5549), pp. 2119-2124, doi:10.1126/science.1064034;

[50] Robock A. (2000): *Vulcanic eruptions and climate*, Rev. Geophys., Vol. 38(2), pp. 191-219, doi:10.1029/1998RG000054;

[51] Romanou A., Liepert B., Schmidt G.A., Rossow W.B., Ruedy R.A., Zhang Y. (2007): *20th Century Changes in Surface Solar Irradiance in Simulations and Observations*, Geophys. Res. Lett., Vol. 34(5), doi:10.1029/2006GL028356;

[52] Russak V. (1990): *Trends of solar radiation, cloudiness and atmospheric transparency during recent decades in Estonia*, Tellus Ser. B, Vol. 42, pp. 206-210;

[53] Ruckstuhl C. and Norris J.R. (2009): *How do aerosol histories affect solar "dimming" and "brightening" over Europe?: IPCC-AR4 models versus observations*, J. Geophys. Res, Vol. 114, D00D04, doi:10.1029/2008JD011066;

[54] Ruckstuhl C., Philipona R., Behrens K., Coen M.C., Dürr B., Heimo A., Mätzler C., Nyeki S., Ohmura A., Vuilleumier L., Weller M., Wehrli C., Zelenka A. (2008), *Aerosol and cloud effects on solar brightening and the recent rapid warming*, Geophys. Res. Lett., Vol. 35, L12708, doi:10.1029/2008GL034228;

[55] Sanchez-Lorenzo A. and Wild M. (2012): *Decadal variations in estimated surface solar radiation over Switzerland since the late 19th century*, Atmos. Chem. Phys., Vol. 12, pp. 8635-8644, doi:10.5194/acp-12-8635-2012;

[56] Sanchez-Lorenzo A., Calbó J., Brunetti M., Deser C. (2009): *Dimming/brightening over the Iberian Peninsula: Trends in sunshine duration and cloud cover and their relations with atmospheric circulation*, J. Geophys. Res., Vol. 114, D00D09, doi:10.1029/2008JD011394;

[57] Sanchez-Lorenzo A., Calbo J., Wild M. (2013): *Global and diffuse solar radiation in Spain: building a homogeneous dataset and assessing their trends*, Glob. Planet. Change, Vol. 100, pp. 343-352, doi:10.1016/j.gloplacha.2012.11.010;

[58] Sanchez-Lorenzo A., Wild M., Brunetti M., Guijarro J.A., Hakuba M.Z., Calbó J., Mystakidis S., Bartok B.: *Reassessment and update of long-term trends in downward surface shortwave radiation over Europe (1939-2012)*, J. Geophys. Res. Atmos., Vol. 120(18), pp. 9555-9569, doi:10.1002/2015JD023321;

[59] Sanchez-Romero A., Sanchez-Lorenzo A., Calbó J., González J.A., Azorin-Molina C. (2014): *The signal of aerosol-induced changes in sunshine duration records: A review of the evidence*, J. Geophys. Res. Atmos., Vol. 119(8), pp. 4657-4673, doi:10.1002/2013JD021393;

[60] Sanchez-Romero A., Sanchez-Lorenzo A., González J.A., Calbó J. (2016): *Reconstruction of long-term aerosol optical depth series with sunshine duration records*, Geophys. Res. Lett., Vol. 43, doi:10.1002/2015GL067543;

[61] Sneyers R. (1992): *On the use of statistical analysis for the objective determination of climate change*, Meteorologische Zeitschrift, Vol. 1(5), pp. 247-256;

[62] Spinoni J., Brunetti M., Maugeri M., Simolo C. (2012): *1961-1990 monthly high-resolution solar radiation climatologies for Italy*, Adv. Sci. Res., Vol. 8, pp. 19-25, doi:10.5194/asr-8-19-2012;

[63] Stanhill G. (1983): *The distribution of global solar radiation over the land surfaces of the Earth*, Solar Energy, Vol. 31(1), pp. 95-104;

[64] Stanhill G. and Cohen S. (2001): *Global dimming: A review of the evidence for a widespread and significant reduction in global radiation with discussion of its probable causes and possible agricultural consequences*, Agric. For. Meteorol., Vol. 107, pp. 255-278, doi:10.1016/S0168-1923(00)00241-0;

[65] Stanhill G. and Cohen S. (2005): *Solar Radiation Changes in the United States during the Twentieth Century: Evidence from Sunshine Duration Measurements*, Am. Meteorol. Soc., Vol. 18(10), pp. 1503-1512;

[66] Stanhill G. and Moreshet S. (1992): *Global radiation climate changes: The world network*, Clim. Change, Vol. 21, pp. 57-75, doi:10.1007/BF00143253;

[67] Stravisi F. (2004): *TRIESTE Dati orari di irradianza solare 1971-2003*, Universitá degli Studi di Trieste-Dipartimento di Scienze della Terra, Rapporti OM N. 105;

[68] Stravisi F. and Cirilli S. (2014): *Irradianza solare globale 2013*, Universit degli Studi di Trieste-Dipartimento di Scienze della Terra, Rap n°159;

[69] Streets D.G., Wu Y., Chin M. (2006): *Two-decadal aerosol trends as a likely explanation of the global dimming/brightening transition*, Geophys. Res. Lett., Vol. 33(15), L15806, doi:10.1029/2006GL026471;

[70] Streets D.G., Yan F., Chin M., Diehl T., Mahowald N., Schultz M., Wild M., Wu Y., Yu C. (2009): *Anthropogenic and natural contributions to regional trends in aerosol optical depth, 1980-2006*, J. Geophys. Res., Vol. 114(D10), pp. 116, doi:10.1029/2008JD011624;

[71] Turnock S.T., Spracklen D.V., Carslaw K.S., Mann G.W., Woodhouse M.T., Forster P.M., Haywood J., Johnson C.E., Dalvi M., Bellouin N., Sanchez-Lorenzo A. (2015): *Modelled and observed changes in aerosols and surface solar radiation over Europe between 1960 and 2009*, Atmos. Chem. Phys., Vol. 15(16), pp. 9477-9500, doi:10.5194/acp-15-9477-2015;

[72] Twomey S.A., Piepgrass M., Wolfe T.L. (1984): *An assessment of the impact of pollution on global cloud albedo*, Tellus Ser. B, Vol. 36, pp. 356-366, doi:10.1111/j.1600-0889.1984.tb00254.x;

[73] USGS (1996): GTOPO 30 Digital Elevation Model, [online] Available from: https://lta.cr.usgs.gov/GTOPO30;

[74] Varga G., Újvári G., Kovács J. (2014): *Spatiotemporal patterns of Saharan dust outbreaks in the Mediterranean Basin*, Aeolian Research, Vol. 15, pp. 151-160, doi:10.1016/j.aeolia.2014.06.005;

[75] Vestreng V., Myhre G., Fagerli H., Reis S., Tarrasón L. (2007): *Twenty-five years of continuous sulphur dioxide emission reduction in Europe*, Atmos. Chem. Phys., Vol. 7(13), pp. 3663-3681, doi:10.5194/acp-7-3663-2007;

[76] Von Storch H. (1995): *Spatial patterns: EOFs and CCA*, in Analysis of Climate Variability: Applications of Statistical Techniques, edited by H. von Storch and A. Navarra, pp. 227-258, Springer, New York;

[77] Wang K.C., Dickinson R.E., Wild M., Liang S. (2012): *Atmospheric impacts on climatic variability of surface incident solar radiation*, Atmos. Chem. Phys., Vol. 12, pp. 9581-9592, doi:105194/acp-12-9581-2012;

[78] Wang Y.W. and Yang Y.H. (2014): *China's dimming and brightening: evidence, causes and hydrological implications*, Ann. Geophys., Vol. 32, pp. 41-55, doi:10.5194/angeo-32-41-2014;

[79] Wild M. (2009): *Global dimming and brightening: A review*, J. Geophys. Res., Vol. 114, D00D16, doi:10.1029/2008JD011470;

[80] Wild M. (2012): *Enlightening global dimming and brightening*, Bull. Amer. Meteor. Soc., Vol. 93, pp. 27-37, doi:10.1175/BAMS-D-11-00074.1;

[81] Wild, M. (2016): *Decadal changes in radiative fluxes at land and ocean surfaces and their relevance for global warming*, Wiley Interdisciplinary Reviews: Climate Change, Vol. 7(1), pp. 91-107, doi:10.1002/wcc.372;

[82] Wild M., Gilgen H., Roesch A., Ohmura A., Long C.N., Dutton E.G., Forgan B., Kallis A., Russak V., Tsvetkov A. (2005): *From dimming to brightening: Decadal changes in surface solar radiation at Earths surface*, Science, Vol. 308(5723), pp. 847-850, doi:10.1126/science.1103215;

[83] Wild M., Trüssel B., Ohmura A., Long C.N., König-Langlo G., Dutton E.G., Tsvetkov A. (2009): *Global dimming and brightening: An update beyond 2000*, J. Geophy. Res. Atmos., Vol. 114, D00D13, doi:10.1029/2008JD011382;

[84] Wilks D.S. (1995): *Statistical methods in the atmospheric sciences*, Int. Geophys. Ser., Vol. 59, pp. 464, doi:10.1007/s13398-014-0173-7.2;

[85] Xia X. (2010): *A closer looking at dimming and brightening in China during 1961-2005*, Ann. Geophys., Vol. 28(5), pp. 1121-1132, doi:10.5194/angeo-28-1121-2010;

[86] Xia X. (2010): *Spatiotemporal changes in sunshine duration and cloud amount as well as their relationship in China during 1954-2005*, J. Geophys. Res. Atmos., Vol. 115(7), pp. 1-13, doi:10.1029/2009JD012879;

[87] Zhang Y.L., Qin B.Q., Chen W.M. (2004): *Analysis of 40 year records of solar radiation data in Shanghai, Nanjing and Hangzhou in Eastern China*, Theor. Appl. Climatol., Vol. 78, pp. 217-227, doi:10.1007/s00704-003-0030-7;

[88] Zhang X., Xia X., Xuan C. (2015): *On the drivers of variability and trend of surface solar radiation in Beijing metropolitan area*, Int. J. Climatol., Vol. 35(3), pp. 452-461, doi:10.1002/joc.3994;

[89] Zhu A., Ramanathan V., Li F., Kim D. (2007): *Dust plumes over the Pacific, Indian, and Atlantic oceans: Climatology and radiative impact*, J. Geophys. Res. Atmos., Vol. 112(16), pp. 1-20, doi:10.1029/2007JD008427.

Chapter 4

Reconstructing sunshine duration and solar radiation long-term evolution for Italy: a challenge for quality control and homogenization procedures

Abstract

In the last two decades, the scientific community has become aware of the fact that the real climate signal in original series of meteorological data is generally hidden behind non-climatic noise caused by a number of factors. Time series of meteorological data can therefore not be used for climate research without facing this issue. In this context, we have recently set up a database of Italian sunshine duration and solar radiation daily records and we have subjected them to a detailed quality check and homogenization procedure. Moreover, as the records are rather sparse and a significant fraction of them have wide gaps, we completed the data and set up a procedure in order to obtain at first a gridded version of the dataset and then average records that are representative of the entire Italian territory. The paper will highlight the main steps of the methodology that allowed us to get these average quality-checked and homogenized records and will discuss some open issues.

4.1 Introduction

In the last two decades, the scientific community has become aware of the fact that the real climate signal in the original series of meteorological data is generally hidden behind non-climatic noise. The non-climatic signals can be caused by station relocations, changes

in instruments and instrument screens, changes in observation times, observers, and observing regulations, algorithms for the calculation of means and so on ([1]; [3]). So, at present, the statement that time series of meteorological data cannot be used for climate research without a clear knowledge about the state of the data in terms of homogeneity has very large consent ([1]; [3]).

The need of facing the homogeneity issue is important for all meteorological variables. However, until now, most of the efforts have been dedicated to temperature and precipitation homogenization and few works about other variables are available in the scientific literature. Therefore, it is imperative to improve our knowledge about the effect of inhomogeneities in masking the climate change signal in other variables. Among them it is of fundamental importance to improve the homogeneity of variables such as sunshine duration (SD) and surface solar radiation (SSR), which are very important to evaluate the temporal change and variability in the energy balance of the climate system and whose measure is subjected to a number of problems ([11]; [12]; [13]) which can hidden the real signal. An additional issue concerning the Italian records is that, even though a rather high number of stations measures SD and SSR since the end of the 1950s, a significant fraction of them covers only a minor time interval. Therefore, beside to a careful homogenization, the study of the temporal evolution of these meteorological variables over Italy requires also the application of methodologies that allow managing the presence of records, which have often more gaps than data. This problem is particularly evident for SD that is here presented for the 1936-2013 period.

Within this context, the goals of this paper are: (a) to present the SD and SSR records available for Italy (Section 4.2), (b) to discuss how we managed the homogeneity issue (Section 4.3), (c) to present the methodology we setup to get monthly, seasonal and annual SD (SSR) records for the 1936-2013 (1959-2013) period which are representative for the entire Italian territory (Section 4.4) and (d) to present and discuss the SD long-term trend and evolution as an example of the results obtained applying these methodologies to the original series (Section 4.5).

4.2 Data

The SD station network considered in this paper is presented in Manara et al. ([6] - Chapter 2). It is based on records from (a) the paper archive of the former Italian Central Office for Meteorology (24 records - 1936-2013), which is managed by CREA (Council for Agricultural Research and Agricultural Economy Analysis), (b) the database of Italian Air Force synoptic stations (AM - Aeronautica Militare) (47 records - 1958-2013), and (c) the National Agrometeorological database (BDAN - Banca Dati Agrometeorologica Nazionale) (59 records - 1994-2013, some of them allow updating corresponding AM records), which is also managed by CREA. In addition, it includes four records (Pontremoli, Varese, Modena, and Trieste) from university and local observatories. The dataset encompasses 104 daily records (Figure 4.1) with data for the 1936-2013 period.

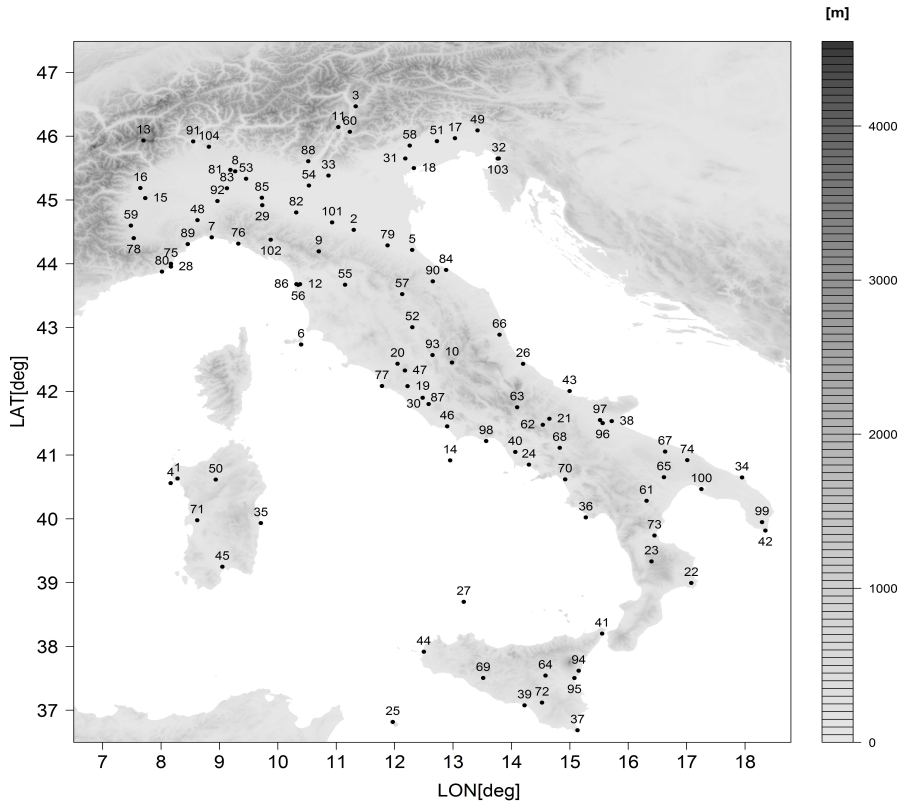

Figure 4.1: Spatial distribution of the SD stations. The stations have the same order as in Table 1 reported by Manara et al. ([6] - Chapter 2). The figure shows the orography of the region too.

The SSR station network considered in this paper is presented in Manara et al. ([7] - Chapter 3). It is mainly based on AM (29 records - 1959-2013 period) and BDAN stations (19 records - 1994-2013 period). Moreover, it includes the observatory of Trieste (1971-2013 period) and five Swiss stations close to the Italian border, from the Swiss Federal Office of Meteorology and Climatology (MeteoSwiss - 1981-2013 period). The dataset encompasses 54 daily records (Figure 4.2) with data for the 1959-2013 period.
We calculated the monthly series for SD and for SSR when the fraction of missing data did not exceed 10% and 20% respectively.

4.3 Quality check and homogenization

At first, the metadata of the records were recovered and the coordinates were checked for consistency, controlling elevation in relation to position. Metadata allow to build the station history that is useful to anticipate and preview which problems could affect the records.
All daily records were checked in order to find out and correct gross errors (negative values and values exceeding the SD/SSR at the top of the atmosphere) ([1]).
We subjected then all our monthly records to a relative homogeneity test ([3]; [9]). In this

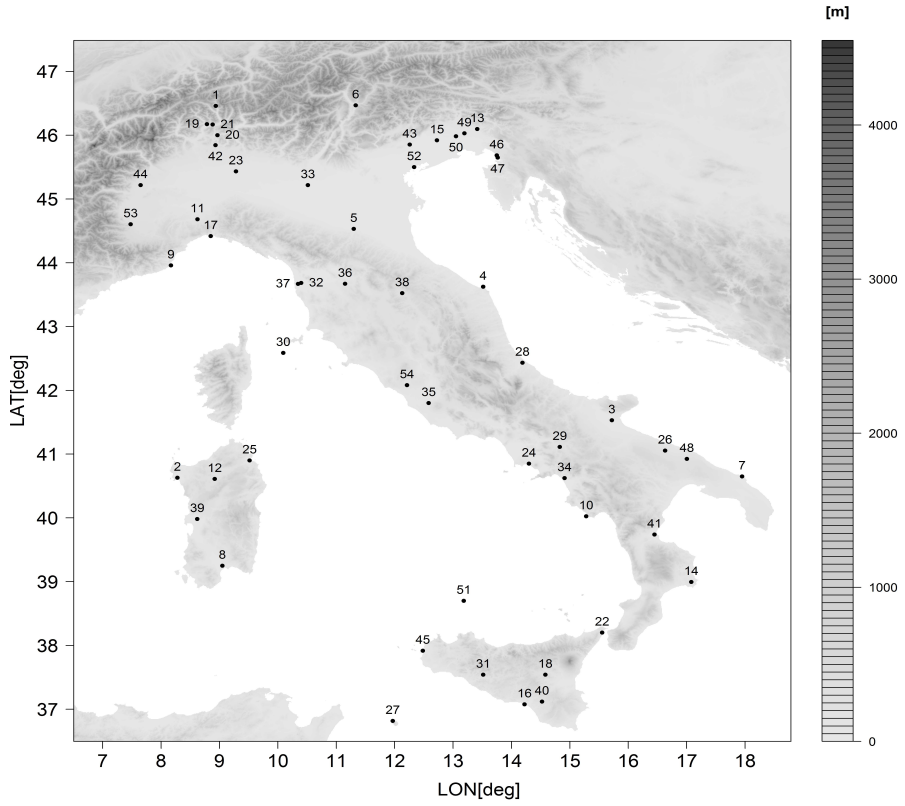

Figure 4.2: Spatial distribution of the SSR stations. The stations have the same order as in Table 1 reported by Manara et al. ([7] - Chapter 3). The figure shows the orography of the region too.

procedure, each series (test series) is tested against 10 other series (reference series) by means of the Craddock test ([15]). The reference series are chosen in the same geographical region of the test series in order to avoid extrapolating the signal of a region to another one. When a break (and so an inhomogeneity) is identified in the test series, the reference series that prove to be homogeneous in a sufficiently long period centered on the break are chosen to estimate the adjustment factors to apply to the test series. Several series are used in order to better identify the break and to get adjustments that are more reliable. For each break, the monthly adjustments are calculated for each reference series. Then, the correcting factors are fitted with a trigonometric function in order to smooth the noise in the adjustment annual cycle and extract only the physical signal. The final set of the monthly adjustments is calculated by averaging all the yearly cycles. When a clear yearly cycle is not evident, the adjustments used to correct the monthly data are chosen constant through the year and they are calculated as the weighted average among the monthly values where the weights are the ratios between monthly mean and the total over the year. When a break is identified, the preceding portion of the series is corrected, leaving the most recent portion of the series unchanged in order to update the records with data yet to be obtained.

The ability of the procedure to detect breaks depends on the spatial coherence of the data and on the density of the record network. Some information on such issues is given by Manara et al. (2015) ([6] - Chapter 2) and Manara et al. (2016) ([7] - Chapter 3) for SD and SSR respectively.

The importance of the homogenization procedure to get reliable single station series is evident from Figure 4.3 where the Italian average annual SD anomaly series (relative anomalies with respect to the period 1984-2013) before and after the homogenization is shown with corresponding Gaussian low-pass filters (11-year window; 3-year standard deviation). These filters allow a better visualization of the decadal variability and long-term trend. The average annual records before and after the homogenization procedure show a different decadal variability during the periods 1936-1959 (average adjustment: 0.981) and 1960-1979 (average adjustment: 1.033) ([6] - Chapter 2). On the contrary, during the period 1980-2013, only small correcting factors have been applied to the original series (average adjustment: 1.004) ([6] - Chapter 2). The necessity of reducing SD before 1960 to get homogeneous series may be due to the strong urbanization which occurred in Italy in the following decades, causing a reduction in the sky-view factor especially for some urban observatories ([6] - Chapter 2).

A similar result is obtained also for SSR especially before 1980s when many instrument changes and recalibrations occurred. More details are given by Manara et al. ([7] - Chapter 3).

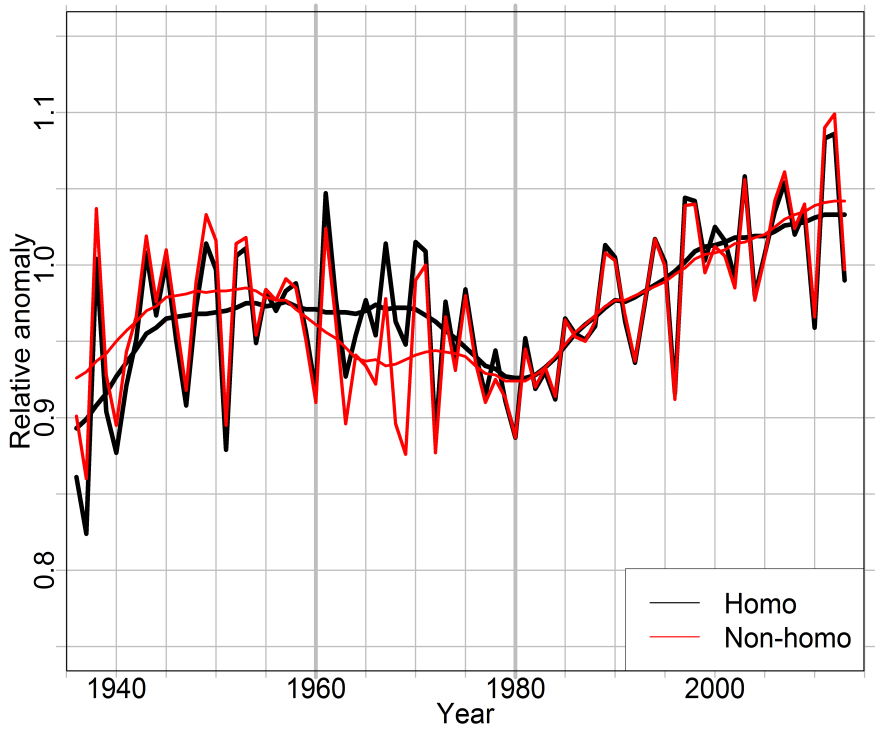

Figure 4.3: Average annual Italian SD anomaly series plotted together with an 11-year window-3-year standard deviation Gaussian low-pass filter before (red line) and after (black line) the homogenization procedure. The anomalies are expressed with respect to 1984-2013 period.

4.4 From the station records to the average regional records

Together with the homogeneity issue, the main problem of the SD and SSR datasets is that most of the records cover only a short time interval with respect to the period covered by the corresponding dataset. This problem is clearly highlighted by dividing the total number of available monthly data (32443 for SD and 18059 for SSR) for the number of months in the period covered by the two datasets. The result gives evidence that the number of available SD data are only 33.4% of the ones that would be necessary to cover without gaps the entire 1936-2013 period. The situation is better for SSR. However, also for this variable we have only 51.6% of the data that would be necessary to cover without gaps the entire 1959-2013 period.

Another problem is that there are periods in the time intervals covered by the two datasets with particularly low data availability, as for example the period before the end of 1950s for SD and the period at the beginning of 1990s for SSR.

In order to better highlight all these problems, we show in Figure 4.4 and 4.5 the data availability for the two datasets. Here the rows correspond to the record numbers as indicated in Figure 4.1 and Figure 4.2, whereas the columns correspond to the years. A year is indicated with a black square if the available monthly values are 12, with a grey square if they are comprised between 9 and 11, with a brown square if they are comprised between 5 and 8 and with a blue square if they are less than 5. A year is indicated with a small cross when no months are available. The many gaps shown in Figure 4.4 and Figure 4.5 make a direct estimation of average Italy SD and SSR records impossible. Such records would in fact be highly vulnerable to fluctuations in spatial coverage, with positive bias when more sunny stations are available and negative bias in the opposite case. For this reason, we transformed the records into anomaly records before averaging them over Italy. The advantage of the anomalies with respect to the absolute values is that their variations take place on a much larger spatial scale. Such a greater spatial coherence causes the anomalies to be less vulnerable to missing data and more suitable for the calculation of regional average or gridded series.

In order to transform the absolute value records into anomaly ones, we had to fill the gaps in the monthly series, at least in the period we used as reference to convert the data into anomalies.

Specifically in Manara et al. ([6] - Chapter 2), each missing SD datum was estimated by means of the most correlated reference record. The selection of the reference record to use for the estimation of the missing datum was performed considering only the records fulfilling three conditions: i) distance within 500km from the record under analysis; ii) availability of at least 10 monthly values in commune with it in the month of the gap and iii) the availability of the datum that is missing in the record under analysis. If no records fulfilled these conditions, the missing datum was not estimated. The reference records fulfilling these conditions were ranked based on a weighting factor defined as the product of two weighting functions depending on the horizontal and vertical distances and

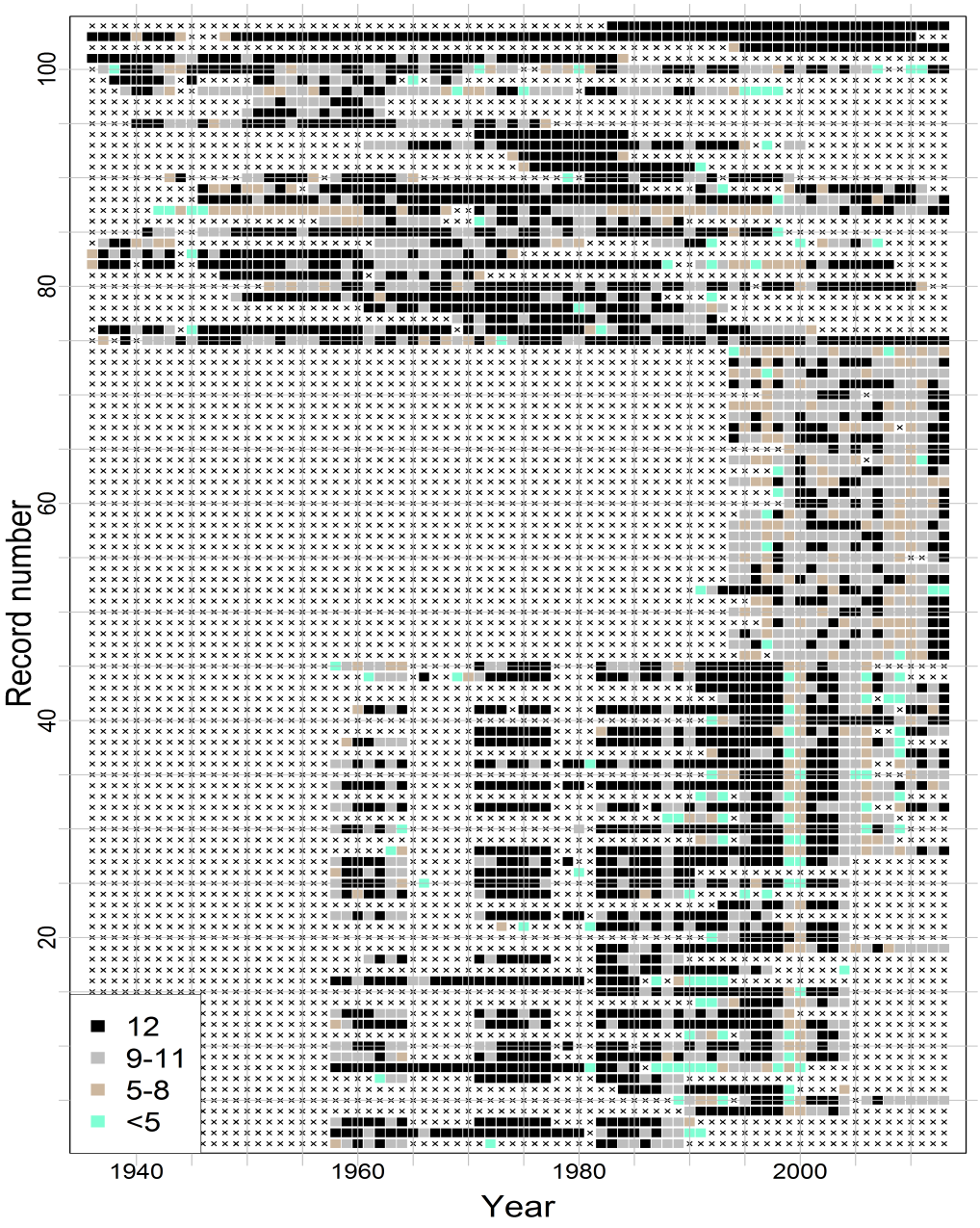

Figure 4.4: Number of available SD months per year for each record. The record number on the y-axis correspond to the number reported in Figure 4.1. A year is indicated with a black square if the available monthly values are 12, with a grey square if they are comprised between 9 and 11, with a brown square if they are comprised between 5 and 8 and with a blue square if they are less than 5. A year is indicated with a small cross when no months are available.

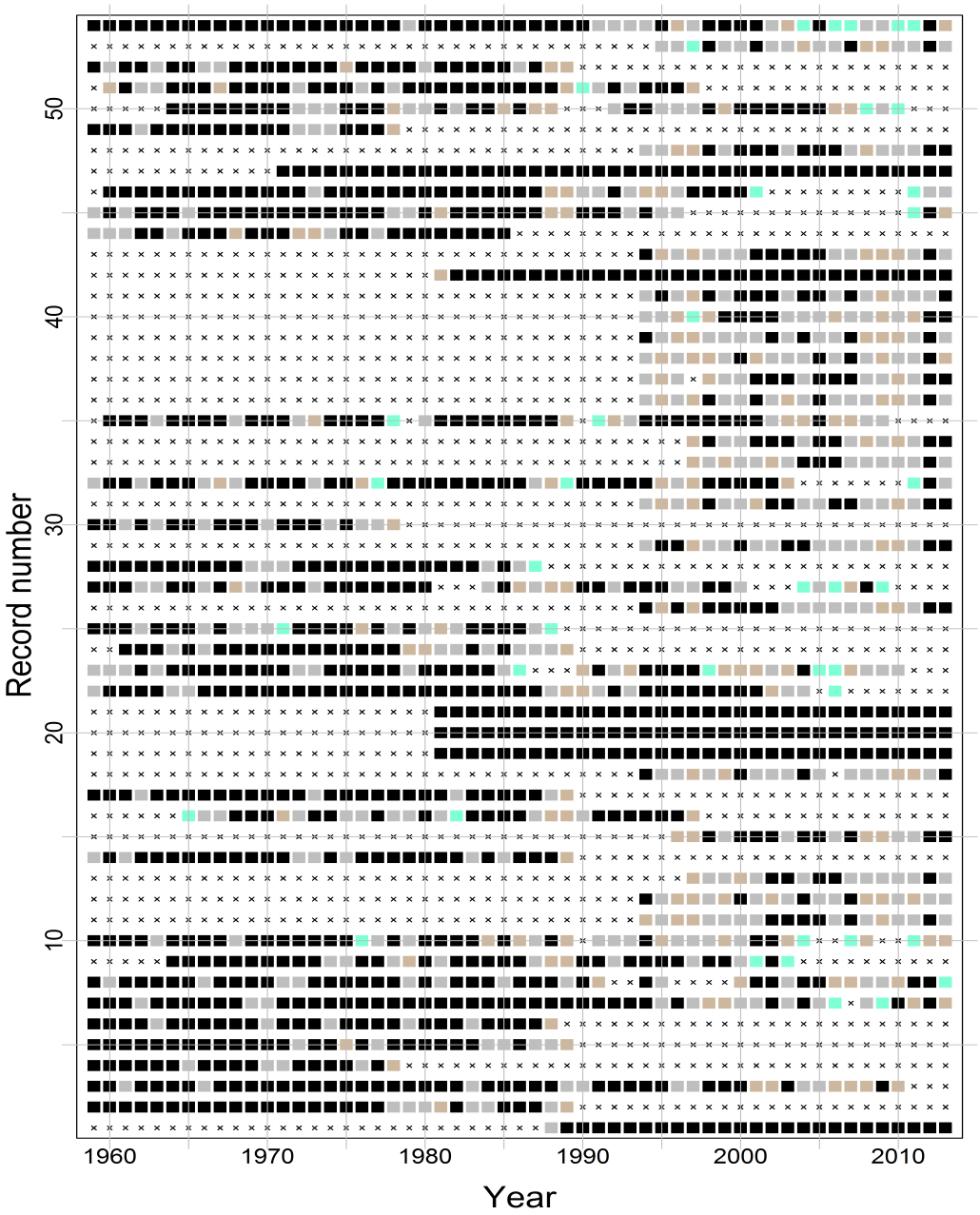

Figure 4.5: Number of available SSR months per year for each record. The record number on the y-axis correspond to the number in Figure 4.2. The data are represented as in Figure 4.4.

the reference record with the highest rank was considered for the estimation of the missing datum. These weighting factors are based on Gaussian functions and they are defined as Brunetti et al. ([4]):

$$w_{i,j}^{var} = \exp\left(-\frac{(\Delta_{i,j}^{var})^2}{c_{var}}\right) \tag{4.1}$$

where i is the series to fill and j the reference series. The weight is calculated for two variables (var - position and elevation), $\Delta_{i,j}^{var}$ is the absolute value of the horizontal or vertical distance between the reference series and the series to be completed. c_{var} is a coefficient which regulates the decrease of the weighting factor. c_{var} can be expressed in terms of the distance $\Delta_{1/2}^{var}$ for which the weight should be 0.5 ([4]):

$$c_{var} = -\frac{(\Delta_{1/2}^{var})^2}{\ln 0.5} \tag{4.2}$$

For the horizontal distance, we used a factor equal to 0.5 at 300km, whereas for the vertical distance we applied the following relation:

$$\Delta_{1/2}^{h} = \begin{cases} 250m & h \leq 500m \\ \frac{h}{2}m & h > 500m \end{cases} \tag{4.3}$$

The introduction of a difference vertical distance factor allowed us using the few high-level sites in our database as much as possible to estimate missing data in high-level records. This is especially useful in winter in northern Italy, where SD/SSR can have significantly different behavior at low and high levels.

Once the reference series was selected, the gap was filled under the assumption of the constancy of the ratio between incomplete and reference series. This procedure has been checked with a leave-one-out approach. Specifically, the procedure was applied to all available data, i.e. each available value of each SD record was considered as missing and estimated by means of the procedure. Then, when original data and the re-estimated ones were compared, about 50% of the ratios between the original values and the estimated ones resulted between 0.95 and 1.05.

This gap filling method may however give rise to outliers resulting from peculiar climatic conditions of the reference series. In order to avoid this problem, the median of a set of five estimated values, corresponding to the five highest correlated reference records, is here selected instead of only the one with the highest rank. The difference between this new procedure and the one we used in Manara et al. ([6] - Chapter 2) is evident for example observing the comparison between the series of the relative SD for the month of January for Milano Linate filled with the old method and the new one (Figure 4.6). The black line represents the original series filled with the old method while the red line represents the original series filled with the new method. The means over the whole period for the original series and the gap-filled series with the two methods do not change while the

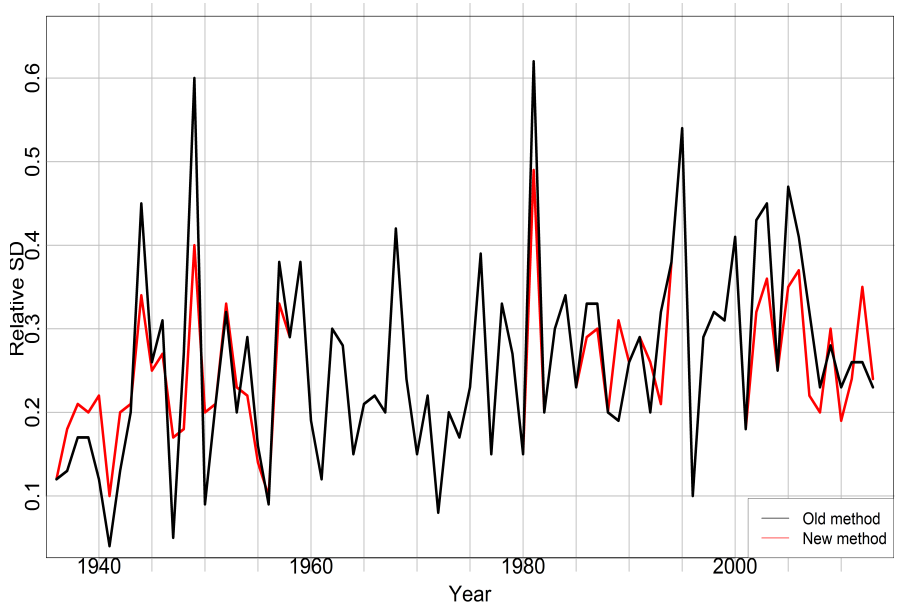

Figure 4.6: The black line represents the original series filled with the old method while the red line represents the original series filled with the new one.

variability of the series completed with the new method (deviation standard: 0.10) is less than the variability of the series completed with the old one (deviation standard: 0.12). In this paper, we use the new method to complete the two database. We used this new method also in Manara et al. ([7] - Chapter 3) for SSR.

For SSR a reference series was considered when it was distant less than 500km from the record under analysis, it had at least 6 monthly values in common with it in the month of the gap and it had the datum that is missing in the record under analysis. When less than five reference records fulfilling the requested conditions were available, the median was calculated with the available reference series.

After the gap filling, we deleted the series with less than 90% of available data over the 1984-2013 (1976-2005) period for the SD (SSR) database. This reduced the SD dataset to 95 records while for the SSR dataset, all series had at least 99% of available data during the 1976-2005 and so all the records were considered for the following analysis. The periods 1984-2013 and 1976-2005 were selected as reference period to calculate the relative monthly, seasonal and annual anomaly series, respectively, for SD and SSR because they are those with the highest data availability after the gap-filling procedure. Then, starting from the gap-filled series we generated a $1° \times 1°$ gridded version of the dataset in order to balance the contribution of areas with a higher number of stations with those that have a lower station coverage. We followed the technique described by Brunetti et al. ([3]) and Sanchez-Lorenzo et al. ([8]), which is based on an Inverse Distance Weighting approach with the addition of an angular term to take into account the anisotropy in spatial distribution of stations. The resulting grid spans from 7° to 19°E and from 37° to 47°N with 68 points over the Italian territory for SD ([6] - Chapter 2) and with 58 points

for SSR ([7] - Chapter 3).
Finally, we calculated the Italian average monthly, seasonal and annual anomaly series from the gridded dataset simply by averaging all grid-point anomaly records.

4.5 Long-term evolution over Italy

As validation of the techniques applied to the original series, in Figure 4.7 the average Italian seasonal and annual SD anomaly records is shown together with the corresponding low-pass filter (11 year window-3-year standard deviation Gaussian low-pass filter). As already reported by Manara et al. ([6] - Chapter 2) for northern and southern Italy, the curves indicate an increase starting from the 1980s (known in literature as "Brightening period" ([10])). This signal concerns all seasons with the only exception of the autumn, that shows an increasing tendency only from the beginning of 1990s. Before this brightening signal, there is a decreasing tendency (known in literature as "Global dimming" ([10])) that is however less intense than the following increase. It concerns especially spring and summer and the period comprised between the middle of the 1960s and the beginning of the 1980s. In the early period, from the 1930s to the 1950s, there is some evidence of an increasing tendency (known in literature as "Early brightening" ([10])). This signal concerns, however, a period in which data availability is low (Figure 4.4), causing a greater uncertainty in the average records.
The overall picture of Italian SD trend is, in good agreement with the trend observed in many areas of the world ([10]). In particular, the resulting trend as reported by Manara et al. ([6] - Chapter 2) turn out to be in good agreement with corresponding records from neighboring areas, as for example the southern part of the Greater Alpine Region ([2]) and eastern Spain ([8]).
SSR (Figure not shown) shows a similar evolution with a significant dimming from the beginning of the series to the mid-1980s and a brightening until the end of the series as reported for northern and southern Italy by Manara et al. ([7] - Chapter 3).

4.6 Conclusions

Considering the importance of solar radiation not only for scientific interest a new database of SD and SSR has been set up over the Italian territory for the 1936-2013 and 1959-2013 period, respectively.
In this paper, the main steps to obtain reliable mean series over the Italian territory starting from the raw series have been illustrated. In particular, it has been shown how the homogenization procedure is important, especially for variables like SD and SSR, underlining how, at regional level, systematic biases in the original records can hide a significant part of the long-term trend. Beside the quality control, particular emphasis is placed also to show how the problem of the gaps in the series should be considered in order to calculate the regional series. This is true especially over areas with a complex

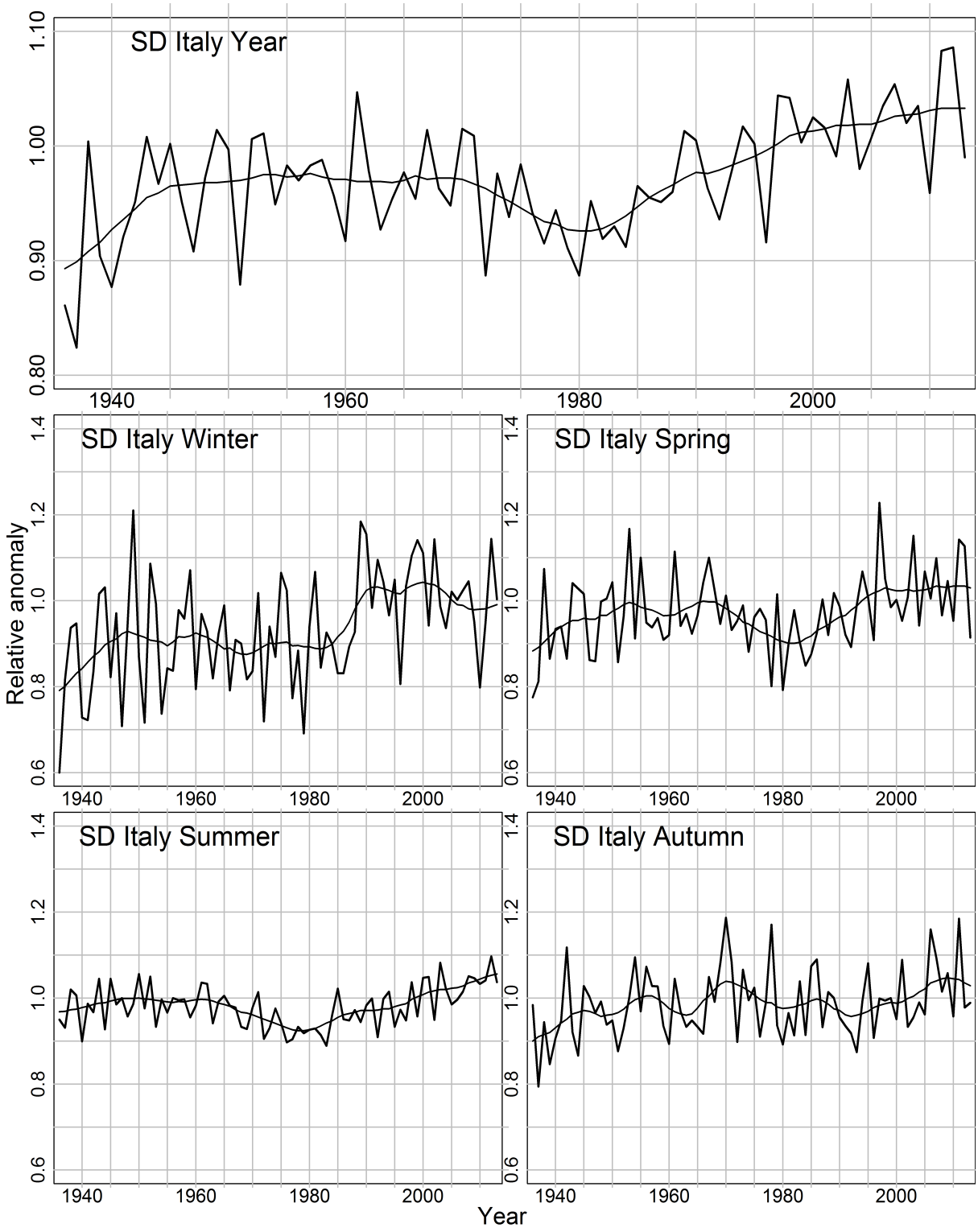

Figure 4.7: Average annual and seasonal Italian SD anomaly series plotted together with the corresponding filter (11 year window-3-year standard deviation Gaussian low-pass filter). The anomalies are calculated with respect to the 1984-2013 period.

orography like Italy.
Finally, considering the length of the Italian SD records, seasonal and annual SD anomaly series over the area are presented as example of the results obtained applying the presented techniques to the original series.

Bibliography

[1] Aguilar E., Auer I., Brunet M., Peterson T.C., Wieringa J. (2003): *Guidelines on Climate Metadata and Homogenization*, WMO-TD No. 1186, pp. 52, World Meteorological Organization, Geneva, Switzerland;

[2] Auer I., Böhm R., Jurkovic A., Lipa W., Orlik A., Potzmann R., Schöner W., Ungersböck M., Matulla C., Briffa K., Jones P., Efthymiadis D., Brunetti M., Nanni T., Maugeri M., Mercalli L., Mestre O., Moisselin J.M., Begert M., Müller-Westermeier G., Kveton V., Bochnicek O., Stastny P., Lapin M., Szalai S., Szentimrey T., Cegnar T., Dolinar M., Gajic-Capka M., Zaninovic K., Majstorovic Z., Nieplova E. (2007): *HISTALP-Historical instrumental climatological surface time series of the Greater Alpine Region*, Int J. Climatol., Vol. 27(1), pp. 17-46, doi:10.1002/joc.1377;

[3] Brunetti M., Maugeri M., Monti F., Nanni T. (2006): *Temperature and precipitation variability in Italy in the last two centuries from homogenized instrumental time series*, Int. J. Climatol., Vol. 26(3), pp. 345-381, doi:10.1002/joc.1251;

[4] Brunetti M., Maugeri M., Nanni T., Simolo C., Spinoni J. (2013): *High-resolution temperature climatology for Italy: Interpolation method intercomparison*, Int. J. Climatol., Vol. 34, pp. 1278-1296, doi:10.1002/joc.3764;

[5] Craddock J.M. (1979): *Methods of comparing annual rainfall records for climatic purposes, Weather*, Vol. 34(9), pp. 332-346, doi:10.1002/j.1477-8696.1979.tb03465.x;

[6] Manara V., Beltrano M.C., Brunetti M., Maugeri M., Sanchez-Lorenzo A., Simolo C., Sorrenti S. (2015): *Sunshine duration variability and trends in Italy from homogenized instrumental time series (1936-2013)*, J. Geophys. Res. Atmos., Vol. 1, No. 120, pp. 3622-3641, doi:10.1002/2014JD022560;

[7] Manara V., Brunetti M., Celozzi A., Maugeri M., Sanchez-Lorenzo A., Wild M. (2016): *Detection of dimming/brightening in Italy from homogenized all-sky and clear-sky surface solar radiation records and underlying causes (1959-2013)*, Atmos. Chem. Phys., Vol. 16, pp. 11145-11161, doi:10.5194/acp-16-11145-2016;

[8] Sanchez-Lorenzo A., Brunetti M., Calbó J., Martin-Vide J. (2007): *Recent spatial and temporal variability and trends of sunshine duration over the Iberian Peninsula from a homogenized data set*, J. Geophys. Res., Vol. 112, D20115, doi:10.1029/2007JD008677;

[9] Venema V.K.C. et al. (2012): *Benchmarking homogenization algorithms for monthly data*, Clim. Past, Vol. 8, pp. 89-115, doi:10.5194/cp-8-89-2012;

[10] Wild M. (2009): *Global dimming and brightening: A review*, J. Geophys. Res., Vol. 114, D00D16, doi:10.1029/2008JD011470;

[11] WMO-No.8 (1969): *Chapter 9, Solar radiation and Sunshine duration*, World Meteorological Organization, Guide to meteorological instruments and observing practices, Third edition;

[12] WMO-No.8 (2008): *Chapter 7, Measurement of radiation*, World Meteorological Organization, Guide to Meteorological Instruments and Methods of Observation, Geneva, Switzerland, ISBN:978-92-63-10008-5;

[13] WMO-No.8 (2008): *Chapter 8, Measurement of Sunshine Duration*, World Meteorological Organization, Guide to Meteorological Instruments and Methods of Observation, Geneva, Switzerland, ISBN:978-92-63-10008-5;

Chapter 5

Homogenization of a surface solar radiation dataset over Italy

Abstract

Observational data cannot be used for climate research without a clear knowledge about the state of the data in terms of temporal homogeneity. The main steps and results of the homogenization procedure applied to a surface solar radiation dataset over the Italian territory for the period 1959-2013 are discussed.

5.1 Introduction

In the last two decades, the scientific community has become aware of the fact that the real climate signal in the original series of observational data can be hidden behind non-climatic noise caused by station relocations, changes in instruments, observation times, observers and so on ([1]). This issue is very important for all meteorological variables ([1]) and is even more important for variables such as surface solar radiation (SSR), whose measurements are subjected to a number of problems ([7]). Therefore, the study of decadal variability and long-term trend of SSR has a strong need of facing the temporal homogeneity issue.

Manara et al. in a recent paper discussed the main points required to set up a SSR database over Italy and to obtain regional average SSR records for Northern and Southern Italy in the 1959-2013 period ([5] - Chapter 3). That paper, however, mainly focuses on the temporal evolution of the considered records, whereas data pre-processing is presented in a rather concise way. Within this context, the aim of the present paper is to discuss in more detail the homogenization of this dataset.

Meteorological series can be tested for homogeneity and homogenized both by direct and indirect methods. The first approach is based on objective information that can be extracted from the station history (metadata), the latter uses statistical methods, generally based on comparison with other series. The direct methodology has the advantage of

providing detailed information about the time location of the inhomogeneities and the sources that caused them, but they are not always available and complete. Moreover, it is generally difficult to convert them into quantitative values useful to correct the discontinuities. On the other hand, the indirect methodology is more suitable to calculate correcting factors to eliminate the breaks. However, the identification of the inhomogeneities is not always easy and unambiguous, as (i) inhomogeneities and errors are present in almost all observational series, making it difficult to objectively assign the breaks to one or another of them and (ii) correlation among data series depends on various factors (e.g., regional patterns, climate elements under analysis, time resolution of data and so on) and when the common variance between the test series and the reference series is too low, the potential discontinuity signal in a homogeneity test disappears into statistical noise ([2]).
The approach we use is based on the indirect methodology. We give however great importance to the metadata as they are very important to help in deciding whether a possible break indicated by the statistical test has actually to be corrected ([2]). In particular, our procedure consists in subjecting the records to a relative homogeneity test ([2]; [6]), where each series (test series) is tested against 10 other series (reference series) by means of the Craddock test ([3]). The reference series are chosen in the same geographical region as the test series in order to avoid extrapolating the signal of a region to another one. When a break (and so an inhomogeneity) is identified in the test series, those reference series that prove to be homogeneous in a sufficiently long period centered on the break are chosen to estimate the adjustment factors to apply to the test series. Several series are used in order to better identify the break and to get adjustments that are more reliable. For each break, the monthly adjustments are calculated from each reference series. Then, the correcting factors are fitted with a trigonometric function in order to smooth the noise in the adjustment annual cycle and extract only the physical signal. The final set of the monthly adjustments is then calculated by averaging all the yearly cycles. When a clear yearly cycle is not evident, the adjustments used to correct the monthly data are chosen constant through the year and they are calculated as the weighted average among the monthly values, where the weights are the ratios between the monthly SSR mean and the total SSR over the year. When a break is identified, the preceding or the following portion of the series is corrected, leaving when possible the most recent portion of the series unchanged in order to update the records with data yet to be obtained. The entire procedure is generally applied to monthly records. It can however be easily extended also to daily ones under the condition that each monthly homogenized value obtained averaging the daily homogenized values is equal to the corresponding monthly homogenized value obtained directly from the homogenization of the monthly series.

5.2 Italian SSR data and metadata

The SSR station network considered in this paper is mainly based on the Italian Air Force synoptic stations (AM - Aeronautica Militare - 29 records) and on the National

Agrometeorological Database (BDAN - Banca Dati Agrometeorologica Nazionale - 19 records). Moreover, it includes the observatory of Trieste and five Swiss stations from the Swiss Federal Office of Meteorology and Climatology (MeteoSwiss) close to the Italian border. The dataset encompasses 54 records with daily resolution covering the 1959-2013 period. The data that come from AM and from Trieste were recorded with the Robitzsch bimetallic actinograph until the 1980s. This instrument was then replaced with the CM11 Kipp & Zonen pyranometer in the first case and with different types of CM Kipp & Zonen pyranometers in the second one. The CM11 Kipp & Zonen pyranometer was also used in the stations included in the BDAN database with the only exception of two stations that use the EP07 Middleton Instruments pyranometer. Finally, the data that come from MeteoSwiss were measured with a CM21 Kipp & Zonen pyranometer. Full details on data and metadata availability are reported in Manara et al. (2016a) ([4] - Chapter 4) and Manara et al. (2016b) ([5] - Chapter 3).

5.3 Homogenization of the italian SSR records

The homogenization of the Italian SSR records was not easy because of three main problems: the low spatial density of the stations, the large fraction of missing data ([4] - Chapter 4) and the presence of a high number of inhomogeneities. The first two problems are enhanced by a fairly low spatial coherence of the records, which causes the common variance between two stations to fall to about 50% at a distance of 150km (Figure 5.1). This makes the selection of the reference series more difficult, considering that they should not only be located close to the test series but must also have available data over the period to homogenize. Hereinafter we show, as an example, the different steps of the homogenization procedure for the Messina station, located in the Southern part of Italy (38.201°N, 15.553°E, 59 m) and with available data for the period 1959-2006. Figure 5.2(a), shows the Craddock test applied to Messina with respect to 10 reference stations. Each curve shows the cumulative normalized differences (s) between the test and the reference series according to the formula:

$$s_i = s_{i-1} + a_i \left(\frac{b_m}{a_m} \right) - b_i \tag{5.1}$$

where a is the reference series, b is test series while a_m and b_m are the time mean series over the whole period.

This test identifies the breaks by means of changes in the slope of the test curves ([3]). The most important breaks seem therefore to be located in the years 1964, 1965, 1969, 1971, 1973, 1979 and 1989. Most of these breaks correspond to changes highlighted by the metadata. Specifically, the breaks of the years 1964 and 1971 correspond to recalibrations of the instrument while the break of the year 1989 corresponds to a change in the instrument (from the Robitzsch bimetallic actinography to the CM11 Kipp & Zonen pyranometer). The first break we corrected is the most recent one (1989). We adjusted

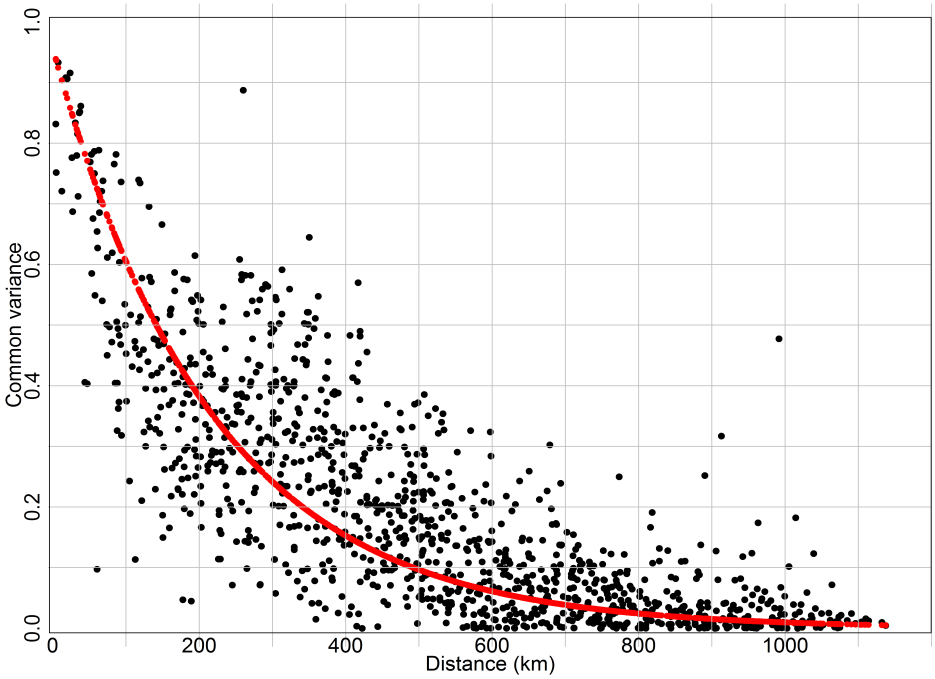

Figure 5.1: Common variance versus distance of monthly SSR records. In order to remove the effect of the annual cycle, the common variance has been calculated after deseasonalization of the records.

therefore all data between the selected break and the preceding one by means of monthly correcting factors (0.91 for the period 1984-1989). They allow to make the data of the selected period homogeneous with those after the break used as reference period to calculate the adjustment factors. The resulting record was obviously not homogeneous as there were other breaks before the one we considered in the first step. We therefore applied the same procedure to all the identified breaks until we got the homogenized record. Figure 5.2(b) shows the Craddock test applied to this final homogeneous record. The Craddock curves of Messina with respect to the different reference series show changes that are amenable more to statistical noise than to non-homogeneity in the test series. The change that is evident in the pink line around the mid of the 1960s is probably due to a break in the reference series and not in the test series considering that this curve is the only one that shows a pronounced variation during these years. The same procedure we applied to the Messina record was applied to all 54 stations of our dataset.

Some statistics on the breaks we corrected are shown in Figure 5.3, which shows the number of corrected breaks vs time in absolute and relative terms (with respect to the number of available series). This figure shows that the Italian SSR records had a rather high number of breaks even if some of them concern only few years or small adjustments. The relative number of breaks is high especially until the 1980s due to the high number of recalibration and instrument changes that occurred in this period. A very interesting issue in relation to data homogenization is to check whether the adjustment factors applied to the station series give raise to a random noise that disappears considering the average

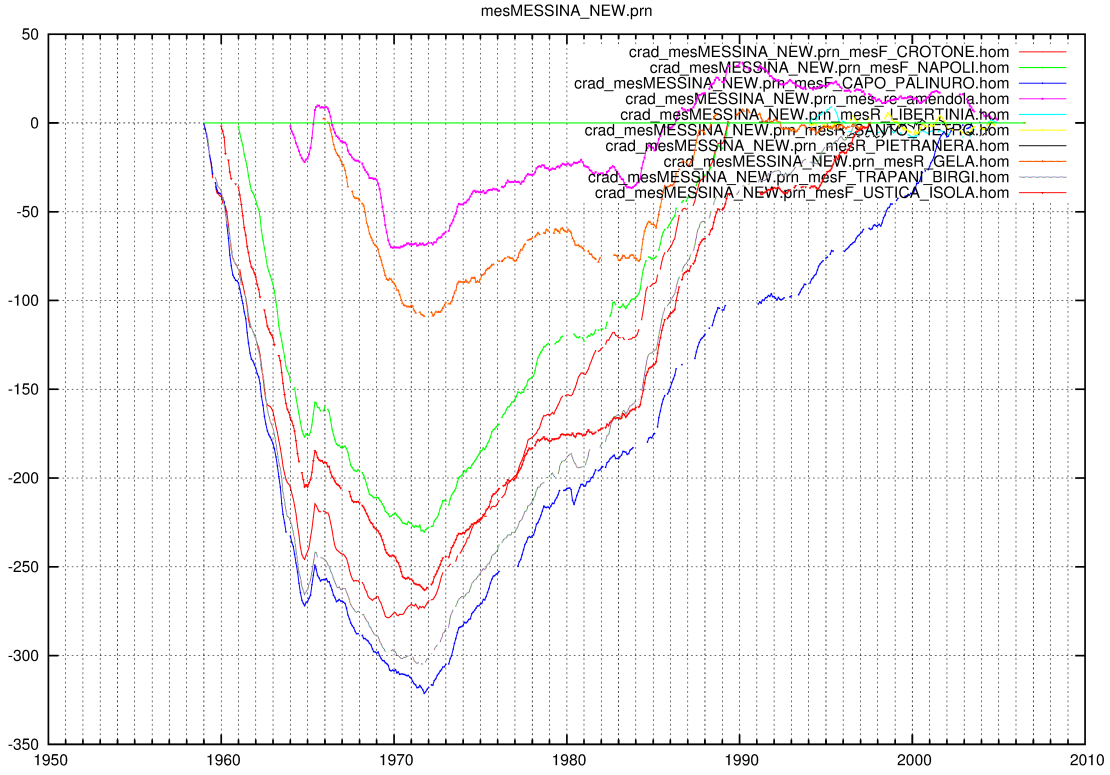

(a)

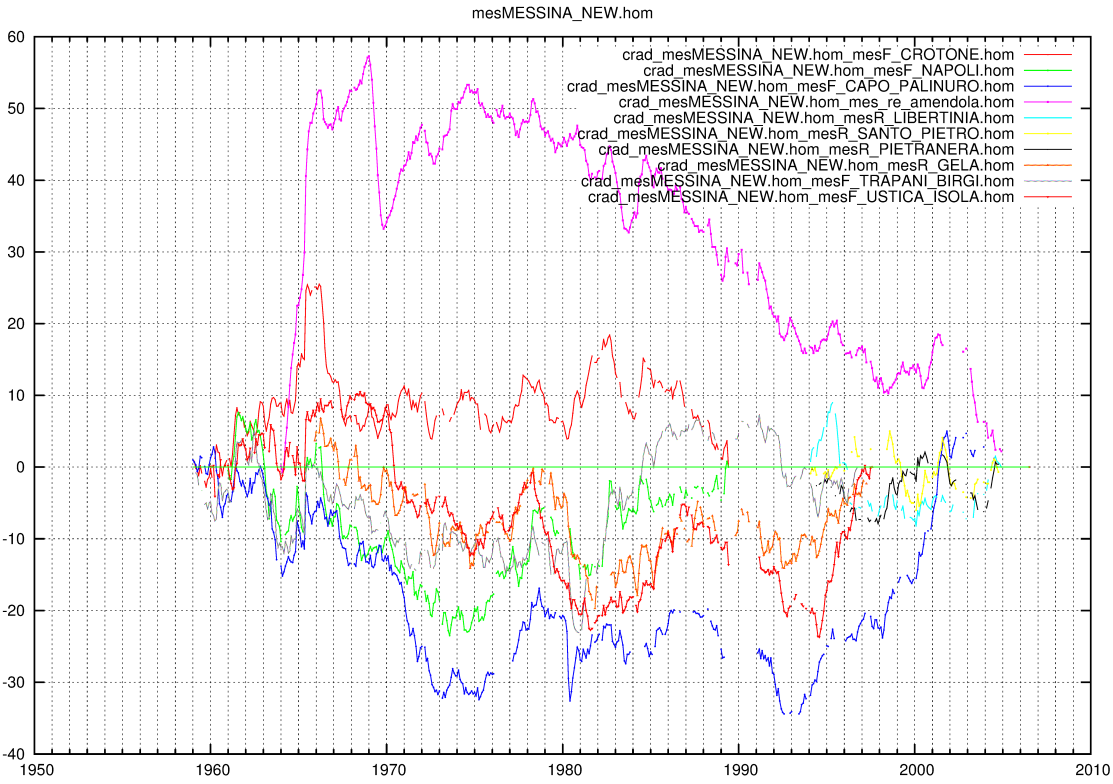

(b)

Figure 5.2: Craddock test applied to Messina with respect to 10 reference series: for the original series (a) and for the final homogeneous series (b). The scale of the y-axis is different to better highlight the signal contained in the series.

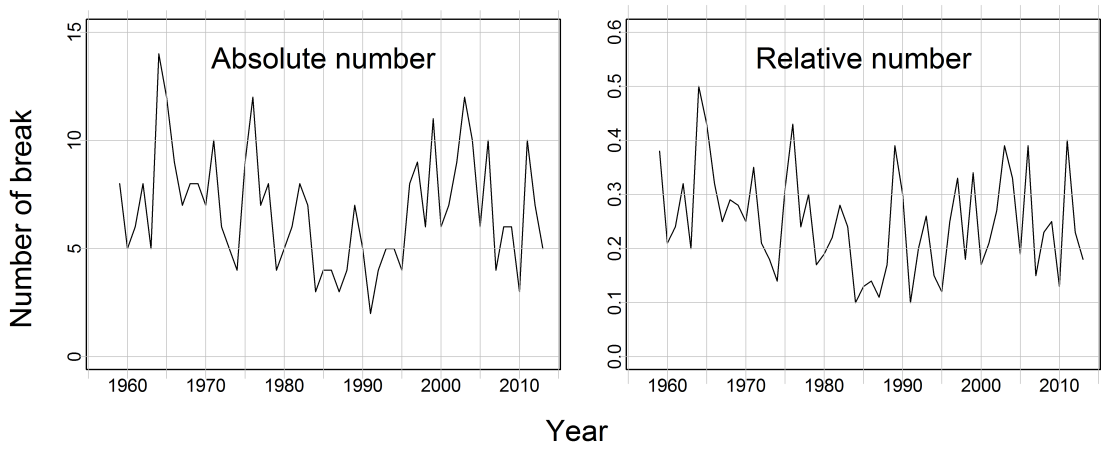

Figure 5.3: Number of detected breaks per year in the SSR dataset (left column) and number of detected breaks normalized by the number of available series (right column).

over a large number of stations (regional average record) or, on the contrary, they produce a long-term signal that masks the real climate tendency. In the first case the ratio between the regional average records calculated from the original and from the homogenized dataset would be around one for the entire record length. For the Italian SSR record this situation concerns only the period after the 1980s where at national scale this ratio is 1.008, whereas before 1980 the effect of the inhomogeneities does not produce a random noise (see Figure 3 in Manara et al. ([5] - Chapter 3)).

5.4 Conclusions

The real climate signal in the original series of observational data can be hidden behind non-climatic noise. So, at present, the statement that time series of meteorological data cannot be used for climate research without a clear knowledge about the state of the data in terms of temporal homogeneity has very large consent, especially when variables such as surface solar radiation (SSR) are considered. In this paper, the main steps of the homogenization procedure applied to an Italian SSR dataset for the period 1959-2013 are described. The procedure adopted is based on an indirect methodology (Craddock test) supported by metadata. The result give evidence that homogenization is a key issue for the study of the temporal evolution of SSR.

Bibliography

[1] Aguilar E., Auer I., Brunet M., Peterson T.C., Wieringa J. (2003): *Guidelines on Climate Metadata and Homogenization*, WMO-TD No. 1186, pp. 52, World Meteorological Organization, Geneva, Switzerland;

[2] Brunetti M., Maugeri M., Monti F., Nanni T. (2006): *Temperature and precipitation variability in Italy in the last two centuries from homogenized instrumental time series*, Int. J. Climatol., Vol. 26(3), pp. 345-381, doi:10.1002/joc.1251;

[3] Craddock J.M. (1979): *Methods of comparing annual rainfall records for climatic purposes*, Weather, Vol. 34(9), pp. 332-346, doi:10.1002/j.1477- 8696.1979.tb03465.x;

[4] Manara V., Brunetti M., Maugeri M.(2016a): *Reconstructing sunshine duration and solar radiation long-term evolution for Italy: a challenge for quality control and homogenization procedures*, Conference proceeding of the 14^{th} IMEKO T10 Workshop Technical Diagnostics - New Perspectives in Measurements, Tools and Techniques for system's reliability, maintainability and safety, 27-28 June 2016, Milan, Italy, pp: 13-18, ISBN: 978-92-990073-9-6, $http://www.imeko.org/publications/tc10-2016/IMEKO-TC10-2016-002.pdf$;

[5] Manara V., Brunetti M., Celozzi A., Maugeri M., Sanchez-Lorenzo A., Wild M. (2016b): *Detection of dimming/brightening in Italy from homogenized all-sky and clear-sky surface solar radiation records and underlying causes (1959-2013)*, Atmos. Chem. Phys., Vol. 16, pp. 11145-11161, doi:10.5194/acp-16-11145-2016;

[6] Venema V.K.C. et al. (2012): *Benchmarking homogenization algorithms for monthly data*, Clim. Past, Vol. 8, pp. 89-115, doi:10.5194/cp-8-89-2012;

[7] WMO-No.8 (2008): *Chapter 7, Measurement of radiation*, World Meteorological Organization, Guide to Meteorological Instruments and Methods of Observation, Geneva, Switzerland, ISBN:978-92-63-10008-5.

Chapter 6

Sunshine duration and global radiation trends in Italy (1959-2013): to what extent do they agree?

Abstract

Two homogenized datasets of sunshine duration (SD) and global radiation ($E_{g\downarrow}$) relative anomalies over Italy are used to investigate to what extent these two variables agree under all-sky and clear-sky conditions in terms of their decadal variations. They are compared for northern and southern Italy over the 1959-2013 common period. All-sky SD records tend to show a shorter and less intense decrease until the 1980s ("global dimming") with respect to $E_{g\downarrow}$ ones, while the agreement is better in the subsequent period where both variables increase ("brightening period"). Moreover, SD shows a trend inversion which anticipates that of $E_{g\downarrow}$. Also the clear-sky $E_{g\downarrow}$ records show a stronger dimming signal than the corresponding SD ones. However, they show a slightly stronger brightening signal too. To investigate whether such behavior can be explained by a different sensitivity of SD and $E_{g\downarrow}$ to atmospheric turbidity variations, the observed clear-sky trends are compared to that estimated by a model based on this variable. The results show that most of the differences observed in the trends of the clear-sky SD and $E_{g\downarrow}$ records can be explained considering the patterns of atmospheric turbidity in the 1959-2013 period. The only exceptions concerns winter and autumn in northern Italy where clear-sky SD does not decrease in the dimming period as much as it should be expected on the basis of the corresponding increase in atmospheric turbidity. The reasons of this discrepancy could be due both to instrumental problems and to the influence of other variables.

6.1 Introduction

The amount of solar energy reaching the Earth's surface provides the energy for a variety of climate processes related to, for example, evaporation, snow melting and diurnal/seasonal cycle of surface temperature ([17]; [36]). Therefore, changes in the amount of solar energy reaching the Earth's surface can have profound environmental, societal and economic implications ([52]; [65]).
Specifically, global radiation (also known as surface solar radiation - $E_{g\downarrow}$) is the solar radiation received from a solid angle of $2\pi sr$ on a horizontal surface and is measured with a pyranometer ([71]). It includes the radiation received directly from the solid angle of the sun's disc (direct radiation - E), as well as the downward component of the diffuse sky radiation that has been scattered in traversing the atmosphere (diffuse radiation - $E_{d\downarrow}$).
In the last decades, the scientific community has become aware of the fact that $E_{d\downarrow}$ is not constant on decadal time scales ([65]), showing a decrease called "global dimming" from the 1950s to the 1980s ([54]; [56]) and a subsequent increase called "brightening period" since the beginning of 1980s ([67]; [68]). Some studies that analyze series starting before the 1950s, report also an increase during the 1930s and 1940s, known as "early brightening" ([55]). For a recent review of the topic see Wild ([66]). The causes of these variations are very complex and not completely clear, especially if studies regarding different areas are compared. The major causes are suspected to be related to changes in anthropogenic aerosols and cloud characteristics ([3]; [27]; [56]; [65]; [66]). It is supposed that clouds are the major contributors to the $E_{g\downarrow}$ variability at the interannual scale, while atmospheric aerosols contribute especially at the decadal scale ([66]) even if they are not completely independent, as they can interact in various ways ([40]).
In particular, increasing anthropogenic aerosol emissions from the 1950s are thought to be the major cause of the observed decadal $E_{g\downarrow}$ reduction until the 1980s ([26]; [34]; [56]). However, the measures to reduce air pollution from the 1970s onward have been suggested to be responsible for the renewed increase of $E_{g\downarrow}$ ([10]; [12]; [13]; [16]; [33]). The reasons for the observed increase during the 1930s and 1940s are more uncertain considering the low availability of long records ([2]; [47]; [66]; [69]).
$E_{g\downarrow}$ records started to become available on a widespread basis only in the late 1950s, with the establishment of numerous radiation sites during the International Geophysical Year (1957-1958) ([52]; [69]). Consequently, one of the main problems in studying the temporal variability of $E_{g\downarrow}$ is the small number of sites with reliable long-term records. Therefore, it is very useful to estimate the temporal variability of $E_{g\downarrow}$ starting from other climatic variables (proxy measures) such as total cloud cover (TCC), visibility or sunshine duration (SD) ([42]; [45]; [54]; [64]). The advantage of these variables is that they are available for a longer period than $E_{g\downarrow}$. The most appropriate proxy for $E_{g\downarrow}$ is probably SD because it is less subjective than the others and data are available since the late nineteenth century ([46]). Moreover, SD is closely correlated to $E_{g\downarrow}$ by means of the Ångström-Prescott formula ([1]; [39]).

According to the World Meteorological Organization (WMO), the SD for a given day is the length of time during which E is above $120 W m^{-2}$ ([72]). Most of the SD data have been recorded with the Campbell-Stokes and Jordan sunshine recorders ([48]). Specifically, the Campbell-Stokes recorder consists of a spherical lens that focuses E onto a paper card, burning a trace if the irradiance exceeds the instrumental threshold ([49]; [53]; [72]). The definition of a correct value for this threshold is not an easy issue: $120 W m^{-2}$ was proposed by WMO as resulting mean after some investigations performed at different stations. It can however vary between about 70 and $280 W m^{-2}$ depending on a number of factors including the atmospheric turbidity and the moisture content of the paper card ([70]). Some studies ([5]; [6]) report that the burning threshold is on average higher in the early morning than in the late evening, hypothetically attributed to dew or other water deposits on the glass sphere and on the paper card. This could produce notable losses in the daily SD values, especially in winter, because more energy is required to burn the trace in the paper card when temperatures are low and relative humidity (RH) is high ([37]).
Besides the problems related to the instrumental threshold, the Campbell-Stokes SD measurements may be affected by other problems ([7]). An example is a situation of very broken cloudiness. In this case, rapid bursts of high E, resulting in short periods during which $E_{g\downarrow}$ is reduced by clouds, may cause continuous traces ([21]; [37]) In this way, an increase of TCC during the day may reduce $E_{g\downarrow}$ without affecting SD ([57]). A further limitation of SD measurements is that they are sensitive to atmospheric aerosols and water vapor ([35]; [74]) only when E is close to the instrumental threshold, whereas $E_{g\downarrow}$ is sensitive to these variables especially when E is highest ([18]). When E is close to the instrumental threshold, RH can have an important influence on SD because it increases the size of the particles via the aerosols hygroscopic effect and therefore changes their radiative properties ([4]; [43]; [59]; [73]). In this way, E can fall under the instrumental threshold and the paper card does not register any SD variation. It is however necessary to consider that SD and, especially, $E_{g\downarrow}$ measurements could also be affected by inhomogeneities due for example to instrument changes or due to recalibrations ([31] - Chapter 5; [63]; [64]). All these well-known problems may cause significant errors in estimating $E_{g\downarrow}$ from SD.
For all these reasons, it is not surprising that $E_{g\downarrow}$ and SD records do not always display consistent trends, as shown by some studies in the literature which try to compare the long-term trends of SD and $E_{g\downarrow}$ for different areas over the world (for a review see Sanchez-Romero et al. ([48])). Thus, for example, Zhang et al. ([75]) report a lower rate of decrease for SD than for $E_{g\downarrow}$ over the period 1961-2000 in Eastern China, while Liang and Xia ([24]) and Che et al. ([9]), extending the study over the whole China for the same period, find a consistent spatial and temporal pattern for the two variables. Stanhill and Kalma ([58]) also find a lower decrease for SD than for $E_{g\downarrow}$, starting from measurements performed in Hong Kong over the period 1958-1992, suggesting that long-term increase in aerosols induces a more significant reduction in $E_{g\downarrow}$ than in SD. Furthermore, stronger and more significant tendencies are reported for $E_{g\downarrow}$ than for SD in Germany for different periods. Specifically, Liepert and Kukla ([25]) find a non significant change in SD and a significant

decrease of $E_{g\downarrow}$ between 1964 and 1990, while Power ([38]) finds a non significant trend in SD but an increase in $E_{g\downarrow}$ between the 1970s and the beginning of the 2000s. Similarly, Stanhill and Cohen ([57]) and Cutforth and Judiesch ([11]) find no long-term SD trend but rather significant reduction of $E_{g\downarrow}$ during the last 50 years of the twentieth century in the United States and in the Canadian Prairie, respectively. They attribute this discrepancy to the different sensitivity of SD and $E_{g\downarrow}$ measurements to diurnal changes in cloud cover, and to the influence of other variables such as RH in addition to the aerosols. Moreover, Soni et al. ([51]) find a significant and consistent decline for both variables during the 1971-2005 period in India. Overall, a large number of studies reported in literature shows stronger tendencies for $E_{g\downarrow}$ than for SD even if every study presents regional peculiarities. Recently, two homogenized datasets of SD ([28] - Chapter 2) and $E_{g\downarrow}$ ([29] - 3) have been setup for the first time for the Italian territory for the periods 1936-2013 and 1959-2013, respectively. This work aims to compare the variations reported in these studies for SD and $E_{g\downarrow}$ records over the common period (1959-2013) under all-sky (Section 6.3) and clear-sky (Section 6.4) conditions. Moreover, the agreement/disagreement in the obtained $E_{g\downarrow}$ and SD clear-sky records is discussed in relation to the variations estimated by means of a model based on Lambert-Beer's law and on a simple estimation of diffuse radiation (Section 6.5). Finally, some conclusive remarks are given (Section 6.6).

6.2 Data: sunshine duration and global radiation

The SD and $E_{g\downarrow}$ seasonal and annual all-sky records used in this paper are those presented by Manara et al. (2015) ([28]) and Manara et al. (2016) ([29]). They are northern and southern Italy average (relative) anomaly records obtained after projecting a large number of homogenized and gap-filled SD and $E_{g\downarrow}$ station anomaly records onto a 1-degree-resolution grid (Figure 6.1).

The station records were obtained from different sources, the major part of them coming from the Council for Agricultural Research and Agricultural Economy Analysis (CREA - Consiglio per la ricerca in agricoltura e l'analisi dell'economia agraria) and the Italian Air Force (AM - Aeronautica Militare Italiana). Full details on data availability, on temporal homogeneity and gap-filling issues are given in Manara et al. ([28]; [29]; [30]; [31] - Chapter 2-5).

The SD regional records cover a larger period (1936-2013) than the corresponding $E_{g\downarrow}$ records (1959-2013). In this paper, we consider only the common period (1959-2013) and in order to better compare SD and $E_{g\downarrow}$, the regional records are expressed for both variables as relative deviations from the 1976-2005 averages.

Beside the all-sky records, we consider also corresponding clear-sky $E_{g\downarrow}$ and SD records. Specifically, the clear-sky days were selected starting from an updated version (both concerning the number of series and the series length) of the TCC database presented by Maugeri et al. ([32]) and considering only the days with a daily TCC mean lower than or

equal to 1 okta. The advantage of 1 okta as the threshold instead of 0 okta (real clear-sky days), is to allow having a higher number of days and more robust clear-sky records even if the selected days are not completely clear. However, this choice does not introduce significant differences in the regional records as discussed by Manara et al. ([29] - Chapter 3). For the series without a corresponding TCC series, we selected the clear-sky days considering the cloudiness data from nearby stations.
As clear-sky records may contain only a small number of days in a month (the average number of clear days per station and month is 18%), the monthly averages may be influenced by the dates in which these days fall, especially in spring and autumn months. We decided therefore to transform the daily $E_{g\downarrow}$ data into clearness index data (i.e., the ratio between $E_{g\downarrow}$ and the corresponding quantity at the top of Earth's atmosphere) and the daily SD data into relative SD data (i.e., the ratio between SD and the time interval between sunrise and sunset) before calculating monthly records from the daily data. These monthly records were then gap-filled, re-transformed into absolute value records and used to calculate seasonal and annual anomalies that were projected onto the same grid used for the all-sky records (Figure 6.1). The grid-point records were finally used to obtain northern and southern Italy SD and $E_{g\downarrow}$ seasonal and annual clear-sky average anomaly records. The clear-sky $E_{g\downarrow}$ records presented in this paper are an updated version of those presented in Manara et al. ([29] - Chapter 3) where the absolute daily values were used instead of the relative daily values even if the same paper demonstrates that this choice does not introduce significant differences in the regional records.

6.3 Comparison between sunshine duration and global radiation records under all-sky conditions

The northern and southern Italy annual and seasonal SD and $E_{g\downarrow}$ records obtained under all-sky conditions are shown in Figure 6.2, together with the corresponding Gaussian low-pass filters (11-year window; 3-year standard deviation) that highlight the decadal variability and long-term trends.

In order to better compare SD and $E_{g\downarrow}$ records, we also show the annual and seasonal $E_{g\downarrow}$/SD ratio records (Figure 6.3 - black line) and the corresponding running trend analysis (Figure 6.4) ([8]). The latter allows estimating the significance (pixel size) and the slope (pixel color) of the trend of these records for each sub-interval of at least 21 years, with significance (p-value ≤ 0.05) estimated by means of the Mann-Kendall non parametric test and slope computed using the Theil-Sen method ([50]; [60]). Specifically, the y and x axes represent the length of the considered window and the starting year, respectively. The Theil-Sen method calculates the trend as the median of the slopes of the lines crossing all possible pairs of points: such methodology is particularly suitable in presence of outliers as it significantly reduces their influence on the results. The idea of investigating the $E_{g\downarrow}$/SD

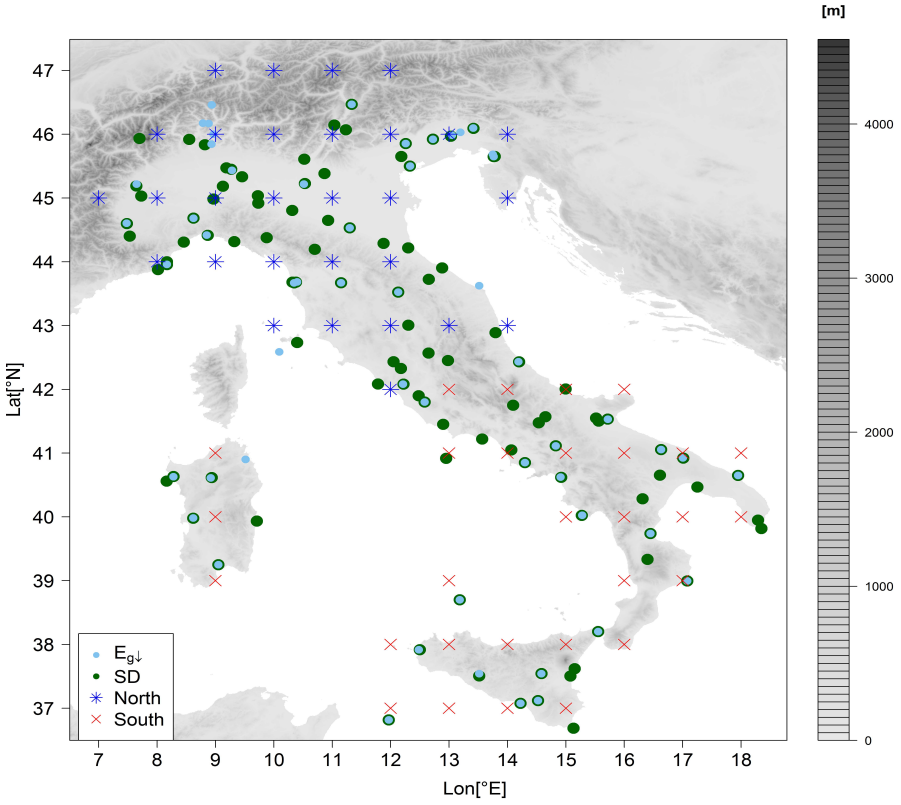

Figure 6.1: Spatial distribution of SD (green points) and $E_{g\downarrow}$ (sky-blue points) station records and of the grid-mode version of the dataset. Blue stars and red crosses represent, respectively, northern and southern Italy grid-points. The figure also shows the orography of the region.

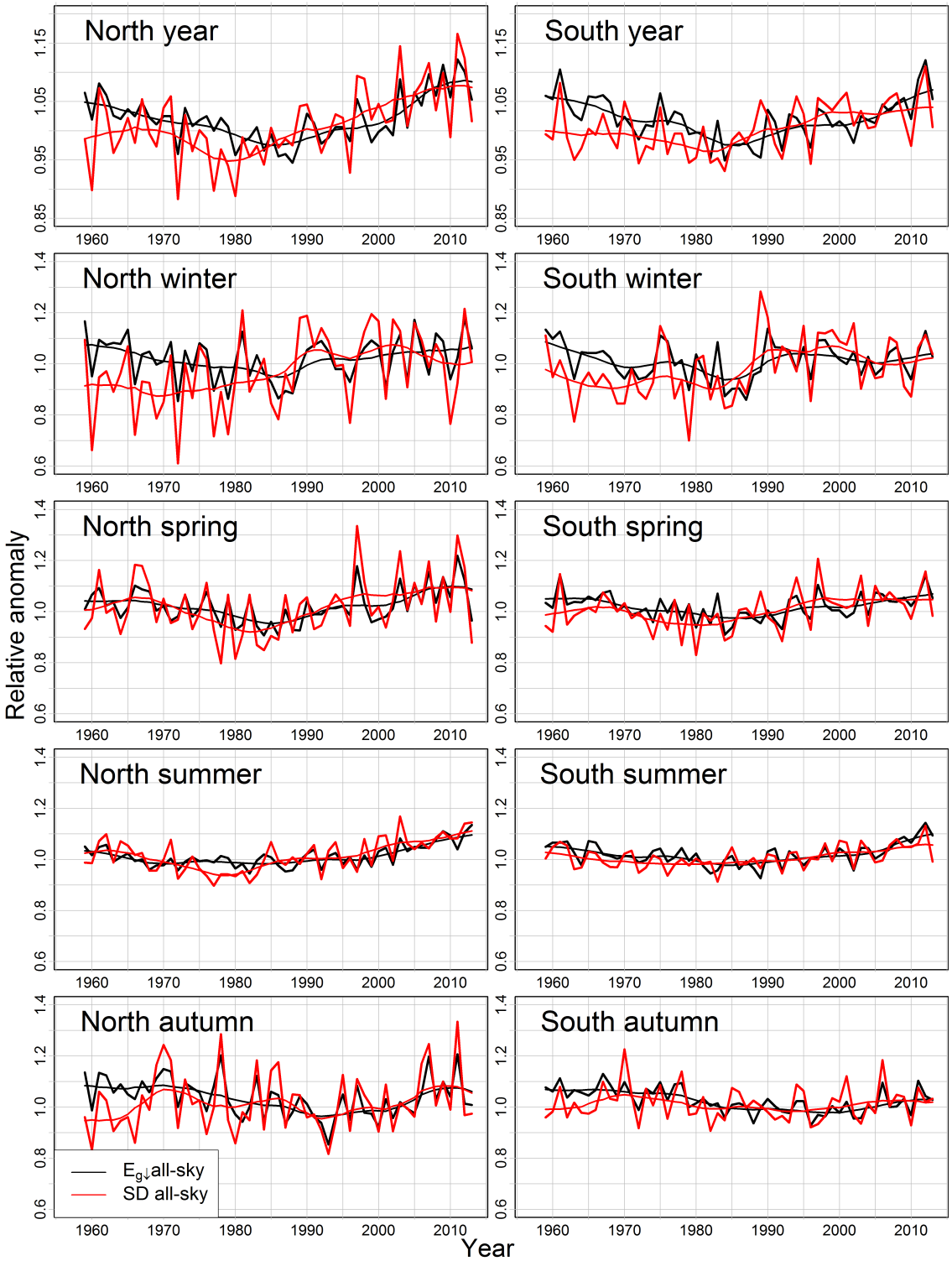

Figure 6.2: Northern (left column) and southern (right column) Italy annual and seasonal SD (red line) and $E_{g\downarrow}$ (black line) records obtained under all-sky conditions, plotted together with 11-year window, 3-year standard deviation Gaussian low-pass filters. The series are expressed as relative deviations from the 1976-2005 averages. Annual graphs are shown with an expanded scale with respect to seasonal ones.

ratios is that any trend in these records reflects the differences in the trends of SD and $E_{g\downarrow}$. Finally, we show in Table 6.1 the correlation coefficients between the records of the two variables over 1959-2013 and over the first and second part of this period (1959-1985 and 1986-2013), corresponding to the $E_{g\downarrow}$ dimming and brightening periods as illustrated by Manara et al. ([29] - Chapter 3). The correlation coefficients are also shown for the Gaussian low-pass filters and for the residuals from them.

Figures 6.2 and 6.3 highlight relevant differences between the all-sky SD (see Manara et al. ([28] - Chapter 2) for a detailed discussion of the trends) and $E_{g\downarrow}$ records (see Manara et al. ([29] - Chapter 3) for a detailed discussion of the trends). Overall, the SD records show a higher interannual variability than the $E_{g\downarrow}$ ones for both regions in all seasons (Figure 6.2), which is probably a consequence of the higher influence of cloudiness on SD day-to-day variability. The discrepancy is maximum in winter (the standard deviation of the residuals from the low-pass filter being 0.07 for $E_{g\downarrow}$ and 0.14 for SD in the northern region and 0.06 for $E_{g\downarrow}$ and 0.10 for SD in the southern region) and minimum in summer (0.02 for $E_{g\downarrow}$ and 0.04 for SD in the northern region and 0.03 for both variables in the southern region) when the cloudiness is lowest and the frequency of clear-sky days is highest.

The agreement between SD and $E_{g\downarrow}$ decadal variability and long-term trends depends on the considered region, season and period. Specifically, the annual SD series present a similar decadal variability to the $E_{g\downarrow}$ series (Figure 6.2) and both variables show for both the regions a dimming/brightening sequence. However, the dimming period for SD is shorter and less intense with respect to that observed for $E_{g\downarrow}$. This is highlighted also by the decrease (stronger in the north than in the south) observed in the ratio records until the end of the 1980s (Figure 6.3). Therefore, the ratio records for the longest windows considered in the running trend analysis (Figure 6.4) have significant negative trend both in the north and in the south (about $-1.5\%decade^{-1}$). Moreover, the SD series show a trend inversion from dimming to brightening at the end of the 1970s/beginning of the 1980s while the $E_{g\downarrow}$ series show it around the mid of the 1980s. This difference is more evident in the north than in the south (Figure 6.2).

During winter the two variables show strong differences until the mid of the 1980s (Figure 6.2), especially in the north, where SD does not show a decreasing tendency in the dimming period as $E_{g\downarrow}$ does. This is also highlighted by the decrease in the ratio records (Figure 6.3) and by the correlation coefficients (Table 6.1) between the low-pass filters of the two variables that during the 1959-1985 period are negative in the north (-0.22) and positive, but rather low, in the south (0.60). Nevertheless, the correlation coefficients of the residuals from the low-pass filters are very high and significant (p-value ≤ 0.05) in both regions (0.96 for the north and 0.83 for the south) underlining a good agreement in terms of the year-to-year variability. The agreement of the low-pass filters is better during the brightening period, where both variables increase and the ratios do not show any significant signal in the south and only few sub-periods with significant positive trend in the north (Figure 6.4). However, this weak increase is especially due to the last decade

			Year			Winter			Spring			Summer			Autumn		
			Anomaly	**Filter**	**Residual**	**Anomaly**	**Filter**	**Residual**	**Anomaly**	**Filter**	**Residual**	**Anomaly**	**Filter**	**Residual**	**Anomaly**	**Filter**	**Residual**
All-sky	**North**	**1959-2013**	0.73	0.73	**0.83**	0.77	0.18	**0.92**	0.90	0.89	**0.93**	0.81	0.89	**0.77**	0.77	0.39	**0.92**
		1959-1985	0.72	0.73	**0.85**	0.85	-0.22	**0.96**	0.93	0.93	**0.94**	0.65	0.72	**0.71**	0.77	-0.10	**0.92**
		1986-2013	0.82	0.96	**0.83**	0.80	0.32	**0.87**	0.89	0.93	**0.93**	0.89	0.97	**0.84**	0.91	0.98	**0.91**
	South	**1959-2013**	0.56	0.48	**0.66**	0.67	0.41	**0.76**	0.77	0.65	**0.85**	0.75	0.84	**0.76**	0.63	0.54	**0.79**
		1959-1985	0.72	0.89	**0.75**	0.80	0.60	**0.83**	0.84	0.86	**0.85**	0.71	0.86	**0.72**	0.68	0.40	**0.82**
		1986-2013	0.61	0.85	**0.59**	0.67	0.70	**0.68**	0.78	0.84	**0.84**	0.80	0.95	**0.79**	0.74	0.76	**0.78**
Clear-sky	**North**	**1959-2013**	0.50	0.65	0.10	0.08	0.01	*0.26*	0.58	0.84	**0.31**	0.64	0.86	0.06	0.31	0.28	**0.42**
		1959-1985	0.55	0.78	-0.04	-0.08	-0.62	0.25	0.60	0.91	0.17	0.47	0.80	0.13	0.37	0.59	0.20
		1986-2013	0.73	0.91	0.20	0.52	0.84	0.28	0.67	0.95	**0.43**	0.75	0.94	0.00	0.71	0.86	**0.52**
	South	**1959-2013**	0.63	0.88	**0.33**	0.16	0.31	0.12	0.61	0.89	**0.39**	0.79	0.93	**0.51**	0.44	0.83	0.08
		1959-1985	0.72	0.94	**0.39**	0.04	-0.13	0.02	0.63	0.98	*0.34*	0.80	0.99	**0.46**	0.49	0.81	0.01
		1986-2013	0.61	0.96	0.26	0.30	0.85	0.19	0.64	0.97	**0.46**	0.80	0.92	**0.56**	0.37	0.95	0.12

Table 6.1: Correlation coefficients between SD and $E_{g\downarrow}$ records (anomalies, low-pass filters and residuals from the filters) for northern and southern Italy under all-sky and clear-sky (see Section 6.4) conditions. For the residuals the significance level is also given: bold for significance level of $p \leq 0.05$, italic for significance level of $0.05 < p \leq 0.1$ and roman for significance level of $p > 0.1$.

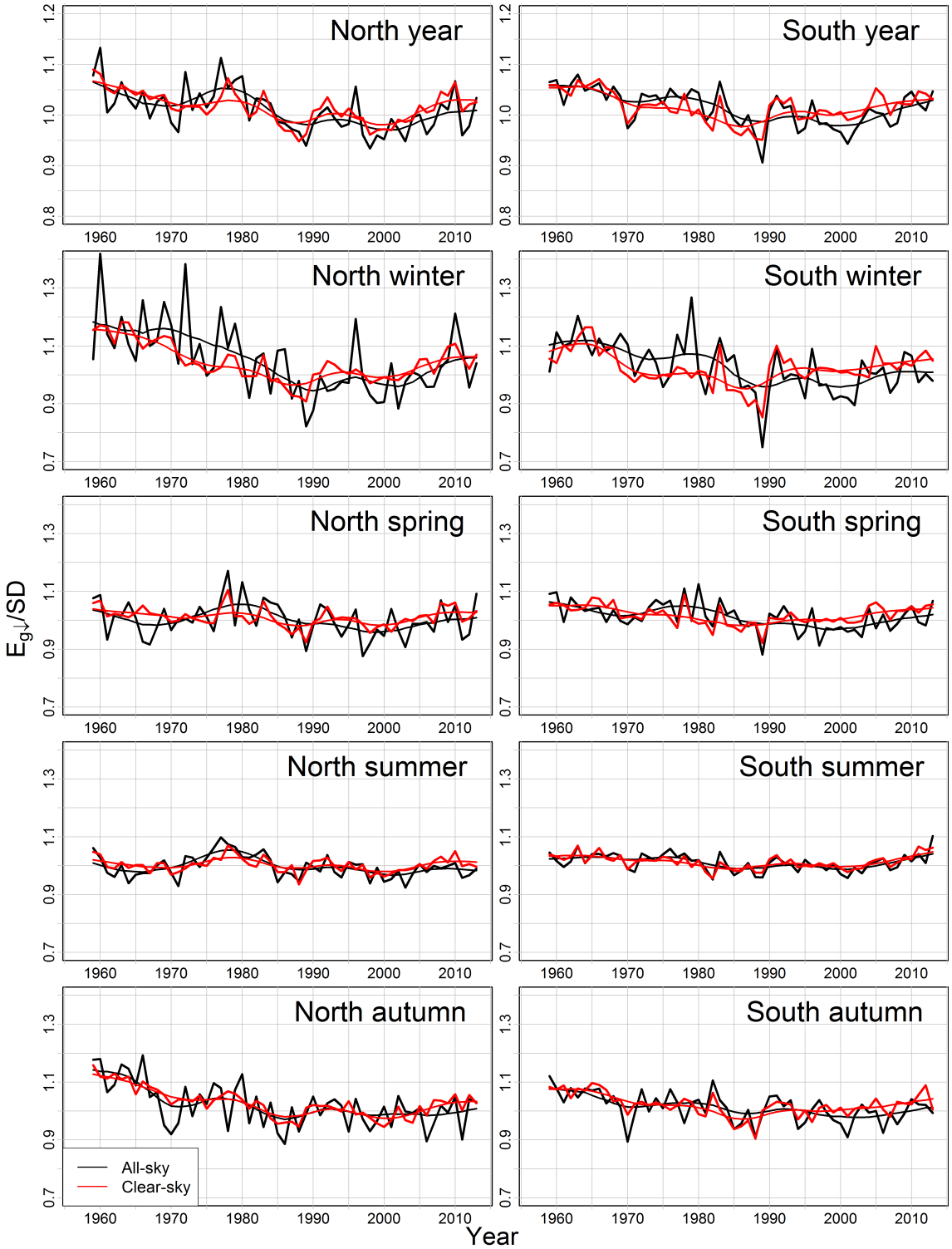

Figure 6.3: Annual and seasonal $E_{g\downarrow}$/SD records for northern (left column) and southern (right column) Italy under all-sky (black line) and clear-sky (red line - see Section 6.4) conditions. The series are plotted together with an 11-year window, 3-year standard deviation Gaussian low-pass filter. Annual graphs are shown with an expanded scale with respect to seasonal ones.

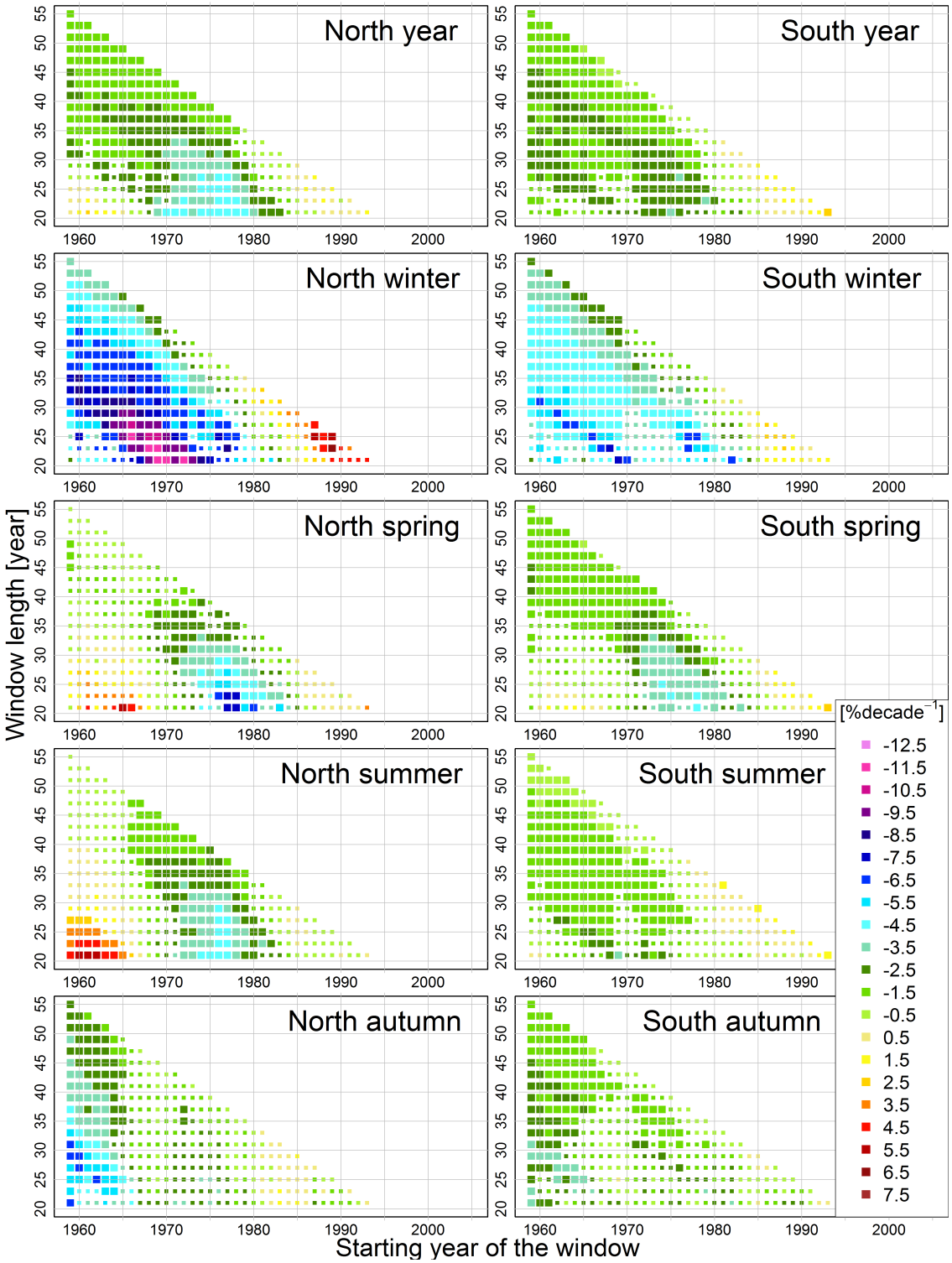

Figure 6.4: Trend of the all-sky $E_{g\downarrow}$/SD records for each sub-interval of at least 21 years. The results are reported both in terms of slopes ($\%decade^{-1}$) and significance levels (large pixels: p≤0.05; small pixels: p>0.05). The y axis represents the window width, and the x axis represents the starting year of the window used for the computation of the trend.

and so it will be necessary to verify this signal when new data will be available in order to confirm it.

During spring and summer the two variables show a decadal variability similar to the annual mean (Figure 6.2) and the ratio records show that the discrepancies between SD and $E_{g\downarrow}$ records are less evident compared to the winter ones (Figures 6.3, 6.4). However, SD shows (more evident in the north than in the south) a trend inversion at the beginning of the 1980s while $E_{g\downarrow}$ shows it around the mid of the 1980s for both seasons (Figure 6.2). Moreover, in the northern region, SD shows a stronger decrease than $E_{g\downarrow}$ in the 1970s and a stronger increase in the 1980s and 1990s, which causes the corresponding increases/decreases in the ratio records. However, the increase in the ratio record is very short and only for few sub-periods has significant trend (Figure 6.4). In the southern region, in the dimming period both in spring and summer, the records show lower decrease for SD than for $E_{g\downarrow}$, which causes a decrease (stronger in spring) of the ratio records (Figures 6.3, 6.4). Interestingly, the best agreement between the two variables in terms of variability at decadal time scale concerns summer that is the season in which the correlation coefficients between SD and $E_{g\downarrow}$ residuals are lowest (for both the regions) (Table 6.1). On the contrary, the lowest agreement between the low-pass filter records (winter in northern Italy over the 1959-2013 period) corresponds to a very high correlation coefficient (0.92) of the residuals, giving evidence that the processes causing the agreement/disagreement of SD and $E_{g\downarrow}$ may be different at yearly and decadal time scales.

During autumn, the two variables show a good agreement even if there are strong differences (more pronounced in the north) in the first decade where the SD records increase while the $E_{g\downarrow}$ ones decrease (Figure 6.2). This is reflected by a clear decrease in the ratio records (Figure 6.3). The decrease of the ratio records continues until the mid of the 1980s (even if the slope is weaker compared to the first decade) due to a stronger dimming in the $E_{g\downarrow}$ records than in the SD ones. The agreement is higher if the subsequent part of the series is considered (especially in the northern region) (Table 6.1 and Figure 6.2) where the ratio records do not show any significant trend (Figure 6.4).

Finally, we show in Table 6.2 the trends estimated by the Theil-Sen ([50]; [60]) method for 1959-2013, 1959-1980 and 1985-2013, which correspond to the whole period analyzed and the dimming and brightening periods according to both the SD and $E_{g\downarrow}$ records.

These values confirm what has already been discussed above. Specifically, the trends during the dimming period (1959-1980) and brightening period (1985-2013) (in $\%decade^{-1}$) are stronger (or comparable) and more significant for $E_{g\downarrow}$ than SD. The only exceptions are: autumn (non-significant trend) for both regions, summer in the north (stronger SD trend than $E_{g\downarrow}$) during the dimming period and winter in the south (non-significant trend) for the brightening period.

	Period	Variable	Year	Winter	Spring	Summer	Autumn
North all-sky	**1959-2013**	$E_{g\downarrow}$	+	+	+	**1.2**	**-1.6**
		SD	**1.7**	**3.5**	+	**2.0**	+
	1959-1980	$E_{g\downarrow}$	**-2.4**	**-6.5**	-2.9	-2.0	-
		SD	-	-	-	**-5.9**	+
	1985-2013	$E_{g\downarrow}$	**4.4**	**5.1**	**5.8**	**4.7**	+
		SD	**3.6**	+	5.5	**4.2**	+
South all-sky	**1959-2013**	$E_{g\downarrow}$	-	-	+	+	**-1.7**
		SD	**1.1**	**2.4**	**1.4**	**0.9**	-
	1959-1980	$E_{g\downarrow}$	**-2.9**	**-5.6**	**-3.5**	**-2.2**	-
		SD	-	-	-	-	+
	1985-2013	$E_{g\downarrow}$	**3.0**	+	**3.5**	**4.3**	+
		SD	**1.9**	+	2.5	**2.3**	+
North clear-sky	**1959-2013**	$E_{g\downarrow}$	-	-	-	+	**-1.1**
		SD	**0.9**	**1.6**	**0.6**	**0.8**	**1.1**
	1959-1980	$E_{g\downarrow}$	**-3.2**	**-5.2**	**-2.5**	**-1.4**	**-5.6**
		SD	-	**2.2**	**-2.1**	**-2.0**	-
	1985-2013	$E_{g\downarrow}$	**4.3**	**5.7**	**3.8**	**3.7**	**4.4**
		SD	**2.2**	**1.7**	**1.8**	**3.0**	**2.7**
South clear-sky	**1959-2013**	$E_{g\downarrow}$	-	-	-	-	**-1.2**
		SD	+	**0.6**	+	+	-
	1959-1980	$E_{g\downarrow}$	**-3.6**	**-4.5**	**-4.0**	**-2.9**	**-4.0**
		SD	-0.9	+	**-1.6**	**-1.8**	-
	1985-2013	$E_{g\downarrow}$	**3.5**	**4.6**	**3.8**	**3.6**	**3.2**
		SD	**1.2**	**1.0**	**1.2**	**1.9**	0.9

[a]Values are expressed in $\%decade^{-1}$. Values are shown in roman for significance level of $0.05 < p \leq 0.1$ and in bold for a significance level of $p \leq 0.05$. For non-significant trends, only the sign of the slope is given. The significance of the trends is evaluated with the Mann-Kendall non parametric test while the trends are estimated by the Theil-Sen method.

Table 6.2: SD and $E_{g\downarrow}$ trends in northern and southern Italy under all-sky and clear sky (see Section 6.4) conditions[a]

6.4 Comparison between sunshine duration and global radiation records under clear-sky conditions

The analysis of the factors causing different decadal variability and long-term trends in SD and $E_{g\downarrow}$ records is very difficult, as in addition to instrumental issues a number of environmental variables should be considered including for example cloudiness, atmospheric aerosols and RH. One approach to reduce the complexity of the problem is to remove the cloudiness effect selecting only the clear-sky days. The northern and southern Italy annual and seasonal SD and $E_{g\downarrow}$ records obtained under clear-sky conditions are therefore shown in Figure 6.5 together with the corresponding low-pass filters.

The $E_{g\downarrow}$ records give evidence of a well-defined dimming/brightening sequence in all seasons for both regions, with rather coherent decadal variability and a transition from dimming to brightening around the mid of the 1980s ([29] - Chapter 3). The removal of the cloud contribution produces on the SD records an effect already observed for the $E_{g\downarrow}$ ones ([29] - Chapter 3): both in the north and in the south the dimming period becomes longer and the corresponding trends more significant in all seasons, with the only exception of winter. Moreover, the increase during the brightening period (spring and summer) becomes weaker (even if the trends are still significant). The most relevant changes are observed in autumn for both regions where under all-sky conditions the SD curves do not show any signal, while under clear-sky conditions the dimming/brightening periods become more significant. The trend is more pronounced during the dimming period in the south (e.g., -1.06 $\%decade^{-1}$, p-value ≤ 0.05 over the period 1959-1985) and during the brightening period in the north (Table 6.2).

For a better visualization of the agreement/disagreement between SD and $E_{g\downarrow}$ clear-sky records, the $E_{g\downarrow}$/SD ratios are reported in Figure 6.3 (red line) and the corresponding running trend analysis in Figure 6.6, whereas the correlation coefficients between the two variables (anomalies, filters and the residuals from them over the periods 1959-2013, 1959-1985 and 1986-2013) are shown in Table 6.1.

Differently from the all-sky records, the clear-sky $E_{g\downarrow}$ records show a comparable (in the north) or slightly higher (in the south) interannual variability than the SD ones over the period 1959-2013. The standard deviations of the residuals from the low-pass filters range from 0.014 (summer in the north) to 0.034 (winter in the south) for $E_{g\downarrow}$ and from 0.010 (annual mean in the north) to 0.022 (winter in the south) for SD. For both variables, the interannual variability is lower for the clear-sky than for the all-sky records, which is an obvious consequence of the relevant role of cloudiness in the year-to-year variability of these variables. It is interesting to highlight that the SD and $E_{g\downarrow}$ residuals from the filters have rather low correlations in clear-sky compared to the all-sky conditions. The highest correlation coefficients for the residuals are observed in spring for both regions, autumn in the north and summer in the south (Table 6.1). However, the common variance between the SD and $E_{g\downarrow}$ residuals is rather low in all seasons and regions (the maximum value is 31% for southern Italy during the 1986-2013 period) and only few correlation coefficients

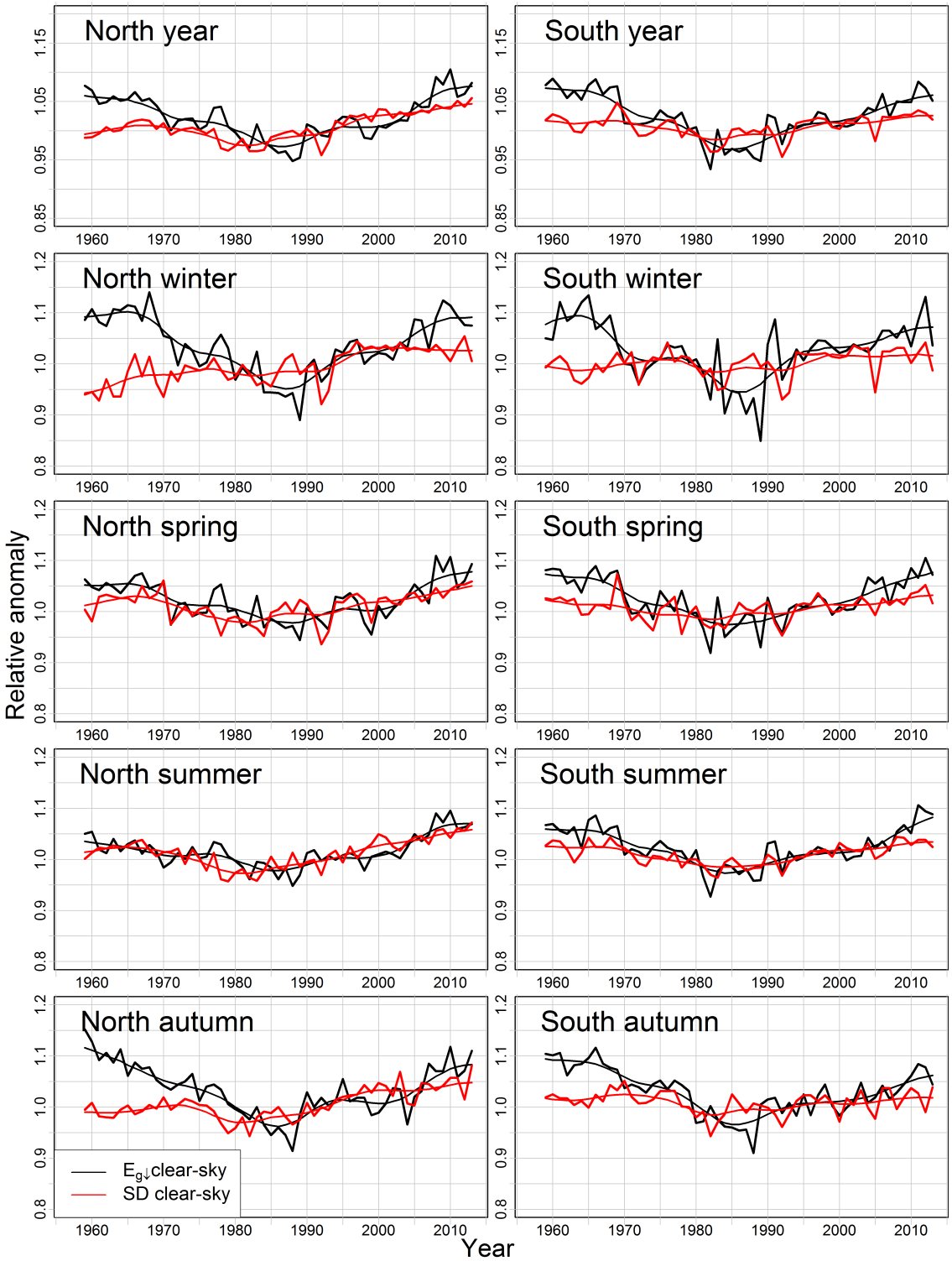

Figure 6.5: Northern (left column) and southern (right column) Italy annual and seasonal SD (red line) and $E_{g\downarrow}$ (black line) records obtained under clear-sky conditions, plotted together with 11-year window, 3-year standard deviation Gaussian low-pass filters. The series are expressed as relative deviations from the 1976-2005 averages. Annual graphs are shown with an expanded scale with respect to seasonal ones.

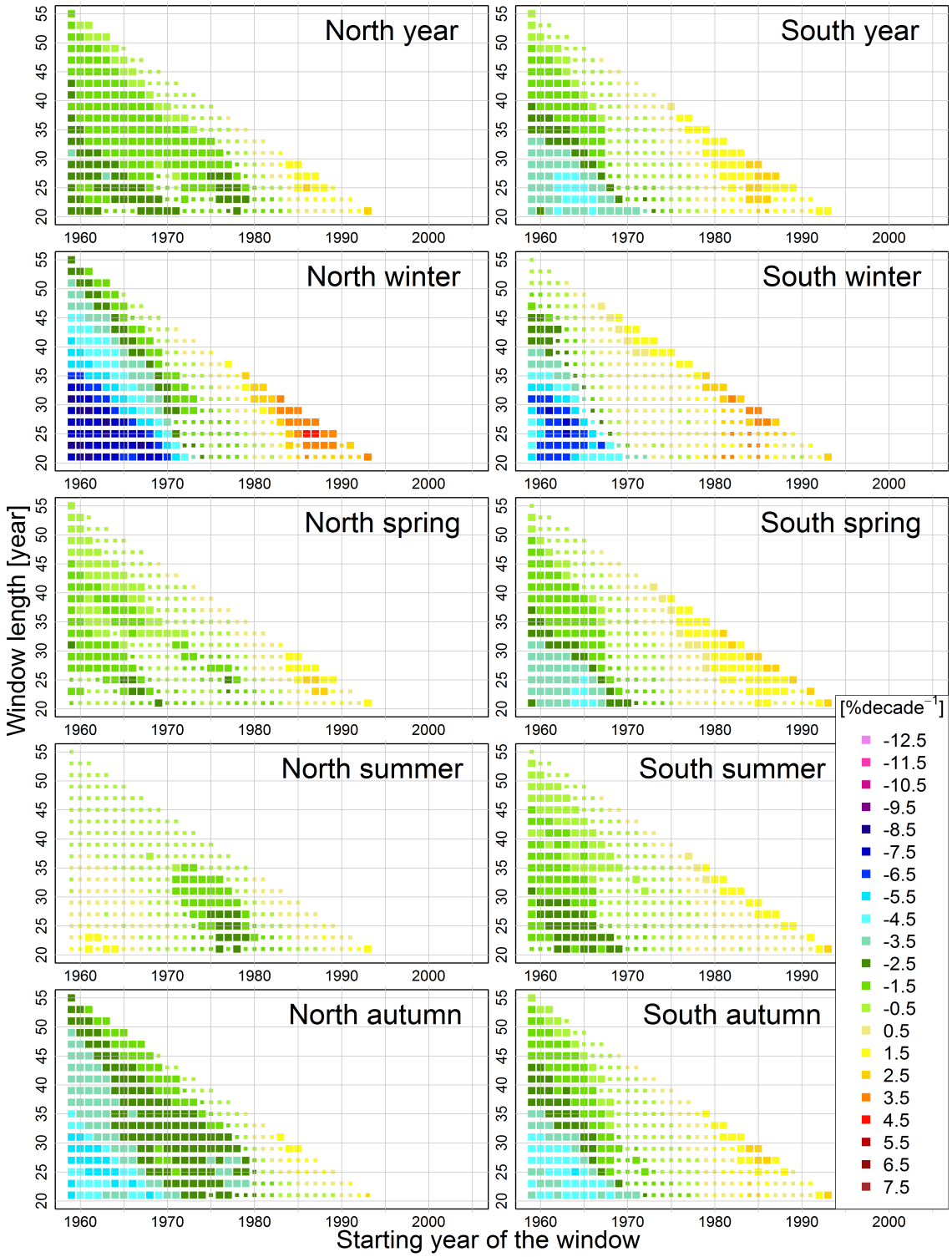

Figure 6.6: Trend of the clear-sky $E_{g\downarrow}$/SD records for each sub-interval of at least 21 years. The results are reported both in terms of slopes ($\%decade^{-1}$) and significance levels (large pixels: p≤0.05; small pixels: p>0.05). The y axis represents the window width, and the x axis represents the starting year of the window used for the computation of the trend.

have a p-value lower than 0.05. Moreover, in most seasons and periods under clear-sky conditions the correlation between the filters is comparable or increases with respect to the all-sky conditions (Table 6.1). This underlines that under clear-sky conditions SD and $E_{g\downarrow}$ are affected by the same factors at decadal time scale, even though their agreement in terms of year-to-year variability is rather low.
As already observed for all-sky conditions, the agreement between clear-sky SD and $E_{g\downarrow}$ decadal variability and long-term trends depends on the considered region, season and period (Figure 6.5). The ratio records show, as already discussed for the all-sky series, a decreasing tendency until the mid-1980s, more pronounced in winter and autumn, for both regions resulting from a stronger dimming of $E_{g\downarrow}$ than of SD (Table 6.2). The corresponding running trend analysis (Figure 6.6) shows significant trends for almost all sub-periods starting in the first decade differently from the all-sky conditions (Figure 6.4) where the decrease was significant in most part of the cases only when longer periods were considered. The agreement between the two variables is higher in the brightening period as both variables increase, even if the $E_{g\downarrow}$ trends present higher values (Table 6.2). This is reflected in some positive sub-periods in the last part of the ratio records, in all seasons and regions (Figure 6.6) differently from the all-sky conditions (Figure 6.4) when very few sub-periods showed a significant trend.
Moreover, the negative trends in the ratio records of the first decades are generally stronger than the trends observed in the following decades causing all series to have a negative slope in the longest sub-periods, even though not all of them are significant (summer in the north and winter, spring and summer in the south). In northern Italy, during summer, the decrease of the first period in the ratio record is not present and only few sub-periods have a significant trend, implying a good agreement between SD and $E_{g\downarrow}$. Here, the few sub-periods with a significant negative trend are due to different reversal years from dimming to brightening for SD (beginning of 1980s) and $E_{g\downarrow}$ (mid-1980s). It is worth noting that this is the only season (as already observed under all-sky conditions) for which SD shows a stronger dimming than $E_{g\downarrow}$ (Table 6.2, northern Italy) as highlighted by the only case in which the running trend analysis shows sub-periods with positive trend during the 1960s (Figure 6.6, northern Italy).

6.5 Sunshine duration and global radiation sensitivity to variations in atmospheric turbidity

The main result highlighted by the comparison between the SD and $E_{g\downarrow}$ clear-sky records is that the latter show generally stronger signals than the former, with a stronger decrease in the dimming period and a slightly stronger increase in the brightening period (the only exception is summer in northern Italy).
In order to investigate whether such behavior can be explained by a different sensitivity

of SD and $E_{g\downarrow}$ to atmospheric turbidity variations, we applied a model based on Lambert-Beer's law to estimate the direct radiation and on a simple estimation of diffuse radiation. The model we applied is based on Rigollier et al. ([41]). It estimates the atmospheric attenuation of $E_{g\downarrow}$ (calculating separately the direct - E and the diffuse - $E_{d\downarrow}$ components) under clear-sky conditions, in terms of the atmospheric turbidity. Indeed, the larger the atmospheric turbidity, the larger the attenuation of the direct radiation (less E) and the larger the portion of the scattered radiation (more $E_{d\downarrow}$) by the atmosphere.
In this model, E is calculated with the following equation ([41]):

$$E(\phi,k) = I_0 * E_0(k) * \int_{\omega_{SR}(\phi,k)}^{\omega_{SS}(\phi,k)} \cos(\theta_{INC}(\phi,k,\omega)) * e^{-0.8662*T_L*m_A(\phi,k,\omega)*\delta_R(\phi,k,\omega)}\, d\omega \quad (6.1)$$

Specifically:

- ϕ is the latitude of the considered point;
- k (k=1,...,12) is the considered month;
- I_0 is the solar constant ($I_0 = 1361 W m^{-2}$, ([22]));
- $E_0(k)$ is the eccentricity factor ([19]);
- $\cos(\theta_{INC}(\phi,k,\omega))$ is the cosine of the solar angle of incidence for a flat surface ([19]);
- T_L is the Turbidity Linke factor: i.e. the number of clean dry atmospheres that would be necessary to pile up in order to obtain the same attenuation of the extraterrestrial radiation as that produced by the actual atmosphere. T_L is related to the total turbidity (aerosol and water vapor) ([20]) and is considered standardized (by means of the 0.8662 factor) for an air mass equal to 2 ([15]);
- $m_A(\phi,k,\omega)$ is the optical air mass ([20]; [41]);
- $\delta_R(\phi,k,\omega)$ is the Rayleigh optical depth ([41]).

The equation is considered for the central day of each month and the integration is performed dividing the length of the day (from sunrise - $\omega_{SR}(\phi,k)$ to sunset - $\omega_{SS}(\phi,k)$) in N intervals (expressed in hour angle - ω). In order to avoid rounding errors, we used a very short time step (N=100000).
In the Campbell-Stokes SD recorder, the paper card is always normal to the direct radiation and therefore the term $\cos(\theta_{INC}(\phi,k,\omega))$ in Equation (6.1) is equal to 1 for each time step when the direct radiation is calculated to obtain SD. Specifically, all time steps for which the direct radiation is higher than 120 $W m^{-2}$ are selected, and the difference between the hour angles corresponding to the maximum and the minimum steps are transformed in hours.
Differently, to calculate E, the term $\cos(\theta_{INC}(\phi,k,\omega))$ is different for each time step during the day and so the daily value is calculated integrating Equation (6.1) from sunrise to

sunset.
$E_{d\downarrow}$ is obtained integrating from the sunrise to the sunset the following equation ([41]):

$$E_{d\downarrow}(T_L, \phi, k, \omega) = I_0 * E_0(k) * T_{rd}(T_L) * F_d(T_L, \phi, k, \omega) \tag{6.2}$$

where $T_{rd}(T_L)$ is the diffuse transmission function at zenith and $F_d(T_L, \phi, k, \omega)$ is the diffuse angular function as given in the following equations:

$$T_{rd}(T_L) = -1.5843 * 10^{-2} + 3.0543 * 10^{-2} * T_L + 3.797 * 10^{-4} * T_L^2 \tag{6.3}$$

$$F_d(T_L, \phi, k, \omega) = A_0(T_L) + A_1(T_L) * \sin(h(\phi, k, \omega)) + A_2(T_L) * \sin(h(\phi, k, \omega))^2 \tag{6.4}$$

where $h(\phi, k, \omega)$ is the solar altitude angle and the coefficients are set as follows:

$$\begin{cases} A_0(T_L) = 2.6463 * 10^{-1} - 6.1581 * 10^{-2} * T_L + 3.1408 * 10^{-3} * T_L^2 \\ A_1(T_L) = 2.0402 + 1.8945 * 10^{-2} * T_L - 1.1161 * 10^{-2} * T_L^2 \\ A_2(T_L) = -1.3025 + 3.9231 * 10^{-2} * T_L + 8.5079 * 10^{-3} * T_L^2 \end{cases} \tag{6.5}$$

$A_0(T_L)$ is subjected to the following condition:

$$if(A_0(T_L) * T_{dr}(T_L)) < 2 * 10^{-3}, A_0(T_L) = \frac{2 * 10^{-3}}{T_{dr}(T_L)} \tag{6.6}$$

This additional condition is necessary because $A_0(T_L)$ becomes negative for $T_L > 6$. When the turbidity increases the diffuse transmission function increases while the angular term decreases. The resulting $E_{d\downarrow}$ decreases if the turbidity increases during the early morning/late evening while it increases during the central part of the day.
Before investigating the SD and $E_{g\downarrow}$ sensitivity to T_L variations, we applied Equations (6.1) and (6.2) to estimate the T_L monthly normal values at each site. Specifically, we searched for the T_L values which give the observed clear-sky $E_{g\downarrow}$ monthly mean values over the period 1959-2013. Such estimation may however have some problems as all the data preprocessing has been performed to ensure the accuracy and temporal homogeneity of the anomaly records, whereas the possible problems of the absolute value records have not been considered. We can therefore not exclude the presence of small biases e.g. due to the fact that the sky-view factor can be partially reduced during the sunrise/sunset in some stations. This could be true for the stations surrounded by hills and mountains or located in urban areas (e.g., records that are collected at urban observatories). Moreover, it should be considered that the T_L values are calculated comparing the simulated $E_{g\downarrow}$ mean values with the observed clear-sky $E_{g\downarrow}$ climatologies obtained using 1 okta as threshold. The monthly T_L normal values we get with this estimation have therefore to be considered only as indicative values. They are higher in all months for the north than for the south, with the southern Italy values about 15-20% lower than the northern Italy ones. The means over all Italian stations range from 3.4 (January) to 5.5 (July). Considering

that the observed clear-sky $E_{g\downarrow}$ normal values could be slightly underestimated (due to the not optimal sky-view factor in some stations and to the threshold adopted to select the clear-sky days), it is reasonable to consider for Italy the following T_L mean values: about 3 in winter, about 5 in summer and about 4 in spring and autumn. This small correction corresponds to the assumption that the actual $E_{g\downarrow}$ normal values are 2-3% higher than those we get from our clear-sky records.

These T_L values correspond however to $E_{g\downarrow}$ normal values over the entire 1959-2013 period. In order to estimate reasonable T_L values for shorter intervals as well, we have to consider that before the dimming period the T_L values were lower than the corresponding 1959-2013 T_L normals. Then, they increased during the dimming period until they reached their maximum values that were higher than the corresponding 1959-2013 T_L normals. Similarly, during the brightening period T_L decreased from their maximum values until the ending values that were again lower than the corresponding 1959-2013 T_L normals. We considered therefore as pre-dimming T_L values, the values which justify the $E_{g\downarrow}$ values in the first years (obtained starting from the $E_{g\downarrow}$ 1959-2013 normals and the relative anomalies - with respect to the 1959-2013 period - of the first years). Then, we used the same approach to identify the most reasonable pre-brightening T_L values and the values of the last years.

We analyzed then the SD and $E_{g\downarrow}$ sensitivity to T_L variations by means of Equations (6.1) and (6.2). Specifically, we considered two points located at sea level and representative of the northern and southern latitudes (45 and 39°N respectively), and we calculated the variations of SD and $E_{g\downarrow}$ for a T_L increase/decrease with respect to starting points equal to each integer and half of integer comprised in a wide interval of values. We report the result of this analysis in Figure 6.7 for the central month of each season (January, April, July and October) and for T_L starting values ranging from the pre-dimming to the pre-brightening values, estimated as above.

The curves in Figure 6.7 concerning 39 and 45°N are very similar both for $E_{g\downarrow}$ and SD. A latitudinal effect is visible almost only for SD in winter and autumn for T_L starting values higher than 4, showing stronger variations for the point located at a higher latitude. We discuss therefore the figure without differentiating the lines concerning the two latitudes. The modelled variations are generally in good agreement with the variations observed under clear-sky conditions (Figures 6.3, 6.5, 6.6), even though for northern Italy some relevant differences are evident in winter and autumn especially during the dimming period. Specifically, in spring (April), considering a pre-dimming T_L value of 3.0-3.5 and a following increase until a pre-brightening value of about 4.5, the modelled $E_{g\downarrow}$ shows stronger variations (decrease) than the modelled SD (e.g., from the panel in row 1 and column 2 of Figure 6.7, for T_L moving from 3.0 to 4.5, SD is expected to decrease about one third less than $E_{g\downarrow}$), as obtained for the observed clear-sky series (Figures 6.3, 6.5, 6.6). The same behavior can be observed starting from the pre-brightening value (about 4.5) and decreasing T_L until an ending value of 3.0-3.5. Also in this case there is a stronger variation (increase) of the modelled $E_{g\downarrow}$ with respect to the modelled SD (e.g., from the panel

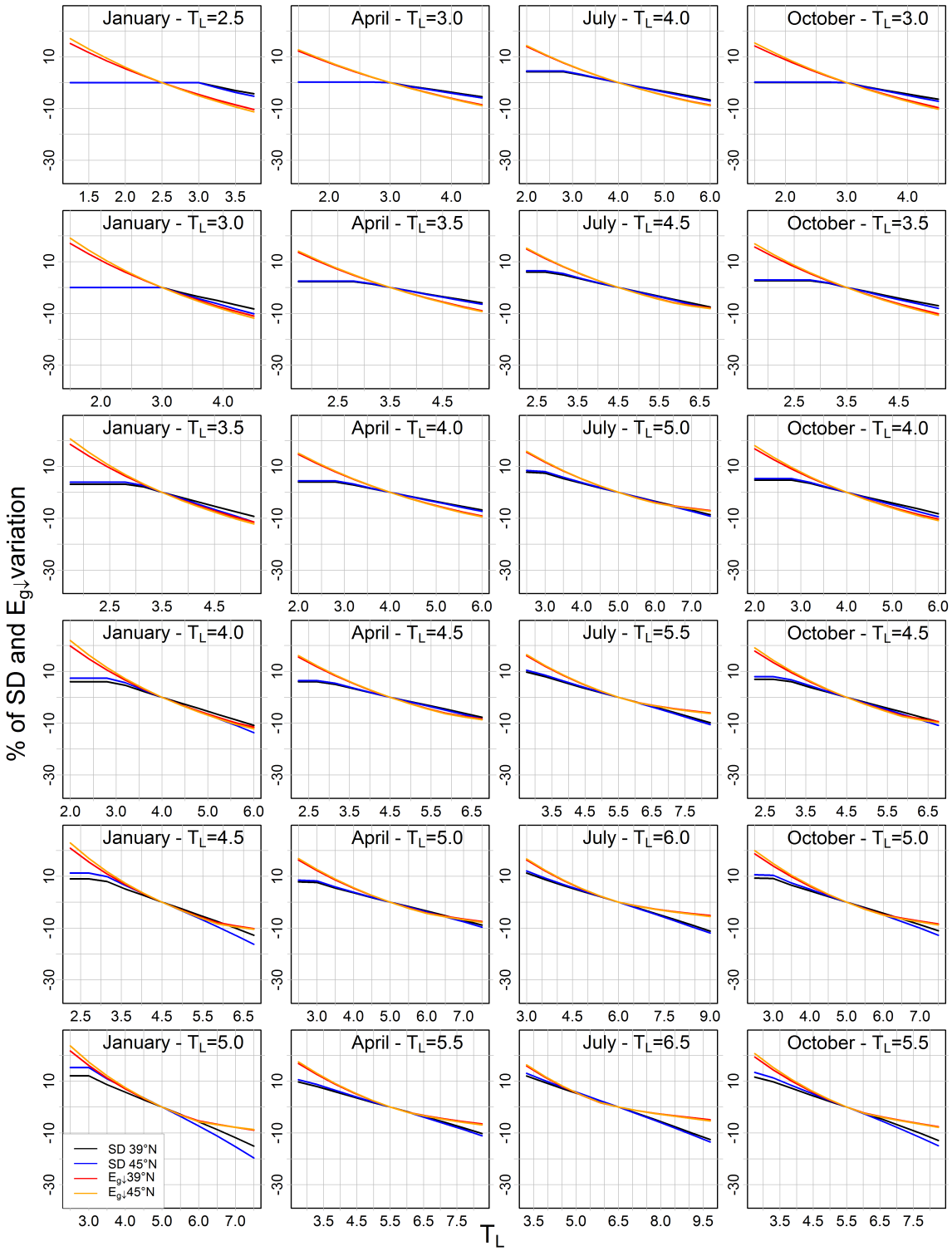

Figure 6.7: Variation (expressed in %) of modelled SD ($E_{g\downarrow}$) for a T_L increase/decrease respect to the starting value indicated in each plot. The black (blue) line represents SD variations for a point located at a latitude of 39°N (45°N) while the red (orange) line represents $E_{g\downarrow}$ variations for a point located at a latitude of 39°N (45°N). The results are shown for the central month of each season.

in row 4 and column 2 of Figure 6.7, for T_L moving from 4.5 to 3.0, SD is expected to increase about one third less than $E_{g\downarrow}$), which is in agreement with the observed clear-sky series (Figures 6.3, 6.5, 6.6).

In summer (July), the modelled $E_{g\downarrow}$ variations are only slightly stronger than the modelled SD ones both when T_L increases between a pre-dimming equal to about 4.5 and a pre-brightening equal to 5.5-6.0 (see e.g., the panel in row 2 and column 3 of Figure 6.7, for T_L moving from 4.5 to 5.5) and when it decreases between 5.5-6.0 and an ending value of about 4 (see e.g., the panel in row 4 and column 3 of Figure 6.7, for T_L moving from 5.5 to 4.0) as obtained for the observed $E_{g\downarrow}$ and SD records (Figures 6.3, 6.5, 6.6). It is also interesting to underline that the higher T_L values in the north could explain the only case for which we obtain that the observed $E_{g\downarrow}$ does not have variations stronger than SD during the dimming period (considering e.g. T_L pre-dimming and pre-brightening values equal to about 5.5 and 6.5).

In autumn (October), from the modelled results (Figure 6.7) $E_{g\downarrow}$ is expected to have higher variations than SD both when T_L increases between a pre-dimming value of 3.0-3.5 to a pre-brightening value of about 4.5 (e.g., from the panel in row 1 and column 4 of Figure 6.7, for T_L moving from 3.0 to 4.5, SD is expected to decrease about one third less than SD) and when it decreases between about 4.5 and an ending value of 3.0-3.5 (e.g., from the panel in row 4 and column 4 of Figure 6.7, for T_L moving from 4.5 to 3.0, SD is expected to increase about one third less than $E_{g\downarrow}$). This is in agreement with the results reported for clear-sky conditions, even though the simulated values do not explain the weak decrease of the observed SD (see Figure 6.5) in the dimming period especially in the north.

A similar behavior is observed in winter (January): also in this season, modelled $E_{g\downarrow}$ is expected to have higher variations than the corresponding SD both when T_L increases from a pre-dimming of 2.5-3.0 to a pre-brightening of 3.5-4.0 (e.g., panel in row 1 and column 1 for T_L moving from 2.5 to 3.5, SD is expected to decrease about two third less than $E_{g\downarrow}$) and when it decreases between 3.5-4.0 and an ending value of 2.5-3.0 (e.g., from the panel in row 3 and column 1 in Figure 6.7 for T_L moving from 3.5 to 2.5, SD is expected to increase about two third less than $E_{g\downarrow}$). In this case for southern Italy the simulated impacts of the atmospheric turbidity evolution on $E_{g\downarrow}$ and SD (Figure 6.7) are in reasonable agreement with the observations (Figures 6.3, 6.5, 6.6), whereas for northern Italy, during the dimming period, relevant discrepancies between the modelled and the observed variations are evident. The previous results show that the SD and $E_{g\downarrow}$ sensitivity to T_L variations strongly depends on the T_L starting value. Specifically, for low T_L starting values $E_{g\downarrow}$ is more sensitive while for high T_L the behavior is opposite. In order to highlight this behavior, we investigated the relative decrease of modelled SD and $E_{g\downarrow}$ corresponding to an increase of T_L of one unit for any integer T_L value in the range 2-7. Specifically, for each one of these T_L values, we calculated the relative decrease of both SD and $E_{g\downarrow}$ for T_L increasing from T_L - 0.5 to T_L + 0.5. The results are shown in Figure 6.8. They highlight that for T_L lower than 4, SD is less sensitive than $E_{g\downarrow}$ (to changes in T_L) for all

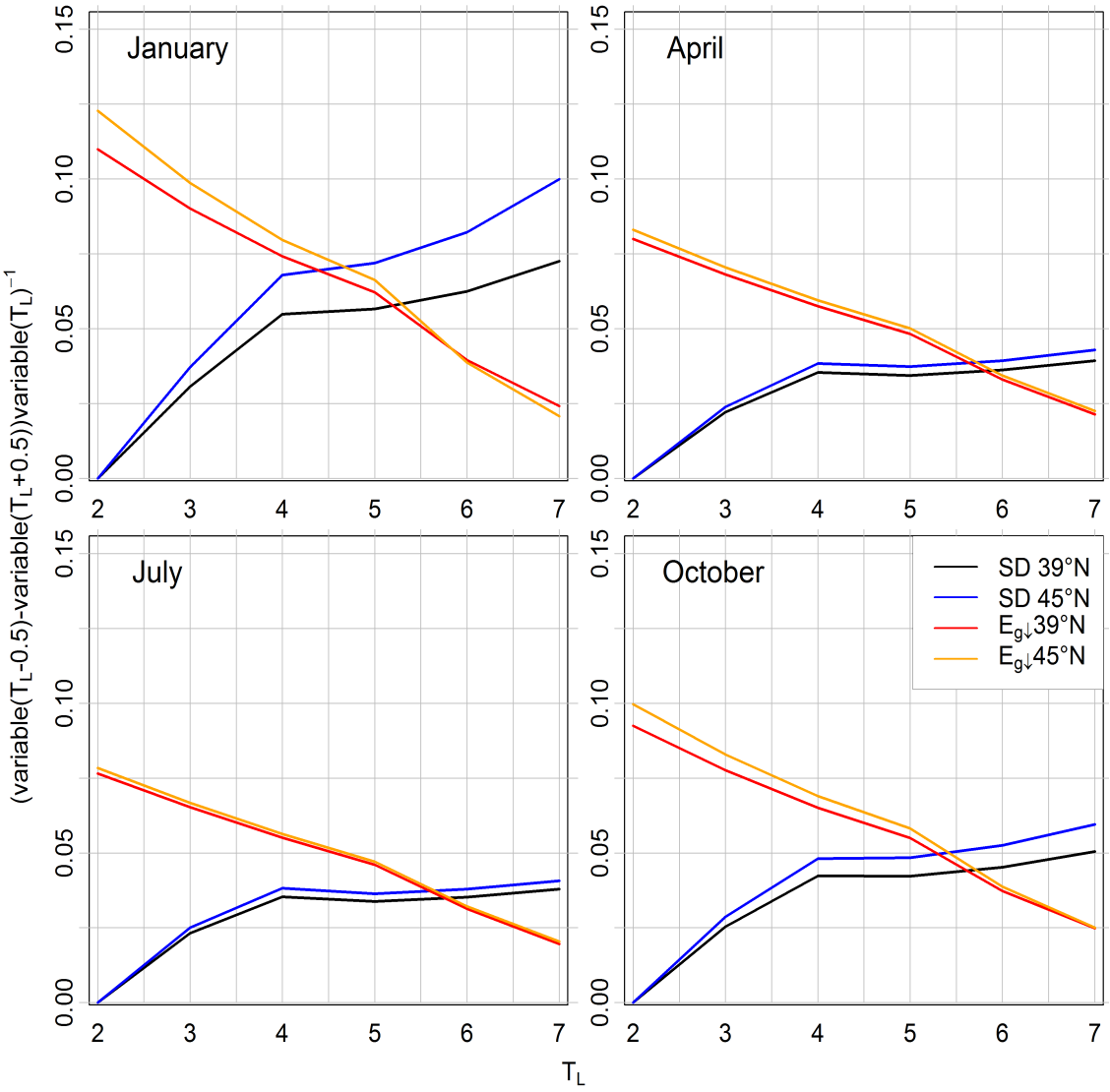

Figure 6.8: Relative decrease of modelled SD($E_{g\downarrow}$) for each integer T_L in the range 2-7 for T_L increasing from T_L - 0.5 to T_L + 0.5. The black (blue) line represents SD variations for a point located at a latitude of 39°N (45°N) while the red (orange) line represents $E_{g\downarrow}$ variations for a point located at a latitude of 39°N (45°N). The results are shown for the central month of each season.

the considered months and for both the considered latitudes while for T_L values higher than 6 the behavior is opposite. In April and July, the intersection between the SD and $E_{g\downarrow}$ curves is around T_L equal to 5-6 for both the points while in January and October, the intersection corresponds to lower T_L values for the north (T_L equal to 4-5 in January and 5-6 in October) than for the south (T_L equal to 5-6 both in January and October). Moreover, the difference in the sensitivity of the two variables is particularly strong for low T_L values especially in January (winter) and October (autumn). Winter is therefore the season for which the most pronounced differences in the SD and $E_{g\downarrow}$ trends are expected because it has both the lowest T_L values and the highest difference in the sensitivity of SD and $E_{g\downarrow}$ to T_L variations. For the other seasons and for their typical T_L values the sensitivity of SD and $E_{g\downarrow}$ to T_L changes is expected to be more similar (Figures 6.7, 6.8) even though in most cases $E_{g\downarrow}$ is more sensitive than SD to changes in T_L, with the only exception of summer for T_L around 6 where a stronger SD sensitivity is expected. These results are actually confirmed by the trends of the observed clear-sky records (Figures 6.3, 6.5, 6.6). However, as already discussed above, the model can only partially explain the observed SD trend of the first period (Figures 6.3, 6.5, 6.6) especially in the northern region.

In order to further investigate the agreement between modelled and observed clear-sky SD trends, we estimated for each decade of the period 1961-2010 the northern and southern Italy T_L values by comparing esa-atmospheric and observed $E_{g\downarrow}$. Then, we applied Equation (6.1) to get the corresponding decadal SD values. Finally, we calculated the relative anomalies (for both the modelled and the observed values) with respect to the averages over these five decades and we compared them. The results are reported in Figure 6.9 for the north and the south and for the 4 months representative of the different seasons. They highlight an excellent agreement between the modelled and the observed SD trends in spring (April) and in summer (July), as already observed from the comparison between the observed clear-sky trends (Figure 6.5) and the modelled variations (Figure 6.7). In the other two seasons, in southern Italy the agreement is rather good, while in the north it is reasonable during the brightening period and very poor during the dimming period, where the modelled and the observed trends do not agree. The discrepancy is stronger in winter than in autumn.

6.6 Discussion and conclusions

Two homogenized datasets of sunshine duration - SD ([28] - 2) and global radiation - $E_{g\downarrow}$ ([29] - 3) records covering the Italian territory were used to investigate to what extent these two variables agree with respect to their temporal evolution, both under all-sky and clear-sky conditions. The analysis has been performed considering annual and seasonal regional relative anomaly records for northern and southern Italy over the 1959-2013 period.

The results highlight that the agreement between the decadal variability and long-term

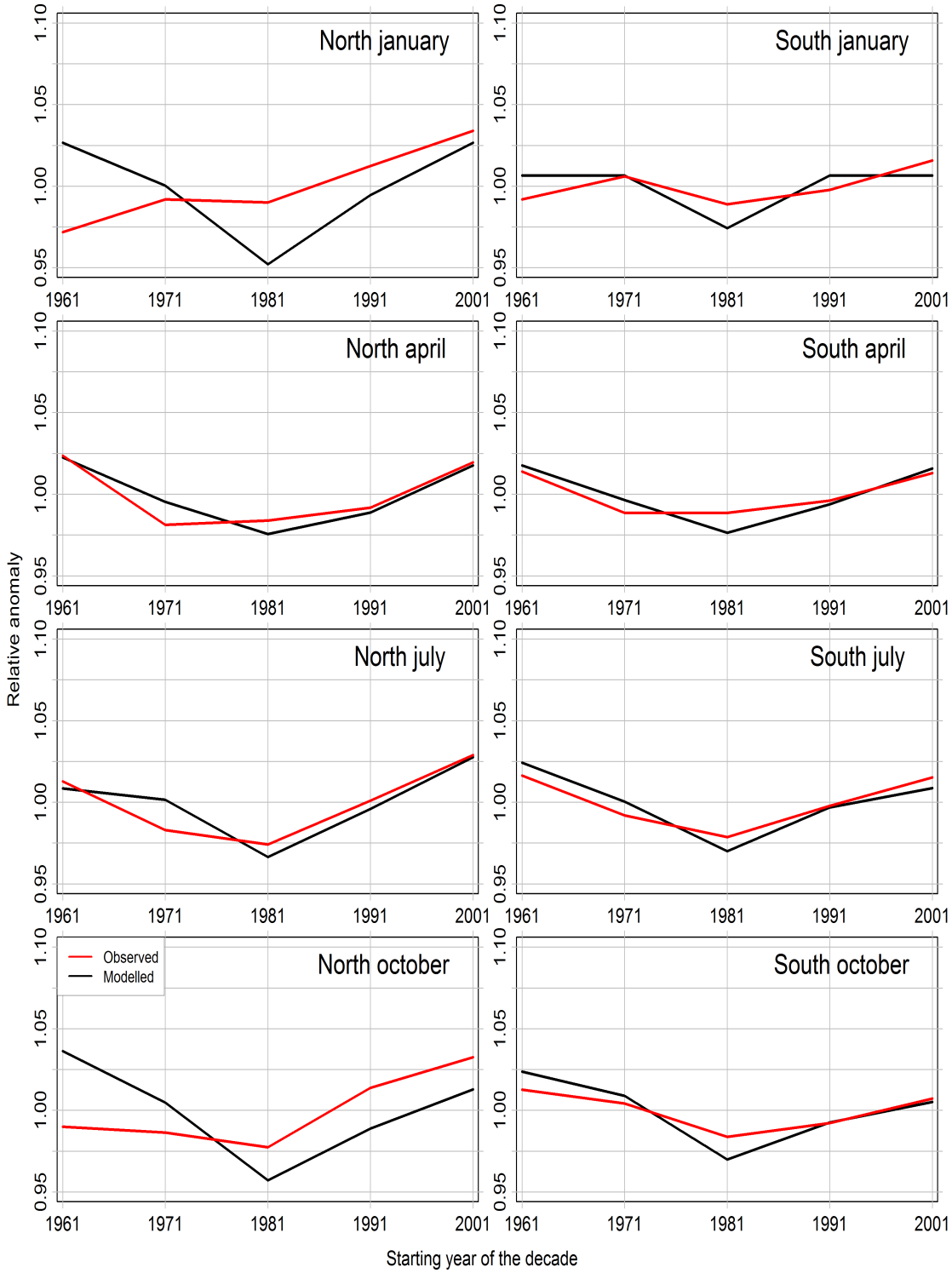

Figure 6.9: Northern (left side) and southern (right side) Italy modelled (red line) and observed clear-sky (black line) SD relative anomalies calculated for each decade of the period 1961-2010. The x-axis show the starting year of the considered decade. The results are shown for the central month of each season.

trends of SD and $E_{g\downarrow}$ depends on the considered region, season and period (Figures 6.2, 6.5). Overall, under all-sky conditions (Figure 6.2), the SD records show a shorter and less intense decrease during the dimming period with respect to the $E_{g\downarrow}$ ones, while the agreement is better if the subsequent period is considered, where both variables show an increasing tendency (Table 6.2). This behavior is reflected in the $E_{g\downarrow}$/SD ratio records (Figure 6.3) that show a significant decrease until the mid-1980s (Figure 6.4), which is more pronounced in winter and autumn (especially due to a lack of a negative SD trend Table 6.2), while in the subsequent period the ratio records do not show any significant trends. Moreover, the SD series show a trend inversion from dimming to brightening at the end of the 1970s/beginning of the 1980s while the $E_{g\downarrow}$ series show it around the mid-1980s (Figure 6.2). Considering only the clear days, the ratio records show again a decrease until the mid-1980s and a weaker increase in the subsequent period. The agreement between SD and $E_{g\downarrow}$ trends is highest in summer in northern Italy (Figure 6.5), which is the only case in which the $E_{g\downarrow}$/SD ratio record does not show the decreasing/increasing tendency, which is present in all other cases (Figure 6.6).

In order to investigate whether the differences in the clear-sky SD and $E_{g\downarrow}$ trends are due to a different sensitivity of these variables to atmospheric turbidity, we first applied a model with the aim of estimating how large the SD and $E_{g\downarrow}$ relative changes are when atmospheric turbidity (expressed by means of the Turbidity Linke Factor - T_L) changes. Then, we considered temporal patterns for T_L representative of the changes from dimming to brightening in the different regions and seasons and we checked if the differences in the observed SD and $E_{g\downarrow}$ trends could be explained on the basis of their different sensitivity to the T_L variations.

The sensitivity analysis showed that clear-sky SD and $E_{g\downarrow}$ sensitivity to T_L variations strongly depends on the T_L absolute value (Figures 6.7, 6.8). Specifically, for low T_L ($T_L < 3$) $E_{g\downarrow}$ is much more sensitive than SD, while for high T_L ($T_L > 6$) SD is slightly more sensitive than $E_{g\downarrow}$. These results give evidence that the use of SD as a proxy for clear-sky $E_{g\downarrow}$ may be problematic especially if T_L is low or if it shows significant changes in time. A further problem may be linked to the position of the stations that could have a non optimal sky-view factor either at sunrise or at sunset or in both circumstances. When the reduction of the sky-view factor is large, this problem can completely hide the response of clear-sky SD to T_L variations. In this case, the direct radiation reaches the Campbell-Stokes sunshine recorder only when its value is already above the instrumental threshold and this is true for a wide range of T_L values. Therefore, the clear-sky SD simply corresponds to the time interval in which the sun is visible from the considered station, independently from T_L and so SD is not sensitive to T_L changes. Our stations are generally located in plain or coastal areas and they have a good sky-view factor. However, in winter T_L values are rather low. We can therefore not exclude that the modelled SD decrease in the dimming period (Figure 6.9) may be slightly overestimated by a non optimal sky-view factor for few stations. This problem is less relevant in the other seasons as the T_L values and the solar elevation angles are higher.

The comparison between the modelled and the observed SD relative trends (Figure 6.9) highlights a very good agreement in southern Italy for all seasons. In northern Italy, the good agreement concerns all seasons only for the brightening period, whereas in the dimming period it concerns only spring and summer. In this period in winter and in autumn, the differences in SD and $E_{g\downarrow}$ observed trends can not be explained based on their different sensitivity to T_L variations. We do not have a conclusive explanation for this problem and we can only speculate on some possible issues which could cause this disagreement. An issue could concern a change over time of the instrumental threshold of the Campbell-Stokes SD recorders, a change that could explain the unexpected signal we observe in winter (and autumn) northern Italy clear-sky SD record. It could be linked to the introduction of paper charts less influenced by high atmospheric humidity: relative humidity is in fact highest in these seasons and in this area. If such change concerned only one or few stations, its effect would be removed by the homogenization procedure. However, if it concerned all stations at the same time, the homogenization procedure would not be able to detect it. Unfortunately, we do not have enough metadata to support and investigate more in depth this hypothesis.

Another issue could be due to a decrease of relative humidity, which was not captured by the method we used to estimate the temporal variations of T_L. This method is in fact based on $E_{g\downarrow}$ records and focuses therefore on the central hours of the day, which are those that most contribute to global radiation. A reduction of relative humidity in the hours of SD sensitivity to T_L (sunrise and sunset) in the 1960s and 1970s could therefore be a physical process which would explain what we observe. Such mechanism could e.g. be driven by an increase of the urbanization close to some of the station sites. High relative humidity may also alter the radiative properties of the particles suspended in the atmosphere increasing their radiative forcing ([23]; [73]). This is particularly important during the winter season in the north where fog episodes are rather frequent. As far as those episodes are concerned, Giulianelli et al. ([14]) report a significant decrease of fog episodes in a Po Plain site (San Pietro Capo Fiume) during the brightening period: unfortunately, their data do not cover the dimming period too. Nevertheless, it is worth noting that in other Mediterranean regions a widespread decrease in relative humidity has been reported during the dimming period ([61]).

All the problems related to the different sensitivity of clear-sky SD and $E_{g\downarrow}$ to T_L do not limit the use of SD as a good proxy to highlight cloudiness induced $E_{g\downarrow}$ variations as shown for other studies ([44]; [62]). They have however to be considered with great attention in studying the temporal evolution of $E_{g\downarrow}$ where the changes in aerosol concentration play a relevant role. A more detailed understanding of the unexpected trend in the winter (and autumn) northern Italy SD record in the dimming period calls for further research including the study of other variables such as relative humidity and visibility.

Bibliography

[1] Ångström A. (1924): *Solar and terrestrial radiation*, Q. J. Royal. Meteor. Soc., Vol. 50(210), pp. 121-126;

[2] Antón M., Vaquero J.M., Aparicio A.J.P. (2014): *The controversial early brightening in the first half of 20th century: a contribution from pyrheliometer measurements in Madrid (Spain)*, Glob. Planet. Change, Vol. 115, pp. 71-75, doi:10.1016/j.gloplacha.2014.01.013;

[3] Bartók B. (2016): *Aerosol radiative effects under clear skies over Europe and their changes in the period of 2001-2012*, Int. J. Climatol., doi:10.1002/joc.4821;

[4] Baynard T., Garland R.M., Ravishankara A.R., Tolbert M.A., Lovejoy E.R. (2006): *Key factors influencing the relative humidity dependence of aerosol light scattering*, Geophys. Res. Lett., Vol. 33, L06813, doi:10.1029/2005GL024898;

[5] Baumgartner T. (1979): *Die Schwellenintensitat des Sonnenscheinautographen Campbell-Stokes an wolkenlosen Tagen*, Arbeitsberichte der Schweizerischen Meteorologischen Zentralanstalt, 84;

[6] Bider M. (1958): *Über die Genauigkeit der Registrierungen des Sonnenscheinautographen Campbell-Stokes*, Archiv fr Meteorologie, Geophysik und Bioklimatologie Serie B, Vol. 9(2), pp. 199-230, doi:10.1007/BF02242909;

[7] Brazdil R., Flocas A.A., Sahsamanoglou H.S. (1994): *Fluctuation of sunshine duration in central and south-eastern Europe*, Int. J. Climatol., Vol. 14, pp. 1017-1034;

[8] Brunetti M., Maugeri M., Nanni T., Auer I., Böhm R., Schöner W. (2006): *Precipitation variability and changes in the greater Alpine region over the 1800-2003 period*, J. Geophys. Res., Vol. 111(D11), D11107, doi:10.1029/2005JD006674;

[9] Che H.Z., Shi G.Y., Zhang X.Y., Arimoto R., Zhao J.Q., Xu L., Wang B., Chen Z.H. (2005): *Analysis of 40 years of solar radiation data from China, 1961-2000*, Geophys. Res. Lett., Vol. 32, L06803, doi:10.1029/2004GL022322;

[10] Chiacchio M. and Wild M. (2010): *Influence of NAO and clouds on long-term seasonal variations of surface solar radiation in Europe*, J. Geophys. Res., Vol. 115, D00D22, doi:10.1029/2009JD012182;

[11] Cutforth H.W. and Judiesch D. (2007): *Long-term changes to incoming solar energy on the Canadian Prairie*, Agr. Forest Meteorol., Vol. 145, pp. 167-175, doi:10.1016/j.agrformet.2007.04.011;

[12] Dutton E.G., Farhadi A., Stone R.S., Long C.N., Nelson D.W. (2004): *Long-term variations in the occurrence and effective solar transmission of clouds as deter-*

mined from surface-based total irradiance observations, J. Geophys. Res. Atmos., Vol. 109(D3), doi:10.1029/2003JD003568;

[13] Dutton E.G., Nelson D.W., Stone R.S., Longenecker D., Carbaugh G., Harris J.M., Wendell J. (2006): *Decadal variations in surface solar irradiance as observed in a globally remote network*, J. Geophys. Res. Atmos., Vol. 111(D19), pp. 1-10, doi:10.1029/2005JD006901;

[14] Giulianelli L., Gilardoni S., Tarozzi L., Rinaldi M., Decesari S., Carbone C., Facchini M.C., Fuzzi S. (2014): *Fog occurrence and chemical composition in the Po valley over the last twenty years*, Atm. Env., Vol. 98, pp. 394-401, doi:10.1016/j.atmosenv.2014.08.080;

[15] Grenier J.C., De la Casiniere A., Cabot T. (1995): *Atmospheric turbidity analyzed by means of standardized Linke's turbidity factor*, J. Appl. Meteorol., Vol. 34, pp. 1449-1458;

[16] Hansen J., Sato M. and Ruedy R. (1997): *Radiative forcing and climate response*, J. Geophys. Res. Atmos., Vol. 102(D6), pp. 6831-6864, doi:10.1029/96JD03436;

[17] Hartmann D.L., Ramanathan V., Berroir A., Hunt G.E. (1986): *Earth Radiation Budget Data and Climate Research*, Rev. Geophys., Vol. 24(2), pp. 439-468;

[18] Horseman A., MacKenzie A.R., Timmis R. (2008): *Using bright sunshine at low-elevation angles to compile an historical record of the effect of aerosol on incoming solar radiation*, Atm. Env., Vol.42(33), pp. 7600-7610, doi:10.1016/j.atmosenv.2008.06.033;

[19] Iqbal M. (1983): *An introduction to solar radiation*;

[20] Jacovides C.P. (1997): *Model comparison for the calculation of Linke's turbidity factor*, Int. J. Climatol, Vol. 17, pp. 551-563, doi:10.1002/(SICI)1097-0088(199704)17:5<551::AID-JOC137>3.0.CO;2-C;

[21] Kerr A. and Tabony R. (2004): *Comparison of sunshine recorded by Campbell - Stokes and automatic sensors*, Weather, Vol. 59(4), pp. 90-95;

[22] Kopp G. and Lean J.L. (2011): *A new, lower value of total solar irradiance: Evidence and climate significance*, Geophys. Res. Lett., Vol. 38(1), pp. 1-7, doi:10.1029/2010GL045777;

[23] Kotchenruther R.A., Hobbs P.V., Hegg D.A. (1999): *Humidification factors for atmospheric aerosols off the mid-Atlantic coast of the United States*, J. Geophys. Res., Vol. 104(D2), pp. 2239-2251, doi:10.1029/98JD01751;

[24] Liang F. and Xia X.A. (2005): *Long-term trends in solar radiation and the associated climatic factors over China for 1961-2000*, Ann. Geophys., Vol. 23(7), pp. 2425-2432, doi:10.5194/angeo-23-2425-2005;

[25] Liepert B.G. and Kukla G.J. (1997): *Decline in global solar radiation with increased horizontal visibility in Germany between 1964 and 1990*, J. Clim., Vol. 10(9), pp. 2391-2401, doi:10.1175/1520-0442(1997)010<2391:DIGSRW>2.0.CO;2;

[26] Liepert B. and Tegen I. (2002): *Multidecadal solar radiation trends in the United States and Germany and direct tropospheric aerosol forcing*, J. Geophys. Res. Atmos., Vol. 107(D12), AAC 7-1 - AAC 7-15, doi:10.1029/2001jD000760;

[27] Liepert B., Fabian P., Grassl H. (1994): *Solar radiation in Germany - observed trends and an assessment of their causes. Part I: regional approach, Contributions to Atmospheric Physics*, Vol. 67(1), pp. 15-29;

[28] Manara V., Beltrano M.C., Brunetti M., Maugeri M., Sanchez-Lorenzo A., Simolo C., Sorrenti S. (2015): *Sunshine duration variability and trends in Italy from homogenized instrumental time series (1936-2013)*, J. Geophys. Res. Atmos., Vol. 1, No. 120, pp. 3622-3641, doi:0.1002/2014JD022560;

[29] Manara V., Brunetti M., Celozzi A., Maugeri M., Sanchez-Lorenzo A., Wild M. (2016): *Detection of dimming/brightening in Italy from homogenized all-sky and clear-sky surface solar radiation records and underlying causes (1959-2013)*, Atmos. Chem. Phys., Vol. 16, pp. 11145-11161, doi:10.5194/acp-16-11145-2016;

[30] Manara V., Brunetti M., Maugeri M.(2016): *Reconstructing sunshine duration and solar radiation long-term evolution for Italy: a challenge for quality control and homogenization procedures*, Conference proceeding of the 14^{th} IMEKO T10 Workshop Technical Diagnostics - New Perspectives in Measurements, Tools and Techniques for system's reliability, maintainability and safety, 27-28 June 2016, Milan, Italy, pp. 13-18, ISBN: 978-92-990073-9-6, $http://www.imeko.org/publications/tc10-2016/IMEKO-TC10-2016-002.pdf$;

[31] Manara V., Brunetti M., Maugeri M., Sanchez-Lorenzo A., Wild M. (2017): *Homogenization of a surface solar radiation dataset over Italy*, Radiation Processes in the Atmosphere and Ocean (IRS2016), AIP Conference Proceedings, Vol. 1810, 090004-1-090004-4, doi: 10.1063/1.4975544, Published by AIP Publishing, ISBN: 978-0-7354-1478-5;

[32] Maugeri M., Bagnati Z., Brunetti M., Nanni T. (2001): *Trends in italian total cloud amount, 1951-1996*, Geophys. Res. Lett., Vol. 28(24), pp. 4551-4554, doi: 10.1029/2001GL013754;

[33] Nabat P., Somot S., Mallet M., Sanchez-Lorenzo A., Wild M. (2014): *Contribution of anthropogenic sulfate aerosols to the changing Euro-Mediterranean climate since 1980*, Geophys. Res. Lett., Vol. 41(15), pp. 5605-5611, doi:10.1002/2014GL060798;

[34] Norris J.R. and Wild M. (2007): *Trends in aerosol radiative effects over Europe inferred from observed cloud cover, solar "dimming", and solar "brightening"*, J. Geophys. Res., Vol. 112, D08214, doi:10.1029/2006JD007794;

[35] Oguz E., Kaya M.D., Nuhoglu Y. (2003): *Interaction between air pollution and meteorological parameters in Erzurum*, Turkey, Int. J. Env. and Poll., Vol. 19(3), pp. 292-300, doi:10.1504/IJEP.2003.003312;

[36] Ohmura A. and Gilgen H. (1993): *Re-evaluation of the global energy balance*, Geophysical Monograph Series, edited by G. A. McBean and M. Hantel, American Geophysical Union, Washington, D. C.;

[37] Painter H.E. (1981): *The performance of a Campbell-Stokes sunshine recorder compared with a simultaneous record of the normal incidence irradiance*, Meteorological Magazine, Vol. 110(1305), pp. 102-109;

[38] Power H.C. (2003): *Trends in solar radiation over Germany and an assessment of the role of aerosols and sunshine duration*, Theor. Appl. Climatol., Vol. 76, pp. 4763, doi:10.1007/s00704-003-0005-8;

[39] Prescott J.A. (1940): *Evaporation from a water surface in relation to solar radiation*, Trans. R. Soc. S. Austr., Vol. 64, pp. 114-118;

[40] Ramanathan V., Crutzen P.J., Kiehl J.T., Rosenfeld D. (2001): *Aerosol, climate, and the hydrological cycle*, Science, Vol. 294(5549), pp. 2119-2124, doi:10.1126/science.1064034;

[41] Rigollier C., Bauer O., Wald L. (2000): *On the clear sky model of the ESRA - European Solar Radiation Atlas with respect to the heliosat method*, Solar Energy, Vol. 68(1), pp. 33-48, doi:10.1016/S0038-092X(99)00055-9;

[42] Román, R., Bilbao J., de Miguel A. (2014): *Reconstruction of six decades of daily total solar shortwave irradiation in the Iberian Peninsula using sunshine duration records*, Atm. Env., 99(November 2016), pp. 4150, doi:10.1016/j.atmosenv.2014.09.052;

[43] Qian Y., Wang W., Leung L.R., Kaiser D.P. (2007): *Variability of solar radiation under cloud-free skies in China: The role of aerosols*, Geophys. Res. Lett., Vol. 34(L12804), doi:10.1029/2006GL028800;

[44] Sanchez-Lorenzo A. and Wild M. (2012): *Decadal variations in estimated surface solar radiation over Switzerland since the late 19th century*, Atmos. Chem. Phys., Vol. 12, pp. 8635-8644, doi:10.5194/acp-12-8635-2012;

[45] Sanchez-Lorenzo A., Calbó J., Brunetti M., Deser C. (2009): *Dimming/brightening over the Iberian Peninsula: Trends in sunshine duration and cloud cover and their relations with atmospheric circulation*, J. Geophys. Res., Vol. 114, D00D09, doi:10.1029/2008JD011394;

[46] Sanchez-Lorenzo A., Calbo J., Wild M. (2013): *Global and diffuse solar radiation in Spain: building a homogeneous dataset and assessing their trends*, Glob. Planet. Change, Vol. 100, pp. 343-352, doi:10.1016/j.gloplacha.2012.11.010;

[47] Sanchez-Lorenzo A., Wild M., Brunetti M., Guijarro J.A., Hakuba M.Z., Calbó J., Mystakidis S., Bartok B.: *Reassessment and update of long-term trends in downward surface shortwave radiation over Europe (1939-2012)*, J. Geophys. Res. Atmos., Vol. 120(18), pp. 9555-9569, doi:10.1002/2015JD023321;

[48] Sanchez-Romero A., Sanchez-Lorenzo A., Calbó J., González J.A., Azorin-Molina C. (2014): *The signal of aerosol-induced changes in sunshine duration records: A review of the evidence*, J. Geophys. Res. Atmos., Vol. 119(8), pp. 4657-4673, doi:10.1002/2013JD021393;

[49] Sanchez-Romero A., Gonzalez J.A., Calbo J., Sanchez-Lorenzo A. (2015): *Using digital image processing to characterize the Campbell-Stokes sunshine recorder and to derive high-temporal resolution direct solar irradiance*, Atm. Meas. Tech., Vol. 8, pp. 183-194, doi:10.5194/amt-8-183-2015;

[50] Sen P.K. (1968): *Estimates of the Regression Coefficient Based on Kendalls Tau*, Journal of the American Statistical Association, Vol. 63(324), pp. 1379-1389, doi:10.1080/01621459.1968.10480934;

[51] Soni V.K., Pandithurai G., Pai D.S. (2012): *Evaluation of long-term changes of solar radiation in India*, Int. J. Climatol., Vol. 32(4), pp. 540-551, doi:10.1002/joc.2294;

[52] Stanhill G. (1983): *The distribution of global solar radiation over the land surfaces of the Earth*, Solar Energy, Vol. 31(1), pp. 95-104;

[53] Stanhill G. (2003): *Through a glass brightly: Some new light on the Campbell-Stokes sunshine recorder*, Weather, Vol. 58(1), pp. 3-11;

[54] Stanhill G. (2005): *Global dimming: a new aspect of climate change*, Weather, Vol. 60(1), pp. 11-14, doi:10.1256/wea.210.03;

[55] Stanhill G. and Achiman O. (2016): *Early global radiation measurements: A review*, Int. J. Climatol., doi:10.1002/joc.4826;

[56] Stanhill G. and Cohen S. (2001): *Global dimming: A review of the evidence for a widespread and significant reduction in global radiation with discussion of its probable causes and possible agricultural consequences*, Agric. For. Meteorol., Vol. 107, pp. 255-278, doi:10.1016/S0168-1923(00)00241-0;

[57] Stanhill G. and Cohen S. (2005): *Solar Radiation Changes in the United States during the Twentieth Century: Evidence from Sunshine Duration Measurements*, Am. Meteorol. Soc., Vol. 18(10), pp. 1503-1512;

[58] Stanhill G. and Kalma J.D. (1995): *Solar dimming and urban heating at hong kong*, Int. J. Climatol., Vol. 15(8), pp. 933-941;

[59] Tang I.N. (1996): *Chemical and size effects of hygroscopic aerosols on light scattering coefficients*, J. Geophys. Res. Atmos., Vol. 101(D14), pp. 19245-19250, doi:10.1029/96JD03003;

[60] Theil, H. (1950): *A rank-invariant method of linear and polynomical regression analysis*, in Proceedings of the Royal Academy of Sciences, pp. 386-392;

[61] Vicente-Serrano S.M., Azorin-Molina C., Sanchez-Lorenzo A., Morán-Tejeda E., Lorenzo-Lacruz J., Revuelto J., López-Moreno J.I., Espejo F. (2014): *Temporal evolution of surface humidity in Spain: recent trends and possible physical mechanisms*, Clim. Dyn., Vol. 42(9), pp. 2655-2674, doi:10.1007/s00382-013-1885-7;

[62] Wang K. (2014): *Measurement Biases Explain Discrepancies between the Observed and Simulated Decadal Variability of Surface Incident Solar Radiation*, Scientific Reports, Vol. 4(1), pp. 6144, doi:10.1038/srep06144;

[63] Wang K., Ma Q., Li Z., Wang J. (2015): *Decadal variability of surface incident solar radiation over China: observations, satellite retrievals, and reanalyses*, J. Geophys. Res. Atmos., Vol. 120, pp. 6500-6514, doi:10.1002/2015JD023420;

[64] Wang K.C., Dickinson R.E., Wild M., Liang S. (2012): *Atmospheric impacts on climatic variability of surface incident solar radiation*, Atmos. Chem. Phys., Vol. 12, pp. 9581-9592, doi:105194/acp-12-9581-2012;

[65] Wild M. (2009): *Global dimming and brightening: A review*, J. Geophys. Res., Vol. 114, D00D16, doi:10.1029/2008JD011470;

[66] Wild, M. (2016): *Decadal changes in radiative fluxes at land and ocean surfaces and their relevance for global warming*, Wiley Interdisciplinary Reviews: Climate Change, Vol. 7(1), pp. 91-107, doi:10.1002/wcc.372;

[67] Wild M. (2012): *Enlightening global dimming and brightening*, Bull. Amer. Meteor. Soc., Vol. 93, pp. 27-37, doi:10.1175/BAMS-D-11-00074.1;

[68] Wild M., Gilgen H., Roesch A., Ohmura A., Long C.N., Dutton E.G., Forgan B., Kallis A., Russak V., Tsvetkov A. (2005): *From dimming to brightening: Decadal changes in surface solar radiation at Earths surface*, Science, Vol. 308(5723), pp. 847-850, doi:10.1126/science.1103215;

[69] Wild M., Trüssel B., Ohmura A., Long C.N., König-Langlo G., Dutton E.G., Tsvetkov A. (2009): *Global dimming and brightening: An update beyond 2000*, J. Geophy. Res. Atmos., Vol. 114, D00D13, doi:10.1029/2008JD011382;

[70] WMO-No.8 (1969): *Chapter 9, Solar radiation and Sunshine duration*, World Meteorological Organization, Guide to meteorological instruments and observing practices, Third edition;

[71] WMO (2008), *Chapter 7, Measurement of Radiation*, in Guide to Meteorological Instruments and Methods of Observation, Geneva;

[72] WMO (2008), *Chapter 8, Measurement of Sunshine Duration*, in Guide to Meteorological Instruments and Methods of Observation, Geneva;

[73] Xia X., Li Z., Holben B., Wang P., Eck T., Chen H., Cribb M., Zhao Y. (2007): *Aerosol optical properties and radiative effects in the Yangtze Delta region of China*, J. Geophys. Res., Vol. 112(D22), pp. 1-16, doi:10.1029/2007JD008859;

[74] You Q., Kang S., Flugel W.A., Sanchez-Lorenzo A., Yan Y., Huang J., Javier M.V. (2010): *From brightening to dimming in sunshine duration over the eastern and central Tibetan Plateau (1961-2005)*, Theor. Appl. Climatol., Vol. 101(6), pp. 445-457, doi:10.1007/s00704-009-0231-9;

[75] Zhang Y.L., Qin B.Q., Chen W.M. (2004): *Analysis of 40 year records of solar radiation data in Shanghai, Nanjing and Hangzhou in Eastern China*, Theor. Appl. Climatol., Vol. 78, pp. 217-227, doi:10.1007/s00704-003-0030-7.

Chapter 7

Past and future solar radiation variability and change over Sicily

Abstract

We estimate Sicily global radiation 1961-2000 monthly climatologies from already available climatologies (2002-2011) and from a regional sunshine duration (SD) anomaly record (1936-2013). We compare these climatologies with corresponding climatologies obtained from 4 RCM-GCM (Regional Climate Model - Global Climate Model) combinations and we present the correcting factors introduced in order to make the model outputs representative of the observational data. Then, we apply the same correcting factors to future model simulations in order to produce monthly climatologies for the 2001-2050 and 2051-2100 period.

7.1 Introduction

High-resolution datasets of monthly climatological normals (i.e. high-resolution climatologies) have proved to be increasingly important in the recent past, and they are likely to become even more important in the future. They are used in a variety of models and decision support tools in a wide spectrum of fields such as, just to cite a few, energy, agriculture, engineering, hydrology, ecology and natural resource conservation ([3]; [4]). One of the most important variables for many possible applications (e.g. energy production and agriculture) is solar radiation.

It is therefore very important to develop and to apply methodologies that exploit as much as possible the information contained in solar radiation observational records: they consist both of global radiation and sunshine duration records. The latter have the advantage of a much larger data availability, especially when long-term records are considered, the former are more frequently available from present-time station networks.

In this context, we set up a methodology for estimating high-resolution solar radiation climatologies from these records. This methodology has been presented at the first con-

ference of the Italian Society of Climate Science (SISC - Società Italiana per le Scienze del Clima)([5]) and it has been applied to a network of 41 Sicily stations available for the 2002-2011 period recovered from an agrometeorological Service of Sicily regional administration (SIAS - Servizio Informativo Agrometeorologico Siciliano - www.sias.regione.sicilia.it) ([5]) using a grid with a resolution of 30 arc-second (30 arc-second resolution GTOPO 30 Digital Elevation Model [7]).
It consists of the following steps that have to be run on a monthly basis:

(a) To calculate global radiation normals for all station sites or to estimate them from sunshine duration normals, when global radiation data are not available;

(b) To estimate, for all station sites, the bias due to shading caused for example by the surrounding orography and to adjust the normal values in order to make them representative of un-shaded sites;

(c) To calculate clearness index (i.e. ratio between the global radiation received by a surface and the exoatmospheric radiation received by the same surface) normals from these shading-bias-adjusted global radiation normals and to decompose global radiation normals into the direct and diffuse components;

(d) To project the shading-bias-adjusted global radiation normals and the direct and diffuse components onto a high-resolution regular grid, considering flat ground;

(e) To evaluate atmospheric turbidity over the same grid by means of the direct component obtained from the shading-bias-adjusted global radiation normals;

(f) To calculate normal values for the direct, diffuse and reflected components of global radiation for any grid-cell, taking into account its slope and aspect (i.e. slope orientation) and considering shading from the cell itself and from the neighboring cells.

It is worth noticing that this procedure can be applied not only to surfaces inclined as the soil but also selecting any combination of slope and aspect. The former solution is particularly useful for agricultural application while the latter is useful for energy applications as solar panels are usually not installed parallel to the ground but in order to collect as much solar radiation as possible.
In this paper, we present a methodology which combines the clearness index normals (available here for the 2002-2011 period)([5]) with sunshine duration records available over a longer period (available for the Italian territory for the 1936-2013 period) (Section 7.2). This makes possible the estimation of the climatologies for any period of the interval in which sunshine duration is available (1936-2013)(Section 7.3). In addition, it makes possible the direct comparison between the clearness index normals obtained from observational data with the clearness index normals obtained from the historical run of the models. This allow to estimate correcting factors to apply to the model output making possible to estimate future scenarios climatologies comparable with those obtained from observational data (Section 7.4).

7.2 Temporal evolution of solar radiation over Sicily in the 1936-2013 period

7.2.1 Introduction

Temporal variability of solar radiation in the last decades is discussed in a number of recent papers ([8]). The results suggest a widespread reduction of solar radiation between the 1960s and the early 1980s and a tendency toward an opposite trend starting from the 1980s. The first phenomenon is known as "Global Dimming", the second as "Brightening Period" ([8]; [9]).
In this context we studied the temporal evolution of solar radiation in the last decades over Italy ([6] - Chapter 2). Specifically we studied sunshine duration (SD): it is defined as the length of time in which direct solar radiation on a plane normal to it is above a certain threshold, usually taken at $120 W m^{-2}$. SD, which is usually measured with an uncertainty of ± 0.1h and a resolution of 0.1h, is directly correlated with solar radiation through Ångström's law ([1]). A very important advantage of SD records is that they usually cover a much longer period than global radiation records.

7.2.2 Data

We collected SD data not only for Sicily, but for the entire Italian territory. The SD records were recovered from three main data sources: the paper archive of CRA-CMA (http://cma.entecra.it/homePage.htm) that is the former Italian Central Office for Meteorology (24 records), the database of Italian Air Force synoptic stations (47 records) and the Italian National Agrometeorological Database (BDAN, 59 records). Beside the records we recovered from these data sources, we considered also two records (Modena and Trieste) from university observatories, one record (Pontremoli) from an observatory managed by a volunteer joining the Italian Society for Meteorology and one record (Varese) from a meteorological observatory managed by a local association.
For some sites we set up composite records, merging data of the same station from different sources. In particular, 18 of the BDAN records were used to update the records provided by Italian Air Force. Moreover, for 8 records we merged data from different sites. They concern stations at short distances and belonging to areas with homogeneous geographical features.
The final dataset encompasses 104 SD daily records covering the entire Italian territory. It refers to the 1936-2013 period. The spatial distribution of the stations is rather uniform, with the only exception of the Alpine area, which is covered only by 3 stations. The station coverage is rather low also in the Apennine area. 11 of the stations are located in Sicily.
Data availability versus time is rather inhomogeneous. The best data coverage concerns 1958-1964, 1971-1977 and 1982-2013 periods, whereas 1965-1970 and 1978-1981 periods have lower data availability. The period with the most critical situation in terms of data

availability corresponds to the first 14 years (1936-1949).

7.2.3 Data pre-processing

Before data analysis, the records were pre-processed in order to get quality checked and homogenized gridded records.

Quality check and calculation of monthly records

All daily records were checked in order to identify and correct gross errors. A further check concerned the position of the stations: all coordinates were checked for consistency (i.e. elevation was checked in relation to position) by means of Google Earth mapping tool. Moreover, we verified the consistency of the coordinates with the information from stations metadata.
All records were expressed in hours and tenths of hour, corresponding to a time resolution of six minutes. They were then converted into relative SD (i.e. the ratio between measured and eso-atmospheric sunshine duration) records and corresponding monthly average records were calculated only when the fraction of missing data did not exceed 10%.

Data homogenization

We subjected all our monthly records to the relative homogeneity Craddock test ([2]). When a break was identified, the portion of the series that precedes it was corrected, leaving the most recent portion of the series unchanged in order to allow an easy updating of the record when new data become available.
Applying the homogenization procedure to the database, only 34 out of 104 records resulted homogeneous, whereas the remaining 70 were homogenized. A total number of 116 breaks was found.

Gap filling and calculation of monthly anomaly records

After homogenization, we filled the gaps in the monthly records. Specifically, each missing datum was estimated by means of the closest record - in terms of distance and elevation difference - among those with available data within the same geographical region. The selection of the record to use for the estimation of the missing datum was performed considering only the records fulfilling two conditions: distance within 500km from the record under analysis and availability of at least 10 monthly values in commune with it in the month of the break. If no records fulfilled these conditions, the missing datum was not estimated.
After gap filling, only the 95 records for which at least 90% of the data were available in the 1984-2013 period were considered. These records were then transformed into anomaly records, with respect to the corresponding monthly normals of this period.

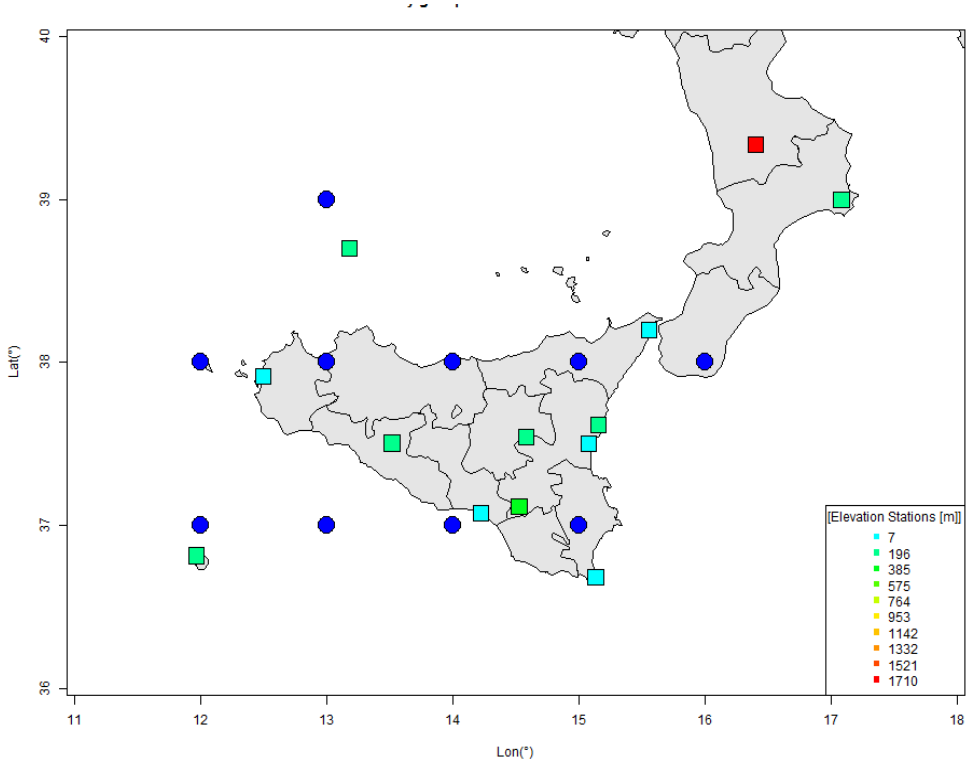

Figure 7.1: Sicily grid-points (blue points) and station records (colored squares) we used to calculate the grid-point series.

Gridding and calculating Sicily average SD record

Starting from the 95 gap-filled anomaly records, we generated a gridded version of monthly SD anomalies. This gridded version has the advantage of balancing the contribution of areas with a higher number of stations with those that have a lower station coverage. We used a grid with 1° resolution both in latitude and longitude, following the technique described by Sanchez-Lorenzo et al. ([10]): it is based on Inverse Distance Weighting approach (distance and elevation difference), with the addition of angular term weight introduced in order to take into account the anisotropy in stations spatial distribution.

The grid was constructed from 7° to 19° E and from 37° to 47° N, selecting 68 points covering the Italian territory. The gridded records in most cases cover the entire 1936-2013 period and there are only a few grid points with some missing data, especially in the first ten years. 10 of the grid-points concern Sicily.

The gridded records can be used to calculate national and regional records simply by averaging all corresponding grid-point anomaly records belonging to the region of interest. Here we present the Sicily record which has been obtained averaging all Sicily grid-point records. Figure 7.1 shows these grid-points, together with the stations that we used to calculate the Sicily grid-point records.

7.2.4 The Sicily sunshine duration record

The average Sicily seasonal and annual SD regional records are shown in Figure 7.2, together with a 3-year standard deviation Gaussian low-pass filter working on 11-year windows. The figure gives evidence of a clear brightening phase starting at about the mid of the 1980s, whereas the dimming phase of the 1960s and 1970s is less evident.
Manara et al. ([6] - Chapter 2) published a paper on the temporal evolution of SD over Italy where a more complete analysis of the records is presented, including the comparison with SD records of other datasets and other areas with records of other proxy variables of solar radiation such as cloudiness and daily temperature range.

7.3 Estimation of global radiation climatologies for any period of the 1936-2013 interval

7.3.1 Ångström's law

The dataset used to obtain the results presented in Manara et al. ([5]) and in Section 7.2 includes both global radiation and SD records. In particular, the 2002-2011 spatial patterns are based on global radiation data, whereas the temporal evolution in the 1936-2013 period is based on SD data.
SD and global radiation are linked by Ångström's equation. It links the clearness index (K_T i.e. the ratio between the global radiation received by a surface (H_T) and the exo-atmospheric radiation received by the same surface (H_0)) to the relative SD (i.e. the ratio between the number of sun hours measured by a sunshine recorder (S) and the solar day length from sunrise to sunset (S_0)) by means of the following linear relation:

$$K_T = a\frac{S}{S_0} + b \tag{7.1}$$

with coefficients a and b depending on the considered month. A detailed discussion on this relation is reported in Spinoni ([11]) and Spinoni et al. ([12]), which report also a and b coefficients obtained by means of about 30 Italian stations with both global radiation and SD long-term records.

7.3.2 From the 2002-2011 climatologies to other reference periods

We used Ångström's equation to estimate the K_T normal values corresponding to any period of the 1936-2013 interval from the 2002-2011 ones. This estimation is rather easy. In fact, considering a fixed month and a given station, we get from Equation 7.1:

$$\overline{K_{T_{A-B}}} - b = a\frac{\overline{S_{A-B}}}{S_0} \tag{7.2}$$

where the over bar denotes a temporal average and A-B denotes the corresponding time period.

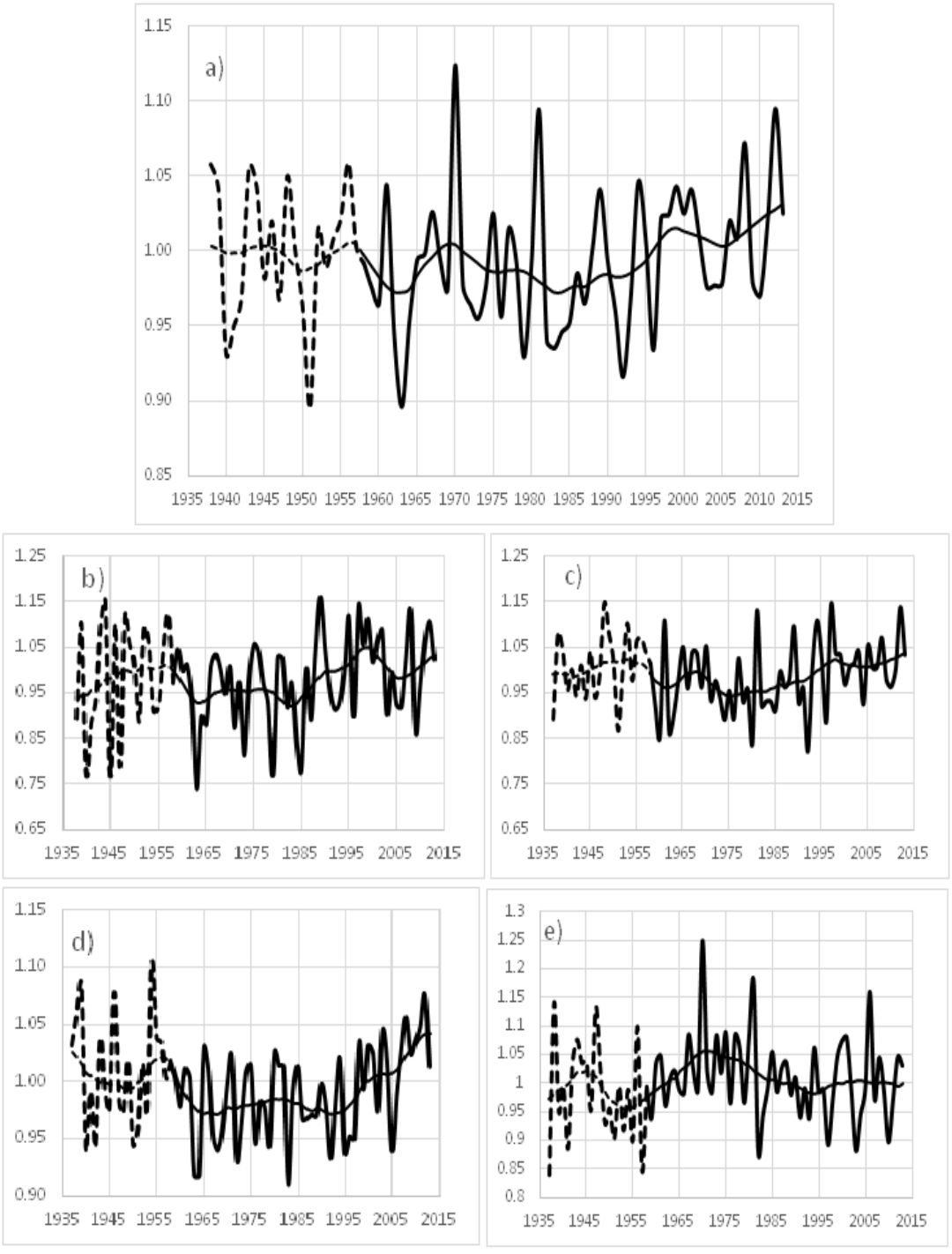

Figure 7.2: Average Sicily sunshine duration (thin line), plotted together with an 11-y window - 3-y standard deviation Gaussian low-pass filter (thick line) for (a) year; (b) winter; (c) spring; (d) summer; (e) autumn. The series are expressed as relative deviations from the 1984-2013 means. Dashed lines are used prior to 1958 owing to the lower number of records for this initial period.

Writing the same equation for period 2002-2011, dividing Equation 7.2 for the corresponding 2002-2011 equation and rearranging the terms, we get:

$$\overline{K_{T_{A-B}}} = \overline{K_{T_{2002-2011}}} \frac{\overline{S_{A-B}}}{\overline{S_{2002-2011}}} + b(1 - \frac{\overline{S_{A-B}}}{\overline{S_{2002-2011}}}) \tag{7.3}$$

If we now divide the SD averages in Equation 7.3 for the corresponding averages in the 1984-2013 period, we have simply to calculate the average of the SD anomaly record over period A-B. It is therefore simply necessary to project the SD anomaly records (see Section 7.2) over the SIAS stations for which the $K_{T_{2002-2011}}$ are already available. This projection was performed with the same technique we used for the projection of the SD anomaly records onto a regular grid (see Section 7.2.3).
This procedure allowed estimating the K_T normal values for the 41 SIAS stations over any period of the 1936-2013 interval. Here we obviously used the shading-bias-adjusted values presented in Manara et al. ([5]).
Once we estimated the K_T monthly normals over period A-B for all 41 SIAS stations, the corresponding climatologies could simply be obtained applying to them all the procedure presented in Manara et al. ([5]).

7.4 Global radiation scenarios for the XXI century

7.4.1 Regional Climate Models

Thanks to the robust high-resolution past reconstruction of global radiation for Sicily, it was possible to evaluate the ability of some ENSEMBLES Regional Climate Model (RCMs) in reproducing global radiation in this region. In particular, we evaluated whether the spatial distribution and the range of the model outputs resulted in agreement with the observational data.
Four RCM-GCM (Regional Climate Model - Global Climate Model) combinations were taken into account: KNMI-ECHAM5, SMHI-ECHAM5, SMHI-BCM and SMHI-Had. We considered the historical run of the models (1961-2000) forced by GCM and their future projections (2001-2100) under the A1B scenario.
Figure 7.3 shows the 78 grid-points we considered for RCMs scenarios. We underline that, in order to allow an easier comparison between model and observational data, we projected the SIAS stations' K_T normals on these grid-points before estimating the climatologies for the 1961-2000 period.

7.4.2 Comparison of observed and modelled global radiation

In order to compare global radiation from the RCMs with observed global radiation, we calculated the K_T monthly normal values from the model records for the 1961-2000 period and compared them with the corresponding observational normals. The results of this comparison are reported in Figure 7.4 - 7.7 that shows the ratios between the model and

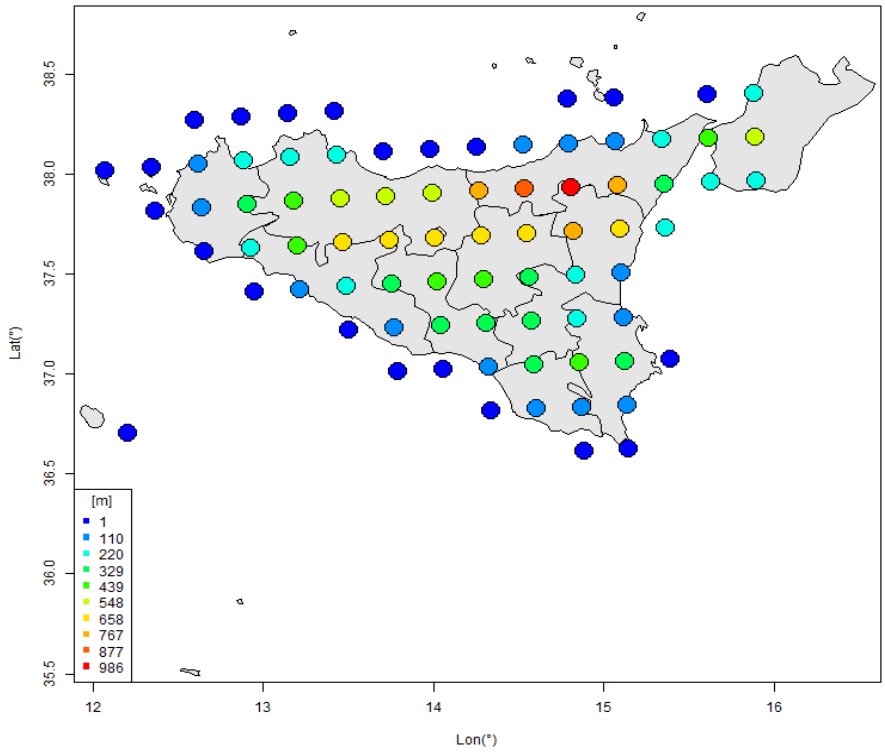

Figure 7.3: Sicily grid-points for the RCMs simulations. The colors indicate the elevation of the model grid-points.

the observational normals for March, June, September and December. These comparisons show that the model outputs have to been adjusted in order to be representative of the real data.

7.4.3 Adjustment of the RCM clearness index normals and estimated future solar radiation climatologies

The ratios between the modelled and the observed K_T normals in the 1961-2000 period have been used to adjust the future climate simulations. More precisely, for each model grid-point, the K_T monthly normals calculated from the model data for the periods 2001-2050 and 2051-2100 have simply been multiplied for the ratio between the K_T normals of the observed and modelled data in the 1961-2000 period.
Once these adjusted K_T normals were available for each model grid-point, the global radiation climatologies were estimated applying the procedure outlined in Manara et al. ([5]). In order to better give evidence of the time evolution of global radiation for the model projections, we show maps (Figure 7.8-7.11) with the ratios between the 2001-2050 and the 1961-2000 climatologies and the ratios between the 2051-2100 and the 1961-2000 climatologies for March, June, September and December. The trend pattern is not well defined, with results depending on the considered month and model. Moreover, the variations from one period to the other are always within the variability of 30-year climatologies

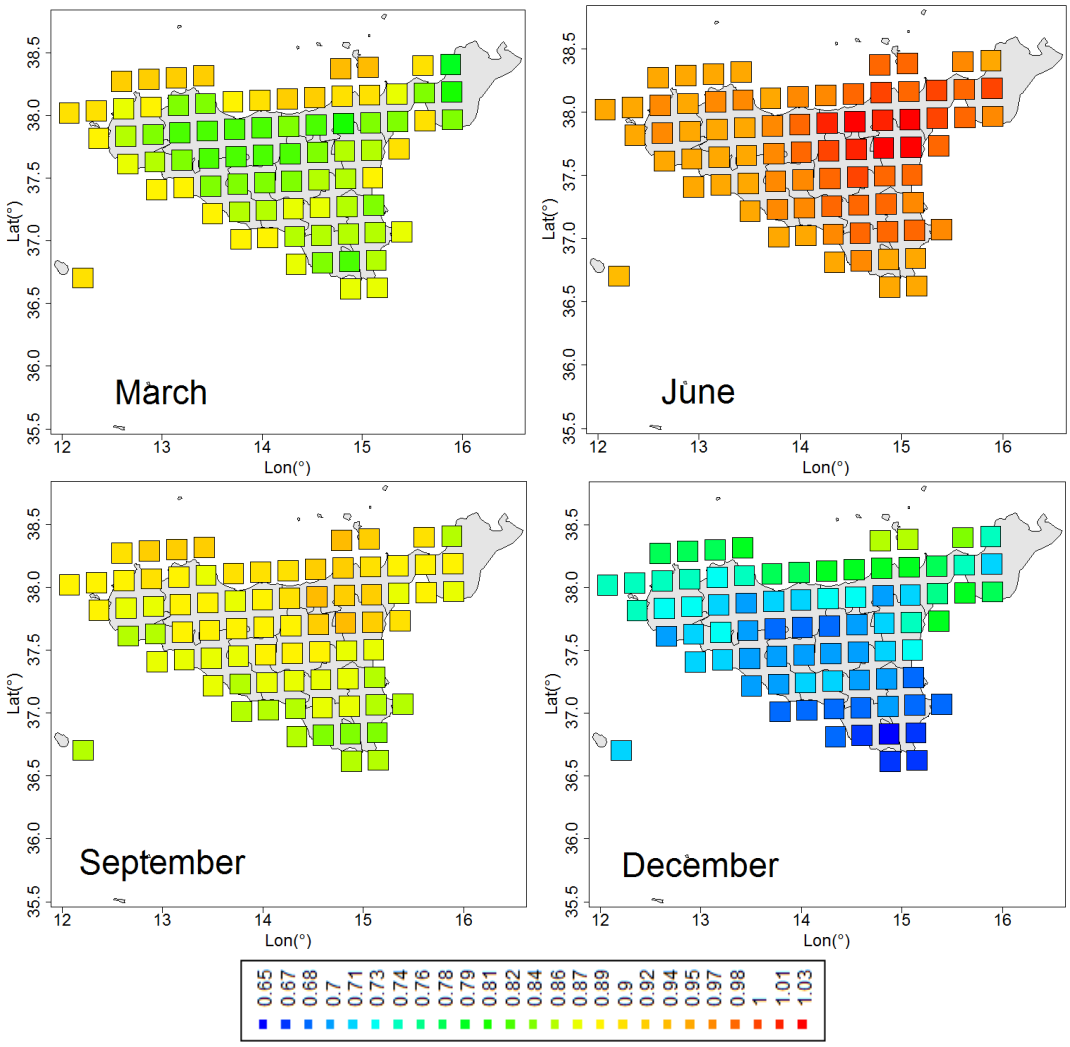

Figure 7.4: Ratios between KNMI-ECHAM5 model and observational normals for the 1961-2000 period: March, June, September and December.

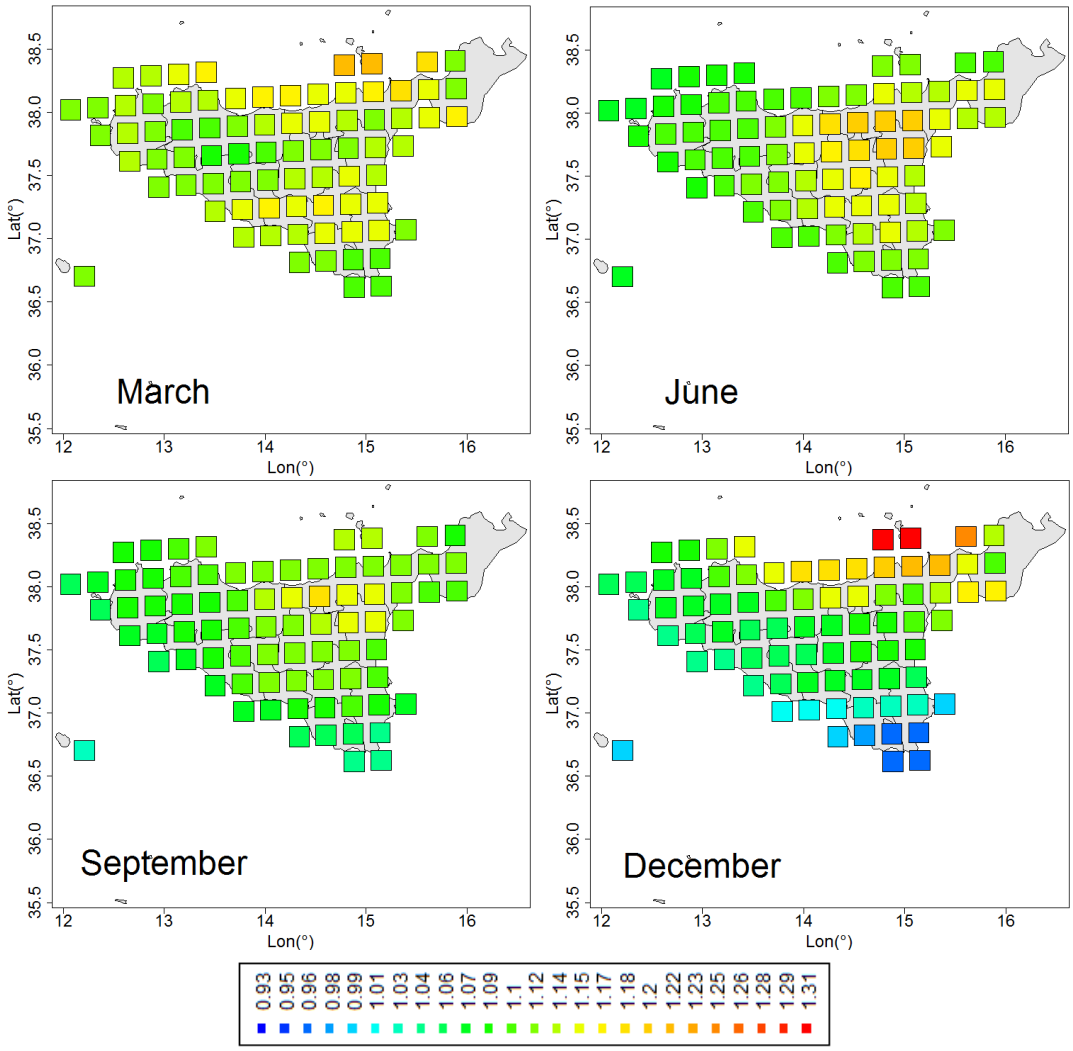

Figure 7.5: Ratios between SMHI-ECHAM5 model and observational normals for the 1961-2000 period: March, June, September and December.

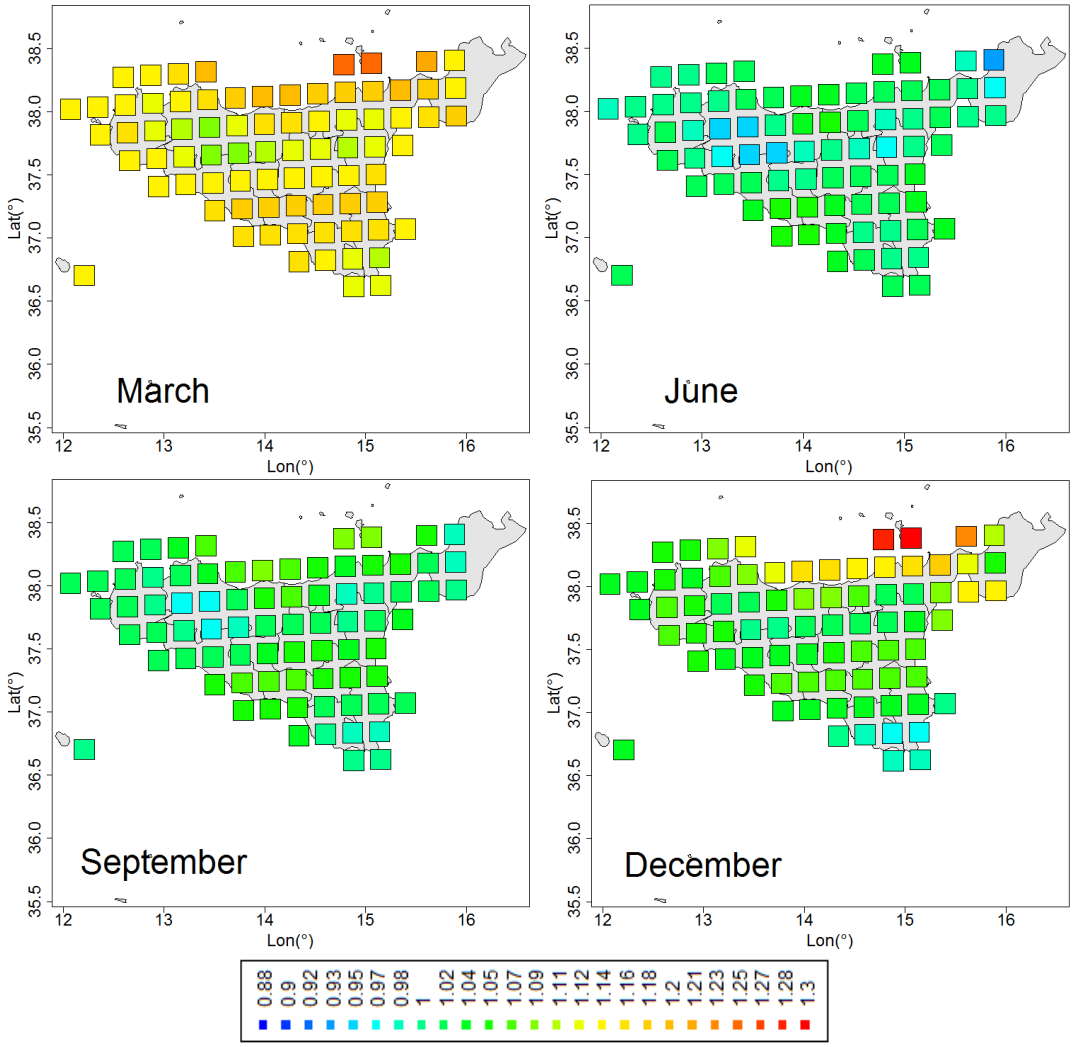

Figure 7.6: Ratios between SMHI-BCM model and observational normals for the 1961-2000 period: March, June, September and December.

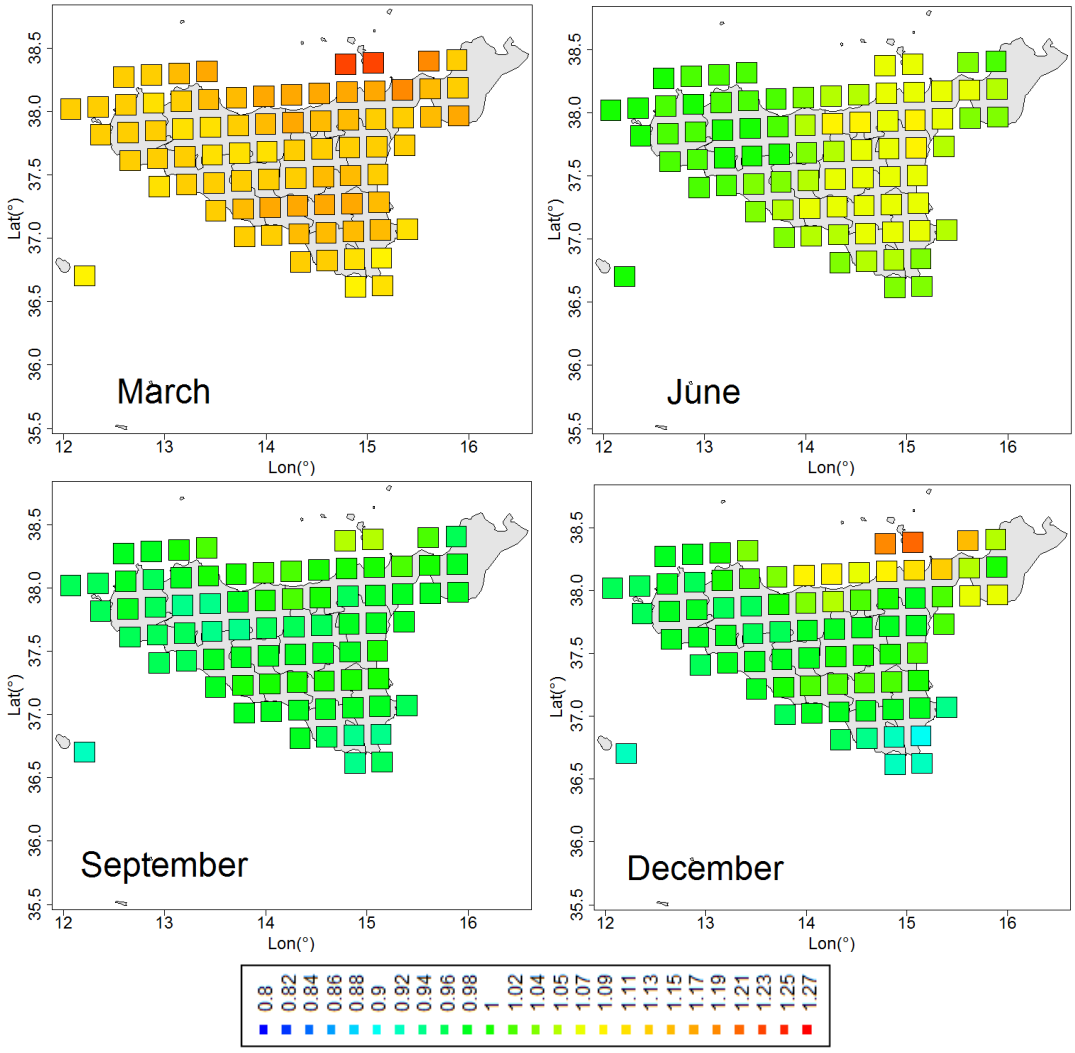

Figure 7.7: Ratios between SMHI-Had model and observational normals for the 1961-2000 period: March, June, September and December.

(e.g. 1951-1980 and 1984-2013 period) derived from the observed data.

7.5 Conclusions

A methodology which allows obtaining Sicily solar radiation climatologies for any period of the 1936-2013 interval has been set up. The K_T normal values of the 1961-2000 period have been used to validate and adjust the outputs of 4 RCM-GCM combinations. The adjusted scenario K_T normals have been used to produce 2001-2050 and 2051-2100 climatologies. These climatologies do not give evidence of well defined global radiation trends. In the future we plan to extend these studies to a wide range of RCM-GCM models and a paper on global radiation scenario will be prepared.

Bibliography

[1] Ångström A. (1924): *Solar and terrestrial radiation*, Q. J. Royal. Meteor. Soc., Vol. 50(210), pp. 121-126;

[2] Craddock J.M. (1979): *Methods of comparing annual rainfall records for climatic purposes, Weather*, Vol. 34(9), pp. 332-346, doi:10.1002/j.1477-8696.1979.tb03465.x;

[3] Daly C. (2006): *Guidelines for assessing the suitability of spatial climate data sets*, Int. J. Climatol., Vol. 26, pp. 707-721;

[4] Daly C., Gibson W.P., Taylor G.H., Johnson G.L.,Pasteris P.A. (2002): *A knowledge-based approach to the statistical mapping of climate*, Clim. Res., Vol. 22, pp. 99-113;

[5] Manara V., Brunetti M., Maugeri M., Pasotti L., Simolo C., Spinoni J. (2013): *Sicily monthly high-resolution solar radiation climatologies*, Conference proceeding: Climate change and its implications on eco system and society, SISC - First Annual Conference, Lecce, Italy, 22-23 September 2013, ISBN: 978-88-97666-08-0, pp. 198-209, *http : //www.sisclima.it/wp − content/uploads/*2014/01/*SISC_Conference_Proceedings.pdf*;

[6] Manara V., Beltrano M.C., Brunetti M., Maugeri M., Sanchez-Lorenzo A., Simolo C., Sorrenti S. (2015): *Sunshine duration variability and trends in Italy from homogenized instrumental time series (1936-2013)*, J. Geophys. Res. Atmos., Vol. 1, No. 120, pp. 3622-3641, doi:10.1002/2014JD022560;

[7] U.S. Geological Survey - USGS (1996): *GTOPO30 Digital Elevation Model*, http://eros.usgs.gov/#/Find Data/Products and Data Available/gotpo30 info;

[8] Wild M. (2009): *Global dimming and brightening: A review*, J. Geophys. Res., Vol. 114, D00D16, doi: 10.1029/2008JD011470;

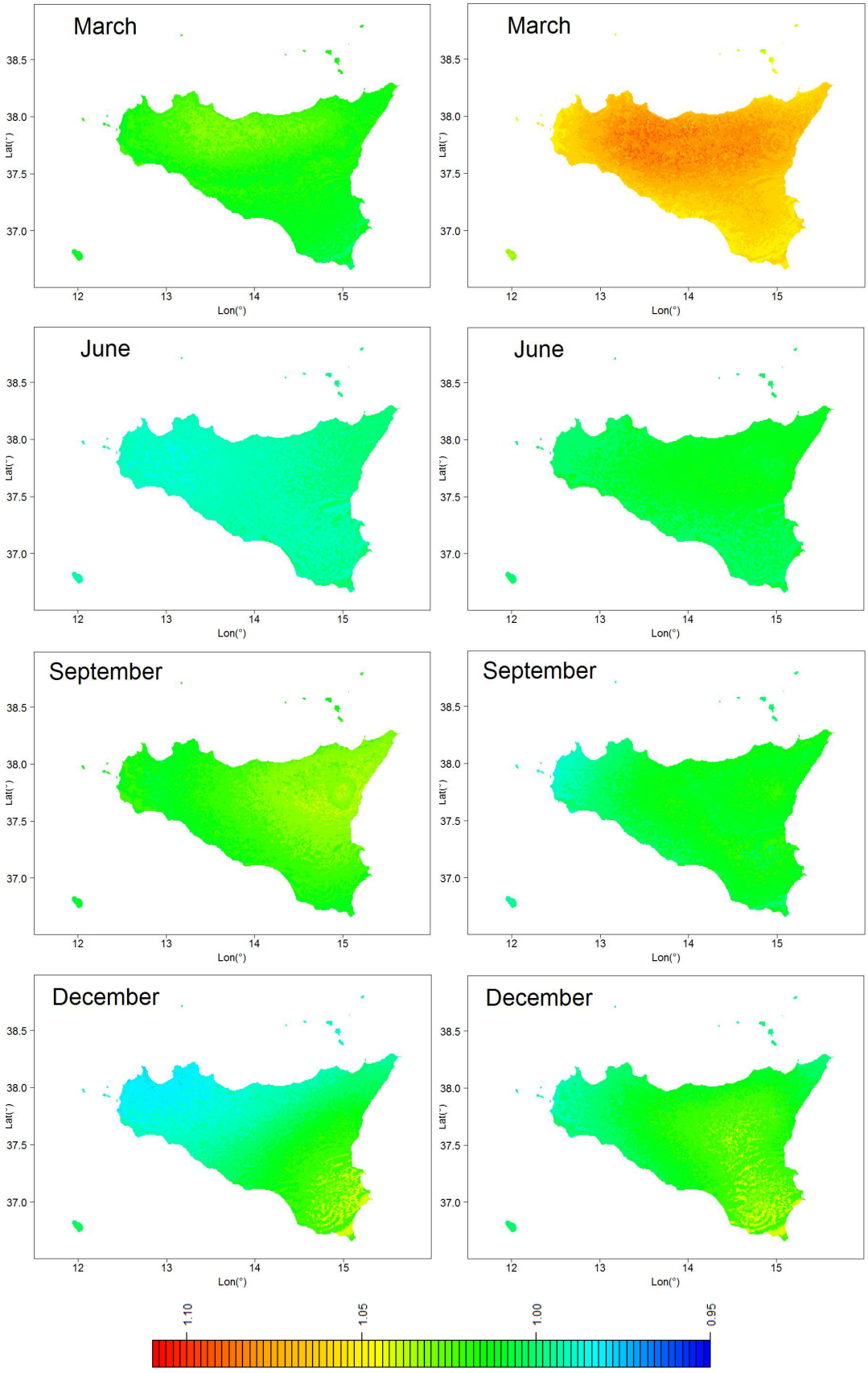

Figure 7.8: Ratios between the 2001-2050 and the 1961-2000 climatologies (left column) and ratios between the 2051-2100 and the 1961-2000 climatologies (right column) for March, June, September and December for the KNMI-ECHAM5 model.

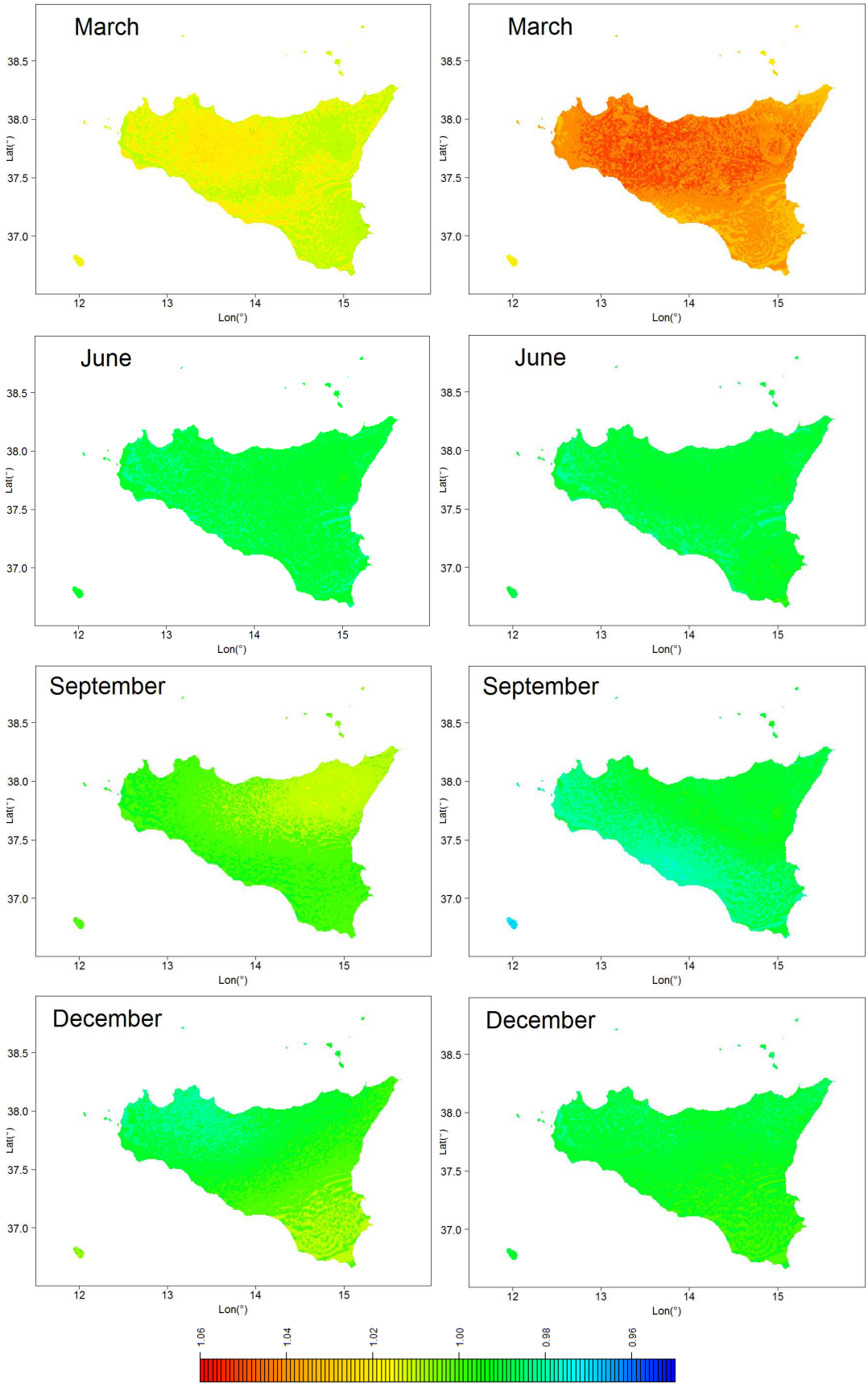

Figure 7.9: Ratios between the 2001-2050 and the 1961-2000 climatologies (left column) and ratios between the 2051-2100 and the 1961-2000 climatologies (right column) for March, June, September and December for the SHMI-ECHAM5 model.

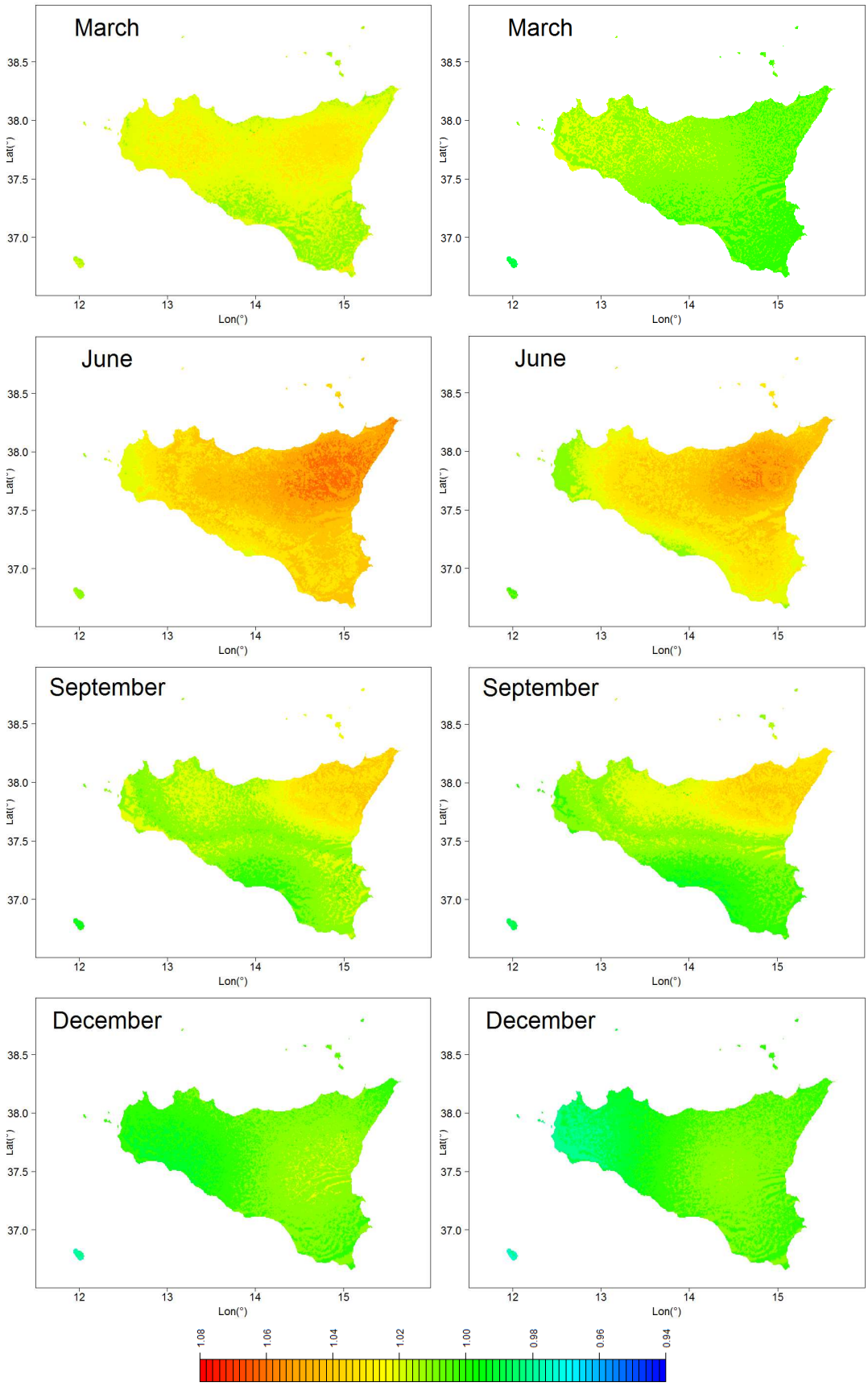

Figure 7.10: Ratios between the 2001-2050 and the 1961-2000 climatologies (left column) and ratios between the 2051-2100 and the 1961-2000 climatologies (right column) for March, June, September and December for the SMHI-BCM model.

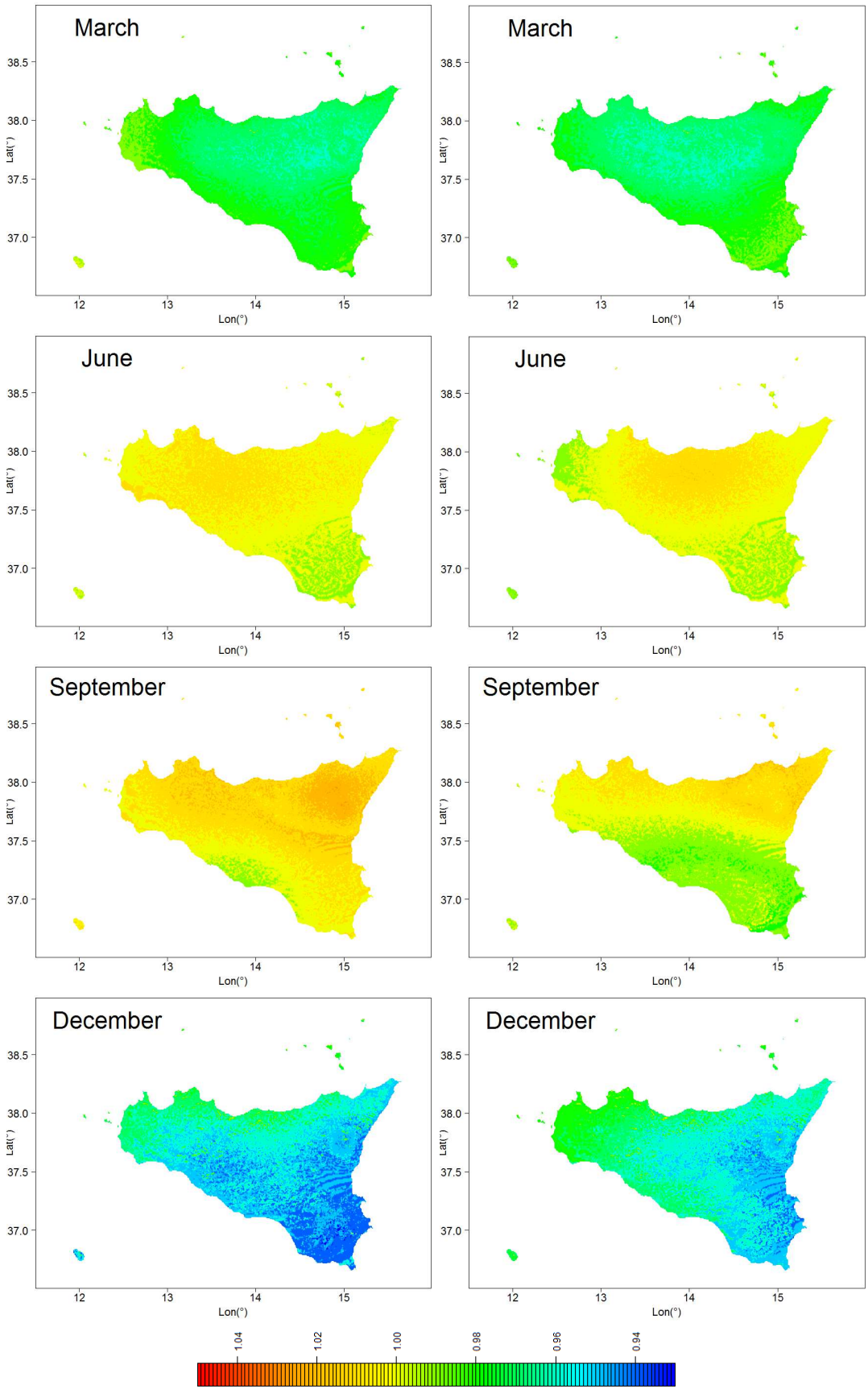

Figure 7.11: Ratios between the 2001-2050 and the 1961-2000 climatologies (left column) and ratios between the 2051-2100 and the 1961-2000 climatologies (right column) for March, June, September and December for the SMHI-Had model.

[9] Wild M. (2012): *Enlightening global dimming and brightening*, Bull. Amer. Meteor. Soc., Vol. 93, pp. 27-37, doi:10.1175/BAMS-D-11-00074.1;

[10] Sanchez-Lorenzo A., Brunetti M., Calbo J., Martin-Vide J. (2007): *Recent spatial and temporal variability and trends of sunshine duration over the Iberian Peninsula from a homogenized data set*, J. Geophys. Res., Vol. 112, D20115, doi:10.1029/2007JD008677;

[11] Spinoni J. (2010): *1961-90 High-Resolution temperature, precipitation, and solar radiation climatologies for Italy*, Ph.D. thesis, Milan University, available at: http://air.unimi.it/bitstream/2434/155260/2/phd unimi R07883 1.pdf;

[12] Spinoni J., Brunetti M., Maugeri M., Simolo C. (2012): *1961-1990 monthly high-resolution solar radiation climatologies for Italy*, Adv. Sci. Res., Vol. 8, pp. 19-21, available at: www.adv-sci-res.net/8/19/2012.

Chapter 8

Conclusions and future developments

The Earth's climate system is powered by solar radiation which governs a large number of processes. It has a central role, not only for scientific interests, but also for its profound environmental, societal and economic implications ([15]). Moreover, in the last decades, the scientific community has become aware of the fact that global radiation ($E_{g\downarrow}$) has not been constant over the time. A large number of sites reported in literature ([17]) show a decreasing tendency between the 1950s and the 1980s, called "Global dimming" and a subsequent increase called "Brightening period". The longest series show also an increasing tendency between the 1940s and 1950s called "Early brightening". The causes of these variations are not completely clear. It has been proposed that changes in the aerosol concentrations and cloudiness are the major causes.
$E_{g\downarrow}$ series started to become available on a widespread basis only at the end of the 1950s during the International Geophysical Year. For this reason, it is very common to study $E_{g\downarrow}$ temporal variability starting from other climatic variables (proxy variables) where probably the most appropriate is sunshine duration (SD). Moreover, studies on the temporal evolution of SD and $E_{g\downarrow}$ in Italy were not available in literature before this work.
For all these reasons, the aims of my PhD project were:

- to set up for the first time an Italian SD and $E_{g\downarrow}$ dataset for the 1936-2013 and 1959-2013 periods, respectively, starting from instrumental time series;
- to study the variability and trends of the obtained seasonal and annual regional (northern and southern Italy) series;
- to determine to what extent SD and $E_{g\downarrow}$ variability could depend on aerosol concentration or on cloudiness changes;
- to compare the obtained SD and $E_{g\downarrow}$ regional records over the common period (1959-2013) in order to investigate to what extent they agree and so to what extent SD can be considered a good proxy variable for $E_{g\downarrow}$;

- to investigate possible applications of the SD and $E_{g\downarrow}$ dataset.

8.1 Sunshine duration and global radiation dataset

In order to set up a SD and $E_{g\downarrow}$ dataset, a large number of daily series (together with the corresponding metadata) were recovered over the whole Italian territory. The largest part of them come from the Council for Agricultural Research and Agricultural Economy Analysis (CREA - Consiglio per la ricerca in agricoltura e l'analisi dell'economia agraria) and the Italian Air Force (AM - Aeronautica Militare Italiana). Some series were also recovered from universities and urban observatories. The final SD dataset encompasses 104 series for the period 1936-2013 while the $E_{g\downarrow}$ dataset encompasses 54 series for the 1959-2013 period.

To obtain reliable series useful to study the variability and trends, it has been necessary to solve a number of problems concerning the quality of the series, their completeness and their spatial distribution ([6]; [7]; [8]; [9] - Chapter 2-5).

So, all the records were subjected to a detailed quality control and homogenization procedure (Craddock test) in order to find out and eliminate non climatic signals. This point has been demonstrated to be very important for variables such as SD and $E_{g\downarrow}$, whose measurements are subjected to a number of problems (e.g., station relocations, changes in instruments, observation times and so on). The results show how at regional level systematic biases in the original records can hide a significant part of the long-term trend. Specifically, the necessity of reducing SD records before the 1960s to get homogeneous series may be due to the strong urbanization which occurred in Italy in the following decades, causing a reduction in the sky-view factor for some urban observatories of the CREA network and producing relatively lower SD in the following years. However, the most relevant inhomogeneities found in the $E_{g\downarrow}$ series are due, before the 1980s, to many instrument changes and recalibrations.

Another problem that has been necessary to solve is that there are periods in the time intervals covered by the two datasets with low data availability, as for example the period before the end of the 1950s for SD and the period at the beginning of the 1990s for $E_{g\downarrow}$. The many gaps make a direct estimation of an average SD and $E_{g\downarrow}$ record impossible. This record were in fact affected by high fluctuations, with positive biases when more sunny stations are available and negative biases when less sunny stations are available. To solve this problem a methodology has been set up in order to fill the gaps in the monthly records. They were estimated under the assumption of the constancy of the ratio between incomplete and reference series.

Then, after the gap-filling, all the series were converted into (relative), seasonal and annual anomaly series and a 1°x1° gridded version of the dataset has been generated in order to balance the contribution of areas with a higher number of stations with those that have a lower station coverage. These series were clustered in two regions (northern and southern Italy) by means of a Principal Component Analysis and finally the grid-point records of

these areas were averaged in order to get the corresponding regional SD and $E_{g\downarrow}$ records for the periods 1936-2013/1959-2013 respectively.
Besides the all-sky records, the corresponding seasonal and annual clear-sky anomaly records (both for SD and $E_{g\downarrow}$) were also obtained ([7]; [10] - Chapter 3; 6). Specifically, starting from the original daily series only the clear-sky days were selected by comparison with corresponding total cloud cover (TCC) series ([11]).

8.2 Sunshine duration and global radiation variability and trends

The obtained all-sky and clear-sky SD and $E_{g\downarrow}$ seasonal and annual anomaly records were analyzed. Specifically, the variability under all-sky conditions is due both to the contributions of clouds and aerosols while the variability under clear-sky conditions is due only to the contribution of aerosol changes ([6]; [7]; [10] - Chapter 2; 3; 6).
The all-sky SD anomaly series show a decreasing tendency ("Global dimming") between the mid-1950s and the beginning of the 1980s and an increasing tendency ("Brightening period") in the subsequent period for both the regions. The intensity of the two signals depends on the considered region and season. Overall, they are comparable in the south while in the north the brightening is both longer and stronger than the previous dimming. In fact, in the north also in the seasons that show a significant dimming in the 1960s and 1970s, the trend over the widest windows is significantly positive (for the 1936-2013 period it ranges from $1.1 \pm 0.3\% decade^{-1}$ in summer to $2.8 \pm 0.7\% decade^{-1}$ in autumn). Differently, in the south, there is a significant positive long-term trend only for the winter record ($1.9 \pm 0.6\% decade^{-1}$ over the 1936-2013 period). In the early period, from mid-1930s to the mid-1950s there is some evidence of an increasing tendency although this signal, "Early brightening", concerns a period in which data availability is very low, causing a greater uncertainty in regional records. The comparison between SD records with corresponding TCC records ([11]) shows that the expected negative correlation between these variables is often not evident as far as long-term tendencies are concerned especially between about the 1960s and 1980s. This suggests that during the dimming period there is an important fraction of SD evolution that cannot be explained by TCC. It must therefore depend on other factors, as for example, changes in aerosol optical thickness.
Considering only the clear-sky SD days, the trends show a longer and more significant dimming period respect to the all-sky series (with the only exception of winter) while the increase during the brightening period becomes weaker (spring and summer). The most relevant changes are observed in autumn for both regions where under all-sky conditions the SD curves do not show any signal, while under clear-sky conditions the dimming/brightening periods become significant.
Similarly, the all-sky $E_{g\downarrow}$ records show a decrease until the mid-1980s and a subsequent

increase until the end of the series even though the strength and persistence of tendencies are not the same in all seasons. In particular, at annual scale the trends of the two periods are comparable especially in the southern region. In fact, the trend for the whole period under analysis is not statistically significant. However, the intensity of the dimming is slightly higher for the south than for the north especially for periods starting in the mid-1960s (about $-3\% decade^{-1}$ for the north and $-4\% decade^{-1}$ for the south), while the brightening is more intense in the north especially for periods starting in the mid-1980s (about $4\% decade^{-1}$ for the north and $2\% decade^{-1}$ for the south). In the clear-sky $E_{g\downarrow}$ records, the dimming and brightening trends become stronger and they are significant for all seasons and for both regions. The most evident differences between all-sky and clear-sky series are observed in winter but also in autumn for both regions, where not only the variations become more intense and significant, but also the change point from dimming to brightening moves from the mid-1990s to the mid-1980s as observed for the other seasons. The length and the intensity of the two periods is comparable even if the dimming period is stronger in spring, summer and autumn in the south while it is stronger in winter in the north.

The resulting trends under clear-sky conditions are in agreement with changes (increase until the mid-1980s and decrease in the subsequent period ([4]; [16])) in anthropogenic aerosols that occurred during the period under analysis. This suggests that anthropogenic aerosols have a relevant contribution on $E_{g\downarrow}$ variations under clear-sky conditions. Moreover, the stronger dimming in the south than in the north, during spring, summer and autumn may give evidence of a contradiction because the north is more affected by air pollution due to higher emissions. Nevertheless, southern Italy is more affected by coarse aerosols ([1]) such as mineral dust from the Sahara and Sahel ([13]). It is confirmed by a good correlation between the $E_{g\downarrow}$ anomaly series and the Sahel Precipitation index especially in the south in summer and autumn. This suggests also a significant contribution of natural aerosols to $E_{g\downarrow}$ variability. Moreover, the fact that the change point under all-sky and clear-sky conditions differs by several years in autumn and the intensity of the two periods changes in all seasons supports the hypothesis that clouds contribute in a significant way to the $E_{g\downarrow}$ variability under all-sky conditions and confirms the hypothesis also formulated for SD, suggesting that cloud cover variations have partially masked the dimming caused by the increasing aerosol concentrations, especially in the northern region.

The obtained trends both for SD and $E_{g\downarrow}$ are in good agreement with those observed in other worldwide areas and Europe, even though some relevant regional peculiarities are evident ([17]; [18]).

8.3 To what extent do sunshine duration and global radiation agree?

SD is often used in literature as proxy variable for $E_{g\downarrow}$, but to what extent do these two variables agree both under all-sky and clear-sky conditions ([10] - Chapter 6)? The results highlight that the agreement between SD and $E_{g\downarrow}$ decadal variability and long-term trends, over the common period 1959-2013, depends on the considered region, season and period. Overall, under all-sky conditions, SD records show a shorter and less intense decrease during the dimming period with respect to $E_{g\downarrow}$ ones, while the agreement is better if the subsequent period is considered, where both the variables show an increasing tendency. Moreover, the SD series show a trend inversion from dimming to brightening at the end of the 1970s/beginning of the 1980s while the $E_{g\downarrow}$ series show it around the mid-1980s. Considering only the clear days, $E_{g\downarrow}$ series show again a stronger decrease than SD ones in the first period, and now also a slightly stronger increase in the subsequent period.

In order to investigate whether the differences in the clear-sky trends are due to a different sensitivity to atmospheric turbidity changes, a model has been applied with the aim of estimating how large are SD and $E_{g\downarrow}$ relative variations when atmospheric turbidity (expressed by means of the Turbidity Linke Factor - T_L) changes. The analysis shows that clear-sky SD and $E_{g\downarrow}$ sensitivity to T_L variations strongly depends on the T_L starting value. Specifically, for low T_L ($T_L < 3$ - typical winter values) $E_{g\downarrow}$ is much more sensitive than SD, for high T_L ($T_L > 6$ - observed in summer in the northern region) SD is slightly more sensitive than $E_{g\downarrow}$, while for the central values (values observed in spring, summer and autumn) the sensitivity is comparable. These results give evidence that the use of SD as a proxy variable for clear-sky $E_{g\downarrow}$ may be problematic especially if T_L is low or if it shows significant changes in time. A further problem may be linked to the position of the stations that could have a non optimal sky-view factor either at sunrise or at sunset or in both moments. In fact, when the reduction of the sky-view factor is large, this problem can completely hide the response of clear-sky SD to T_L variations especially in winter. However, the Italian stations are located in area with a good sky-view factor even if it can not be excluded that few of them have non optimal location at the sunrise or at the sunset in winter.

The comparison between the modelled and the observed SD relative trends highlights a very good agreement in the southern Italy for all seasons while in the northern Italy the good agreement concerns all seasons only for the brightening period, whereas in the dimming period it concerns only spring and summer. In this period, in winter and in autumn, the differences in SD and $E_{g\downarrow}$ observed trends can not be explained by their different sensitivity to T_L variations. These disagreement could be both connected to instrumental problems (e.g., low performance in the first years of the paper card for high values of the relative humidity) or to a decrease of relative humidity in the period under analysis (e.g., decrease of fog occurrences especially during the brightening period ([3])).

8.4 Application: Global radiation climatologies for the past, present and future

SD and $E_{g\downarrow}$ datasets are useful in a wide number of fields. They can be used for example to validate satellite data ([14]), outputs from RCM-GCMs (Regional Climate Models - Global Climate Models) and reanalysis series ([12]).
In this work, a methodology has been set up ([5] - Chapter 7) to project the data of a station network onto a high resolution grid and to transform the normal values of a given period in those of any another period. These steps are very important in comparing the station observations and the RCM-GCMs simulations. In fact, they allow to evaluate the ability of the models to capture the real behavior of SD and $E_{g\downarrow}$ and to adjust their outputs in order to make them representative of real data. Moreover, they allow to estimate SD and $E_{g\downarrow}$ climatologies for any time interval, considering the orography, the astronomical parameters and the composition of the atmosphere. It is worth noticing that this procedure can be applied not only to surfaces inclined as the soil but also selecting any combination of slope and aspect. The former solution is particularly useful for agricultural applications while the latter is useful for energy applications. Specifically, the methodology has been set up in the frame of an European project ECLISE (Enabling Climate Information Services for Europe), that aimed to take the first step towards the realization of an European Climate Service. It has been applied to a network of 41 Sicily stations in order to obtain 2002-2011 $E_{g\downarrow}$ climatologies. Then, starting from the 2002-2011 $E_{g\downarrow}$ normal values, it has been possible to calculate the normal values for any period of the 1936-2013 interval (period of SD data availability) and then to adjust the output of 4 RCM-GCMs combinations using the $E_{g\downarrow}$ normal values obtained for the 1961-2000 period. Finally, it has been possible to obtain the corresponding climatologies for every interval for which the normal values are available.

8.5 Future developments

During my PhD project, I have highlighted solar radiation variability in Italy over the last decades and I have investigated the underlying causes. In spite of the clear results on SD and $E_{g\downarrow}$ trends, there are some relevant open issues. It will be necessary to understand more in detail how aerosol concentrations have changed during the dimming and brightening periods. It will be possible to do it for example analysing the visibility records. Moreover, it will also be interesting to understand more in detail how the relative humidity has changed during the same period and so how the aerosol optical properties have changed. Another opened point concerns clouds and so how the total cloud cover and the different types of clouds have changed.
Moreover, it will be interesting to further develop the possibility to exploit the use of SD and $E_{g\downarrow}$ station data and spatio-temporal fields for a wide range of applications.

Bibliography

[1] Bonasoni P., Cristofanelli P., Calzolari F., Bonafé U., Evangelisti F., Stohl A., Sajani Zauli S., van Dingenen R., Colombo T., Balkanski Y. (2004): *Aerosol-ozone correlations during dust transport episodes*, Atmos. Chem. Phys., Vol. 4, pp. 1201-1215, doi:1680-7324/acp/2004-4-1201;

[2] Cubasch U., Wuebbles D., Chen D., Facchini M.C., Frame D., Mahowald N., Winther J.G. (2013): *Introduction.* In: Climate Change 2013: The Physical Science Basis. Contribution of Working Group I to the Fifth Assessment Report of the Intergovernmental Panel on Climate Change [Stocker T.F., Qin D., Plattner G.K., Tignor M., Allen S.K., Boschung J., Nauels A., Xia Y., Bex V., Midgley P.M. (eds.)]. Cambridge University Press, Cambridge, United Kingdom and New York, NY, USA;

[3] Giulianelli L., Gilardoni S., Tarozzi L., Rinaldi M., Decesari S., Carbone C., Facchini M.C., Fuzzi S. (2014): *Fog occurrence and chemical composition in the Po valley over the last twenty years*, Atm. Env., Vol. 98, pp. 394-401, doi:10.1016/j.atmosenv.2014.08.080;

[4] Maggi V., Villa S., Finizio A., Delmonte B., Casati P., Marino F. (2006): *Variability of anthropogenic and natural compounds in high altitude-high accumulation alpine glaciers*, Hydrobiologia, Vol. 562, pp. 43-56, doi:10.1007/s10750-005-1804-y;

[5] Manara V., Brunetti M., Maugeri M., Pasotti L., Simolo C. (2014): *Past and future solar radiation variability and change over Sicily*, Conference proceeding: Climate change: scenarios, impacts and policy SISC Second Annual Conference, Venice, Italy, September 2014, ISBN: 978-88-97666-04-2, pp: 397-415; *http* : $//www.sisclima.it/wp-content/uploads/2014/10/SISC\_Conference\_Proceedings-2014.pdf$;

[6] Manara V., Beltrano M.C., Brunetti M., Maugeri M., Sanchez-Lorenzo A., Simolo C., Sorrenti S. (2015): *Sunshine duration variability and trends in Italy from homogenized instrumental time series (1936-2013)*, J. Geophys. Res. Atmos., Vol. 1, No. 120, pp. 3622-3641, doi:10.1002/2014JD022560;

[7] Manara V., Brunetti M., Maugeri M.(2016): *Reconstructing sunshine duration and solar radiation long-term evolution for Italy: a challenge for quality control and homogenization procedures*, Conference proceeding of the 14^{th} IMEKO T10 Workshop Technical Diagnostics - New Perspectives in Measurements, Tools and Techniques for system's reliability, maintainability and safety, 27-28 June 2016, Milan, Italy, pp. 13-18, ISBN: 978-92-990073-9-6, *http* : $//www.imeko.org/publications/tc10-2016/IMEKO-TC10-2016-002.pdf$;

[8] Manara V., Brunetti M., Celozzi A., Maugeri M., Sanchez-Lorenzo A., Wild M. (2016): *Detection of dimming/brightening in Italy from homogenized all-sky and clear-*

sky surface solar radiation records and underlying causes (1959-2013), Atmos. Chem. Phys., Vol. 16, pp. 11145-11161, doi:10.5194/acp-16-11145-2016;

[9] Manara V., Brunetti M., Maugeri M., Sanchez-Lorenzo A., Wild M. (2017): *Homogenization of a surface solar radiation dataset over Italy*, Radiation Processes in the Atmosphere and Ocean (IRS2016), AIP Conference Proceedings, Vol. 1810, 090004-1-090004-4, doi: 10.1063/1.4975544, Published by AIP Publishing, ISBN: 978-0-7354-1478-5;

[10] Manara V., Brunetti M., Maugeri M., Sanchez-Lorenzo A., Wild M.: *Sunshine duration and global radiation trends in Italy (1959-2013): to what extent do they agree?*, submitted to J. Geophys. Res. Atmos.

[11] Maugeri M., Bagnati Z., Brunetti M., Nanni T. (2001): *Trends in italian total cloud amount, 1951-1996*, Geophys. Res. Lett., Vol. 28(24), pp. 4551-4554, doi: 10.1029/2001GL013754;

[12] Nabat P., Somot S., Mallet M., Sanchez-Lorenzo A., Wild M. (2014): *Contribution of anthropogenic sulfate aerosols to the changing Euro-Mediterranean climate since 1980*, Geophys. Res. Lett., Vol. 41, pp. 5605-5611, doi:10.1002/2014GL060798;

[13] Prospero J.M. (1996): *Saharan dust transport over the North Atlantic Ocean and Mediterranean: An overview, The Impact of Desert Dust across the Mediterranean*, Vol. 11, pp. 133-151, doi:10.1007/978-94-017-3354-0;

[14] Sanchez-Lorenzo A., Wild M., Trentmann J. (2013): *Validation and stability assessment of the monthly mean CM SAF surface solar radiation dataset over Europe against a homogenized surface dataset (1983-2005)*, Remote Sens. Environ., Vol. 134, pp. 355-366, doi:10.1016/j.rse.2013.03.012;

[15] Stanhill G. (1983): *The distribution of global solar radiation over the land surfaces of the Earth*, Solar Energy, Vol. 31(1), pp. 95-104;

[16] Vestreng V., Myhre G., Fagerli H., Reis S., Tarrasón L. (2007): *Twenty-five years of continuous sulphur dioxide emission reduction in Europe*, Atmos. Chem. Phys., Vol. 7, pp. 3663-3681, doi:10.5194/acp-7-3663-2007, 2007;

[17] Wild M. (2009): *Global dimming and brightening: A review*, J. Geophys. Res., Vol. 114, D00D16, doi:10.1029/2008JD011470;

[18] Wild, M. (2016): *Decadal changes in radiative fluxes at land and ocean surfaces and their relevance for global warming*, Wiley Interdisciplinary Reviews: Climate Change, Vol. 7(1), pp. 91-107, doi:10.1002/wcc.372;

Acknowledgements and Data

I gratefully thank all the institutions that allowed access to the data for research purposes and contributed to setting up the 1936-2013 sunshine duration database and the 1959-2013 global radiation database.

Sunshine duration data

CREA ("Consiglio per la ricerca in agricoltura e l'analisi dell'economia agraria"). The original data are available at: *http* : *//cma.entecra.it/homePage.htm* since 1994. The data of the previous years have to be requested at CREA.
The Italian Air Force ("Servizio dell'Aeronautica Militare Italiana" refer to:
http : *//clima.meteoam.it/istruzioni.php* for data access) data have been received in the frame of an agreement between Italian Air Force and the Italian National Research Council.
Luca Lombroso and Maurizio Ratti provided the series of the Geophysical Observatory of Modena, and the series of the Meteorological Observatory of Pontremoli ("Osservatorio meteorologico Marsili").
The Trieste series is available online at: *http* : *//www.meteo.units.it/*.
The Varese data are available on request at "Centro Geofisico Prealpino-Società Astronomica G.V. Schiaparelli" (*http* : *//www.astrogeo.va.it/*).
The HISTALP data are available online at: *http* : *//www.zamg.ac.at/histalp/*.
The Spanish data come from the Spanish Meteorological Agency (AEMET) and for data access refer to: *http* : *//www.aemet.es/es/portada*.

Global radiation data

The Italian Air Force data ("Servizio dell'Aeronautica Militare Italiana") have been received in the frame of an agreement between the Italian Air Force and the Italian National Research Council (for data access refer to *http* : *//clima.meteoam.it/istruzioni.php*).
For the BDAN ("Banca Dati Agrometeorologica Nazionale") data refer to:
http : *//cma.entecra.it/homePage.htm*.
For Trieste data refer to: *http* : *//www.meteo.units.it/*.

The Swiss data have been obtained from the Swiss Federal Office for Meteorology and Climatology (MeteoSwiss) and they are available at *http* : *//www.meteosvizzera.admin.ch/* and *https* : *//gate.meteoswiss.ch/idaweb/login.do*.
The Sicilian data come from the Agrometeorological Service of Sicily Regional Administration (for data access refer to: *http* : *//www.sias.regione.sicilia.it/*).

Other data

The total cloud cover data come from the Italian Air Force ("Servizio dell'Aeronautica Militare Italiana") and they have been received in the frame of an agreement between the Italian Air Force and the Italian National Research Council (for data access refer to: *http* : *//clima.meteoam.it/istruzioni.php*).
The Sahel precipitation index data (doi:10.6069/H5MW2F2Q) come from the Joint Institute for the Study of the Atmosphere and Ocean and they are available at:
http : *//research.jisao.washington.edu/datasets/sahel/*.